



Horizon 2020
Programme

MUSA

Research and Innovation Action (RIA)

This project has received funding from the European
Union's Horizon 2020 research and innovation programme
under grant agreement No 847441

Start date : 2019-06-01 Duration : 48 Months

Review of uncertainty methodologies and tools applicable to SA codes for the prediction of ST

Authors : Dr. Victor Hugo SANCHEZ-ESPINOZA (KIT), Dr. Karine Chevalier Jabet (IRSN)

MUSA - Contract Number: 847441

Project officer: Angelgiorgio IORIZZO

Document title	Review of uncertainty methodologies and tools applicable to SA codes for the prediction of ST
Author(s)	Dr. Victor Hugo SANCHEZ-ESPINOZA, Dr. Karine Chevalier Jabet (IRSN)
Number of pages	0
Document type	Deliverable
Work Package	WP3
Document number	D3.1
Issued by	KIT
Date of completion	2021-04-08 15:10:09
Dissemination level	Public

Summary

This deliverable describes the review of the uncertainty quantifications methodologies and tools to be applied within the MUSA-project by the partners to assess the uncertainty of different severe accident codes in predicting the radiological source term of various reactor designs. It reflects the different tasks of the SubWP3.1 i.e. 1) main features of UQ tools 2) experience from previous applications of UQ-tools 3) applicability of UQ-tools to SA and 4) Usability of UQ-tools on large HPC.

Approval



Date	By
2021-04-08 15:11:47	Dr. Victor Hugo SANCHEZ-ESPINOZA (KIT)
2021-04-08 16:17:34	Dr. Luis e. HERRANZ (CIEMAT)

D.3.1 – *Review of UQ methodologies and tools applicable to SA codes for the prediction of ST*

K. Chevalier (IRSN), V. Sanchez (KIT)

Version 06 – 08/04/2021

Document type	Deliverable / Milestone / Minutes / Report
Document number	D.3.1 version 06
Document title	Review of UQ methodologies and tools applicable to SA codes for the prediction of ST
Authors	K. Chevalier (IRSN), V. Sanchez (KIT)
Release date	13/11/2020
Contributing partners	S. Beck (GRS), M. Berdaï (CNSC), R. Bocanegra (CIEMAT), A. Bousbia Salah (BELV), G. Caruso (UNIROMA1), G. Clark (JACOBS), I. Lamont (JACOBS), A. Dethioux (TRACTEBEL), M. D'Onorio (UNIROMA1), F. Gabrielli (KIT), F. Giannetti (UNIROMA), W. Giannotti (NINE), L. E. Herranz (CIEMAT), A. Hoefer (FRAMATOME), M. Kloos (GRS), M. Malicki (TRACTEBEL), F. Mascari (ENEA), E.M. Pauli (FRAMATOME), C. Sarrette (BELV), L. Tiborz (GRS), V. Vileiniskis (LEI), X. Zheng (JAEA)
Dissemination level	Restricted to MUSA Consortium

Version	Short description	Main author	WP leader	Coordinator
#01	First release	K. Chevalier (IRSN)	V. Sanchez (KIT)	L. Herranz (CIEMAT)
#02	Revision 2	29.09.2020	4.10.2020	
#03	Revision 3		09.10.2020	
#04	Revision 4	12.11.2020	01.02.2020	
#05	Final		13.11.2020	
#06	Revision		08.04.2021	
Signature			 Dr. V. Sanchez	

Summary

This deliverable describes the review of the uncertainty quantifications methodologies and tools to be applied within the MUSA-project by the partners to assess the uncertainty of different severe accident codes in predicting the radiological source term of various reactor designs. It reflects the different tasks of the SubWP3.1 i.e. 1) main features of UQ tools 2) experience from previous applications of UQ-tools 3) applicability of UQ-tools to SA and 4) Usability of UQ-tools on large HPC.

Chapter 2 introduces the main objectives of this deliverable and lists the UQ-tools and severe accident codes intended to be applied in MUSA WP4, WP5 and WP6. In Chapter 2, a synthesis of the UQ-methods is given based on the information provided by the involved partners. Here, the overall problem, the type of uncertainties and how the different UQ-tools treat them as well as the key-features of the UQ-tools, the interface between the UQ-tools and the SA-codes are summarized. The synthesis also briefly describes the sampling and uncertainty propagation methods, the post-processing capabilities of the different UQ-tools, and the different correlations and methods available in the UQ-tools of MUSA for sensitivity analysis.

The focus of this report is put on the role of uncertainty parameters, their characteristics and data needed to be defined for each of them in order to propagate the uncertainties from the input to the output. Different couples of uncertainty methods and severe accident codes are going to be used in MUSA by different partners. Hence, the existing interface between them, the ways of uncertainty propagation and sampling, the different correlations and methods for sensitivity analysis, the different options for post-processing and finally the numerical noise of some severe accident codes are discussed to some extent. The data assimilation tools intended to be applied by two partners and the accumulated experience using these methods are discussed in a separate chapter.

An overview of the UQ-tools and the previous experience of the partners applying UQ-tools to different numerical tools e.g. neutronic, thermo-mechanic, thermal hydraulic, containment tools, and severe accident codes is summarized in a table. It includes the analysis of thermal hydraulic test facilities (e.g. FEBA), LOCA-tests (IFA-650.9-10), severe accident tests (e.g. QUENCH, Phebus), DBA-sequences (e.g. PWR REA, LB-LOCA, VVVER-1000 MCP Restart) and few severe accident sequences (MCCI, aerosol behavior, DCH, Hydrogen in containment, PWR-900 SA-sequence, PWR SBLOCA SA-sequence).

The potential of UQ and data assimilation tools of the partners for HPC-applications is also collected. Finally, conclusions are drawn in view of the tasks to be done in MUSA WP4, WP5 and WP6.

The Appendix 1 of this Deliverable includes the methods, main features, the kind of uncertainty parameters (initial conditions, boundary conditions, model parameters, etc.), propagation methods and finally the advantages and disadvantages of the UQ-tools to be used in MUSA e.g. SUSAN, SUNSET, URANIE, DAKOTA, RAVEN. In Appendix 2, the extensive and divers experience of the partners using and applying the UQ-tools in connection with different severe accident codes for different problems are collected and their relevance for the MUSA goals is emphasized. The Appendix 3 summarizes the applicability of the different UQ/data assimilation tools in a high performance computer (HPC) environment, which is of paramount importance for the MUSA project. Appendix 4 deals with the data assimilation tools while Appendix 5 describes the noise analysis of severe accident codes that may be considered/discussed when performing uncertainty quantifications.

Content

Summary	3
Content	4
Abbreviations and acronyms	5
List of Tables	6
1 Introduction	7
2 Synthesis	8
2.1 Define the problem	8
2.2 Definition of the uncertain parameters.....	9
2.3 Description of the uncertain parameters to be fed to the uncertainty propagation.....	10
2.3.1 Epistemic uncertainty.....	10
2.3.2 Aleatory/Stochastic uncertainty	10
2.4 Definition of interfaces with SA codes	11
2.5 Sampling and propagation methods.....	11
2.6 Post-processing	12
2.7 Sensitivity Analysis	12
3 Overview of applications of UQ-tools of MUSA-partners	13
3.1 Potential of UQ and data assimilation tools for HPC applications.....	15
4 Conclusions	15
5 Bibliography	16

Appendix-1: Uncertainty quantification methods (Task 1 and 3)

Appendix-2: Experience from application of the UQ-methods (Task 2)

Appendix-3: Potential of UQ for HPC applications (Task 4)

Appendix-4: Data Assimilation (Task 1)

Appendix-5: Noise Analysis

Abbreviations and acronyms

Abbreviation	significance
BE	Best Estimate
BEPU	Best Estimate Plus Uncertainties
CDF	Cumulative Distribution Function
CIAU	Capability of Internal Assessment of Uncertainty
CSA	Containment Safety Analyses
CV	Control Volume
DOE	Design Of Experiments
DST	Dempster–Shafer theory
EM	Evaluation Model
FOM	Figure Of Merit
FP	Fission Product
GSA	Global Sensitivity Analysis
IUQ	Input Uncertainty Quantification
OAT	One at a Time
PDF	Probability Density Function
PIRT	Phenomena Identification Ranking Table
SA	Severe Accident
SET	Separate Effect Test
UMAE	Uncertainty Method based on Accuracy Extrapolation
UQ	Uncertainty Quantification

List of Tables

Table 1: UQ-tools and SA-codes to be used in the MUSA-project 7

Table 2: Available frameworks for the different types of uncertainties 10

Table 3: Statistical tools features for input parameters pdf estimation..... 11

Table 4: Statistical tools/ SA codes interface features 11

Table 5: Statistical tools available for sensitivity functionalities..... 12

Table 6 : Overview of the application of UQ-tools/DBA and SA-codes of MUSA-partners 13

Table 7: HPC availability for UQ and data assimilation tools 15

1 Introduction

The overall objective of WP3.1 is to review and assess methodologies or tools used by the different partners of MUSA for uncertainty and sensitivity analyses when applying severe accident codes for the prediction of the radiological source term of different reactor designs and corresponding severe accident sequences.

As the quantification of uncertainty sources (IUQ) is performed in WP2, the scope of the report is limited to the overall review of the different UQ-methodologies to be used by the MUSA-partners in order to quantify the propagation of the uncertainties of the input parameters to the output uncertainties of severe accident codes (UQ). Therefore, both Severe Accident codes as well as the UQ-tools are given, where the couple of UQ and SA-codes can be observed. For uncertainty quantification, these computer codes have been coupled (or will be) coupled to probabilistic tools, such as DAKOTA, RAVEN, SUNSET, SUSA, URANIE. Table 1 shows the association between the UQ-tools and the Severe Accident codes, where the blue color meaning that the coupling is functional and has already been used, and the pink color indicates that the coupling remains to be done.

Table 1: UQ-tools and SA-codes to be used in the MUSA-project

	DAKOTA	RAVEN	SUNSET	SUSA	URANIE
ASTEC					
AC2					
MAAP					
MELCOR					
RELAP/SCDAP					

The statistical framework used by the different UQ-tools is similar e.g. Monte Carlo i.e. random or LHQ sampling, although other frameworks are provided. There is a large experience using these UQ-tools for the quantification of the uncertainty of system thermal hydraulic codes, most recently their application is being extended to other kind of codes e.g. subchannel codes, core solvers, etc. that are applied in the domain of physical phenomena during design basis accidents. The differences between the various UQ-tools lie mostly in extra-functionalities.

It is worth to mention, that the application of UQ-tools to quantify the uncertainty and sensitivity of severe accident codes in predicting the radiological source term, as it is foreseen in MUSA, is new and there is only limited experience applying these UQ-tools to severe accident phenomena, for example to in-vessel core degradation, MCCI, chemistry within the containment, and fission product and transport within containment, etc.

In this report, the following chapters will describe the four tasks of the subWp3.1 in the following order:

- First of all, a synthesis of the capability and limitations of the UQ-tools, their key-features, models, peculiarities, etc. that was extracted from the contributions provided by the MUSA-partners (code developers, users) will be described. The MUSA-partner will use these tools in WP4, WP5, and WP6. Emphasis will be put on the relevance of the experience of the partners using the UQ-tools in connection with severe accident tools for the investigations to be done for PHEBUS (WP4), different reactor designs (WP5) and for spent fuel pools (WP6).
- The main features, models, etc. of each UQ-tools to be applied in MUSA is described based on the contributions delivered by the involved partners in Appendix-1 while in Appendix -2 the experience of the partners in using UQ-tools in connection with SA-codes for dedicated applications is presented.
- Appendix-3 summarizes the potential of the different couple of UQ/SA-tools for their application in large computer clusters (HPC).
- Appendix 3 describes the applicability of the different UQ/data assimilation tools in a high performance computer (HPC) environment, which is of paramount importance for the MUSA project.
- Appendix 4 deals with the data assimilation tools including modeling issues and capabilities.
- Finally, Appendix 5 describes the noise analysis of severe accident codes that may be considered/discussed when performing uncertainty quantifications.

2 Synthesis

The community of severe accidents does not rely anymore entirely on the use of conservative approach, since it showed its limitation in a number of situations. For example, for molten corium concrete interaction, if we consider the basemat breakthrough instant, we might be conservative on the parameters that tend to maximize the concrete vertical erosion and lower the heat exchange with the containment atmosphere in order to get the shortest breakthrough times in our safety analysis. If we consider the containment failure due to pressurization, we would tend to favour the energy release towards the containment atmosphere and favour the situations where water can flow onto the corium, for example by favouring homogenous corium configurations ensuring sufficient radial erosion of the cavity pit. Other examples like that can be found, including examples involving accident management strategies. Because the phenomenology is complex and represents a hopefully closed system, being conservative in one aspect may result in being dramatically optimistic in another aspect. Consequently, a more realistic called “best-estimate approach” is followed worldwide that requires the quantification of the embedded uncertainty of the codes used for safety assessment. This safety assessment approach is named Best Estimate Plus Uncertainty.

Therefore, the seek for realism is a key issue, and uncertainty quantification, as mentioned previously, is mostly based on the increased use of different stochastic methods e.g. Monte-Carlo sampling for the quantification of severe accident codes that is common praxis since many years for numerical tools applied for the analysis of events of the safety level 1 to 3 of the defence-in-depth concept. The principle of this kind of method is the sampling of a vector of input parameters characterized by a range of variations and a probability density function (pdf), then performing the corresponding calculations, and getting a vector of output of the same size as the sample. Alternately, the RAVEN-tool uses an adaptive sampling; not yet applied in connection to the severe accident codes.

An additional argument for the quantification of the code's uncertainties is the existence of cliff-edge effects in the codes, difficult to anticipate due to the high dimensionality of the problem and the time dependencies. A major drawback of best-estimate analysis plus uncertainty is the CPU cost of some integral severe accident codes needed to simulate a considerable large number of long-lasting severe accident scenarios of LWR, required to achieve an acceptable probability content and confidence. Furthermore, it has to be noted that the quality of the quantification of the uncertainty of a numerical tool (for any physical domain) also depends on the range of the uncertainty input parameters and the selected pdf that the analyst uses for the analysis. Finally yet importantly, the overall quality of the uncertainty quantification is determined by the degree of coupling (interface) of the UQ-tool and the SA-code, meaning that if it is possible to consider as uncertainty parameters not only the initial and boundary conditions but also the model parameters.

One alternative to alleviate the long-lasting CPU time of the simulation of LWR severe accident sequences using integral plant models may be the build-up of surrogate models. It may be possible when a specific phenomenon is going to be investigated e.g. MCCI but it may be very challenging to develop a surrogate model for a complete nuclear power plant considering all key-phenomena impacting the radiological source term prediction. Moreover, the surrogate models tend to shift the problem if one desires sufficient precision and representativeness.

In view of the huge and cheap available computer (HPC) in Europe and some members states, it seems very attractive to explore the use of such computer clusters to perform in an automatized manner a huge number of simulations with SA-codes including the quantification of the embedded uncertainties and sensitivity analysis based on Monte-Carlo sampling methods or alternative methods. The majority of the UQ-tools selected by the MUSA-partners belongs to this class of tools. In the following Chapters, a synthesis of these methods will be given.

2.1 Define the problem

A vast range of different modelling options can be chosen, listed hereafter with increasing level of complexity and physical selectivity: in all cases a temporal window of the accident is defined (with eventually key phases identification), corresponding roughly to a panel of physical phenomena to be taken into account as follows:

1. All the phenomena likely to occur in the period are modelled and taken into account. No assumption is made about the availability of systems, treated as uncertain parameters. Initiator is often determined. The uncertainties one might have about physical phenomena are taken into account. This option is used when a global synthetic representation of a set of various accidental situation is needed, with dynamic representation (for PSA for example).
2. Choose a given sequence with the whole phenomenology represented from the initiator time; assumptions are made on the initiator and the availability of the systems at some point (the point that ensures the chosen sequence happens), but also on the uncertainties one might have about physical phenomena;
3. Choose a given sequence with only a part of the phenomenology represented from the initiator time; this could be the case for example for a source term calculation with imposed thermal hydraulic conditions. In terms of CPU it is less expensive than (2); the assumptions are the same than (2); in that case the accuracy and representativeness of the boundary conditions through time (assessed via other means) of the computation is at stake; the underlying hypothesis is that there is insignificant effect of the chosen FOMs on the rest of the phenomenology of the accident (i.e. no feedback of source term related variable on thermal hydraulics for example);
4. Choose a physical aspect of the accident at a given period of the accident. Use roughly the same assumption types as in (2) except that the simulation starts at the onset of the target physical problem, which might not be the initiator time. In that case the accuracy of the initial state (assessed via other means) of the computation is at stake; this type of assessment is also particularly useful when working on Separate Effect Tests (SET).

At this point, the problem is specified and one has a precise idea of the phenomenon to be examined, and consequently the FOMs are known.

Several additional key issues have to be mentioned:

- a. The limits of the physical modelling; certain effects are not taken into account and might lead to errors; this has to be distinguished from epistemic uncertainty, where the modelling exists but is imperfect. When adding a new model, there is no guarantee that the uncertainty range remains the same. An example for that is the addition in a model of a FP species, which can be filtered differently than in the previous version of the model; this is the reason why it shall be considered as a bias or error rather than an uncertainty ;
- b. The faithfulness of the representation of the system; it is a compromise between precision and CPU cost. When performing UQ, it is implicitly assumed that the development of the input deck has been made and qualified to a best estimate geometric, material composition, operational conditions, etc... For example, this could be important for the representation of the core, leading to errors in vessel rupture if not precise enough and dramatic changes as cliff-edges effects occur when geometrical refinement increases. Another example is the refinement of containment description with regard to hydrogen explosion.
- c. As faithful as the representation might be, numerical errors remain and may have effects on the results of the assessment; if possible the developers of the SA-codes reduce them, but the residual part has to be assessed and compared to the uncertainty range one gets at the end of the UQ (hopefully it is negligible).

2.2 Definition of the uncertain parameters

The WP2 of MUSA is extensively dealing with this the selection of input parameters for different reactor designs with the goal of perform an uncertainty quantification of SA-codes when simulating a severe accident sequence to predict the radiological source term (Beck, et al., 2020).

2.3 Description of the uncertain parameters to be fed to the uncertainty propagation

In the framework of MUSA project, the following uncertainties types namely epistemic and aleatory will be considered in the uncertainty quantification process by the different UQ-methodologies. Hereafter, a short description of these types is given.

2.3.1 Epistemic uncertainty

This uncertainty is due to incomplete knowledge. It comes from our limited ability to model the system. This uncertainty can be reduced either by improvements in measurement techniques or by increasing our understanding of the involved phenomena. It is associated to an imprecise but fixed quantity. The epistemic uncertainties are addressed via various frameworks, e.g.

- Probabilistic: as the uncertain parameter is fixed but unknown, the probability represents some degree of belief associated to a given value of this parameter,
- Interval analysis: the values limiting an interval correspond to a certain degree of belief. In the case of possibilities, an upper and lower probability bound characterizes the belief corresponding to the degrees of possibility and necessity associated to the interval. The output is therefore two sets of distributions, corresponding to a maximum and minimum value of the probabilities.

2.3.2 Aleatory/Stochastic uncertainty

It is due to natural or random variability and is inherent to the system being studied. It can be described, but cannot be reduced; stochastic uncertainty characterizes a precisely known but variable quantity. The probabilistic framework is therefore generally used. When the knowledge of the distribution is incomplete, the theory of imprecise probabilities can be used.

Because of the coexistence of these two types of uncertainties, the use of a single probabilistic framework when taking into account the two types is semantically difficult, as probabilities do not have the same meaning for both. A nested assessment is therefore often performed (double loop). In Table 2, a summary of the type of probabilities of the MUSA UQ-tools is shown.

Table 2: Available frameworks for the different types of uncertainties

Code	Epistemic	Aleatory	Comment
SUSA	probabilities	probabilities	
SUNSET	probabilities/possibilities	probabilities	In that implementation possibilities require the checking of monotony on the sampled interval
DAKOTA	probabilities/interval	Probabilities/imprecise probabilities (upper and lower probability boxes)	
URANIE	probabilities	probabilities	
RAVEN	probabilities	probabilities	

When assessing the distributions (pdf), for both types of uncertainties, the use of expert judgment is chosen as a last resort when no other information is available. The principle of minimal specificity (which states that when no information about a variable is known, then each value has to be considered equally probable) is then used when little information is available.

When sufficient information is available, the building of a distribution is then possible based on observations. In that case, the tools generally provide methods for the estimation of their fitness to the observations or for the estimation of their parameters. Table 3 gives an overview of the main features of the statistical tools of the MUSA UQ-methods.

Table 3: Statistical tools features for input parameters pdf estimation

Code	Tools	Comment
SUSA	probabilities	
SUNSET	(χ^2 , Kolmogorov – Smirnov)	Estimation of fitness of a particular distribution
	moment method, non-parametric (moving window) method	Building of distribution
DAKOTA	maximum likelihood method	
URANIE	Dedicated module: UncertModeler (χ^2 , Kolmogorov – Smirnov)	Estimation of fitness of a particular distribution
	Estimation by maximum likelihood, moment method, non-parametric (histogram, kernel) methods	Building of distribution
RAVEN		No tool available for that part

2.4 Definition of interfaces with SA codes

In Table 4, an overview about the availability of interfaces between the UQ-tools for initial and boundary conditions as well as for model parameters is exhibited.

Table 4: Statistical tools/ SA codes interface features

Code	Initial conditions	Boundary conditions	Model parameters
SUSA	Yes	Yes	Yes
SUNSET	Yes	Yes	Yes
DAKOTA	Yes	Yes	Yes
URANIE	Yes	Yes	Yes
RAVEN	Yes	Yes	Yes

2.5 Sampling and propagation methods

All UQ-tools to be used in MUSA have the capability for pure random (Monte Carlo) and Latin hypercube sampling (LHS). The determination of the sample size rely mostly on Wilks formula for pure random sampling, allowing a certain confidence level associated to a given percentile which can be selected by the analyst. It has been empirically noted in the framework of severe accident that LHS sampling converges faster than pure random sampling. This is the case when the response is a monotonous function of the input parameters or when the response rely only on a limited set of parameters [1][2].

The usually available laws for sampling (PDF) are (common denominator between MUSA partners): Bernoulli, binomial, Poisson, beta, gamma, exponential, Gumbel, normal, lognormal, chi2, triangular, uniform, loguniform, and Weibull.

2.6 Post-processing

After the numerous simulations of the severe accident sequence with the MUSA SA-codes is performed, a huge number of data is available to be statistically post-processed with the UQ-tools. By means of scripts or other tools, the data of interest are extracted from the output or result files of the SA-codes and written in the files in the formats needed by the UQ-tools.

The following statistics indicators are usually provided by all the MUSA UQ-tools:

- Minimum, maximum values
- Mean, standard deviation,
- Cumulative density function,
- Probability density functions, and
- Quantiles.

2.7 Sensitivity Analysis

Table 5 gives a list of the available sensitivity functionalities of the MUSA UQ-tools. They generally come with their associated design of experiments (Stratified, factorial, Sobol, Morris, FAST, etc.). Some of the sensitivity measures require an important CPU-cost like global sensitivity analysis.

The use of sensitivity indexes (correlations) like Spearman require the verification of monotony, which might be difficult in case of multiple input variables.

Table 5: Statistical tools available for sensitivity functionalities

Code	indicator	Comment
SUSA	<ul style="list-style-type: none"> • Correlation indexes: Spearman, Pearson, Kendall, Blomqvist • Variance based techniques: Standard regression coefficient, coefficient of determination, Sobol, Scatter plots 	
SUNSET	<ul style="list-style-type: none"> • Correlations: Spearman, Pearson (included partial) • Variance based techniques: Standard multilinear regression coefficient, coefficient of determination • Scatter plot: no graphical interface, export to CSV instead 	Weighted regression available
DAKOTA	<ul style="list-style-type: none"> • Correlation : Spearman, Pearson • Scatter plots 	
URANIE	<ul style="list-style-type: none"> • Correlations: Pearson, Spearman, • Screening (OAT, Morris, etc.), • Variance based techniques: Sobol' indexes (FAST, RBD, Sobol/Saltelli) 	
RAVEN	<ul style="list-style-type: none"> • Multilinear regression coefficients, computed via linear regression method • Covariance • Correlations: Pearson • Variance Dependent Sensitivity • Global sensitivity analysis 	Sobol

3 Overview of applications of UQ-tools of MUSA-partners

In view of the MUSA main goal i.e. the quantification of the uncertainty of severe accident codes when predicting the radiological source term of different reactor designs and selected severe accident sequences, it is of paramount importance to summarize the experience of the MUSA-partners at the begin of the MUSA-project. In Table 6 an overview of the previous experience of the MUSA-partners in applying UQ-tools and severe accident codes is given.

As can be observed there, only the IRSN did an uncertainty quantification of ASTEC using SUNSET for a severe accident sequence where the key figure of merit is the radiological source term available at the containment for release into the atmosphere. All other UQ-studies were performed for specific SA-phenomena. It is worth to mention that another study was devoted to the source term prediction but for Sodium cooled fast reactors where the physical phenomena and containment design differs from the ones of LWRs.

Table 6 : Overview of the application of UQ-tools/DBA and SA-codes of MUSA-partners

UQ-tool	DBA/SA Simulation code	DBA-application (relative MUSA relevance)	SA-Application (high MUSA relevance)
SUSA			
GRS	ATHLET-CD / AC2	BEMUSA, Reflood (Premium Benchmark) PWR REA analysis using SUSA	Phebus FPT1 using COCOSYS-IAM and SUSA, PWR Konvoi SB-LOCA using SUSA focused on in-vessel and containment phenomena including radiological source term
LEI	RELAP5/SCDAPSIM		QUENCH-03/-06, Early In-vessel
LEI	ASTEC2.0		In-vessel, containment
LEI	COCOSYS		Phebus FPT2, Containment
LEI	COCOSYS		MISTRA Facility for SA, Atmospheric stratification, hydrogen in containment
LEI	ASTEC/CPA		Generic containment (SBLOCA)
BeIV	RELAP5/PARCS	VVER-1000 MCP-restart transient	
SUNSET			
IRSN	ASTEC2.0		PWR-900 SA radiological source term in case of LFW
LEI	ASTEC2.0		Quench-03, Early in-vessel
DAKOTA			
ENEA	MELCOR		SFR source term CSTF-AB1 tests
ENEA	MELCOR		PWR in-vessel phenomena
ENEA	TRACE	PWR LB-LOCA	
CIEMAT	SPARC-90		Suppression pool in BWR-SBO (FU1 conditions)
TBL	FRAPCON/FRAPTRAN	Integral LOCA test IFA-650.9-.10	
TBL	MELCOR		MCCI, aerosol behaviour, DCH
TBL	RELAP5	FEBA, PERICLES Reflood (Premium Benchmark)	
URANIE			
KIT	ASTEC2.2		Quench-08, early in-vessel PWR
BELV	CATHARE2 V2.5	FEBA, PERICLES	

		Reflood (Premium Benchmark)	
RAVEN			
JAEA	MELCOR2.2		Coupling under development

3.1 Potential of UQ and data assimilation tools for HPC applications

The Table 7 sums up the potential usability of the UQ-tools within a HPC-framework. Detailed information is available at Appendix 3.

Table 7: HPC availability for UQ and data assimilation tools

Code	HPC usability	Comment
SUSA	unknown	Windows
SUNSET	yes	LINUX, Windows
DAKOTA	yes	Linux platform, MPI has to be installed
URANIE	yes	HPC, Linux-clusters MPI, SLURM, SGE, LSF installed
RAVEN	yes	Use of PSB queuing system
MOCABA	Potentially easy to implement	
NEMM	Not applicable	

4 Conclusions

Based on the review of the key-features, functionalities, models of the MUSA UQ-tools (Appendix 1), the experience of the involved partners described in Appendix 2 as well as the potential use of the UQ-tools and SA-codes in an HPC-environment (Appendix 3), the following conclusions can be drawn:

- Uncertainty quantification tools (SUSA, SUNSET, URANIE, DAKOTA, RAVEN)
 - Almost all UQ-tools considered in MUSA have similar capabilities and they are developed for quite different computer architectures (Linux, Windows)
 - SUSA is based on Excel with an interface to ATHLET and AC2
 - DAKOTA is an open source platform that can be used within SNAP for different codes e.g. TRACE, MELCOR in a Linux/Windows environment or outside SNAP using dedicated scripts under Linux or Windows.
 - URANIE is an open source statistical platform running under Windows and Linux. A Python-based interface has been developed for the ASTEC code, while more efforts are needed for other severe accident codes, e.g. MELCOR.
 - RAVEN is an open source general purposed tool with an interface for MELCOR and it can be run under Windows and Linux
 - SUNSET is a statistical software strongly linked to ASTEC able to perform uncertainty and sensitivity analysis
 - Previous application relevant for MUSA i.e. for severe accidents and radiological source term prediction
 - SUNSET was already applied to quantify the uncertainty and sensitivity of ASTEC in predicting the radiological source term for a French PWR reactor
 - URANIE was already applied to quantify the uncertainty and sensitivity of ASTEC for the prediction of the hydrogen source term during the QUENCH-06 and -08 tests
 - DAKOTA was already applied to quantify the uncertainty and sensitivity of MELCOR predictions for the hydrogen production in a PWR core, for the source term CSTF-AB1 test, and the in-pool fission product retention in a BWR-SBO
 - SUSA was already applied to quantify the uncertainty and sensitivity of ASTEC and COCOSYS for the analysis of the PHEBUS FPT1 and FPT2 experiments, respectively, and of RELAP/SCDAPSIM for the QUENCH-03 and -06 tests

- Experience applying UQ-tools to SA-codes covering the full SA-sequence (in-vessel, ex-vessel, containment) to predict the radiological source term is limited
 - IRSN performed the uncertainty quantification for ASTEC using SUNSET tool for a LOF-sequence in PWR
 - GRS experience in performing U&S-analysis for a severe accident SBLOCA using SUSANA and ATHLET-CD/COCOSYS focus on both in-vessel and containment issues including source term.
- Experience of MUSA-partners in HPC-applications of UQ/SA-codes for the uncertainty quantification of SA-sequences in NPPs ranging from the initiation up to the radiological source term
 - IRSN explored the use of HPC for the uncertainty quantification of ASTEC using SUNSET tool
 - KIT is exploring the use of a large HPC cluster (ForLHR II) at the Steinbuch Center of Computing (SCC) to perform the uncertainty quantification of ASTEC/URANIE for the prediction of the radiological source term for a German PWR
- Data assimilation tools (MOCABA, NEMM)
 - MOCABA application to severe accidents will be done for the first time in connection with ASTEC in MUSA.
 - NEMM is a new tool under development for severe accident applications. Hence, no experience exist on the field of severe accidents.

5 Bibliography

Beck, S., Sonnenkalb, M., Herranz, L. E. & Coindreau, O., 2020. *Identification of uncertain parameters for MUSA*, EU: D2.1.

Appendix 1: Uncertainty quantification methods (Task 1 and 3)

K. Chevalier (IRSN), V. Sanchez (KIT)

Version 06 – 08/04/2021

Content

Content	3
List of figures	5
1 SUSAS (GRS).....	6
1.1 Description of the method	6
1.2 Description of main features	7
1.3 Initial conditions	8
1.4 Boundary conditions	8
1.5 Model parameters	8
1.6 Propagation of uncertainties	8
1.6.1 Quantification of input uncertainties	8
1.6.2 Sample generation	10
1.6.3 Computer code runs	10
1.6.4 Uncertainty analysis	11
1.6.5 Sensitivity analysis	13
1.6.6 Scatter & Cobweb Plots	15
1.7 Pros and Cons	17
2 SUNSET (IRSN)	18
2.1 Description of the method	18
2.2 Description of main features	20
2.2.1 Uncertainty analysis	20
2.2.1.1 STEP 1: sample generation	20
2.2.1.2 Random sampling	20
2.2.1.3 Interval sampling	20
2.2.1.4 STEP 4: analysis	20
2.2.2 Sensitivity analysis	20
2.3 Initial conditions	21
2.4 Boundary conditions	21
2.5 Model parameters	21
2.6 Propagation of uncertainties	21
2.7 Pros and Cons	21
3 DAKOTA (ENEA, TRACTEBEL, CIEMAT).....	22
3.1 A BRIEF INTRODUCTION TO DAKOTA	22
3.1.1 Description of main features	22
3.1.1.1 Aleatory methods	22
3.1.1.2 Epistemic methods	23
3.1.2 DAKOTA Output	23
3.2 CIEMAT METHODOLOGY APPLIED TO DAKOTA	24
3.2.1 Description of the method	24
3.2.2 Methodology Basis	24
3.2.3 Best-estimate modelling	24
3.2.3.1 Description	24
3.2.3.2 Decision	24
3.2.3.3 Modeling	25
3.2.4 Uncertainty Quantification	25
3.2.4.1 Identification	25
3.2.4.2 Uncertain Input Parameters Identification	25
3.2.4.3 Parameters Uncertainty Characterization	26
3.2.5 Quantification	26
3.2.6 Interpretation	26
3.3 DAKOTA (TRACTEBEL)	27
3.3.1 Description	27
3.4 DAKOTA toolkit in SNAP (ENEA).....	27
3.4.1 DAKOTA/SNAP Description of main features	28

•	STEP1: “Edit Uncertainty Configuration/DAKOTA Properties”	29
•	STEP 2: “Edit Uncertainty Configuration View/Variables”	29
•	STEP3: “Edit Uncertainty Configuration View/Distribution”	29
•	STEP 4: “Edit Uncertainty Configuration View/Report”	29
3.5	Initial conditions	34
3.6	Boundary conditions	34
3.7	Model parameters	34
3.8	Propagation of uncertainties	34
3.9	Pros and Cons	34
3.9.1	probabilistic method to propagate the input uncertainty	34
3.9.2	Analysis methods	35
3.9.2.1	Pure Monte Carlo	35
3.9.2.2	Wilks approach	35
3.9.2.3	Interval analysis	35
3.9.2.4	Evidence theory	35
3.9.3	DAKOTA limitations	35
3.9.4	User oriented features or functionalities, user friendliness	35
4	URANIE (KIT, BELV)	37
4.1	Description of the method	37
4.2	Description of main features	38
4.3	Initial conditions	40
4.4	Boundary conditions	40
4.5	Model parameters	41
4.6	Propagation of uncertainties	41
4.7	Pros and Cons	41
5	RAVEN (UNIROM1, JAEA)	42
5.1	Description of the method	42
5.2	Description of main features	44
5.2.1	Uncertainty analysis	44
5.2.1.1	Distributions	44
5.2.1.2	Sampling strategies	45
5.2.1.3	Statistical Post-processing	46
5.2.2	Sensitivity analysis	46
5.2.3	Dynamic PRA	46
5.3	Initial conditions	47
5.4	Boundary conditions	47
5.5	Model parameters	47
5.6	Propagation of uncertainties	47
5.7	Pros and Cons	47
6	References	47

List of figures

Figure 1: SUSAs Main window	7
Figure 2: SUSAs Documentation of uncertain input parameters	8
Figure 3: SUSAs Quantification of uncertainties in terms of probability distributions	9
Figure 4: SUSAs Quantification of dependence information	10
Figure 5: SUSAs Uncertainty analysis option	11
Figure 6: SUSAs 100 curves of a time/index-dependent result	12
Figure 7: SUSAs Two-sided (95 %; 95 %) tolerance limits over time	13
Figure 8: SUSAs Sensitivity analysis options	14
Figure 9: SUSAs Pearson's ordinary correlation coefficient as sensitivity measure	14
Figure 10: SUSAs Spearman's rank correlation coefficient as sensitivity measure over time	15
Figure 11: SUSAs Scatter plots	16
Figure 12: SUSAs Cobweb plots	16
Figure 13: General presentation of an ASTEC/SUNSET sequence of action for an uncertainty study	18
Figure 14: General sketch of uncertainty analysis using SUNSET and ASTEC	19
Figure 15: LHS strata subdivision for a normal-distributed parameter	23
Figure 16: LHS pairing example where X1 and X2 are the sampled variables and the dots are the samples sites [21], [24], [20], [19]	23
Figure 17: The DAKOTA uncertainty/sensitivity analysis process [8].	27
Figure 18: DAKOTA uncertainty analysis workflow for MELCOR code in a SNAP environment/architecture	28
Figure 19: MELCOR/DAKOTA uncertainty stream done in SNAP	28
Figure 20: "Edit Uncertainty Configuration/DAKOTA Properties" SNAP Tab	30
Figure 21: "Edit Uncertainty Configuration/DAKOTA Properties" SNAP Tab, insufficient number of sampling warning.	30
Figure 22: "Edit Uncertainty Configuration/Variables" SNAP Tab	31
Figure 23: Example of input uncertain parameter distribution representation in the SNAP Tab	31
Figure 24: "Edit Uncertainty Configuration/Report" SNAP Tab	31
Figure 25: Peak cladding temperature Pearson's simple response correlation coefficient (double-ended LBLOCA simulation with TRACE code coupled with DAKOTA for a generic PWR-900) [45]	33
Figure 26: Peak cladding temperature Spearman's simple response correlation coefficient (double-ended LBLOCA simulation with TRACE code coupled with DAKOTA for a generic PWR-900) [45]	33
Figure 27: The URANIE Platform: Main Modules and their interdependencies (green) and the external dependencies (light purple boxes) [55]	38
Figure 28: The URANIE Platform: General Steps for Uncertainty and Sensitivity Analysis [55]	39
Figure 29: The URANIE Platform: General Steps for Uncertainty and Sensitivity Analysis [55]	40
Figure 30: Schematic representation of the RAVEN software [58]	43
Figure 31: MELCOR-RAVEN coupling interface	44

1 SUSANA (GRS)

In deterministic safety analyses (DSA) for nuclear power plants (NPPs), it has become common practice to apply best estimate computer codes for calculating postulated accidents in a realistic and not in a conservative way. If a best-estimate code is used in combination with realistic input data, it is generally required (IAEA, 2009) that relevant epistemic (lack of knowledge) uncertainties which may affect the computational result (e.g., the peak cladding temperature in a loss of coolant accident) shall be considered and that their influence on the result shall be quantified [1]. There are several sources of epistemic uncertainty which may influence a computational result. Important sources are the model formulations implemented in a computer code. They are mostly based on a scattering of measurements or may be rather simplified so that the level of predictive accuracy of a model – even a validated model – may not be precisely known.

Further uncertainty sources are numerical solution algorithms, which commonly include approximations and simplifications somehow affecting the result, the initial and boundary conditions of the application case, plant specific data and measurement errors [1].

Intuitively the most appropriate method to account for the uncertainty sources of a computational result and to get a quantification of their influence is the Monte Carlo (MC) method. It considers a range of values instead just one value for each uncertain input parameter of the computer code. Each value selected for a parameter is combined with a value selected for each other uncertain parameter and supplied as input to corresponding computer code runs. Based on the sample of values finally provided for a computational result, a quantification of the uncertainty of the result is obtained by applying statistical methods [1].

An extra sensitivity analyses or, more precisely, an uncertainty importance analysis is supplemented to the uncertainty analysis to identify those uncertain input parameters, which mostly contribute to the uncertainty of a computational result (Hofer 1999). It provides information on where to improve the state of knowledge in order to reduce the (epistemic) uncertainty of the computational result most effectively [1].

The development of SUSANA started mid-1980s. Since then, SUSANA has been constantly improved mainly according to the needs in the field of deterministic (DSA) and probabilistic (PSA) safety analyses. The approach implemented in SUSANA for considering uncertainties is acknowledged worldwide and applied in licensing processes in France, USA, Korea and Lithuania. In the project 'Best Estimate Methods – Uncertainty and Sensitivity Evaluation (BEMUSE)' of OECD NEA (2003 -2011), where different methods for uncertainty and sensitivity analyses were applied, most of the participating organizations applied the approach developed at GRS and implemented in SUSANA.

1.1 Description of the method

SUSANA is developed to facilitate the performance of uncertainty and sensitivity analyses of computational results based on the MC method, [2]. SUSANA is an important part of the GRS code system for safety analyses of nuclear power plants (NPPs). It provides support to quantify input uncertainties in terms of probability distributions and to specify associations between input uncertainties in terms of correlations or other measures and functions. For Monte Carlo simulation, the simple random and the Latin Hypercube sampling procedures are available. To prepare and launch computer code runs, a selection of code interfaces is implemented. Rather comfortable are the interfaces to selected codes applied in the field of safety analyses of NPPs. However, in principal, SUSANA can be coupled to any code. Many options exist for quantifying the uncertainty of a computational result and for performing a sensitivity analysis. SUSANA combines well established methods from mathematical statistics with a comfortable graphical user interface (GUI). The GUI guides through the main analysis steps, re-requests input data where necessary, checks for input errors, performs data transfers and performs all other actions up to the final representation of results.

1.2 Description of main features

The GUI of SUSAs is written in Visual Basic .NET (VB .NET). The main SUSAs window consists of a bar of menus representing the main analysis steps. Nine different menus are available, Figure 1. The first menu to select is the Project menu where a new project must be specified, or an existing project must be selected. Selection of the other men-us depends on the analysis status already achieved in the course of a project. Selection of a menu usually starts on the left and goes step-by-step further to the right.

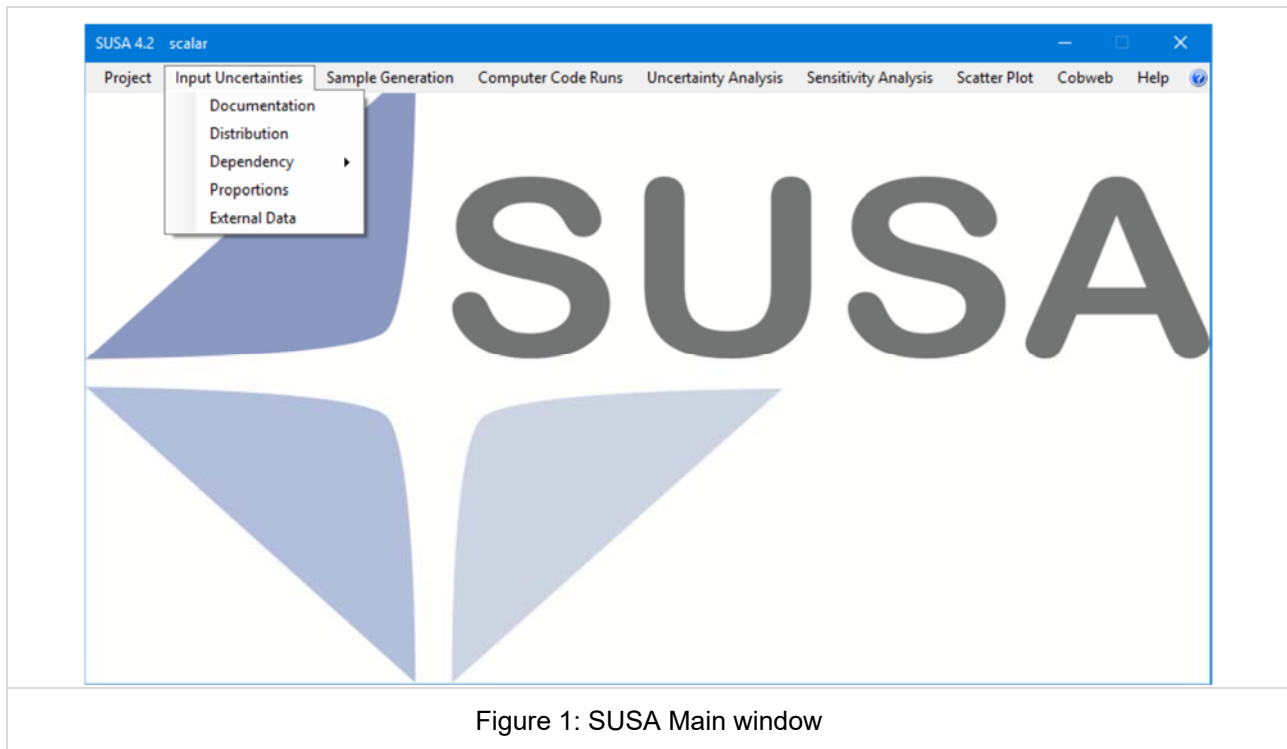


Figure 1: SUSAs Main window

The menu 'Input Uncertainties' must be selected to enter the uncertain input parameters of a project and to quantify the corresponding uncertainties probabilistically. In the menu 'Sample Generation', a sample of different sets of parameter values can be generated. The menu 'Computer Code Runs' is intended for launching computer code runs based on the sampled sets of parameter values and for preparing the computational results in the format required in the subsequent analysis steps. The menu 'Uncertainty Analysis' includes options for quantifying the uncertainty of a computational result. Sensitivity indices which help to identify the main uncertainty sources of a computational result can be found within the menu 'Sensitivity Analysis'. The menus 'Scatter Plot' and 'Cobweb' provide additional graphical output supporting the uncertainty and sensitivity analysis. The Help menu includes the user's guide and a tutorial for SUSAs. A context related online help function is implemented as well. Each menu of SUSAs consists of several items or submenus for specific tasks to be per-formed within the analysis step represented by the menu. For instance, the menu 'Input

Uncertainties' includes the five items Documentation, Distribution, Dependency, Pro-portions and External Data, Figure 1. Selection of the Documentation item is necessary in order to specify and document the uncertain parameters of a project. The Distribution item should be chosen to quantify the uncertainties of the documented parameters in terms of probability distributions. Selection of the Dependency item is important, if dependencies between uncertain parameters are to be quantified. The item 'Proportions' offers the possibility to categorize selected uncertain parameters as proportions of the same whole which have to sum up to 1. Selection of the item 'External Data' al-lows for assigning values provided by external sources to uncertain parameters. If an item of a menu or submenu is selected, SUSAs opens corresponding dialog windows requiring the input data of the respective analysis step. Errors in the input data are immediately communicated to the user who must revise the input in order to continue with the analysis step. The calculations of SUSAs are performed by Fortran program modules automatically loaded when needed during an application. For graphics generation, SUSAs applies the free Java plotting tool AptPlot, which offers GUI support for a subsequent revision of plot defaults. SUSAs is available for 32-bit and 64-bit computer systems.

1.3 Initial conditions

In principal, SUSAs applies to any type of uncertain input parameters. Restrictions are described in section 3.2.

1.4 Boundary conditions

SUSA can consider boundary conditions in the analysis.

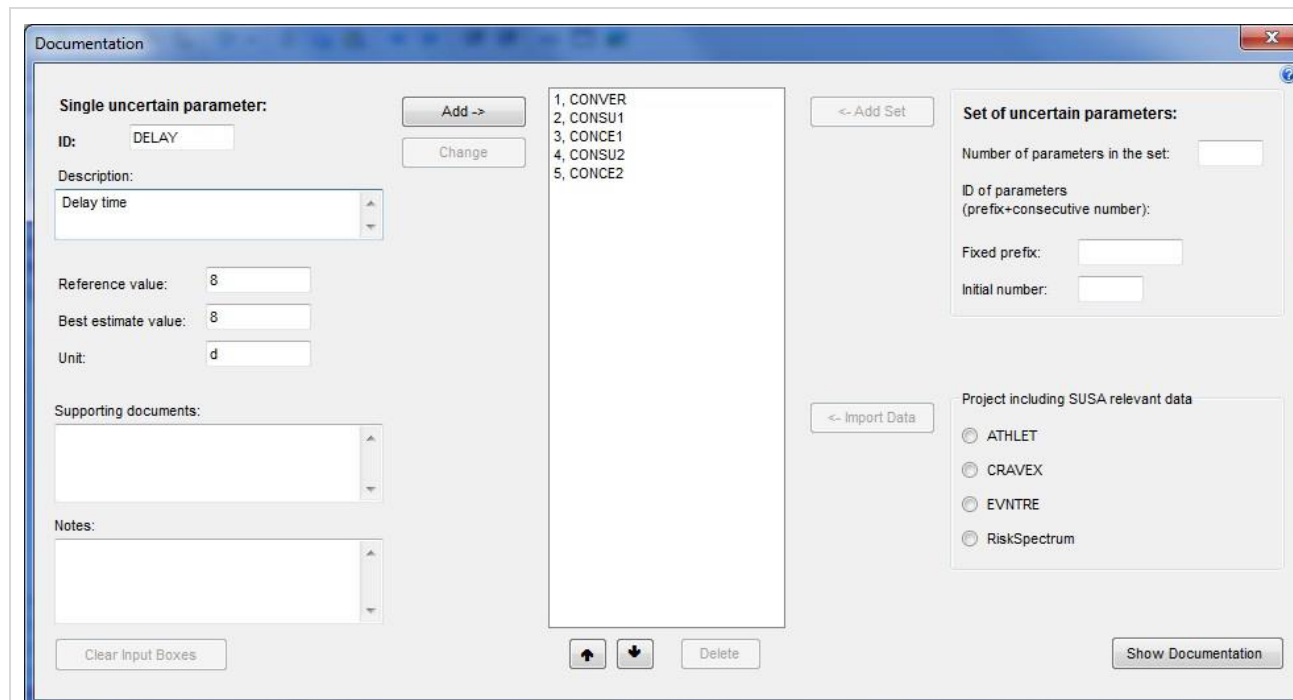
1.5 Model parameters

Also model parameters can be consider as “input uncertain parameters” in SUSA.

1.6 Propagation of uncertainties

1.6.1 Quantification of input uncertainties

Before input uncertainties can be quantified within SUSA, it is necessary to document and specify the uncertain input parameters of the computer code application, Figure 2. If this step is completed, the uncertainties of the parameters may be quantified in terms of probability distributions and/or appropriate association measures and or functions. There is also the possibility to assign a set of potential values to an uncertain parameter.



The screenshot shows the 'Documentation' window in SUSA. It is divided into several sections:

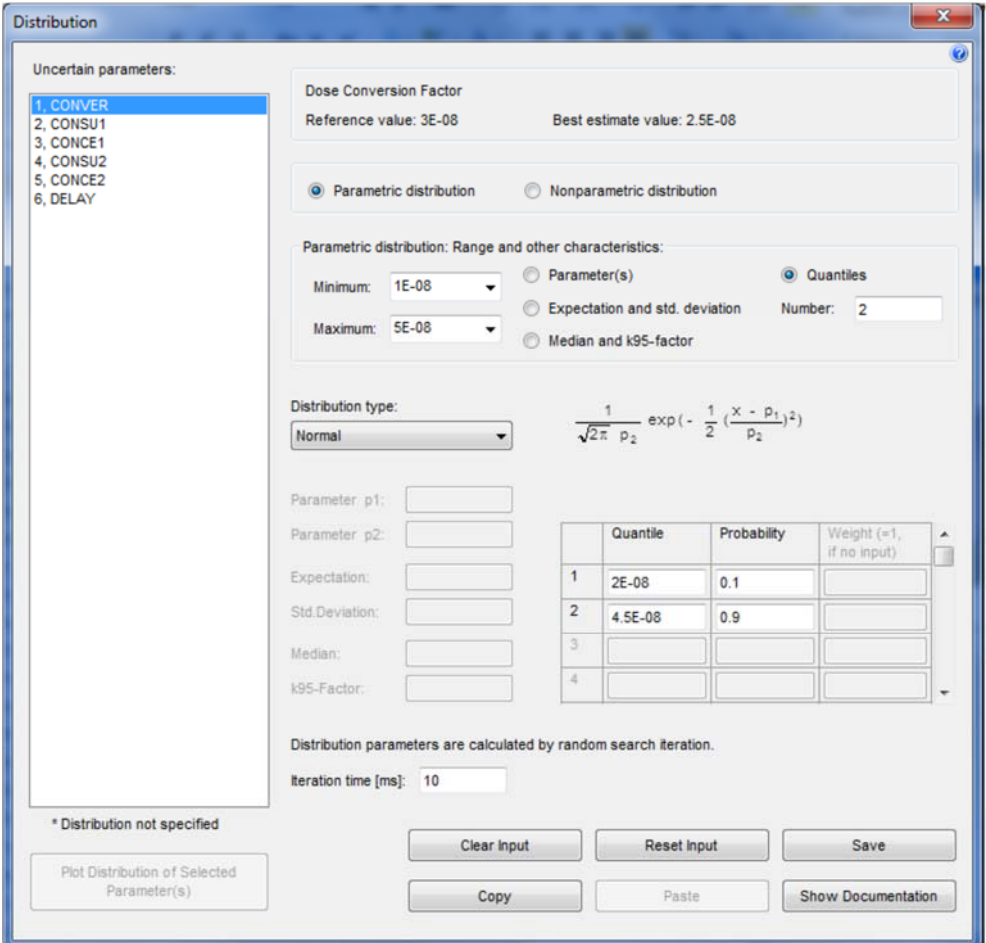
- Single uncertain parameter:**
 - ID:** DELAY
 - Description:** Delay time
 - Reference value:** 8
 - Best estimate value:** 8
 - Unit:** d
 - Supporting documents:** (empty text area)
 - Notes:** (empty text area)
- Buttons:** 'Add ->' and 'Change' are next to the single parameter section.
- Parameter List:** A central list box contains:
 - 1, CONVER
 - 2, CONSU1
 - 3, CONCE1
 - 4, CONSU2
 - 5, CONCE2
- Buttons:** '<- Add Set' is above the list, and '<- Import Data' is below it.
- Set of uncertain parameters:**
 - Number of parameters in the set:** (empty input field)
 - ID of parameters (prefix+consecutive number):** (empty input field)
 - Fixed prefix:** (empty input field)
 - Initial number:** (empty input field)
- Project including SUSA relevant data:**
 - ☐ ATHLET
 - ☐ CRAVEX
 - ☐ EVNTRE
 - ☐ RiskSpectrum
- Buttons:** 'Clear Input Boxes' is at the bottom left, and 'Show Documentation' is at the bottom right.

Figure 2: SUSA Documentation of uncertain input parameters

Primarily, SUSA expects the uncertainty of a parameter to be quantified as a probability distribution Figure 3. To this purpose, a wide range of distribution types is implemented. If the user has no idea which distribution to specify, SUSA offers a selection of distributions, which might be appropriate, dependent on what is known on the range and on characteristics such as quantiles, expectation, std. deviation, median and k95-factor. If the parameters of a distribution are not known, SUSA calculates them from what is known. This is done either

analytically or by applying a random search algorithm. Distributions which normally have an infinite minimum and/or maximum are truncated at the values indicated as minimum and maximum. The distribution assigned to an uncertain parameter can be plotted separately or compared with other distributions in a single diagram.

Dependencies between uncertain parameters can be specified in terms of association measures, conditional distributions, mathematical functions (formulae) and inequalities. Furthermore, full dependency can be specified in case the potential value of a parameter is completely determined by the value assigned to another parameter, Figure 4. Most of the dependence relationships specified in SUSANA can be visualized in the form of scatter plots.



Distribution

Uncertain parameters:

- 1, CONVER
- 2, CONSU1
- 3, CONCE1
- 4, CONSU2
- 5, CONCE2
- 6, DELAY

Dose Conversion Factor

Reference value: 3E-08 Best estimate value: 2.5E-08

☒ Parametric distribution ☐ Nonparametric distribution

Parametric distribution: Range and other characteristics:

Minimum: 1E-08 ☐ Parameter(s) ☒ Quantiles

Maximum: 5E-08 ☐ Expectation and std. deviation Number: 2

☐ Median and k95-factor

Distribution type: **Normal**

$$\frac{1}{\sqrt{2\pi} p_2} \exp\left(-\frac{1}{2} \left(\frac{x - p_1}{p_2}\right)^2\right)$$

Parameter p1:

Parameter p2:

Expectation:

Std.Deviation:

Median:

k95-Factor:

	Quantile	Probability	Weight (=1, if no input)
1	2E-08	0.1	
2	4.5E-08	0.9	
3			
4			

Distribution parameters are calculated by random search iteration.

Iteration time [ms]: 10

* Distribution not specified

Plot Distribution of Selected Parameter(s)

Clear Input Reset Input Save

Copy Paste Show Documentation

Figure 3: SUSANA Quantification of uncertainties in terms of probability distributions

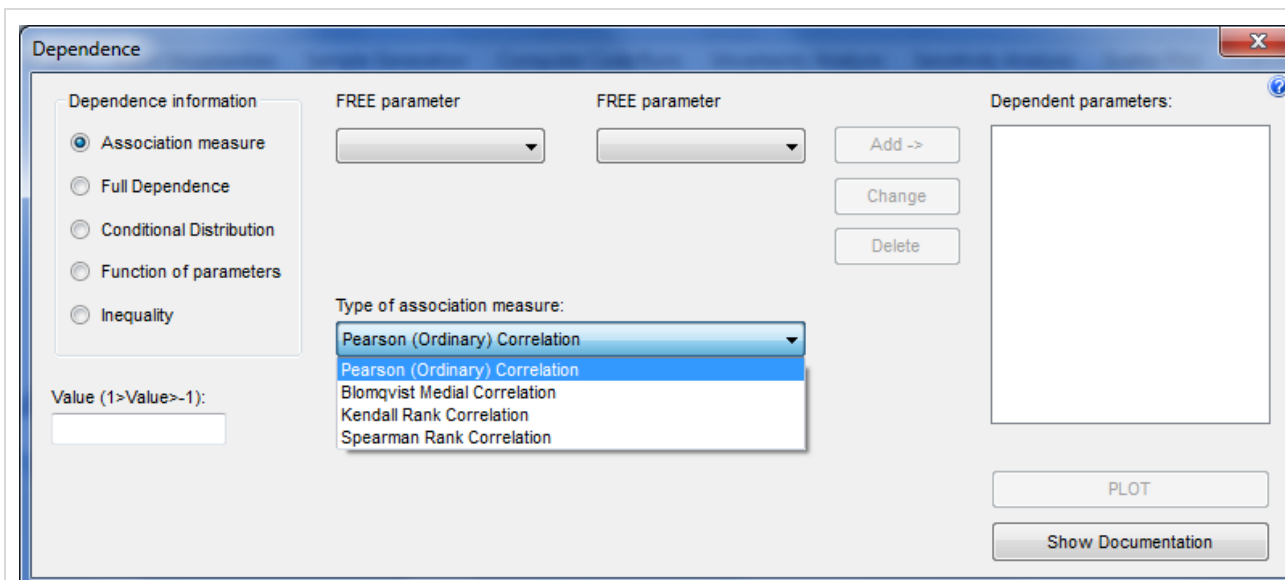


Figure 4: SUSA Quantification of dependence information

Another option available in SUSA for specifying input uncertainties is the characterization of uncertain parameters as proportions of the same whole, which sum up to one. This option is useful to handle the uncertain branching probabilities of an event tree model in a PSA. All uncertain parameters, probability distributions and dependence structures entered within SUSA are displayed in clear tables which can be printed or copied into papers or reports. More details can be found in [2].

1.6.2 Sample generation

Two procedures are currently implemented in SUSA to sample the values of uncertain parameters, namely the simple random sampling (SRS) and the Latin Hypercube sampling (LHS) procedure [3] [4]. The SRS procedure provides values randomly sampled from a multivariate probability distribution defined by the distributions and dependencies specified as input. The LHS procedure provides values covering the range of each uncertain parameter evenly in probability. To this purpose, the range of each parameter is divided into equiprobable intervals and, then, one value is selected from each interval. This value is either the median or a randomly selected value of the interval. The values selected for each parameter are finally per-muted in order to comply with specified correlations between parameters.

The random values to be generated by SUSA can be controlled by the initial seed value and the selected (pseudo) random number generator.

From the sample values finally generated, SUSA can calculate the sample-related correlation coefficients between the uncertain parameters. This information is useful to detect unintentional (spurious) correlations due to numerical effects which may affect the results of the uncertainty and sensitivity analysis.

The results of the sample generation including specified inputs and realized sample-related correlations are documented in a text file.

1.6.3 Computer code runs

SUSA can automatically start a computer code run for each available set of parameter values. If the computer code is run based on an input file, SUSA can automatically generate the input files corresponding to the different sets of parameter values and launch the corresponding runs. The computational results to be analysed can be selected via a code-specific key file or the address of the results in the corresponding code output file. SUSA automatically transfers the selected code results from all runs to a file adequately formatted so that the results are accessible in the subsequent analysis steps.

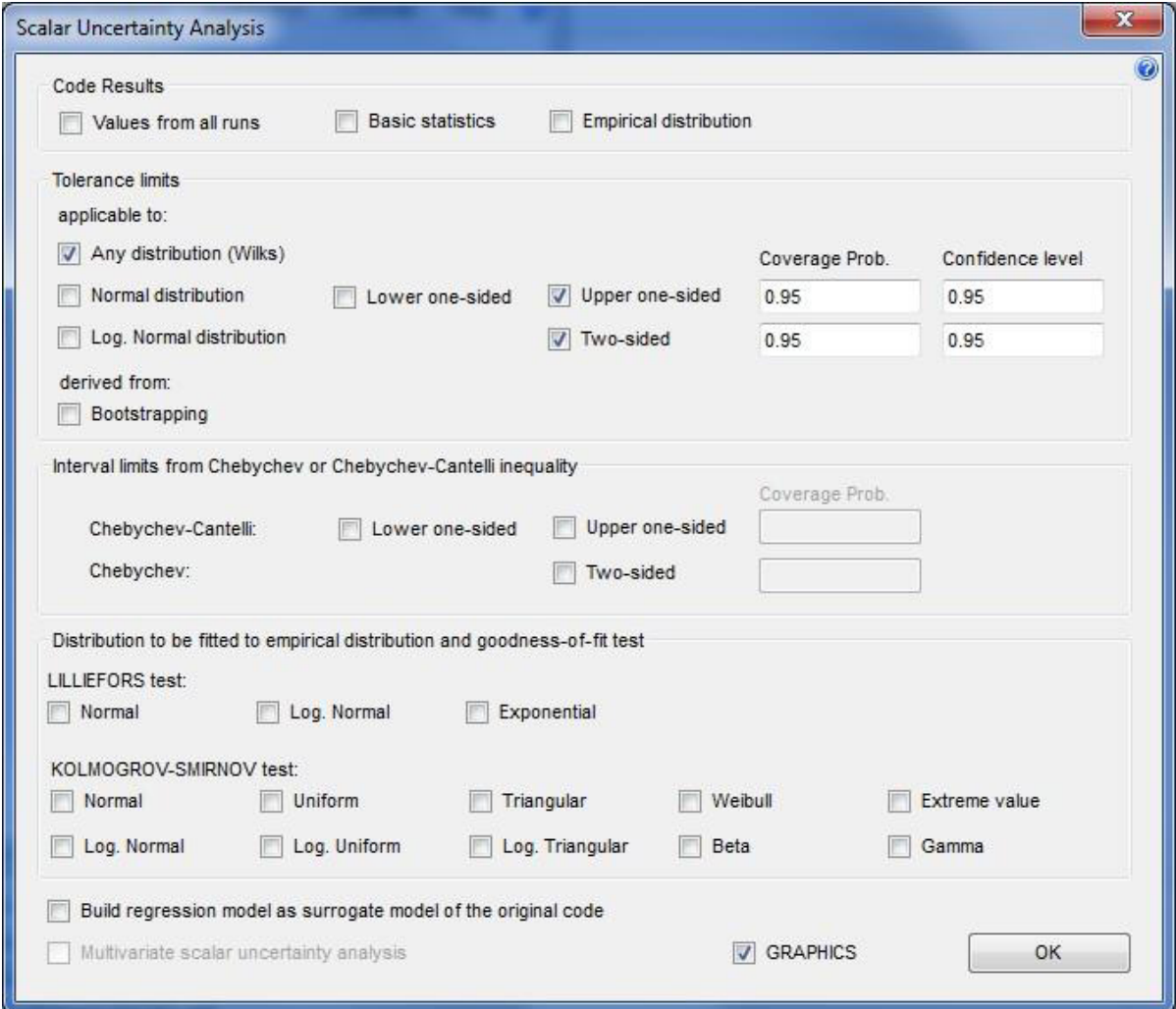
A special feature of SUSA is that it can automatically prepare a Fortran code template already including the code instructions for considering the uncertain parameters and the corresponding sample values. This template can be extended by a Fortran code for the actual model (e.g. a sub-model of a complex code, Figure

5. For compiling the whole Fortran code, SUSAs loads the free GNU Fortran Compiler which is automatically in-stalled with SUSAs.

In principal, any computer code can be coupled with SUSAs. Comfortable interfaces are implemented for codes frequently used for DSA and PSA.

1.6.4 Uncertainty analysis

SUSAs provides various options to quantify the uncertainty of a computational result Figure 6. The uncertainty analysis can be performed for scalar as well as time/index-dependent computational results. A scalar result is just a single value per computer code run, whereas a time/index-dependent result is a series of values over time, space, etc.



Scalar Uncertainty Analysis

Code Results

☐ Values from all runs ☐ Basic statistics ☐ Empirical distribution

Tolerance limits

applicable to:

	Coverage Prob.	Confidence level
<input checked="" type="checkbox"/> Any distribution (Wilks)	0.95	0.95
<input type="checkbox"/> Normal distribution		
<input type="checkbox"/> Log. Normal distribution		

derived from:

☐ Bootstrapping

Interval limits from Chebychev or Chebychev-Cantelli inequality

	Coverage Prob.
Chebychev-Cantelli: <input type="checkbox"/> Lower one-sided <input type="checkbox"/> Upper one-sided	
Chebychev: <input type="checkbox"/> Two-sided	

Distribution to be fitted to empirical distribution and goodness-of-fit test

LILLIEFORS test:

☐ Normal ☐ Log. Normal ☐ Exponential

KOLMOGOROV-SMIRNOV test:

☐ Normal ☐ Uniform ☐ Triangular ☐ Weibull ☐ Extreme value
☐ Log. Normal ☐ Log. Uniform ☐ Log. Triangular ☐ Beta ☐ Gamma

☐ Build regression model as surrogate model of the original code

☐ Multivariate scalar uncertainty analysis

☒ GRAPHICS **OK**

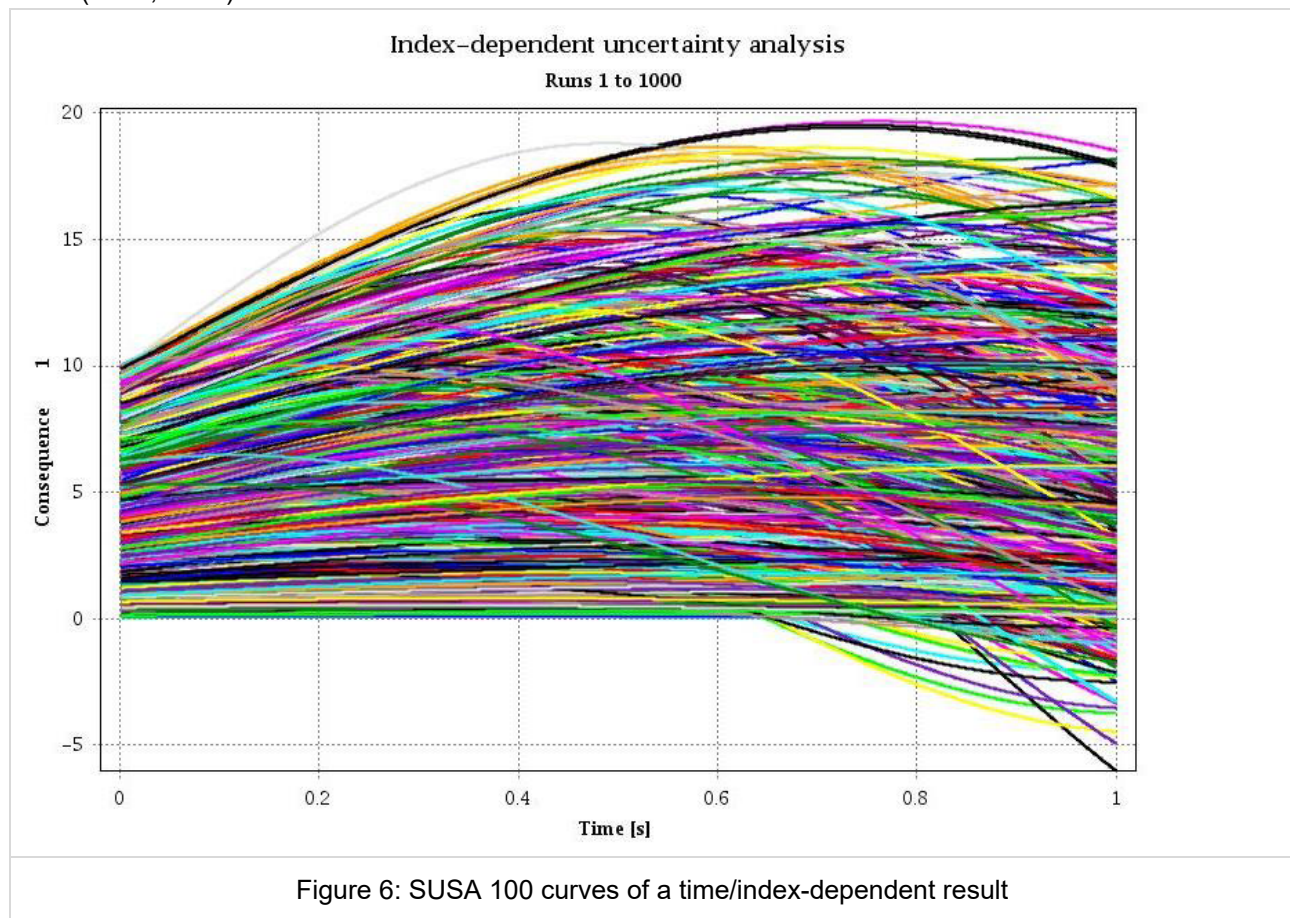
Figure 5: SUSAs Uncertainty analysis option

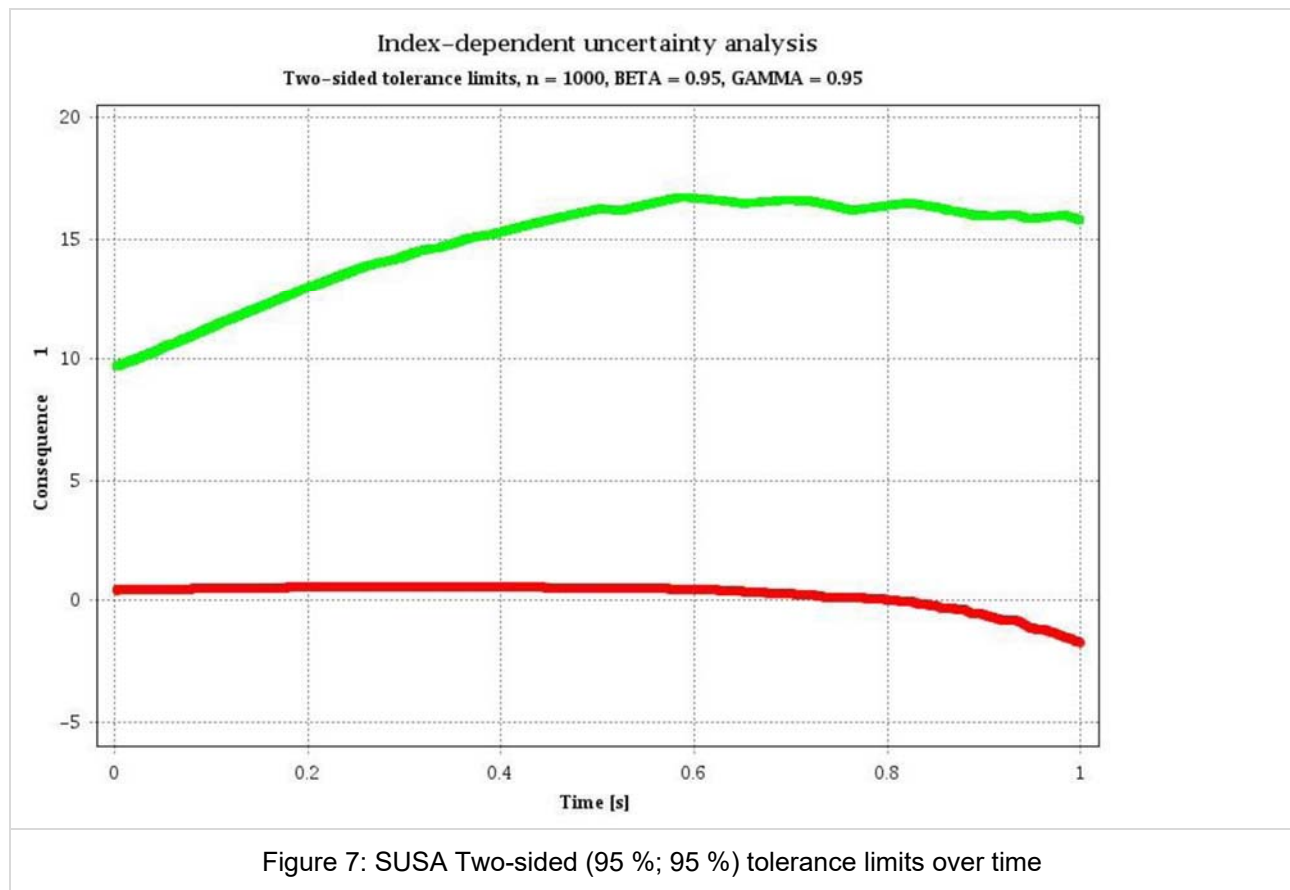
If the uncertainty of a computational result is to be quantified in terms of quantiles or intervals including a proportion of values, SUSAs can provide empirical quantiles as well as Wilks' non-parametrical tolerance limits, [5] [6]. These ($\beta \cdot 100\%$; $\Gamma \cdot 100\%$) tolerance limits are often applied in the frame of a DSA using $\beta = 0.95$ and $\Gamma = 0.95$, [7]. The calculation of Wilks' tolerance limits is independent of the number of uncertain parameters. It just requires a minimum number of runs to be performed. For instance, at least 59 runs must be performed to get a one-sided (95 %; 95 %) tolerance limit.

If the uncertainty of a computational result is to be quantified in terms of a probability distribution, SUSAs helps to find an appropriate distribution. It can perform the Lilliefors-or Kolmogorov-Smirnoff test which informs on the goodness-of-fit of a selected para-metric distribution to the (empirical) distribution of a code result [8].

SUSA can even build a regression model which is linear in the uncertain parameters and which may serve as a so-called response surface. Such a response surface may be of interest, if a quite large set of values for a computer code result is to be per-formed and just a single code run is found to be rather time consuming. SUSA can per-form Monte Carlo simulation based on the regression model and compare the (empirical) distribution of the result with the distribution of the result of the original model. If the regression model provides acceptable results, it can be used instead of the original model in order to provide a large data basis for quantifying the uncertainty of the computational result.

Exemplary results of an uncertainty analysis of a time/index-dependent result are shown in Figure 6 and Figure 7 shows the curves of a time-dependent result from 100 computer code runs. It shows the corresponding two-sided (95 %; 95 %) tolerance limits.





1.6.5 Sensitivity analysis

The sensitivity analysis with SUSA is performed with the same sample data as already generated for the uncertainty analysis. Like the uncertainty analysis, it can be performed for scalar as well as time/index-dependent computational results.

The following types of correlation-based sensitivity indices are implemented, Figure 8 and Figure 9:

- Pearson's ordinary correlation
- Spearman's rank correlation
- Blomqvist's medial correlation
- Kendall's rank correlation

If the sensitivity indices shall be applied to individual parameters, SUSA calculates the ordinary and partial correlation coefficient, the standardized regression coefficient and the coefficient of determination (R^2) for each correlation type, [9] [10].

If the sensitivity indices shall be applied to parameter groups, SUSA calculates the multiple correlation coefficient for each correlation type.

Besides correlation-based sensitivity indices, SUSA can calculate the following variance-based sensitivity indices for individual parameters:

- Correlation Ratio from raw and rank transformed data [11] [12] [13]
- Sobol's sensitivity index [14] [15]

For scalar code results (output variables), SUSA can additionally provide association measures from 2x2 contingency tables [16] or regression coefficients derived from a stepwise (rank) regression.

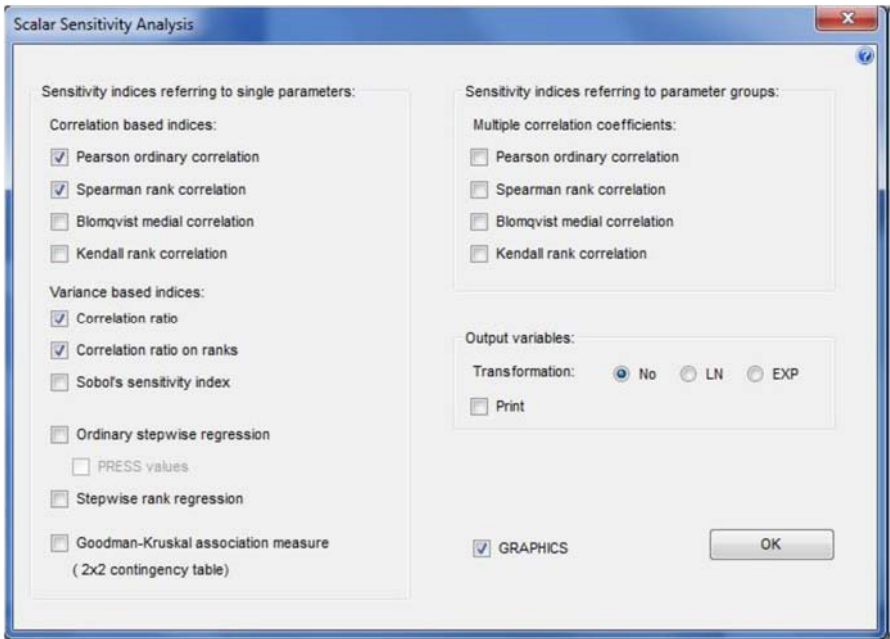


Figure 8: SUSA Sensitivity analysis options

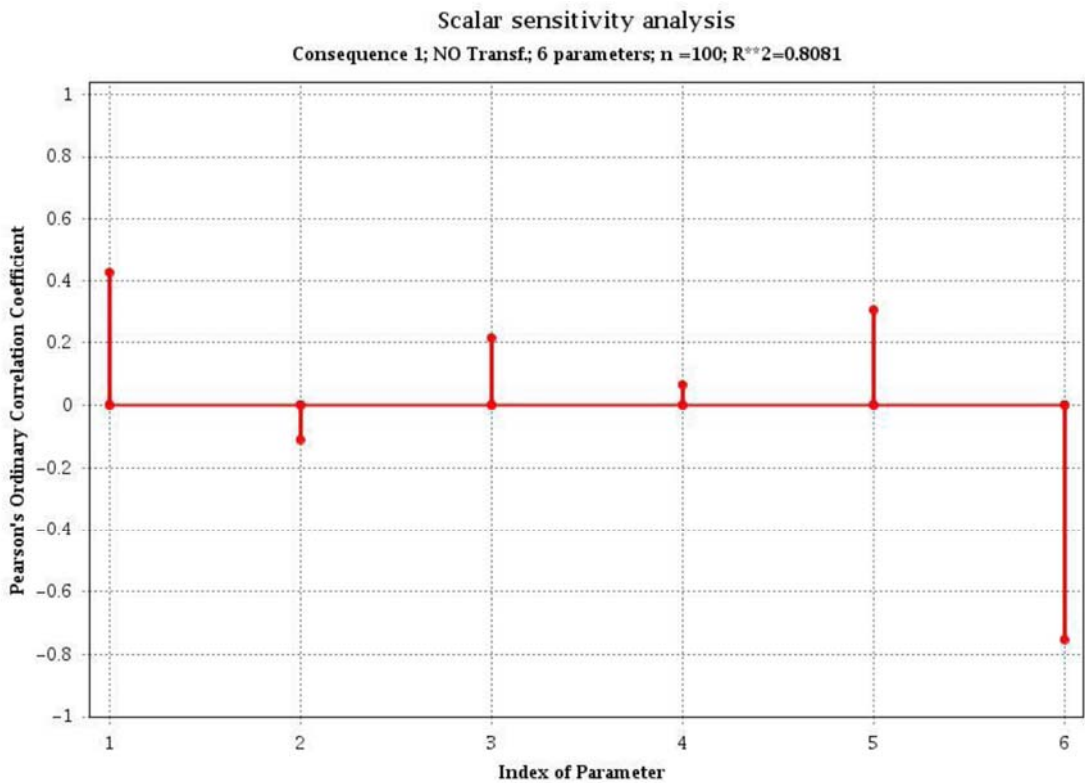
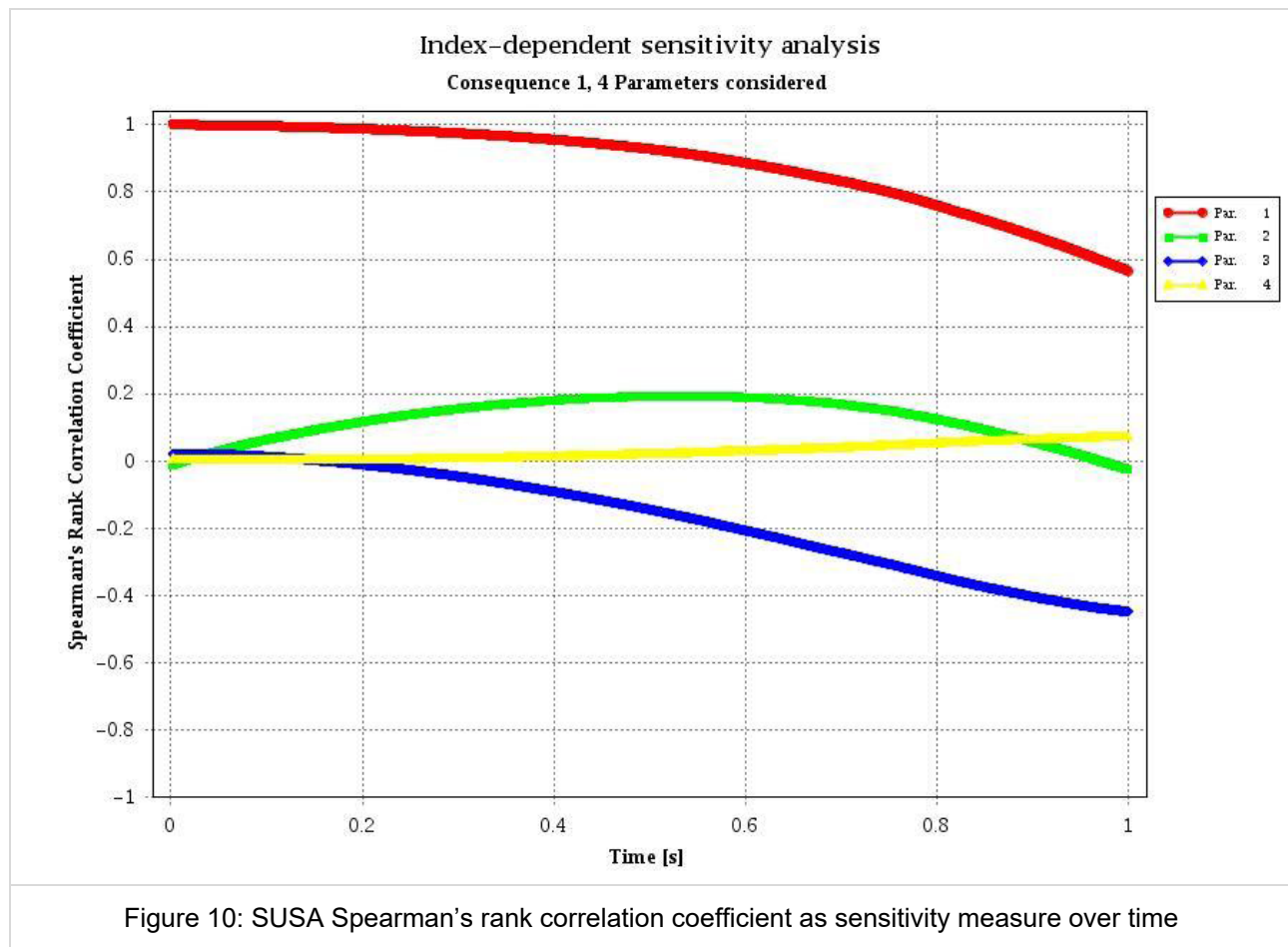


Figure 9: SUSA Pearson's ordinary correlation coefficient as sensitivity measure



1.6.6 Scatter & Cobweb Plots

SUSA can produce scatter and cobweb plots to visualize dependencies and sensitivities. Scatter plots can be generated for selected pairs of parameters and/or code results. Figure 11 shows an exemplary scatter plot between an uncertain parameter and a computational result. A cobweb plot allows for investigating the local sensitivity of a computational result. For instance, it can show how the high or low values of a computational result are associated with the values of the uncertain input parameters. A cobweb plot may also help to detect sensitivities with respect to combinations of uncertain input parameters. An exemplary cobweb plot is shown in Figure 12. Each dotted vertical line in this figure represents an uncertain input parameter except the left-most one, which represents the computational result. Each polygonal curve links each of the 10 largest values of the computational result (e.g. ranks 91-100) to the corresponding set of parameter values represented by their ranks.

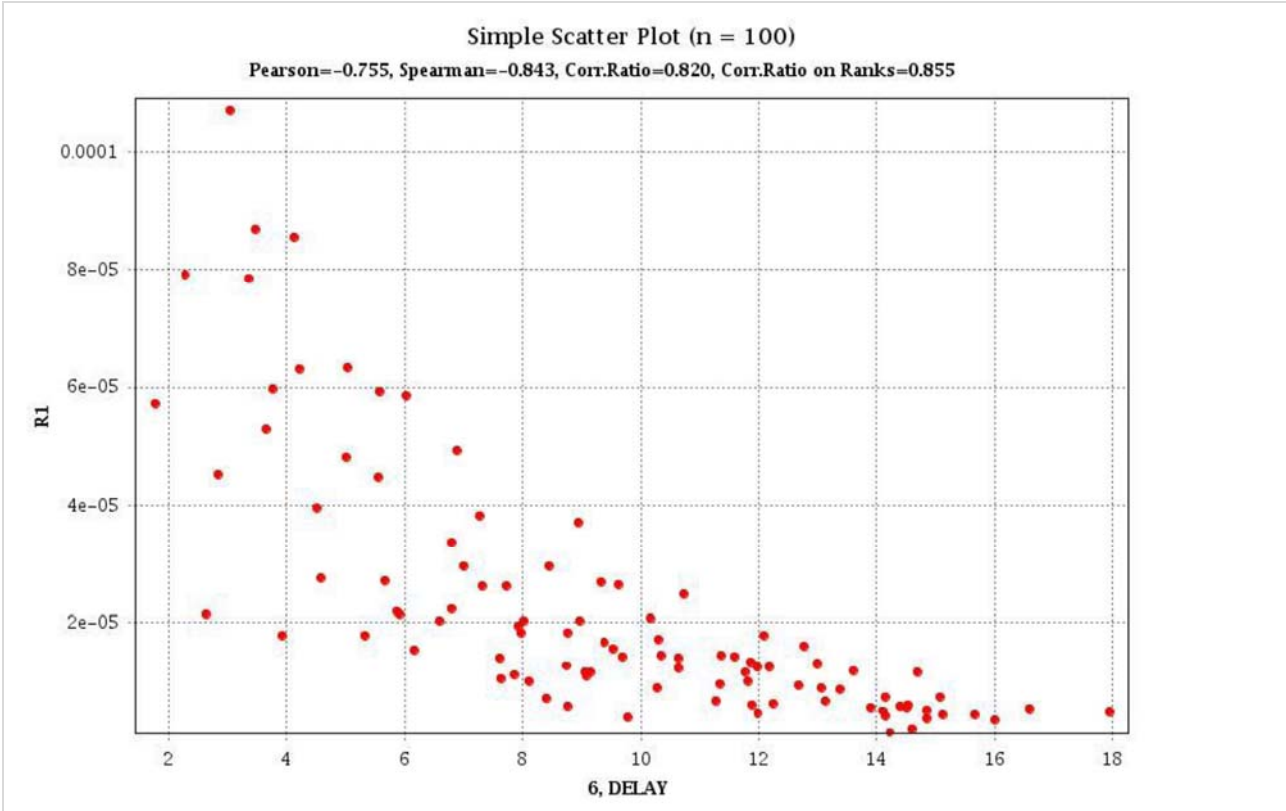


Figure 11: SUSA Scatter plots

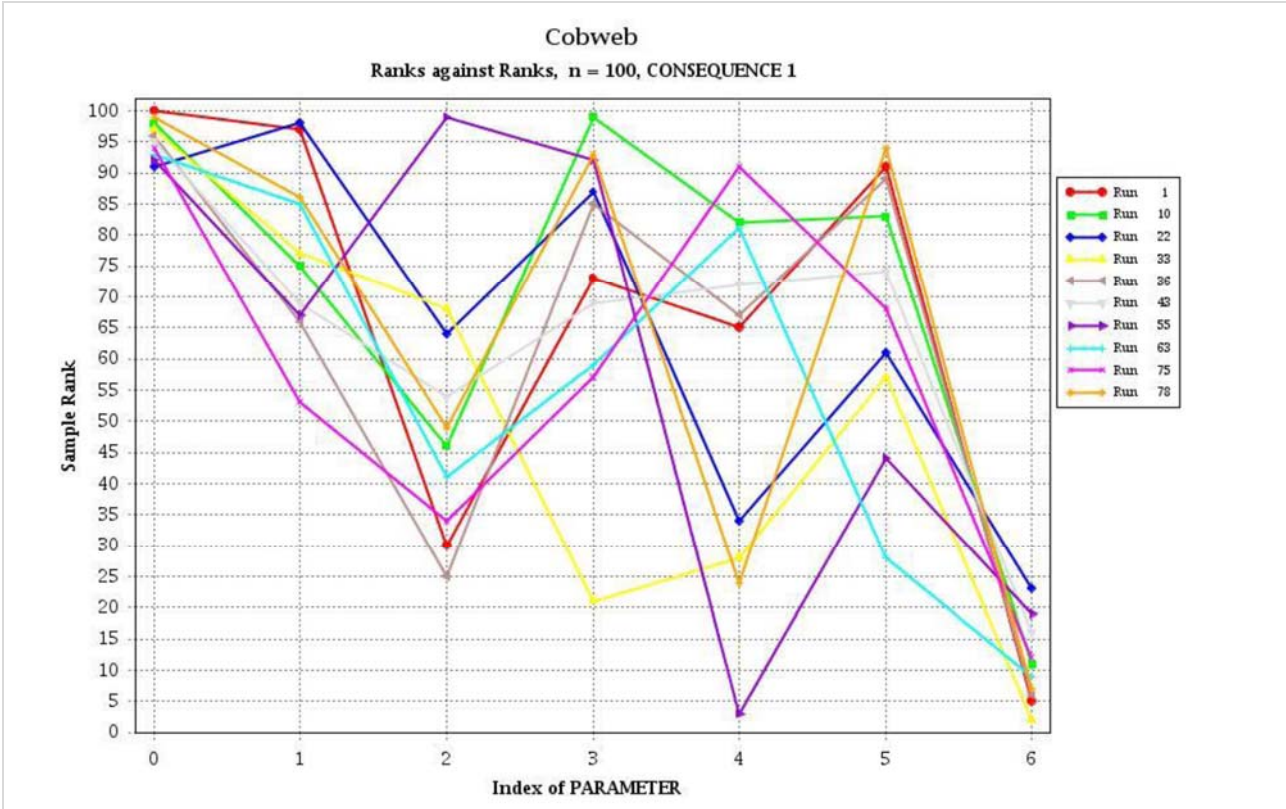


Figure 12: SUSA Cobweb plots

1.7 Pros and Cons

PROS:

SUSA does not have any limitations with respect to the uncertain parameters, the Monte Carlo simulation runs and the number of results, which can be considered in an application. The GUI of SUSA is very comfortable and supports the user to perform the analysis steps. It checks for input errors, performs data transfers, calls the Fortran program modules which are needed for calculation, presents the corresponding results in text form and visualizes the results using the tool AptPlot. The uncertain parameters associated with the specified probability distribution and dependence information are documented in a table, which can be easily included in a paper or report.

SUSA includes comfortable interfaces to selected codes applied in nuclear safety analyses. It also offers an interface to any other simulation code running based on an input file.

CONS:

So far, SUSA is only available for Windows operating systems. Nevertheless, current developments are aimed to make SUSA platform-independent. The method implemented in SUSA for considering uncertainties is MC simulation. It allows for considering either epistemic or aleatory uncertainties. For considering both types of uncertainties and for quantifying their common and separate influence, a double loop Monte Carlo (MC) simulation can be performed. However, the steps to be performed for this kind of analysis are not as convenient as for analyses considering just one type of uncertainties. Some analysis steps of a double loop MC simulation must be carefully prepared, since they are not automatically performed by SUSA.

SUSA is not the right tool for considering aleatory uncertainties with features of very low probabilities such as the performance of a safety system which mostly operates as intended and fails extremely rarely. In this case, MC simulation is not practicable in general, since a huge number of runs is necessary to consider the failure of the system. A tool recommendable in this context is the MCDET tool, which performs a combination of MC and Dynamic Event Tree (DET) simulation, [17]. MCDET can also account for an interaction between aleatory uncertainties and the system dynamics simulated by a code. Such an interaction is not supported by SUSA.

2 SUNSET (IRSN)

2.1 Description of the method

The SUNSET (Statistical UNcertainty and Sensitivity Evaluation Tool) software [18], developed by IRSN, is a statistical tool designed for uncertainty and/or sensitivity analysis of mathematical or physical models like computer codes.

It is composed of two parts:

- A set of statistical computing and interface functions, based on C++ language.
- A Graphical User Interface allowing the call of statistical functions, in Java language.

The tool runs on Linux and Windows environment.

SUNSET is a versatile tool: a study performed is a sequence of actions that the user has to define; the result of one action is given as an input of one of the following actions. A sequence of actions might take the form as illustrated at Figure 13, where an action is associated to sampling building, which output is filled to the action of ASTEC calculation launching, the result of which is filled to the action of post-processing.

The available SUNSET functions cover the following fields :

- utilities/data management : import/export data to csv format for example,
- generation of numerical values : design of experiment, sampling, sample aggregation
- sample propagation, through coupling with codes, or analytic functions defined in SUNSET
- uncertainty analysis
- sensitivity analysis
- evaluation and synthesis of information
- Multicriteria decision aid
- Data reconstruction

Uncertainty and sensitivity functions are described hereafter.

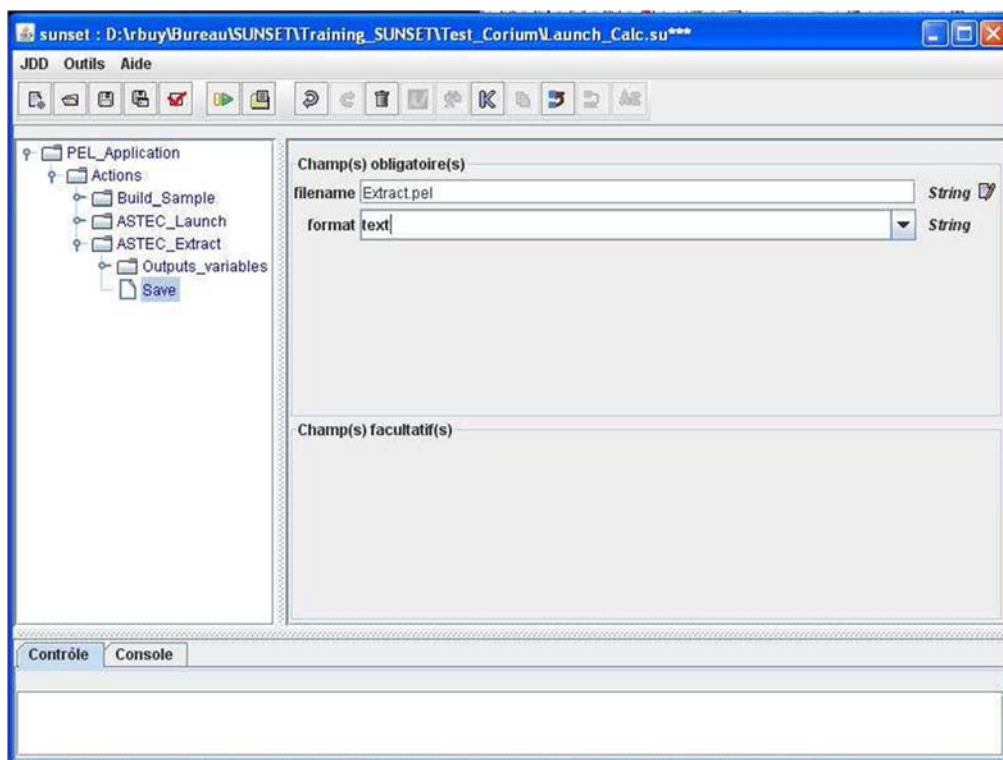


Figure 13: General presentation of an ASTEC/SUNSET sequence of action for an uncertainty study

In the framework of severe nuclear accidents, SUNSET has been coupled to ASTEC code. The general sketch of uncertainty analysis, based on Monte-Carlo simulations is presented at Figure 14.

The first step consists in the modeling of input uncertainties, choosing a probabilistic framework, possibilistic framework, or joint frameworks, and preparing the Monte-Carlo sampling.

Stochastic uncertainties are handled by probability theory. In that case, the probability density represents the frequency of a value for given variable.

For epistemic uncertainties, the user can choose either possibility or probabilistic frameworks, although in this latter case, the probability represents a measure of the degree of confidence in the value of a variable, and not a frequency.

The second and third steps are related to the preparation of ASTEC input deck and the launching of calculations; this will be discussed in another paragraph.

The uncertainty analysis techniques implemented in SUNSET are used for probabilistic variables and result in the production of estimators like mean, variance, or percentiles. In case of use of possibility framework, the sampling leads to a set of intervals and to a pair of data tables containing the extremity of each sampled interval. Therefore, each table can be seen as an occurrence of a random variable and the probabilistic techniques described below, can also be applied (ie. two cumulative density curves are produced instead of one).

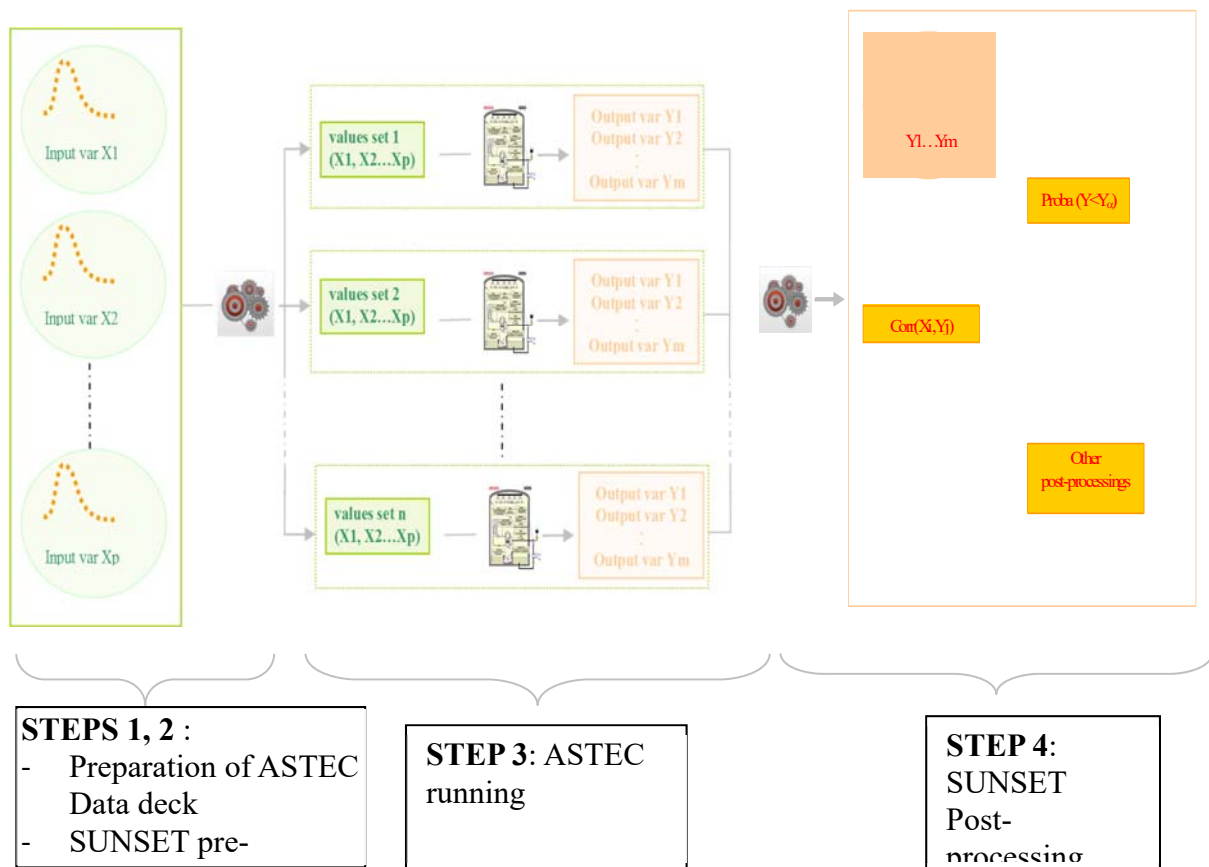


Figure 14: General sketch of uncertainty analysis using SUNSET and ASTEC

2.2 Description of main features

2.2.1 Uncertainty analysis

2.2.1.1 STEP 1: sample generation

2.2.1.2 Random sampling

The following methods are available for random sampling:

Simple random sampling: each occurrence is drawn independently of the previous one; the random sampling algorithm implemented in SUNSET is reproducible for a specified seed of the random number generator. The seed can be user defined; the necessary size of the sample can be calculated as a function of the statistical tolerance limits using a one or two sided estimator based on Wilks formula.

Dependence Modeling:

The dependences in SUNSET are modelled using a linear correlation of the rank of the variables. The principle of such a procedure is first to generate a sample of n values, for each of the variables. The values associated with each variable are then permuted according to the correlations on the ranks defined by the user.

Latin Hypercube sampling: for a sample size N of k independent variables, the interval of variation for each input variable X_j where $j=1, \dots, k$ is divided into N sub-intervals of equal marginal probabilities $\frac{1}{N}$. Once a sub-interval has been drawn, it is then excluded for the following drawings. Therefore for each variable, all parts of its distribution is represented among the input values once at least and at most.

Marginal probability distributions: Sunset provides discrete laws (Bernoulli, binomial, Dirac, uniform discrete, Poisson, piecewise-constant empirical cumulative distribution) and continuous laws (beta, gamma, exponential, Gumbel, normal, lognormal, chi2, triangular, uniform, loguniform, Weibul)

2.2.1.3 Interval sampling

Possibility: a possibility distribution is a set of nested confidence intervals to which “belief” masses are attributed. The possibility degree of a given event measures the extent of the plausibility of the event. The possibility of an event can be seen as the upper probability degree associated this event. Its dual measure is the necessity.

Necessity: the necessity of an event can be interpreted as the lower degree associated with the probability of this event.

simple sampling method : this method combines the various variables and their values taken at the same level of confidence

random sampling method : (RaFu method) The different variables and their values are combined with random confidence levels.

Possibility distributions: Sunset provides normal, uniform, trapezoidal, triangular, polygonal possibility distributions

2.2.1.4 STEP 4: analysis

Statistical indicators: average, standard deviation, variance

Order statistics: percentiles, one or two sided Wilks estimator,

General functions: cumulative density function estimation, density estimation, fit tests of distributions (χ^2 , Kolmogorov – Smirnov)

2.2.2 Sensitivity analysis

The following global sensitivity estimators are available in Sunset:

- regression coefficient,

- determination coefficient,
- correlation coefficient,
- partial correlation coefficients,
- simple determination coefficient, and
- partial determination coefficient.

These estimators measure how much explanatory the uncertain input parameters are for the response, presumably a linear function of the input. As an extension to nonlinear problems, the same coefficient is available for ranks instead of values, and therefore a ranking function is available. In that case, the response is supposed to be monotonous.

2.3 Initial conditions

Initial conditions can be set in ASTEC input deck as instructions read from sunset output of uncertain parameters.

2.4 Boundary conditions

Boundary conditions can be set in ASTEC input deck as instructions read from sunset output of uncertain parameters.

2.5 Model parameters

Model parameters can be set in ASTEC input deck as instructions read from sunset output of uncertain parameters.

2.6 Propagation of uncertainties

Please refer to paragraph 2.2.1.

2.7 Pros and Cons

On the use of probabilistic framework vs possibility framework, possibility theory allows the representation of imprecise information taking into account known information only, unlike probabilistic framework. RaFu method allows an efficient numerical treatment for sampling and reduces the computational cost of the propagation step. But the counterpart is that one has to verify the monotony of the response over the sampled variables in order to get correct results, which can take some time. On the contrary, the use of probability framework is straightforward. The counterpart is that the combination of the input pdf of independent variables can lead to the phenomenon of compensation, leading to the lesser representation of extreme values.

On the use of sampling methods for probabilistic framework, the LHS method is based on an independence assumption in uncertain parameters; it gives better results than the SRS method in cases where the response is dominated by only some of the input variables or if the response is a monotonic function of each of its arguments. The estimators obtained from an LHS have less variance than those obtained by SRS.

Considering sensitivity analysis, the global sensitivity coefficients allow checking the influence of a parameter over all the variation interval of the parameters, leading to local information being missed. On another hand, local method (not present in sunset) always require a lot of calculations, often not affordable when dealing with long duration and full phenomenological severe accident sequence.

3 DAKOTA (ENEA, TRACTEBEL, CIEMAT)

3.1 A BRIEF INTRODUCTION TO DAKOTA

DAKOTA [19] [20] [21] is an open source software written in C++ and developed by Sandia National Laboratories to perform parametric and uncertainty analysis in a fast and automatic way. The aim of this toolkit is to bridge simulation codes and analysis methods for parametric evaluation, uncertainty quantification and system optimization. The DAKOTA code was originally conceived to more readily interface simulation codes and optimization algorithms, but recently, it includes other iterative analysis methods such as Uncertainty Quantification (UQ). DAKOTA can be used for UQ analysis through the SNAP platform [22], where USNRC codes (e.g. MELCOR, TRACE, etc.) are already “coupled”, and therefore it makes the setup and analysis more “user-friendly”. Its handicap is that its methods and functions for UQ are limited in comparison with DAKOTA stand alone.

However, DAKOTA can be also used “stand-alone” to allow performing UQ analysis with almost every code. This option becomes more complicated or tedious, but in contrast, it allows to make use of all its potential for the applicability in UQ. As in the case DAKOTA-SNAP, DAKOTA (stand-alone) is able to perform forward uncertainty propagation in which probability information for input parameters is mapped to probability information for output response functions. However, in addition, it also includes the possibility of performing what are denominated “Nested models”, which permit layering one DAKOTA method over another, enabling algorithms like mixed epistemic-aleatory or second order UQ. To have more information on DAKOTA the following references can be used [19] [20] [21].

3.1.1 Description of main features

Aleatory and epistemic methods are separated in different packages in DAKOTA:

3.1.1.1 Aleatory methods

The aleatory UQ methods in DAKOTA include various sampling-based approaches, such as “Monte-Carlo Sampling” or LHS. They are both included in the LHS package. The variable distributions allowed are limited to normal, lognormal, uniform, log-uniform, triangular, exponential, beta, gamma, Gumbel, Frechet, Weibull, Poisson, binomial, negative binomial, geometric, hypergeometric, and user-supplied histograms. What is denominated in DAKOTA as “Monte Carlo (MC) sampling” is in fact a Simple Random Sampling (SRS) method where samples are chosen randomly according to the specified PDF.

The LHS method [23] is a stratified sampling technique where each uncertain variable is divided into N strata of equal probability (Figure 15), coinciding N with the number of samples n. The length of each of the strata is consistent with the PDF that follows the uncertain variable. LHS becomes a more effective technique since, in general, fewer samples than SRS are needed for the same accuracy in statistics [4].

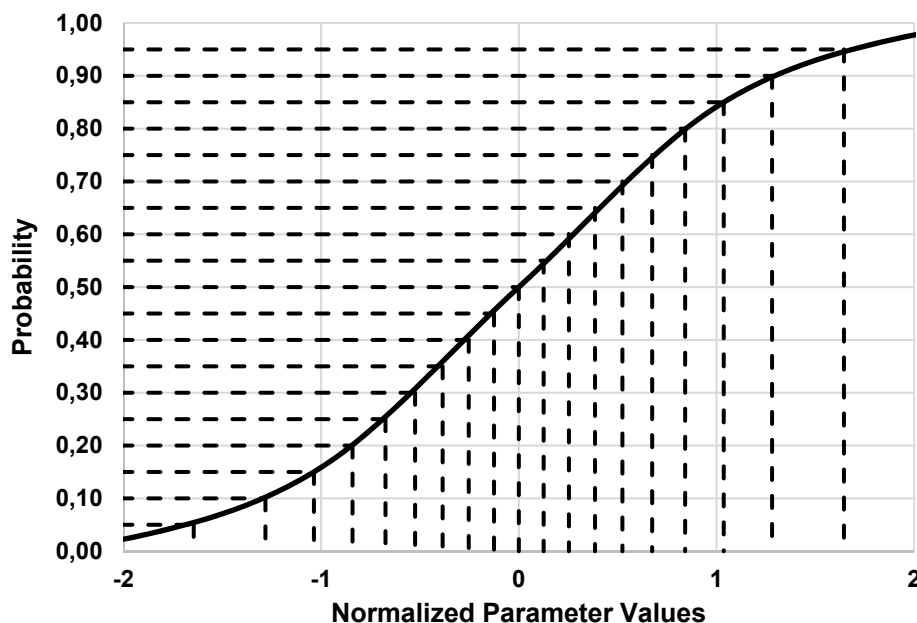


Figure 15: LHS strata subdivision for a normal-distributed parameter

Sampling methods in DAKOTA generate sets of samples based on the PDFs of the uncertain variables which then are mapped into sets of response functions. Means, standard deviations, Coefficients Of Variation (COVs), and confidence intervals are computed for the response functions. To obtain the responses, the MC method is employed, where the samples are paired to obtain a number of code inputs equal to the sample size of the uncertain input variables. The pairing process is random when the “MC sampling” method is employed. However, if LHS is applied, the pairing process results biased since every row and column in the hypercube formed by all the partitions has exactly one sample (Figure 16). Consequently, samples obtained by this method cannot be considered independent.

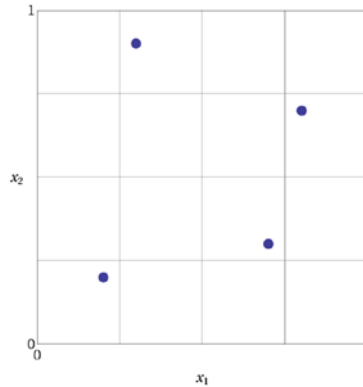


Figure 16: LHS pairing example where X_1 and X_2 are the sampled variables and the dots are the samples sites [21], [24], [20], [19]

Finally, the code is executed to propagate the input variable uncertainties obtaining its corresponding responses which are computed to obtain the desired statistics. In addition, if “random” sampling is selected, the non-parametric approach developed by Wilks [5] can be applied. Non-parametric methods do not assume any parametric distribution for the probability of the target variable. The Order Statistics (OS) are used to obtain the tolerance limits by assuming that the range between the highest and lower statistics follows a beta distribution independently of the distribution shape of the aleatory variable (code outputs). This, along with a given probability (β) and confidence (γ) can be derived to obtain the minimum number of cases needed to assure such coverage.

3.1.1.2 Epistemic methods

The epistemic UQ methods include interval analysis and Evidence theory. In DST, the uncertain input variables are modeled as sets of intervals. BPAs are assigned to each interval, indicating how likely it is that the uncertain input falls within such interval. Two methods are available, global and local evidence. Both of these methods perform DST calculations. The difference is that the local method uses a local optimization algorithm to calculate the interval bounds and the global method uses either sampling or a global optimization approach to calculate an interval bound. It has to be specify “lhs” for performing a LHS and to obtain the minimum and maximum of the samples within each cell as the bounds.

Mixed aleatory and epistemic methods for problems with a mixture of epistemic and aleatory uncertainties, it becomes necessary to segregate the two uncertainty types within a nested analysis. In this nested approach, an outer epistemic level selects realizations of epistemic parameters. In the case where the outer loop is evidence-based, the approach generates epistemic *Bel.* and *Pl.* bounds on aleatory statistics.

3.1.2 DAKOTA Output

The response function statistics returned by DAKOTA includes sample means, standard deviations, skewness and kurtosis. It also returns confidence intervals on the means and standard deviations of the responses and also the Cumulative Distribution Function (CDF) pairs.

In addition to obtaining statistical summary information of the results, correlations are also supplied. Four types of correlations are returned in the output: simple and partial “raw” correlations, and simple and partial “rank” correlations. The simple raw correlation coefficients are Pearson’s correlation coefficients. Partial correlation

coefficients are similar to simple correlations but adjusting for the effects of the other variables. The rank correlations in DAKOTA are obtained using Spearman's rank correlation.

3.2 CIEMAT METHODOLOGY APPLIED TO DAKOTA

3.2.1 Description of the method

The Best Estimate (BE) approach has been gaining momentum in the nuclear safety community as a means to achieve more realistic calculations than the original conservative approach applied for decades. However, a single BE calculation needs to be somehow complemented so that the calculation scatter due to input and code uncertainties is comprehensively quantified. During the last decades, many methodologies have been developed for quantifying calculation uncertainties. They can be classified into two main groups: probabilistic and deterministic approaches.

The BEPU methodology employed by CIEMAT in the framework of the MUSA project is based on the BEPU-CSA methodology [25]. It is a method originally developed for high-fidelity Containment Safety Analyses (CSA). However, as it presents a generic structure based on the Regulatory Guide 1203 [26], it can be applied to other kind of analyses such as severe accidents. The codes employed are the MELCOR code for modeling and calculation of the severe accident phenomena, and the DAKOTA tool for the statistical analysis.

3.2.2 Methodology Basis

The BEPU-CSA methodology is structured into two main sections, namely "Best Estimate Modeling" and "Accuracy Assessment". It has to be pointed out that only uncertainties (no numerical errors nor model biases are considered) will be considered during the accuracy assessment, which is the main goal of the MUSA project.

The BEPU-CSA methodology has been built around three main principles:

- a) Expert judgment will be limited. Instead of a subjective Parameter Identification and Ranking Table (PIRT), all the uncertain parameters identified will be initially considered in the analysis. This might be softened if unforeseen difficulties show up during the application.
- b) The distinction between aleatory, epistemic and imprecise uncertainties [27].
- c) Calculation time has to be also considered to assure the methodology pragmatism. This can be heavily condition the BEPU-CSA application given the long transient time in case of severe accidents. Therefore, either the EM (Evaluation Model) developed for the analysis or the full uncertainty parameters consideration (a) or both, will be consolidated in such a way that the methodology becomes computationally affordable.

3.2.3 Best-estimate modelling

It is divided in three main phases, being these the description phase, focused on the scenario and the plant that will be analyzed; the decision phase, where the modeling strategy and the code that will be used is depicted; and finally, the modeling phase, which describes the Evaluation Model (EM) setup process.

3.2.3.1 Description

Description of the transient is essential for choosing the code to be employed in the calculation and the modeling strategy to be followed. Different phenomena might be present during different accident sequences and different time spans in the same accident, which are also dependent on the plant design. For instance, in

A conceptual pre-analysis is recommended at this stage. By identifying key expected phenomena, the accident could even be phased [28], which might be useful for the analysis. The definition of FOMs is to be done in this stage of the analysis. Modeling strategy might to some extent (i.e., nodalization) be affected by FOMs nature, either integral or instantaneous, or either volume average or local.

3.2.3.2 Decision

This phase concerns codes suitability to address severe accident simulation. Even though, in principle most popular codes (i.e., MELCOR, ASTEC, MAAP, AC2, etc.) are mature enough, modelers should make it sure that they match what requires a full-scope SA simulation (i.e., phenomena considered, proper integration, numerical stability, etc.). From this standpoint, the MELCOR code [29] is a reference code in SA simulation,

with a sound coverage of Source Term phenomena. Nevertheless, it should be highlighted that fission product (FP) chemistry is not dealt with during FP transport, particularly iodine chemistry modeling is incomplete and outdated. This drawback along with the impossibility to capture 3D phenomena that might affect hydrogen distribution, for instance, should be kept in mind when modeling SA scenarios. Anyway, the code may be considered qualified for the MUSA purpose.

3.2.3.3 Modeling

Since the goal is to perform a BE analysis, the EM has to be as precise and detailed as possible, and that means that plant data needed to feed the code has to be equally detailed. The source of these data usually come from a huge amount of plant schematics, diagrams, and other related documents. To properly face the difficulties in dealing with that amount of documents, the EM setup process is divided into two practical steps:

- a) The construction of plant CAD model is the first step in the modeling phase [25]. In order to organize the plant data available, it is highly recommended to start setting-up a high-fidelity CAD model. Since many important parameters are difficult to gather (containment free volume, heat sink surfaces, geometric distribution, etc.), joining all the data in one digitalized document allows to achieve it with no major problems. The data gathered from the CAD model is then used to setup the Control volume (CV) parameters. A mesh assessment should be performed to assure that nodalization is adequate for predicting key phenomena. Heat structure data, such as the wall thickness, heights or surfaces, are also extracted from the CAD model, as well as the flow connections between components. Depending on the scenario to be analyzed, safeguards systems which are assumed to be available may also be modeled.
- b) The development of the MELCOR EM. The process and recommendations for plant modeling with MELCOR for severe accident analyses is depicted in several public documents, but the CIEMAT's EM is based on the documentation extracted from the SOARCA project best practices guidelines [30].

3.2.4 Uncertainty Quantification

An EM will never reproduce real physics since many simplifications and approaches are necessary when modeling a SA scenario. The quantification of uncertainties may be structured in three phases *Identification*, *Quantification*, and *Interpretation*.

3.2.4.1 Identification

The response (FOM) uncertainty is produced by a combination of different uncertainty and error sources. Experimental data; plant data; model inadequacy; numerical schemes; geometry simplification; and user effect are the main uncertainty and error sources.

Aleatory uncertainties come from the natural variability of a phenomenon (i.e. droplet sizes from a flashing liquid, or number of resultant neutrons from a fission reaction) and measurements (instrument accuracy). In the latest, it may be differentiated between instrument calibration, which add a bias (error) to the measurement; and the instrument precision, which adds dispersion (randomness). In some cases, there may be lack of information for a correctly characterizing of a aleatory uncertainty (i.e. only the mean is known or the PDF parameters are based on a sample set instead of the whole population). In such situations, the uncertainty of this parameter may be considered an imprecise uncertainty.

Epistemic uncertainties are those produced due to the lack of knowledge. Usually, availability of real plant schematics and documentation is not trivial. Hence, the information for plant modeling could be incomplete, and incompleteness of data is by definition an epistemic uncertainty. Consequently, these uncertainties may affect critical parameters, such as the definition of the free volume and/or heat sink areas.

Numerical & systemic errors are normally produced due to the lack of control over the code structure, inadequacy of physical models used, and/or the complexity of the simulated phenomena. Therefore, code errors are related to physical models adequacy (including scale distortions), discretization schemes (spatial and temporal), iterative process (residuals), round-off error, and user effect, [27]. As was previously stated, errors will be not considered by CIEMAT in the MUSA context.

3.2.4.2 Uncertain Input Parameters Identification

For determining uncertain input parameters, the MELCOR models of relevant phenomena for the scenario to be addressed will be studied. Correlation coefficients will not be considered uncertain parameters, since they

were used to calibrate the mathematical model to fit real physics, and therefore, they add bias (error) and not dispersion to the calculation.

3.2.4.3 Parameters Uncertainty Characterization

Ranges and probability distributions are generally used to characterize parameter uncertainties. There are different methods to characterize input uncertainties, remarking SAPIUM [31] and part of the SOARCA project [32], [33] outcomes.

When characterizing uncertainties, the case of aleatory uncertainties is clear, since the most appropriate mathematical representation for them is the classical probabilistic framework. Therefore, if the information is complete, uncertainty of parameters can be characterized with an adequate PDF applying the Classical Probability Theory (CPT), whose basis can be found in almost every textbook related to statistics and probability, such as in [34]. The data for characterizing the parameter uncertainty will be extracted from experiments, in a similar way as was performed in the SAPIUM project [31].

However, it is not common to have all the information needed available. Or maybe, there are different sources of information for a parameter in particular. In these cases, the uncertainty becomes incomplete or imprecise. In such situation, the characterization will be driven by the *Principle of Minimal Specificity* [5], and a method based on bounded probabilities (or probability boxes) will be employed. Instead of a single value of probability, the parameter uncertainty will be represented by a bound defined by upper and lower probability values [35] [36].

For the case of purely epistemic uncertainties (total ignorance about the value(s) of a parameter), there is no other way but applying the expert judgment for estimating the uncertainty range. The uncertainty characterization in these cases will be driven by the *Principle of Insufficient Reason* [37] by assigning a uniform distribution to it.

3.2.5 Quantification

It is proposed to apply the Wilks approach [5] [6][6], [7][5], [6]. In that manner, the number of iterations needed will be dependent only on the tolerance and confidence limits established, being for instance, 59 runs to establish the 95th percentile at 95-percent confidence (95/95) for one tolerance limit.

The DAKOTA tool will be used for the statistical analysis. To do that, a coupling between MELCOR and DAKOTA becomes necessary. If both codes are used under the SNAP interface [22], this coupling is already done by the SNAP itself. However, CIEMAT plans to use DAKOTA in the stand-alone format, since it allows a better control over the DAKOTA and MELCOR capabilities. That means that a script to couple these two codes is required, and therefore, it has been developed in Python.

3.2.6 Interpretation

The application of the Wilks approach by itself only assures a tolerance region of specified content and specified probability. However, the influence of each of the input uncertainties in the EM output is still unknown, making necessary a sensitivity analysis. Since a “reduced” set of Monte-Carlo iterations has been already performed, uncertainty statements and sensitivity measures are available simultaneously for all singled-value as well as continuous-valued output quantities of interest from the same variation of input and code calculations.

The Pearson product-moment Correlation Coefficient (PCC) [30] [31] [38] will be employed to observe the linear correlation between the FOM(s) and the input parameters. The Spearman’s Correlation Coefficient (SCC) [6] will be used to analyze the monotonic correlation between them (a monotonic correlation is considered when a perturbation in one of the two parameters implies a change in the other parameter, but not necessarily at a proportional rate).

However, since these two regression coefficients are obtained from a relatively small sample, a p –values analysis will be performed to check its consistency. Confidence Intervals (CIs) will be also estimated to consider the so-called “statistical error”. For that, the classical method stated by Student [39] is proposed.

3.3 DAKOTA (TRACTEBEL)

3.3.1 Description

The uncertainty and sensitivity analysis process using DAKOTA as stand-alone tools is shown in Figure 17. For the applications to multi-physics code package presented in this paper, the defined input uncertainty parameter ranges and distributions for each simulation code, as well as the chosen uncertainty analysis method and number of samples are defined in the DAKOTA Input File.

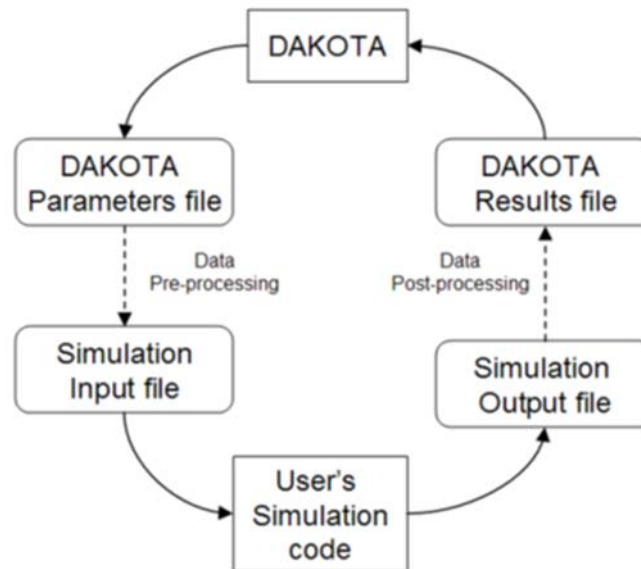


Figure 17: The DAKOTA uncertainty/sensitivity analysis process [8].

Based on the sampled or assigned values of input uncertainty parameters in the DAKOTA Parameter Files, various scripts have been developed to create the simulation code input files, to execute the simulation code runs, and to collect relevant calculation results from the simulation code output files into the DAKOTA Results Files. The DAKOTA Executable will then perform the requested statistical uncertainty and sensitivity analysis and provide the information in the DAKOTA Output Files.

3.4 DAKOTA toolkit in SNAP (ENEA)

In the framework of deterministic safety analyses, DAKOTA toolkit is also provided as a plug-in [22] for the Symbolic Nuclear Analysis Package (SNAP), which is a graphical user interface designed to support the use of USNRC nuclear codes (e.g. TRACE, RELAP, MELCOR, etc.). Using SNAP, it is possible to build the input-deck in a graphical environment and to have a direct visualization of the code calculated data by using its animation capability [40] [41] [42]. SNAP is a suite of integrated applications including a “Model Editor”, “Job Status”, the “Configuration Tool” client applications and a “Calculation Server”. In particular, the “Model Editor” is used for the nodalization development and visualization and for the visualization of the selected calculated data by using its graphical and animation model capability. Through SNAP it is possible to set-up the DAKOTA uncertainty analysis [22] and to perform automatically all the steps to apply the probabilistic method to propagate input uncertainty. Figure 18 shows a schematic representation of DAKOTA uncertainty analysis workflow in a SNAP environment/architecture for MELCOR applications. Figure 19 shows the equivalent MELCOR/DAKOTA uncertainty stream done in SNAP.

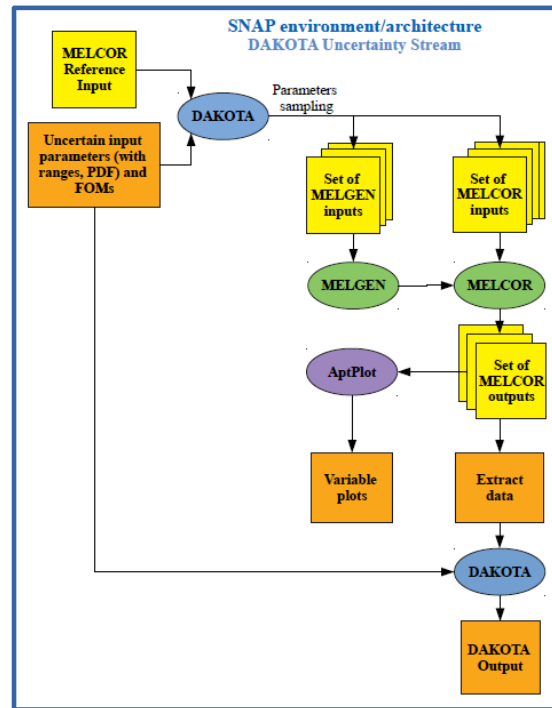


Figure 18: DAKOTA uncertainty analysis workflow for MELCOR code in a SNAP environment/architecture.

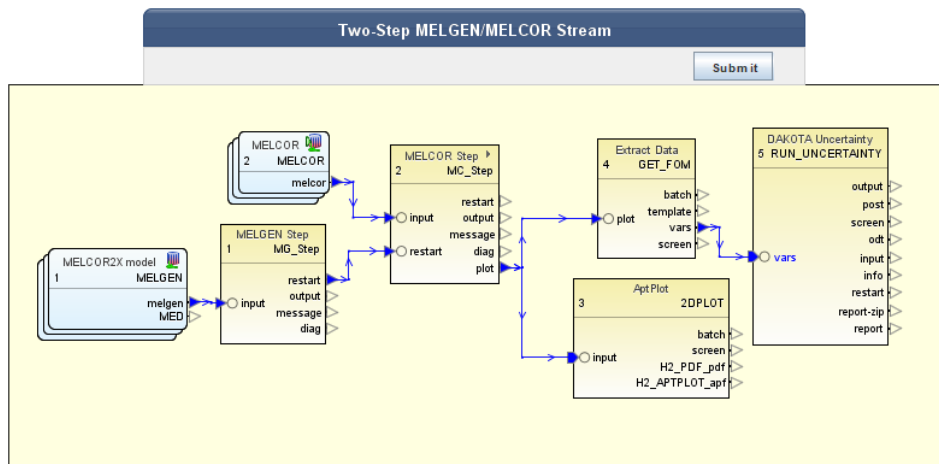


Figure 19: MELCOR/DAKOTA uncertainty stream done in SNAP.

3.4.1 DAKOTA/SNAP Description of main features

DAKOTA plugin [22] for SNAP allows to:

- 1) Enter the selected uncertain input parameters (together with their range and PDF type);
- 2) Select the sampling method (Monte Carlo or Latin Hypercube);
- 3) Enter the desired FOMs for the analysis;
- 4) Set the final report, automatically generated at the end of the uncertainty quantification analysis, which contains the results of the uncertainty analysis application.

In Figure 18 it is presented the DAKOTA workflow in SNAP coupled with MELCOR code. Starting from the reference MELCOR input-deck, the selected uncertain input parameters (together with their range and PDF) and the FOMs, DAKOTA samples the input parameters creating a set of N MELGEN and MELCOR inputs. The minimum number of code runs N depends on the requested probability content α , the confidence level β and the number of FOMs. In case only one FOM is investigated, for the one-sided tolerance interval, the

required number of code runs can be found, based on Wilks [5] [6] by solving the following equation with respect to N:

$$1 - \alpha^N \geq \beta \quad (1)$$

If more than one FOM is investigated, for the one-sided tolerance interval, the required number of code runs can be found by solving the following equation with respect to N [43]:

$$\beta = \sum_{j=0}^{N-p} \frac{N!}{(N-j)!j!} \alpha^j (1 - \alpha)^{N-j} \quad (2)$$

where p is the number of FOMs. More information on statistical aspects of best estimate analyses can be found in [44].

The different steps necessary to define the uncertainty analyses in a DAKOTA application in SNAP are :

- **STEP1: “Edit Uncertainty Configuration/DAKOTA Properties”**

As shown in Figure 20, in the first SNAP Tab of the uncertainty stream, “Edit Uncertainty Configuration/DAKOTA Properties”, the sampling process (e.g. number of samples, sampling method, etc.) can be characterized and the FOMs for the Uncertainty Application (UA) can be introduced.

- **STEP 2: “Edit Uncertainty Configuration View/Variables”**

In the second SNAP Tab of the DAKOTA Uncertainty Stream configuration, “Edit Uncertainty Configuration View/Variables”, it is possible to add the selected input uncertain parameters, Figure 22, previously defined in the MELCOR input-deck, and characterizes them.

- **STEP3: “Edit Uncertainty Configuration View/Distribution”**

In the Third SNAP Tab of the DAKOTA Uncertainty Stream configuration, “Edit Uncertainty Configuration View/Distribution”, it is possible to quantitatively characterize the input uncertain distribution previously defined. In particular it is possible to define the Distribution Type (Normal, Lognormal, Uniform, Loguniform, Triangular, Exponential, Beta, Gamma, Gumbel, Frechet, Weibull, Histogram) and the distribution parameters that characterize each of them. In Figure 23 is reported an example with the triangular distribution. In the right of this Tab it is visualized the Probability Density and Cumulative Distribution resulting from the characterization of the input uncertain parameter.

- **STEP 4: “Edit Uncertainty Configuration View/Report”**

In the fourth Tab “Edit uncertainty configuration/Report”, Figure 24, it is possible to characterize the report configuration, automatically generated by DAKOTA, and the plot variables in the “Plotted Values Table” (Input uncertainty parameter VS iteration index, FOM VS input uncertain parameters, FOM VS iteration index).

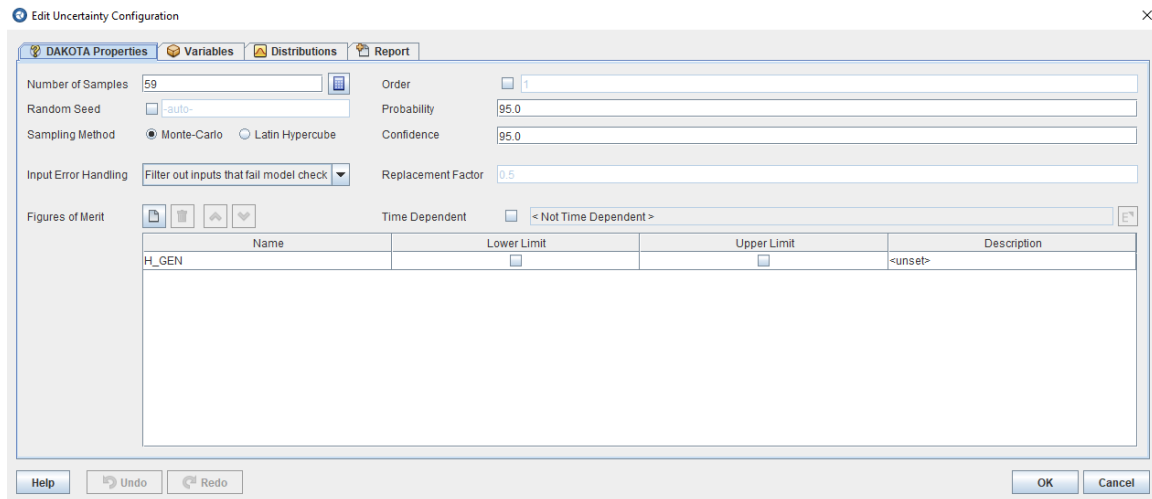
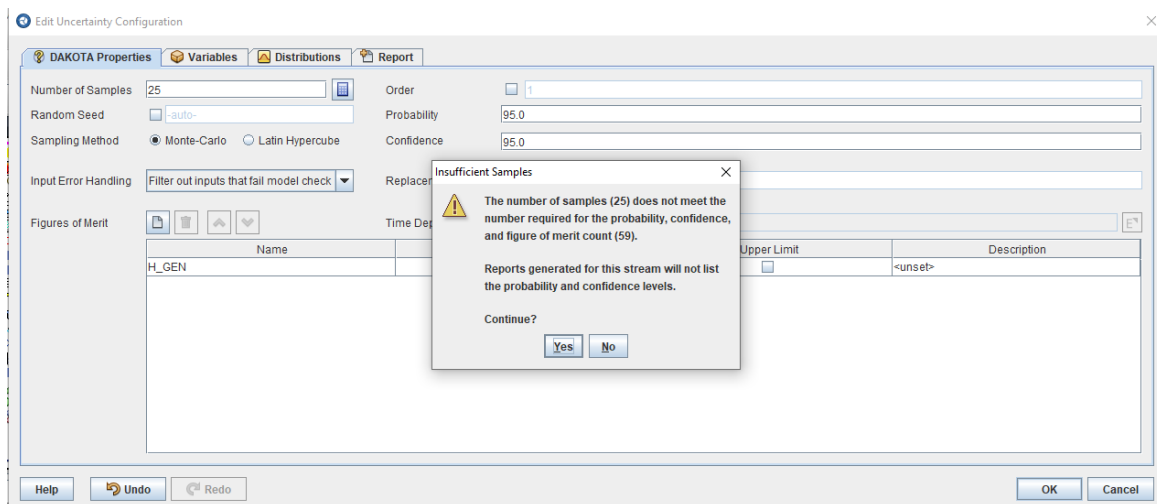


Figure 20: “Edit Uncertainty Configuration/DAKOTA Properties” SNAP Tab.

Figure 21: “Edit Uncertainty Configuration/DAKOTA Properties” SNAP Tab, insufficient number of sampling warning¹.

¹ A “Calculated Samples” button is available to the user to evaluate the required number of tasks considering the Order, Probability and Confidence selected by the user. The required number of tasks is visualized in the “Number of Samples” field. The user can define independently a number of tasks. If the number of tasks, selected by the user, is minor than the required tasks a warning message of insufficient sampling is displayed, Figure 33. This evaluation is based on the Wilks method [17]. As shown in Figure 32, the Order, Probability and Confidence can be selected on the right of the mask in the “Order”, “Probability”, “Confidence” field.

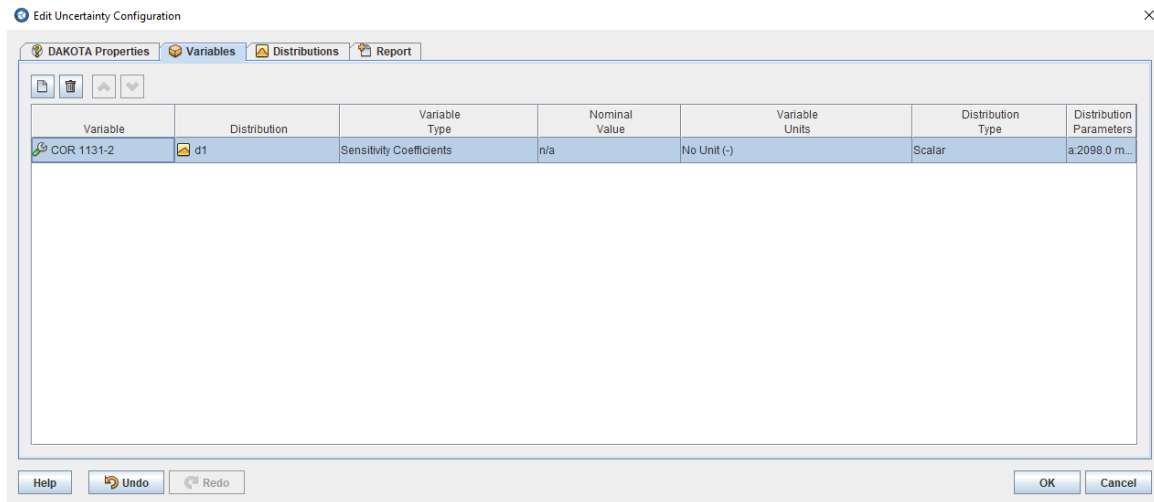


Figure 22: “Edit Uncertainty Configuration/Variables” SNAP Tab.

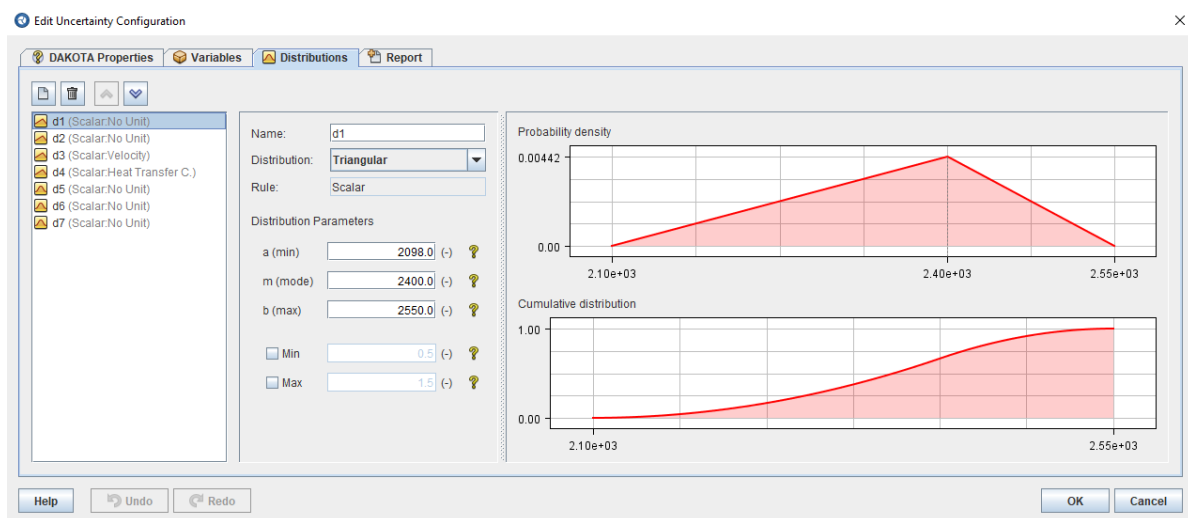


Figure 23: Example of input uncertain parameter distribution representation in the SNAP Tab.

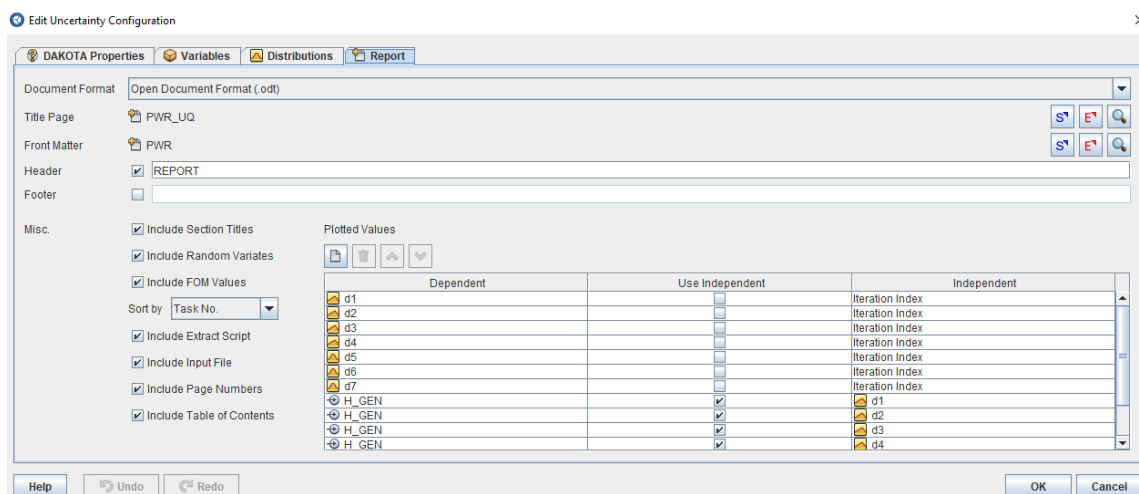


Figure 24: “Edit Uncertainty Configuration/Report” SNAP Tab.

REPORT: Variate and Response data

As shown in Figure 18, an initial DAKOTA run is performed using the specified input parameters to generate a set of variates for each task. The individual tasks are then performed and the FOMs are extracted from the completed calculations.

The plots present in the DAKOTA automatically generated report are:

- Input uncertain parameter against iteration index (e.g. **Error! Reference source not found.**);
- FOM VS input uncertain parameters (e.g. **Error! Reference source not found.**);
- Input uncertain parameter VS another input uncertain parameter.

It is reported in a tabular form:

- The value of the response data for each task, for the instants selected;
- The value of each uncertain parameter for each task.

REPORT: DAKOTA results

As shown in Figure 18, a second DAKOTA run was performed using the variate and extracted FOM values to obtain the statistical results and a cumulative distribution function for the FOM. DAKOTA also calculates the response correlations for the FOM.

In relation to the DAKOTA statistical results of the FOM, the following information can be found in the automatically generated report:

- Plot (e.g. **Error! Reference source not found.**, **Error! Reference source not found.** on the right):
 - o Cumulative distribution function;
 - o Probability density function.
- Tabular (e.g. **Error! Reference source not found.**, **Error! Reference source not found.**)
 - o Statistical results:
 - Min value and the related task;
 - Max value and the related task;
 - Mean value;
 - Median value and the related task;
 - Standard deviation;
 - Coefficient of Variance.

REPORT: Uncertainty analyses response correlation

As a result of the uncertainty analysis, DAKOTA [19] [22] [45] [46] computes four response correlation coefficients: simple, partial, simple rank and partial rank. The simple coefficient is related to the actual input and output data. The simple coefficient r between an input variable x and an output variable y , in n samples, is computed using the Pearson's correlation. It is a measure of the degree of linear correlation between the two variables and its value is comprised between -1 and 1. If $r < 0$ the correlation is negative (an increment of x leads to a reduction in y), if $r = 0$ there is no correlation between the two variables, if $r > 0$ the correlation is positive (an increment of x leads to an increment of y). The partial correlation coefficient is computed similarly to simple one but taking into accounts the effects of the other variables. This is useful, for example, if there is a strong correlation between two inputs; in this way the correlation of the second input on the output may be adjusted after having considered the correlation between the first input and the output [19]. Rank correlation coefficients use the ranked data instead of the actual ones. Ranks are obtained by ordering the data in ascending order, and are more convenient to be used when inputs and outputs are characterized by sensible difference in magnitude; it is possible to understand if the input sample with the lower rank is associated to the output with the lower rank and so on [19] [47]. To compute the rank correlation, DAKOTA uses the Spearman's rank correlation that is similar to Pearson's one but with the ranked data instead of the actual values. If two variables are monotonically related, without repetitions, the Spearman coefficient is -1 or +1 (depending if the function is monotonically decreasing or increasing), since the ranked values are used. Moreover, Spearman's correlation is less sensitive to possible outlier values of the variables than Pearson's one.

Error! Reference source not found. and **Error! Reference source not found.** show the response correlation reported in the automatically generated DAKOTA report for the ENEA CASE 1 and 2 respectively for a selected instant. For completeness, as example of time dependence computation of response correlation coefficient,

the peak cladding temperature Pearson and Spearman coefficient are reported based on a TRACE [48] (USNRC best estimate thermal hydraulic system code) analyses of a double ended guillotine break in a generic PWR-900 [45], Figure 25 and Figure 26.

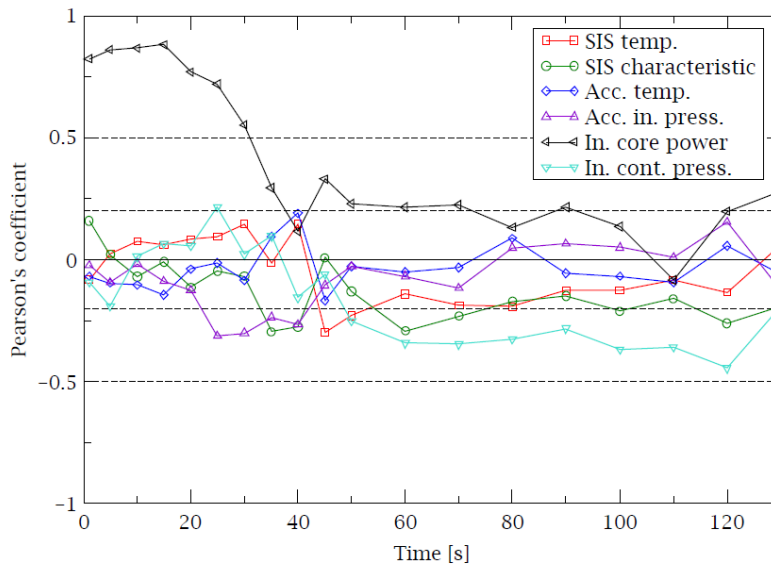


Figure 25: Peak cladding temperature Pearson's simple response correlation coefficient (double-ended LBLOCA simulation with TRACE code coupled with DAKOTA for a generic PWR-900) [45]

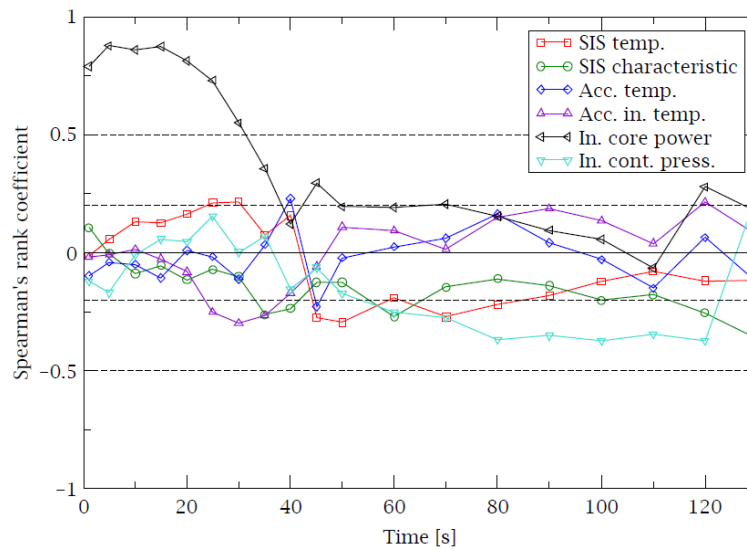


Figure 26: Peak cladding temperature Spearman's simple response correlation coefficient (double-ended LBLOCA simulation with TRACE code coupled with DAKOTA for a generic PWR-900) [45]

3.5 Initial conditions

DAKOTA can treat the code input as an uncertain variable and provide tools for insertion of the sampled values in the studied code input files. The freedom provided to the user by the use of scripts permit to generate input variables from sampled parameter. For example, DAKOTA samples fuel rod diameters, because those are the values affected by the fabrication tolerance, and the script calculates the results thicknesses that the code need. Also, the sample can be variables used by a script to generate a skewed axial profile.

On the specific aspect of case initial conditions, the same user liberty permits to perform sampling both on a first initialisation case, then on the test case itself. One example [10] is the simulation of irradiation of a fuel rod up to the adequate burnup with a steady-state code before the simulation of an experiment with a transient code. This includes the required adaptations of input parameters and the potential rework of the results from the initialisation case before passing them to the test case.

Initial conditions can be used as input uncertainty parameters also using DAKOTA in a SNAP environment/architecture.

3.6 Boundary conditions

See previous sections. The use of scripting will facilitate the handling of aspects like code coupling.

Boundary conditions can be used as input uncertainty parameters also using DAKOTA in a SNAP environment/architecture.

3.7 Model parameters

Model parameters can be treated if they are code inputs. In some cases [11], the studied code has been modified to create an additional input which contain factors to multiply the appropriate subcode results and consequently apply uncertainties on model behaviour.

Model parameters can be used as input uncertainty parameters if they are code inputs also using DAKOTA in a SNAP environment/architecture.

3.8 Propagation of uncertainties

DAKOTA is well suited for the non-parametric order statistics by Monte-Carlo sampling of all uncertain parameters according to the analyses by Tractebel. Other methods are available: LHS sampling, reliability methods, stochastic expansion methods (based on polynomial chaos and stochastic collocation), plus several epistemic and mixed aleatory/epistemic methods.

3.9 Pros and Cons

3.9.1 probabilistic method to propagate the input uncertainty

The probabilistic method to propagate the input uncertainty [45] [7], is, in brief, based on a random sampling of the input uncertain parameters selected by the user; a set of N code runs having in the input a combination of the uncertain parameters is created and solved with the selected code (e.g. MELCOR). Then, it is possible to perform the statistical analysis and to characterize, through response correlations, the relationship between the selected uncertain input parameters and the FOMs..

One of main advantages of this method is that, by for example using a non-parametric method, the number of code runs does not depend on the number of input uncertain parameters. In addition, it is not necessary a prior development of a Phenomena Identification and Ranking Table (PIRT), which is a long process. Each uncertain input parameter should be defined by its range of variation and its Probability Density Function (PDF); this means that even if the exact value of a parameter is uncertain, some values are more likely to be close to the real one than others. The definition of the PDF is one of the most challenging tasks in the application of the probabilistic method to propagate input uncertainties. If there is no evidence or information to choose a particular PDF, the uniform distribution can be used; in fact, at a fixed range, it assigns the same probability to all the values in the range of variation of the parameter. The drawback is that this can lead to a results

spreading larger than the one obtained with the use of peaked type distributions. More information about deriving parameter PDF can be found in [49].

3.9.2 Analysis methods

3.9.2.1 Pure Monte Carlo

It is a parametric method and therefore, it may be more accurate for estimating the FOMs uncertainty. However, its accuracy will depend on the sample size, which will be proportional to the number of input variables combined to obtain the FOM responses. It would make this method computationally expensive when several input variables are considered.

3.9.2.2 Wilks approach

It is a non-parametric method, and therefore, there is no dependency between the sample size needed and the input variables considered. Sample size will depend on the coverage and confidence needed in the analysis. Since this method relies on more general statements, like that the FOM distribution is continuous, it is less accurate, but conservative, than parametric methods.

3.9.2.3 Interval analysis

Interval analysis method could be considered non-probabilistic since every uncertain variable is treated as an interval. Extreme values for each interval are used to compute the uncertainty bands of FOMs. Every possible combination between variable values are considered. Therefore, the cases needed in the analysis will be dependent on the input variables so that 2^n code runs will be necessary (where n is the number of input variables). It could make the UQ analysis computationally expensive if many of them are considered.

3.9.2.4 Evidence theory

This method is similar to that the interval analysis since the uncertain variables are defined by intervals. The difference is that every variable could be defined by several intervals, making it even more expensive (in code runs) than the interval analysis. In fact, interval analysis may be considered a particular case in DST, where all the input variables are define by a unique interval. Its advantage is that no subjective considerations are stated about the input variables uncertainty.

3.9.3 DAKOTA limitations

The need of extra scripts (pre- and post-processing)

Nested analysis limited by the DAKOTA structure. For instance, double Wilks cannot be performed neither apply Wilks approach to the outer loop.

DAKOTA output is limited to that described in 3.1.2. If other test and/or analysis is desired, brute output data have to be used for computing it.

3.9.4 User oriented features or functionalities, user friendliness

Pros:

- Choice between graphical user interface and input files. DAKOTA can be controlled by command line and introduced in scripts.
- Good access to the data to perform pre and post treatments. This permits to study complex calculations with several codes involved.
- Free
- Versatility: Large and varied set of methods available.
- Good management of parallel computing.
- Community to help users.
- Can manage large numbers of random variables and code responses (e.g. several hundred responses for a transient problem).
- Sensitivity analysis is automatically performed.

Cons:

- Knowledge of scripting needed. It is up to the user to manage the transfer of data to and from the studied code (even if tools are provided to help).

4 URANIE (KIT, BELV)

4.1 Description of the method

URANIE [50] [51] is an open source platform for uncertainty and sensitivity analysis developed by CEA within the ROOT analysis Framework [52] [53]. In addition to the classical uncertainty and sensitivity studies, URANIE has also the capability to perform surrogate model generation and calibration, reliability analysis, optimisation and construction of design-of-experiment. In this sense, it is similar to other open source platforms such as DAKOTA, Open-TURNS, and UQLab.

The URANIE platform is written in C++ and it runs in multiple platforms (UNIX, Windows) and it can be used via a C++ (CINT), Python (PYROOT) or Ruby interface. URANIE takes profit of many ROOT-features as an advanced data visualisation tools, a hierarchical machine independent and highlight compressed object-oriented database and many statistical analysis tools (RooStats, RooFit, etc). A simple data access is provided in the formats: flat ASCII file, XML, JSON, internal ROOT format (TTree) and to SQL-database. Important for the UQ of severe accident codes is the parallel capability of URANIE which is based on different mechanisms e.g. simple fork processing, shared-memory distribution (pthread), splint-memory distribution (mpirun) and GPU. A complete documentation can be found in the URANIE site [54].

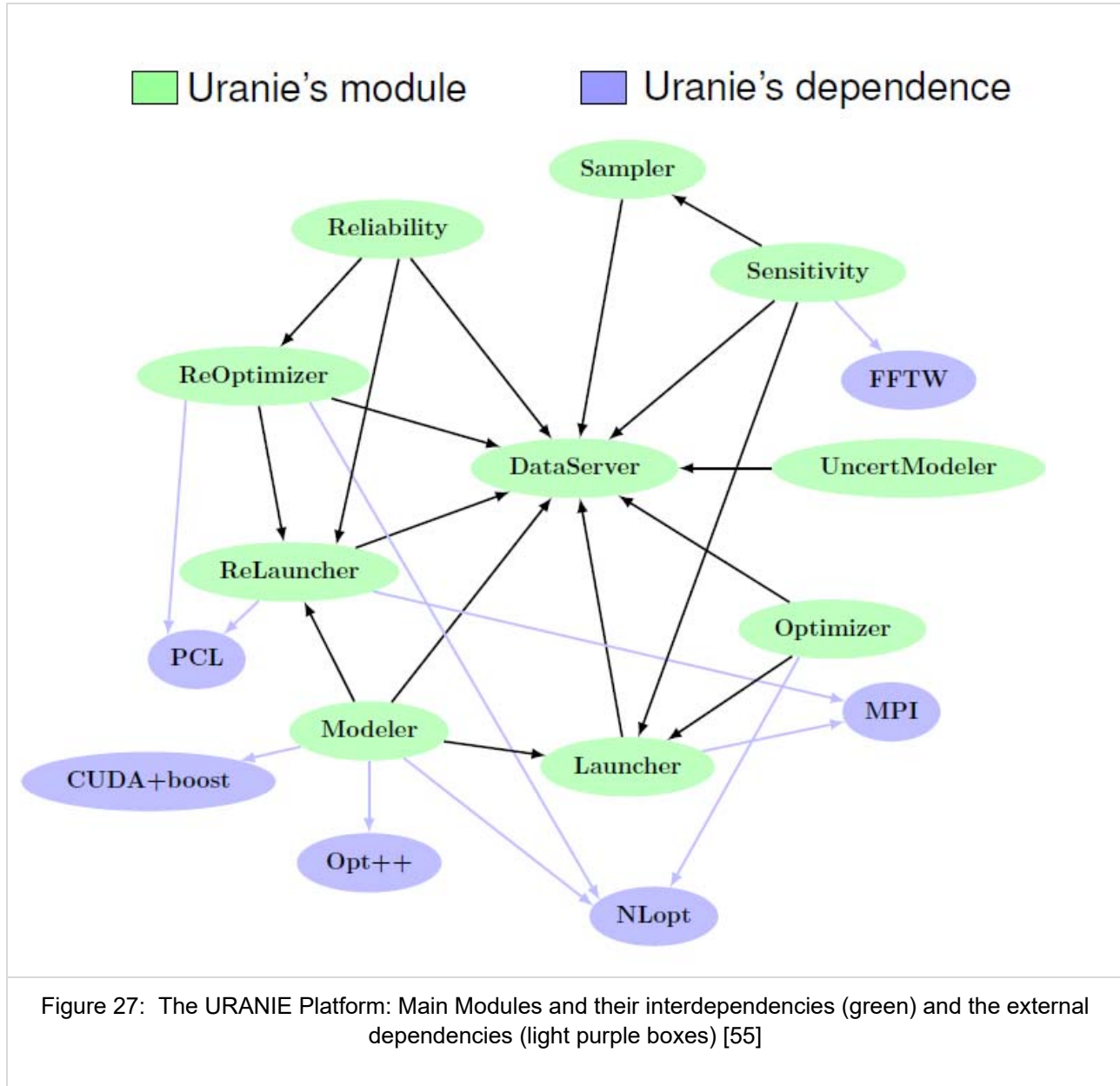
Key features of the URANIE platform are accessibility, modularity, genericity and universality. **Modularity** is assured by the modular organisation so that only needed modules can be loaded for a specific analysis while **Genericity** means that the platform can handle codes or functions as black-boxes using non-intrusive methods and hence it can be applied to all scientific fields. **Universality** means that the platform can export data and surrogate models in many formats (ASCII, XML, JSON) for use within URANIE or by other platforms. Finally, a peculiarity of URANIE is the fact that both samples and results are stored in a common object, called **TDataServer**, which is the centre of all the statistical treatments performed by the users [50].

In Figure 27, the main URANIE modules and their interdependencies are shown. Hereafter, a brief description of selected modules is given:

- **DataServer** is the core module for data handling and first statistical computation e.g. mean, standard deviation, min, max, normalization, correlation matrices, and quantile. It also define variables using pre-defined statistical laws e.g. uniform, Gaussian, exponential, triangular, etc. and it contains all the necessary information about the variables of a problem (names, units, probability laws, etc.). Finally it creates plots and import/export data in different formats e.g. ASCII, XML, JSON. The **DataServer** library defines the **TDataServer** object which contains all information about the uncertain variables for the use in a UQ-study.
- **ReLauncher**: it is the interface to code or/and function handling i.e. it applies an analytical function or an external simulation code on the content of a TDataServer. The content can either result from a design-of-experiments generated using the Sampler module, or can be loaded into the TDataServer from an external source. The ReLauncher can deal with code, Python functions, C++ interpreted and compiled functions.
- **Sampler**: it is used to create the design- of-experiments that represents the starting point for many analyses. It uses the attributes of the TDataServer, which are random variables. This module consist of the following main categories: stochastic and deterministic design. Examples for stochastic design are e.g. Simple Random Sampling (SRS), Latin Hypercube Sampling (LHS), One-At-a-Time Sampling (OAT), etc. Some examples for deterministic designs are e.g. Sobol sequence (quasi Monte Carlo), sparse grid sampling, space filling design.
- **UncertModeler**: This module examines how well a sample of data agrees with a given distribution as its population with goodness-of-fit techniques.
- **Sensitivity**: it allows to perform sensitivity analysis of the response y with respect to the inputs x in order to rank the inputs with respect to their impact on the outputs of a code or a function. Several kind of methods are available e.g. local finite differences, regression methods (Pearson values, Spearman ranks), screening (OAT, Morris, etc.), Sobol indexes (FAST, RBD, Sobol/Saltelli).
- **Modeler**: It is the module for surrogate model generation in order to reproduce the behavior of data provided. Some of the available models are: polynomial regressions, generalized linear models, , k-Nearest neighbor, Kernel methods, Artificial Neural Networks (ANN), chaos polynomial expansion,

Gaussian processes e.g. kriging with gpLib. All these models can be exported in different formats (C++, fortran, PMML) for later on use.

- **ReOptimizer:** Different types of optimization problems e.g. minimization of Single Objective (SO) or Multi Objectives (MO), optimization of parameters with impact on an objective and find possible constraints on these parameters. For it, many tools are available such as Minuit, Opt++, NLOpt and Vizir.
- **Reliability:**



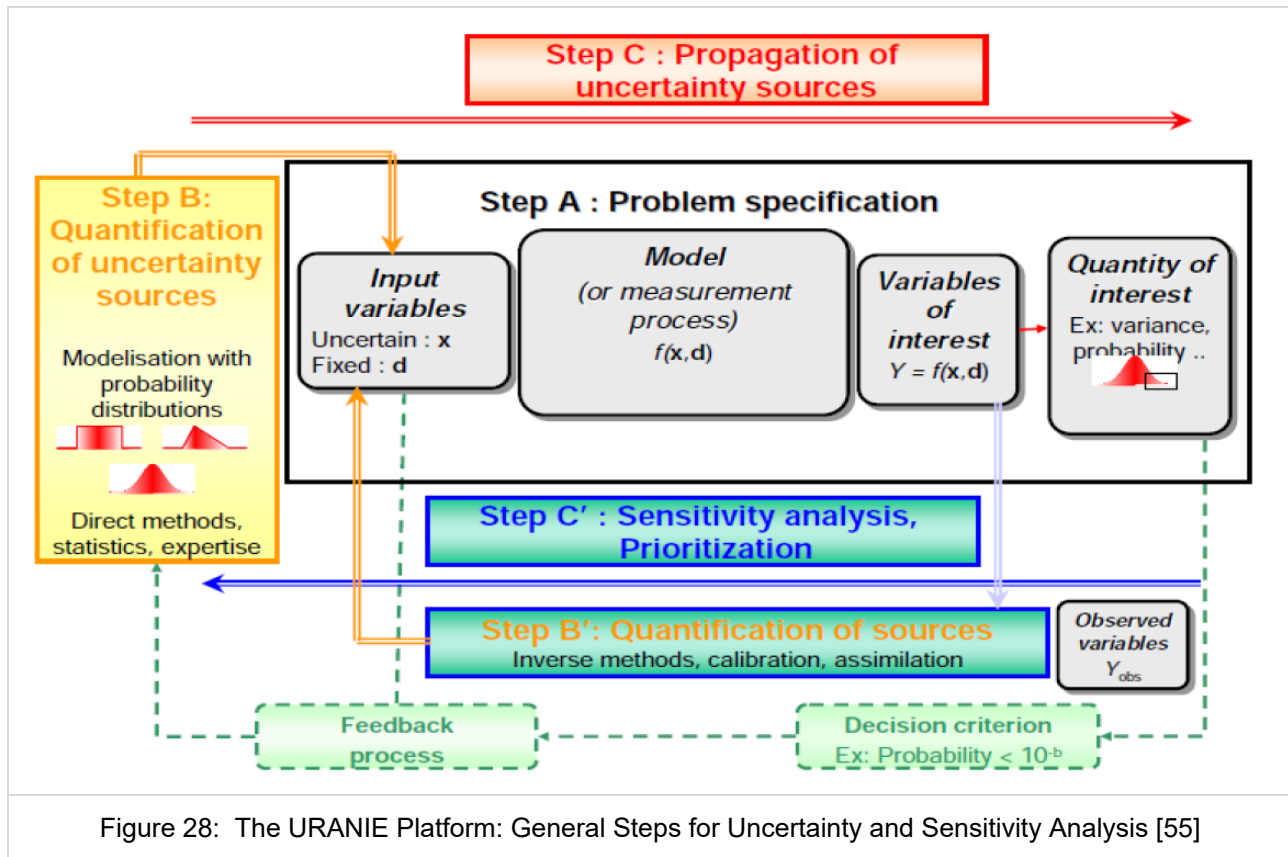
4.2 Description of main features

The general flowchart for uncertainty and sensitivity analysis using URANIE is depicted in Figure 28. According to [10], the main steps for the uncertainty propagation are listed here:

- **Step A:** Problem specification,
- **Step B:** Quantification of uncertainty sources, and
- **Step C:** Propagation of uncertainty sources.

If the view is focus on general sensitivity methods, additional steps are added e.g.:

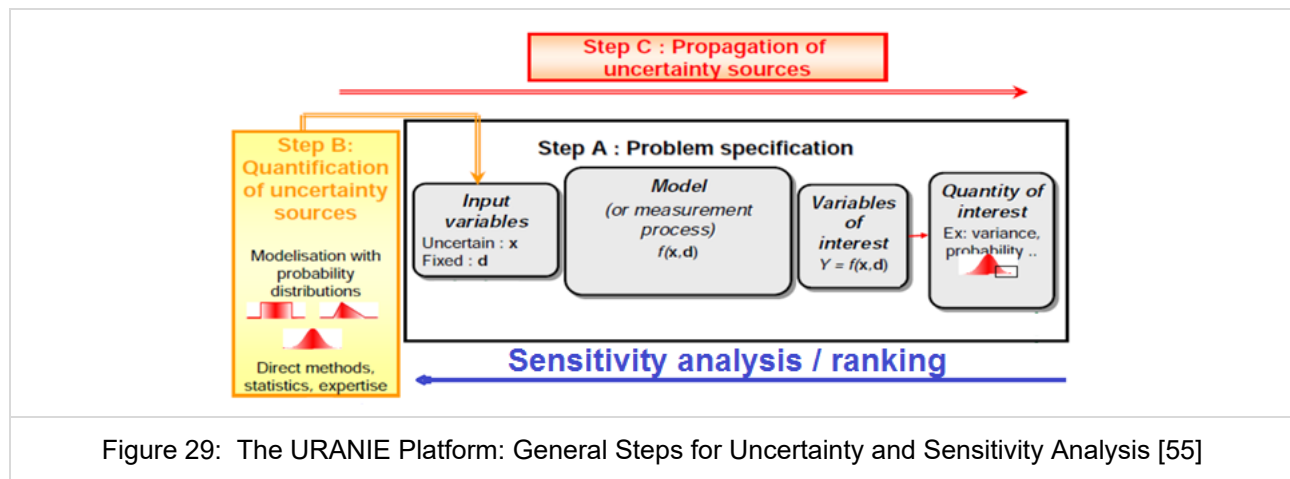
- Step B': Quantification of sources (inverse methods, calibration and data assimilation) and
- Step C': Sensitivity analysis, prioritization.



In the problem specification, Step A in Figure 29, the computer code is selected i.e. ASTEC (f) and for it the uncertain parameters (x) to be considered in the analysis of a specific accidental sequence are chosen together with the parameter range (i.e. max and min values as well as the reference value) and the corresponding probability density function (pdf). The selected uncertain parameters are a subset of the input parameters, initial conditions, boundary conditions, etc. of the specific SA-code. It means that the other parameters not considered as uncertain (x) are represented by d so that the model / code is $f(x,d)$. The output variables of interest are given by $y = f(x,d)$. Finally, the quantities of interest performing an uncertainty propagation can be classified as follows:

- Location: mean (μ), Min, Max, Median, Quantile
- Dispersion: standard deviation (σ), Variance (σ^2), Range (Max-Min), coefficient of variation ($\delta = \sigma/\mu$)
- Probability density functions (PDF), cumulative density function (CDF).

In the Step B, appropriate PDFs for each uncertain parameter needs to be determined or generated. For it, experimental data if available need to be evaluated and applying a mathematical algorithm (e.g. FFT) the proper PDF for the uncertain parameter of interest can be computed[11]. If no experimental data is available for the uncertain parameter of interest, a pdf e.g. uniform function is selected based on expert judgement. For example, if experimental data is available, the PDF can be obtained by different data fitting methods e.g. parametric (maximum likelihood, moment method, and non-parametric (histogram, kernel) methods, and statistical (Chi-squared χ^2 , Empirical Distribution Function (EDF) e.g. Kolmogorov-Smirnov D) tests or Bayesian/Bootstrap methods if the data sets are small.



In the Step C, the propagation of uncertainty sources from the input into the output is done considering the following sub-steps:

- URANIE sub-step “Design of Experiments (DoF)”: All the selected uncertainty parameter with the corresponding values (reference, MAX, MIN) and the PDFs e.g. are random sampled for example based on the Monte Carlo sampling considering the interdependences of the “uncertain variables” and the probability content as well as the level of confidence. According to the Wilk’s formula and depending if a one-side or two-side analysis is going to be done, a minimal number of cases i.e. code calculations (in URANIE: “Points of DoE”) will be generated by the tool. In order to perform N runs, each uncertain parameter is varied N-times independently of each parameter as long as the uncertain parameters are not correlated. The values for each parameters are then obtained by e.g. the random Monte Carlo sampling method. Finally yet importantly, it has to be decide if a “point” analysis or a time dependent analysis is going to be done.
- The SA-code will be run for N-times considering the values of the uncertainty parameters determined by the random Monte Carlo sampling either in sequential or in a parallel mode. This steps is normally automatized using Python scripts. As next, the output of the SA-code predicted for the variables of interest need to be extracted from the output files of the SA-codes. This process is also automatized using Python scripts, which will generate a data file in the format expected by URANIE for a subsequent treatment. URANIE offers different surrogate models (linear, polynomial, artificial neural network, kriging) to reduce the computational times of the code evaluations if needed.
- Finally, the analysis of the quantity of interest using URANIE statistic capabilities is done to obtain for example the uncertainty band of quantities of interest during the accident progression.
- A sensitivity analysis of the uncertain parameters (input) can be done afterwards regarding the variables of interest (target variables) using parametric or non-parametric correlations e.g. Spearman’s rank correlation or the Pearson’s product momentum correlation, etc.

4.3 Initial conditions

The initial conditions are specified in the input deck of the SA code and transferred to URANIE. For example, in the case of ASTEC (see Chapter 4 in the Appendix 2) such transfer is performed through a Python interface.

4.4 Boundary conditions

The boundary conditions are specified in the input deck of the SA code and transferred to URANIE. For example, in the case of ASTEC (see Chapter 4 in the Appendix 2) such transfer is performed through a Python interface.

4.5 Model parameters

The model parameters are specified in the input deck of the SA code and transferred to URANIE. For example, in the case of ASTEC (see Chapter 4 in the Appendix 2) such transfer is performed through a Python interface.

4.6 Propagation of uncertainties

Please, see Paragraph 4.2 in the Appendix 1.

4.7 Pros and Cons

The main advantages of the URANIE platform is the fact that it is an open source platform under continuous development at CEA that includes a lot of statistical tools not only for uncertainty propagation and sensitivity analysis but also for optimization, etc.. Since it is developed under Linux and it includes parallel capabilities (to be tested) is very attractive for the application in connection with severe accident codes to analyze severe accident progression, which per se are CPU-time intensive compared to the system thermal hydraulic codes.

One of the main discouraging issues for beginner user of URANIE is that it requires the installation of external packages, which have to be installed before URANIE is installed. Some of them are mandatory (ROOT, Cmake) since URANIE is built as a layer on top of ROOT in order to take profit of key features such as C++ on-the-fly compiler (CLING), Python automatic transcription, access to SQL-databases, optimal and efficient model handling, visualization, etc. Other external packages are optional e.g. CPPUnit, OPT++, FFTW, NLOpt, PCL, MPI, CUDA.

5 RAVEN (UNIROM1, JAEA)

5.1 Description of the method

The RAVEN (Risk Analysis Virtual Environment) software is open-source and can be downloaded from GITHUB [56]. The RAVEN development has begun in early 2012 at the Idaho National Laboratory (INL) to perform parametric and probabilistic analysis based on the response of complex system codes, in order to quantify the safety margins of safety-related events. Nowadays RAVEN is a multi-purpose probabilistic and uncertainty quantification platform, capable to be coupled with any system code.

RAVEN development is performed under a strict Software Quality Assurance process. Actually, it is qualified as NQ1-Lvl. 2. The overall goal was to conceive a tool to enable Risk Informed Safety Margin Characterization (RISMC):

1. Evaluating risk (uncertainty propagation)
2. Understanding risk (limit surface, ranking, sensitivity, data mining)
3. Mitigating risk (optimization)

RAVEN has been developed in a highly modular and pluggable way in order to enable easy integration of different programming languages (i.e., C++, Python) and, coupling with any system code [12]. It is capable of investigating the system response as well as the input space using Monte Carlo, Grid, or Latin Hyper Cube sampling schemes, but its strength is focused toward system feature discovery, such as limit surfaces, separating regions of the input space leading to system failure, using dynamic supervised learning techniques.

As for all PRA software, the capability to control the plant evolution during the simulation is a plus for uncertainty propagation. In system safety analysis codes, a similar need is expressed by the implementation of the control logic of the plant. As a consequence, the optimization of resources imposes the integration of this task under a common project that is RAVEN. Consequently, the plant control logic is simulated by RAVEN; this also offers the flexibility to easily implement proprietary control logic without changing RELAP or MELCOR source code.

In summary, from a user prospective, RAVEN is a tool that [57] :

1. Determines the calculation flow to achieve the most accurate evaluation of risk accounting for probabilistic behaviour and uncertainty propagation;
2. Visualizes simulations results (thousands and more) and provides the data mining capability to deeply understand the plant behaviour;
3. Provides the capability to investigate risk mitigation strategies by suggesting directions and quickly assessing impacts.

The main idea behind the design of the RAVEN framework is the creation of a multi-purpose platform characterized by high flexibility with respect to the possible performable analysis. The framework must be capable of constructing the analysis/calculation flow at run-time, interpreting the user-defined instructions and assembling the different analysis tasks following a user specified scheme. In order to achieve such flexibility, combined with reasonably fast development, a programming language naturally suitable for this kind of approach was needed: Python [58].

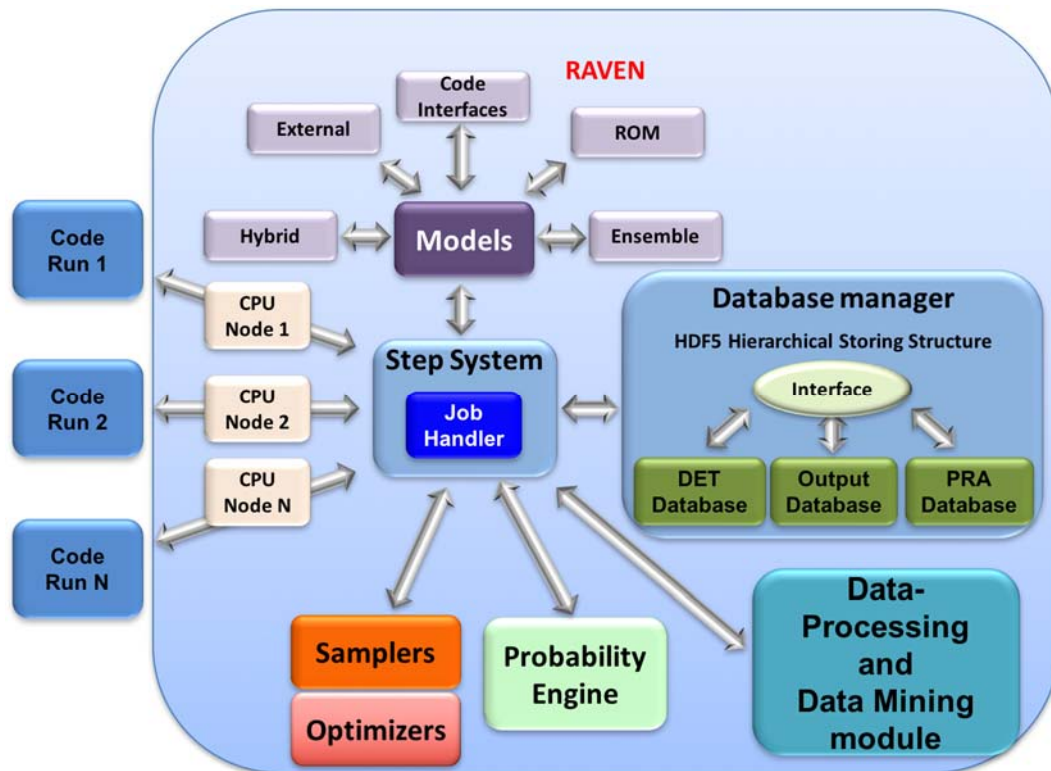


Figure 30: Schematic representation of the RAVEN software [58]

As can be inferred from above, RAVEN is coded in Python and is characterized by an object-oriented design. The core of the analysis performable through RAVEN is represented by a set of basic components (objects) the user can combine, in order to create a custom analysis flow. A list of these components and a summary of their most important functionalities are reported as follow [59]:

1. *Distribution*: In order to explore the input/output space, RAVEN requires the capability to perturb the input space (initial conditions of a system code). The initial conditions, that represent the uncertain space, are generally characterized by probability distribution functions (PDFs), which need to be considered when a perturbation is applied. In this respect, a large library of PDFs is available to choose from.
2. *Sampler*: A proper approach to sample the input space is fundamental for the optimization of the computational time. In RAVEN, a “sampler” employs a unique perturbation strategy that is applied to the input space of a system. The input space is defined through the connection of uncertain variables and their relative probability distributions.
3. *Model*: A model is the representation of a physical system (e.g. Nuclear Power Plant, etc.); it is therefore capable of predicting the evolution of a system given a coordinate set in the input space.
4. *Reduced Order Model (ROM)*: The evaluation of the system response, as a function of the coordinates in the input space, is very computationally expensive, especially when brute-force approaches (e.g. Monte Carlo methods) are chosen as the sampling strategy. Reduced Order Models could be used to lower this cost, reducing the number of needed points and prioritizing the area of the input space that needs to be explored. They can be considered as an artificial representation of the link between the input and output space for a particular system. It is not particularly indicated for SA applications due to the numerosity of cliff-edge effects.

In the framework of severe nuclear accidents RAVEN has been coupled to MELCOR code by Sapienza University of Rome. The general sketch of the process is shown in Figure 30.

The interface has three main functions [13] :

1. interpret the information coming from RAVEN;
2. translate such information in the input of the driven code;
3. manipulate output data file to create a database.

To allow RAVEN storing output data coming from MELCOR, a Python output parser has been developed to convert the plot binary file generated by MELCOR into a CSV file. To overcome the handling of large datafiles

the interface allows to create a CSV file with only variables required by the users. So, it is possible to obtain a database that comprises the required variables from all MELCOR packages. Figure 31 shows the procedural framework used for sensitivity and uncertainty analyses. A MELCOR input deck is used as template, the chosen parameters are specified as string with special characters. RAVEN can identify such parameters and replaces the string with values sampled from a specified distribution. The sampled values are implemented into N number and consequently N-MELCOR input decks are generated. Data resulting from simulations are stored into a database that can be used to perform statistical analyses.

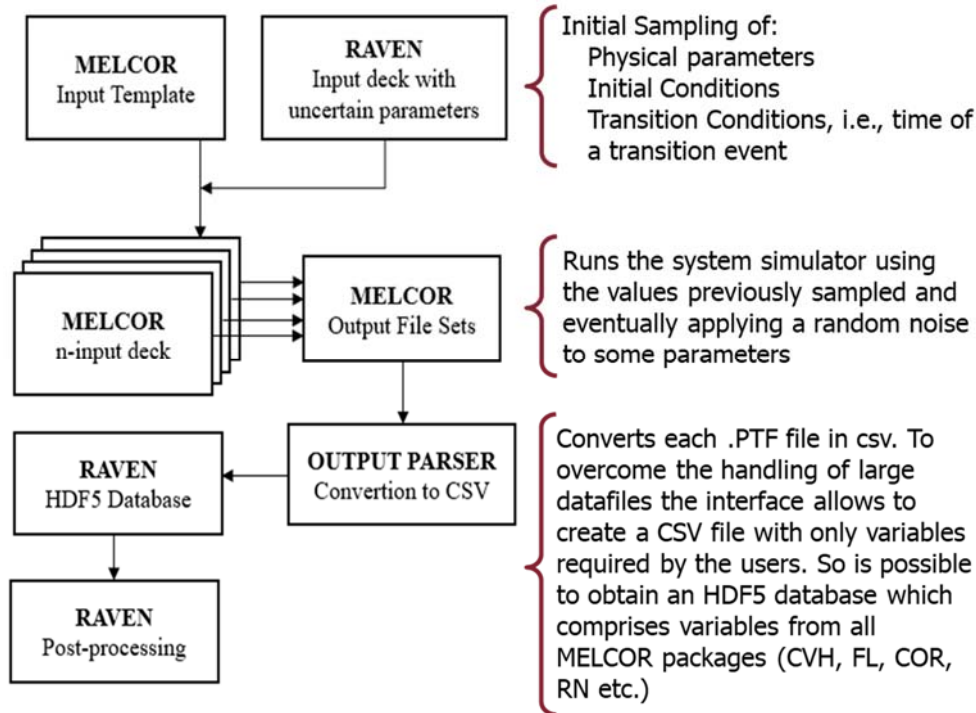


Figure 31: MELCOR-RAVEN coupling interface

5.2 Description of main features

5.2.1 Uncertainty analysis

5.2.1.1 Distributions

RAVEN provides support for several probability distributions. Currently, the user can choose among several 1-dimensional distributions and N-dimensional ones, either custom or multidimensional normal.

1. *One-Dimensional Probability Distributions*: both continuous and discrete distributions can be used. Each distribution has a pre-defined, default support (domain) based on its definition, however these domains can be shifted/stretched and truncated using the appropriate parameters where applicable. The continuous distribution supported by RAVEN are as follow:
 - Beta Distribution
 - Exponential Distribution
 - Gamma Distribution
 - Laplace Distribution
 - Logistic Distribution
 - LogNormal Distribution
 - LogUniform Distribution
 - Normal Distribution
 - Triangular Distribution
 - Uniform Distribution
 - Weibull Distribution

RAVEN currently supports 3 discrete distributions. In the following paragraphs, the input requirements are reported:

- Bernoulli Distribution
- Binomial Distribution
- Geometric Distribution
- Poisson Distribution
- Categorical Distribution
- Markov Categorical Distribution

2. *N-Dimensional Probability Distributions*: allow the user to model stochastic dependences between parameters. Thus, instead of using N distributions for N parameters, the user can define a single distribution lying in a N-Dimensional space. The following N-Dimensional Probability Distributions are available within RAVEN:

- Multivariate normal distribution
- ND Inverse Weight interpolation distribution
- ND spline interpolation distribution

5.2.1.2 Sampling strategies

The sampler is probably the most important entity in the RAVEN framework. It performs the driving of the specific sampling strategy and, hence, determines the effectiveness of the analysis, from both an accuracy and computational point of view. The samplers, that are available in RAVEN, can be categorized into three main classes:

1. *Forward*: collects all the strategies that perform the sampling of the input space without exploiting, through dynamic learning approaches, the information made available from the outcomes of calculations previously performed (adaptive sampling) and the common system evolution (patterns) that different sampled calculations can generate in the phase space (dynamic event tree). In the RAVEN framework, several different “Forward” samplers are available:
 - Monte Carlo
 - Stratified
 - Grid Based
 - Sparse Grid Collocation
 - Sobol Decomposition
 - Response Surface Design of Experiment
 - Factorial Design of Experiment
 - Ensemble Forward Sampling strategy
 - Custom Sampling strategy

Among these, the Monte-Carlo sampling approach is one of the most well-known and widely used approaches to perform exploration of the input space. The main idea behind Monte-Carlo sampling is to randomly perturb the input space according to uniform or parameter-based probability density functions.

2. *Dynamic Event Tree* (still under development for MELCOR): this sampling strategy is designed to take the timing of events, in transient/accident scenarios, explicitly into account. In practice, a single simulation is spawned and a set of triggers is added to the system code control logic. Every time a trigger is activated (one of the CDF thresholds in the grid is exceeded), a new set of simulations (branches) is spawned. Each branch carries its conditional probability. In the RAVEN code, the triggers are defined by specifying a grid using a predefined discretization metric in the mode input space. RAVEN provides two discretization metrics: 1) CDF, and 2) value. Thus, the trigger thresholds can be entered either in probability or value space.
3. *Adaptive*: provides the possibility to perform smart sampling (also known as adaptive sampling) as an alternative to classical “Forward” techniques. The motivation is that system simulations are often computationally expensive, time-consuming, and high dimensional with respect to the number of input parameters. Thus, exploring the space of all possible simulation outcomes is infeasible using finite computing resources.

5.2.1.3 Statistical Post-processing

The RAVEN framework provides the capability to store and retrieve data to/from an external database. Currently RAVEN has support for only a database type called HDF5. Starting from the database, different kind of data objects (PointSet, HistorySet, DataSet) can be obtained to perform statistical post-processing, which is one of the most assessed ways to investigate the impact of the intrinsic variation of the input space among several figure of merits.

Currently, the following types are available in RAVEN:

- BasicStatistics
- ComparisonStatistics

The BasicStatistics post-processor is the container of the algorithms to compute many of the most important statistical quantities. It is important to notice that this post-processor can accept as input both PointSet and HistorySet data objects, depending on the type of statistics the user wants to compute.

Currently the scalar quantities available for request are:

- expectedValue: expected value or mean
- minimum: The minimum value of the samples
- maximum: The maximum value of the samples
- median
- variance
- sigma: standard deviation
- percentile
- variationCoefficient
- skewness
- kurtosis (also known as Fisher's kurtosis)
- samples: the number of samples in the data set used to determine the statistics.

The matrix quantities available for request are:

- sensitivity: matrix of sensitivity coefficients, computed via linear regression method
- NormalizedSensitivity: matrix of normalized sensitivity coefficients
- covariance: covariance matrix
- pearson: matrix of correlation coefficients
- VarianceDependentSensitivity: matrix of sensitivity coefficients dependent on the variance of the variables

The ComparisonStatistics post-processor is capable to compare the obtained results with experimental results (or with another calculation) through a numerical quantification of the differences. The available methods for the comparison are:

- CDF area difference (Minkowsky L1 metric)
- PDF area difference
- difference PDF metric [60]

These functions are useful especially for the validation of new models or codes.

5.2.2 Sensitivity analysis

Global sensitivity estimators described in the previous paragraph can be used also to perform sensitivity analyses in RAVEN.

5.2.3 Dynamic PRA

The PRA analysis needs an approximation to this distribution for selected consequence variables. A way to achieve this goal is an Event Tree approach. In dynamic PRA analysis, Conventional Event Tree sequences are run simultaneously starting from a single initiating event. The branches occur at user specified problem times and/or when an action is required by the operator and/or the system, creating a deterministic sequence of events based on the time of their occurrence. One of the disadvantages of this method is that the timing/sequencing of events and system dynamics is not explicitly accounted for in the analysis. In order to overcome these limitations a "dynamic" approach is needed. The Dynamic Event Tree (DET) technique brings

several advantages, among which is the fact that it simulates probabilistic system evolution in a way that is consistent with the severe accident model. The dynamic PRA, in general, and the Dynamic Event Tree methodologies in particular, are designed to take the timing of events explicitly into account, which can become very important especially when uncertainties in complex phenomena are considered.

5.3 Initial conditions

Initial conditions can be set in MELCOR2.2 input deck, which is text-based and can be perturbed by RAVEN.

5.4 Boundary conditions

Boundary conditions can be set in MELCOR2.2 input deck, which is text-based and can be perturbed by RAVEN.

5.5 Model parameters

Model parameters and other options can be set in MELCOR2.2 input deck, which is text-based and can be perturbed by RAVEN.

5.6 Propagation of uncertainties

Uncertainty propagates from random input sampling, input deck perturbation, MELCOR2.2 execution and finally to output data analysis.

5.7 Pros and Cons

RAVEN is a very flexible instrument ready to carry out the UQ for SA codes as MELCOR and MAAP. It is open source, a large number of statistical instruments are available, and the dynamic PRA analysis is a useful tool for the evaluation of the SA transients.

Actually, a GUI is not available, but the input is in XML format and then it is easy to develop a GUI capable to generate the XML input.

6 References

- [1] M. Kloos, "Main features of the tool SUSA 4.0 for uncertainty and sensitivity analyses. Proceedings of," in *ESREL Conference*, Zürich, Schweiz, 2015.
- [2] M. Kloos, "SUSA - Software for uncertainty and sensitivity analyses, Version 4.2, User's Guide and Tutorial. GRS-P-5, Vol. 1, Rev. 5," GRS, Garching, 2019.
- [3] H. JC and D. FJ, "Latin hypercube sampling and the propagation of uncertainty in analyses of complex systems.," *Reliab Eng Syst Safety*, p. 23–69., 81 2003.
- [4] H. JC, D. FJ and J. JD, "A comparison of uncertainty and sensitivity analysis results obtained with random and Latin hypercube sampling," *Reliab Eng Syst Safety*, p. 305–330, 89 2005.
- [5] S. S. Wilks, "Determination of Sample Sizes for Setting Tolerance Limits," *Ann. Math. Stat.*, p. 91–96, 1941.
- [6] S. S. Wilks, "Statistical Prediction with Special Reference to the Problem of Tolerance Limits," *Ann. Math. Stat.*, p. 400–409, Nr.4 Vol.13 1942.
- [7] H. Glaeser, " "GRS method for uncertainty and sensitivity evaluation of code results and applications," *Sci. Technol. Nucl. Install.*, 2008.
- [8] K. S. and J. N. L., *Encyclopedia of statistical sciences*, Volume 4, Wiley & Sons, 1983.

- [9] E. Hofer, “ Sensitivity analysis in the context of uncertainty analysis for computationally intensive models,” *Computer Physics Communications*, , pp. 21-34, 1999.
- [10] M. Kloos, “Sensitivity analyses supplemented to epistemic uncertainty analyses for PSA results,” in *Proceedings of PSAM 11*, Helsinki, Finland., 2012.
- [11] K. M. G. and S. A., *The advanced theory of statistics, Vol. 2: Inference and relationship*. 3rd ed, New York: MacMillan Publishing Co., 1973. .
- [12] I. R.L. and H. S. C., “A robust measure of uncertainty importance for use in fault tree system analysis,” *Risk Analysis*, p. 401–406, 1990 .
- [13] M. D. McKay, “ Variance-based methods for assessing uncertainty importance, NUREG-1150 analyses. LA-UR-96-2695; 1–27.” USA , 1996.
- [14] I. Sobol, “ Sensitivity estimates for nonlinear mathematical models.,” *Math Model & Computational Experiments*, p. 407–414, 1 1993.
- [15] S. A., K. Chan and E. Scott, *Sensitivity analysis*, Wiley Series in Probability and Statistics, Wiley, 2000.
- [16] G. L. A. and K. W. H., “Measures of Association for Cross Classification,” *Journal American Statistical Association*, pp. 310-364, 1963.
- [17] M. Kloos and e. al., “MCDET: A Tool for Integrated Deterministic Probabilistic Safety Analyses,” in *Advanced Concepts in Nuclear Energy Risk Assessment and Management*, World Scientific Publishing Company., 2018.
- [18] E. Chonacki and a. J. Baccou, “SUNSET V2.1: Theory Manual and User Guide,” IRSN, Cadarache, 2013.
- [19] B. M. Adams and e. al., “Dakota, A Multilevel Parallel Object-Oriented Framework for Design Optimization, Parameter Estimation, Uncertainty Quantification, and Sensitivity Analysis: Version 6.6 Theory Manual. SAND2014-4253,” Sandia Nat. Lab., USA, 2014.
- [20] B. M. Adams and et.al., “Dakota, A Multilevel Parallel Object-Oriented Framework for Design Optimization, Parameter Estimation, Uncertainty Quantification, and Sensitivity Analysis: Version 6.6 Reference Manual. SAND2014-5015,” Sandia Nat. Lab, USA, 2014.
- [21] “Dakota homepage,” Sandia Nat. Lab., 2020. [Online]. Available: <https://dakota.sandia.gov/>.
- [22] Applied Programming Technology Inc., “Symbolic Nuclear Analysis Package (SNAP). User ’ s Manual.,” APT, USA, 2012.
- [23] M. M. D., R. J. Beckman and C. and W. J., “A comparison of three methods for selecting values of input variables in the analysis of output from a computer code,” *Technometrics*, p. pp. 55–61, 42 No.1 2000.
- [24] B. M. Adams et al., “Dakota, A Multilevel Parallel Object-Oriented Framework for Design Optimization, Parameter Estimation, Uncertainty Quantification, and Sensitivity Analysis: Version 6.6 User's Manual,SAND2014-4633,” Sandia, USA, 2014.
- [25] R. Bocanegra, G. Jimenez and a. M. Fernandez-Cosials, “Development of a PWR-W GOTHIC 3D model for containment accident analysis,” *Ann. Nucl. Energy*, p. 547–560, 2016.
- [26] U. NRC, “AN APPROACH FOR DETERMINING THE TECHNICAL ADEQUACY OF PROBABILISTIC RISK ASSESSMENT RESULTS FOR RISK-INFORMED ACTIVITIES, Regulatory Guide 1.203,” December 2005. [Online]. Available: <https://www.nrc.gov/docs/ML0535/ML053500170.pdf>.
- [27] C. J. Roy and W. L. Oberkampf, “A comprehensive framework for verification, validation, and uncertainty quantification in scientific computing,” *Comput. Methods Appl. Mech. Eng.*, p. 2131–2144, Nr. 25-28 Vol.200 2011.
- [28] R. Orive, I. C. G. P. J., J. Arias, J. R. Alonso and a. J. Á. Martinez, “Uncertainties Study into the LWR Containment Analyses,” in *ICAPP-5023*, Seoul, Korea, 2015.

- [29] L. L. Humphries, R. K. Cole, D. L. Louie, V. G. Figueroa and a. M. F. Young, "MELCOR Computer Code Manuals, Vol. 1: Primer and Users' Guide. SAND2015-6691 R," SANDIA Nat. Lab, USA, 2015.
- [30] K. W. Ross, J. Phillips, R. O. Gauntt and a. K. C. Wagner, "MELCOR Best Practices as Applied in the State-of-the-Art Reactor Consequence Analyses (SOARCA) Project, Nureg/Cr-7008, p. 133," ANL , USA, 2014.
- [31] J. Baccou and et.al., "SAPIUM: Development of a Systematic APproach for Input Uncertainty quantification of the physical Models in thermal-hydraulic codes, Good Practices Guidance Report,," NEA/CSNI/R(2019)xx, Paris, France, 2019.
- [32] P. Mattie and et.al., "State-of-the-Art Reactor Consequence Analyses Project , Uncertainty Analysis of the Unmitigated Long-Term Station Blackout of the Peach Bottom Atomic Power Station, NUREG/CR-7155," USA, 2016.
- [33] Sandia National Lab, "Severe Accident Analysis Department, State-of-the-Art Reactor Consequence Analyses (SOARCA) Project. Sequoyah Integrated Deterministic and Uncertainty Analyses, NUREG/CR-7245," US NRC, USA, 2019.
- [34] R. E. Walpole, R. H. Myers, S. L. Myers and a. K. E. Ye, Probability & Statistics for Engineers & Scientists, MyLab Statistics Update. Pearson..
- [35] J. C. Helton, J. D. Johnson, W. L. Oberkampf and and C. J. Sallaberry, "Representation of Analysis Results Involving Aleatory and Epistemic Uncertainty, SAND2008-4379," Sandia Nat. Lab, USA, 2008.
- [36] S. Destercke, *Epistemic uncertainty propagation in risk/reliability analyses: an introduction to imprecise probabilities.,* 2017., France: CRNS, 2017.
- [37] P.-S. D. Laplace, "Essai Philosophique sur les probabilités," France, 1814.
- [38] F. Galton, "Co-relations and their measurement, chiefly from anthropometric data," *Proc. R. Soc. London*, p. 135–145, Vol 45 1889.
- [39] Student, "The Probable Error of a Mean," *Biometrika*, pp. 1-25, Nr.1 Vol.6 1908.
- [40] F. Mascari, G. Vella, B. G. Woods, K. Welter and a. F. D'Auria, "Analysis of Primary/Containment Coupling Phenomena Characterizing the MASLWR Design During a SBLOCA Scenario," IntechOpen, 2012, p. Ch. 8., Vienna, Austria.
- [41] F. Mascari and et.al., "Analysis of the OSU-MASLWR 001 and 002 Tests by using TRACE code, NUREG/IA-0466," US NRC, USA, 2016.
- [42] F. Mascari, J. C. D. L. R. Blul, M. Sangiorgi and a. G. Bandini, " Analyses of an Unmitigated Station Blackout Transient in a Generic PWR-900 with ASTEC , MAAP and MELCOR Codes, NUREG/IA-0515," 2019., US NRC, USA, 2019.
- [43] S. M. Bajorek and a. C. Gingrich, "Uncertainty Methods Framewor. Development for the TRACE Thermal-Hydraulics Code by the U.S.NRC," in *Proc. OECD/CSNI Work. Best Estim. Methods Uncertain. Eval. NEA/CSNI/R(2013)8/PART2*, pp. 148–157, 2013.
- [44] A. Guba, M. Makai and L. Pál, "Statistical aspects of best estimate method-I," *Reliab. Eng. Syst. Safety*, p. 217–232, Nr.3 Vol.80 2003.
- [45] A. Bersano and F.Mascari, "Evaluation of a Double-Ended Guillotine Break Transient in a Three-Loop PWR-900 Like with TRACE Code Coupled with DAKOTA Uncertainty Analysis," *Int. J. Nucl. Power, November/December, Oct. 2019*, no. 64 Issue 11/12 vol. 1 2019.
- [46] K. A. Gamble and a. L. P. Swiler, "Uncertainty quantification and sensitivity analysis applications to fuel performance modeling," in *Top Fuel 2016: LWR Fuels with Enhanced Safety and Performance, SAND2016-4597C*, 2016, pp. 1289–1298.
- [47] F. Mascari, "ENEA ACTIVITIES IN THE FIELD OF SEVERE," ENEA, Italy, 2019.

- [48] USNRC, "TRACE TRACE V5.840 Theory manual, Field equations, solution methods, and physical models," U. S. Nuclear Regulatory Commission, Washington, DC, U.S., 2013.
- [49] M. E. Stephens, B. W. Goodwin and a. T. H. Andres, "Deriving parameter probability density functions," *Reliab. Eng. Syst. Safety*, p. 271–291, Vol.42 1993.
- [50] J.-B. Blanchard, G. Damblin, J.-M. Martinez, G. Arnaud and a. F. Gaudier, "The Uranie platform: an open-source software for optimisation, meta-modelling and uncertainty analysis," *EPJ Nucl. Sci. Technology*, p. 4, Vol5 2019.
- [51] F. Gaudier, "URANIE : The CEA/DEN Uncertainty and Sensitivity platform," *Procedia Social and Behavioral Sciences*, p. 7660–766, 2 2010.
- [52] R. Brun and F. Rademakers, "ROOT- An object oriented data analysis framework," *Nuclear Instruments and Methods in Physics Research, Section A*, pp. 81-86, 1997.
- [53] I. Antcheva, . M. Ballintijn, B. Bellenot, M. Biskup, R. Bruna, N. Buncica, P. Canal, D. Casadei, O. Couet, V. Fine, 1. G. G. L. Franco, A. Gheata, D. G. Maline, M. Goto, J. Iwaszkiewicz, A. Kreshuk, D. M. Segura, R. Maunder, L. Moneta and A. Naumann, "ROOT-A C++ framework for petabyte data storage, statistical analysis and visualization," *Computer Physics Communications*, pp. 2499-2512, 180 2009.
- [54] URANIE, "Uranie," 2020. [Online]. Available: <https://sourceforge.net/projects/uranie>.
- [55] E. d. Rocquigny, "Quantifying uncertainty in an industrial approach: an emerging consensus in an old epistemological debate," *Surveys and Perspectives Integrating Environment and Society*, Vol.2 2.1 2009.
- [56] Raven, "RAVEN homepage on github," Idaho National Laboratory, 2020. [Online]. Available: <https://github.com/idaholab/raven>.
- [57] A. Alfonsi et al., "RAVEN User Guide. INL/EXT-18-44465," INL, USA, 2017.
- [58] A. Alfonsi, "Raven as a tool for dynamic probabilistic risk assessment: Software overview," INL, USA, 2013.
- [59] A. Alfonsi and et.al., "RAVEN Theory Manual,RAVEN Theory Manual,INL/EXT-16-38178 Revision 3," INL, Idaho Falls, 2016.
- [60] V. Narcisi, P. Lorusso, F. Giannetti, A. Alfonsi and a. G. Caruso, "Uncertainty quantification method for RELAP5-3D© using RAVEN and application on NACIE experiments," *Ann. Nucl. Energy*, p. 419–432, Vol.127 2019.

Appendix 2: Experience from application of the UQ-methods (Task 2)

K. Chevalier (IRSN), V. Sanchez (KIT)

Version 06 – 08/04/2021

Content

Content	3
List of figures	4
List of Tables	6
1 SUSA (GRS, LEI, BELV)	7
1.1 Experience of the GRS applying SUSa with a SA-Code (GRS)	7
1.2 Modelling of experiments using best estimate approach (LEI).....	9
1.3 Modelling of accidents using Theory of Probabilistic Dynamics (LEI)	13
1.4 Experience from the application of SUSa (Bel V)	15
2 SUNSET (IRSN, INRNE, LEI, TUS)	17
2.1 Epistemic variables using probabilistic framework (IRSN)	17
2.2 Best estimate approach for modelling of QUENCH-03 experiment (LEI)	19
3 DAKOTA (ENEA, CIEMAT, TRACTEBEL).....	20
3.1 MELCOR/DAKOTA/SNAP Applications (ENEA).....	20
3.1.1 CASE 1: MELCOR/DAKOTA coupling against CSTF-AB1 test	20
3.1.2 CASE 2: MELCOR/DAKOTA coupling for a PWR.....	24
3.2 Uncertainty quantification of in-pool fission product retention during BWR station Black-out sequences (CIEMAT)	27
3.3 Uncertainty quantification for different codes (Tractebel).....	27
4 URANIE (KIT, BELV)	29
4.1 The ASTEC/URANIE platform (KIT).....	29
4.1.1 Application of the ASTEC/URANIE platform to QUENCH-08 Experiment	30
4.1.2 The ASTEC/URANIE results for the QUENCH-08 Experiment.....	33
4.1.3 Performance of the ASTEC/URANIE application to the QUENCH-08 Experiment.....	35
4.2 Bel V Experience from the application of URANIE	36
5 RAVEN (UNIRM1, JAEA)	37
5.1 Source term uncertainty quantification and global sensitivity analysis.....	37
5.2 Other applications.....	37
6 References	38

List of figures

Figure 1: Time point of the vessel failure.....	7
Figure 2: Cumulated hydrogen production	8
Figure 3: I ₂ concentration in gas shown (209 selected runs; reference calculation of the I ₂ concentration in gas (red) and experimental values (blue marks)); RI concentration in gas (209 selected runs; reference calculation of the RI concentration in gas (red) and experimental values (yellow marks))	9
Figure 4: Results of RELAP/SCDAPSIM calculation of QUENCH-06 experiment: a) behaviour of cladding temperatures of the fuel rod imitator from the inner rod ring at 750 mm-height; b) amount of generated hydrogen	9
Figure 5: Influence of uncertain parameters to the calculation results: a) cladding temperature of the fuel rod imitators in the outer ring at 750 mm-height. Heat up phase and transient phase; b) hydrogen calculation results	10
Figure 6: Results of ASTEC calculation of PHEBUS FPT1 experiment: a) fuel cladding temperature at 700 mm elevation; b) total hydrogen generation	10
Figure 7: Mass of aerosols in gas phase of containment (maximum, minimum, median, average and experiment values)	11
Figure 8: Spearman's rank correlation coefficients for suspended aerosol mass (only parameters with values >0.3 at least at one point are highlighted)	11
Figure 9: Spearman's rank correlation coefficients for aerosol deposition on containment floor.....	11
Figure 10: Spearman's rank correlation coefficients for aerosol deposition on the condensers and in a sump	11
Figure 11: Comparison of the parameter uncertainty and the user effect standard deviation bands: a) pressure; b) hydrogen concentration	12
Figure 12: Obtained sensitivity measures (Spearman's coefficients): a) for pressure; b) for hydrogen concentration in the dome	13
Figure 13: Obtained tolerance limits of vertical profiles at the end of the experiment: a) steam volume fraction; b) temperature	13
Figure 14: Example of time-dependent uncertainty analysis of rupture probability estimate	14
Figure 15: Example of time-dependent sensitivity analysis providing PCC	14
Figure 16: Mean axial power distribution during steady state.	16
Figure 17: Uncertainty results for axial power profile during steady state.....	16
Figure 18: Spearman's Rank coefficients for the steady state axial power distribution.	17
Figure 19: Experience from application of the UQ-methods, IRSN, epistemic variables using probabilistic framework: iodine related source term	18
Figure 20 : Depending on the scenario the iodine release ranges from ~0.1g to ~5g	18
Figure 21: Results of ASTEC calculation of QUENCH-03 experiment: a) cladding temperatures of the fuel rod imitator from the outer ring at 750 mm height; b) amount of generated hydrogen.....	19
Figure 22: Influence of uncertain parameters to the calculation results: a) cladding temperature of the fuel rod imitators in the outer ring at 750 mm height; b) hydrogen calculation results	20
Figure 23: DAKOTA SNAP property Tab for the ENEA CASE 1.	21
Figure 24: Variate and Response data: input uncertain parameter vs iteration index for the ENEA case1. ...	22
Figure 25: Variate and Response data: FOM VS input uncertain parameters: SUSP and MMD VS D1 (CHI) and d2 (GAMMA) for the ENEA Case 1.	22

Figure 26: SUSP dispersion of the results against the experimental data, cumulative distribution function, and probability density function (ENEA CASE 1).	23
Figure 27: SNAP JOB-STATUS during the DAKOTA uncertainty application (ENEA CASE2).	25
Figure 28: Total hydrogen mass generated dispersion, cumulative distribution function, and probability density function (ENEA CASE 2).	25
Figure 29: DAKOTA input reported in the automatically generated report.....	27
Figure 30: Uncertainty quantification of FRAPCON/FRAPTRAN using DAKOTA for the IFA-LOCA test	28
Figure 31: Approach followed for the Uncertainty quantification in the frame of PREMIUM benchmark.....	29
Figure 32: Flowchart of the ASTEC/URANIE Platform developed at KIT [24]	30
Figure 33: Sketch of the QUENCH facility [25].....	31
Figure 34: QUENCH-08 experiment.....	31
Figure 35: ASTEC/URANIE results: H2 mass and production rate [24].....	33
Figure 36: Sensitivity of the H2 production on the input parameters for the geometry and the scenario [24]	34
Figure 37: Sensitivity of the H2 production on the input parameters for radiative and convection heat exchange [24]	34
Figure 38: Sensitivity of the H2 production on the input parameters for relocation and oxidation of the molten material [24]	35
Figure 39: Uncertainty Propagation for PERICLES tests – Cladding Temperatures	37

List of Tables

Table 1: Distribution of aerosol deposition	12
Table 2: Rank of uncertain parameter according to their effect on the axial power distribution	17
Table 3: Variation of correlation coefficients through time	18
Table 4: Uncertainty input parameters range (ENEA CASE1) [12] [17] [11].....	21
Table 5: Statistical results, reported in the automatically generated DAKOTA report, for SUSP-FOM (ENEA CASE 1).	23
Table 6: Response correlation, reported in the automatically generated DAKOTA report, for SUSP FOM (ENEA CASE 1).	23
Table 7: Uncertainty Quantification Input Options - Model Variables and Distributions (ENEA CASE2).	24
Table 8: Statistical results based on the 59 samples (ENEA CASE 2).	26
Table 9: Response correlation reported in the automatically generated DAKOTA report based on the 59 samples (ENEA CASE 2).	26
Table 10: Input parameters of the ASTEC/URANIE analysis of the QUENCH-08 test [24].....	32
Table 11: CPU wall-clock time of URANIE: original vs. update	35

1 SUSAs (GRS, LEI, BELV)

1.1 Experience of the GRS applying SUSAs with a SA-Code (GRS)

SUSA can be used in any application area. It has been mainly applied with the codes of the GRS code system AC2 (ATHLET, ATHLET-CD und COCOSYS) as well as with the codes TESPA-ROD, QUABOX/CUBBOX, EVNTRE and ASTEC. Moreover, SUSA is part of the GRS program system SUnCISTT for considering uncertainties in the frame of criticality analysis. Outside GRS, SUSA is mainly used in combination with the codes RELAP5, MAAP (version MAAP-CANDU) and DYN3D.

The approach implemented in SUSA for considering uncertainties is acknowledged worldwide and applied in licensing processes in France, USA, Korea and Lithuania. In the project 'Best Estimate Methods – Uncertainty and Sensitivity Evaluation (BEMUSE)' of OECD NEA (2003 – 2011), where different methods for uncertainty and sensitivity analyses were applied, most of the participating organizations applied the approach developed at GRS and implemented in SUSA.

BETMI-2 calculation (Benchmark Exercise on the TMI-2 Plant): The simulation for the surge-line break with simultaneous loss of offsite power (Sequence 2) has been complemented by an uncertainty and sensitivity analysis [1]. In the study 25 uncertain parameters have been considered. These parameters were related to the thermal hydraulics, the boundary conditions, the oxidation modelling, the formation and relocation of metallic as well as ceramic melt, and some additional parameters. Altogether 100 calculations have been performed, for which the input parameters have been determined by simple random sampling. The analyses comprised of 10 scalar and 12 time-dependent variables.

For the scalar output variables the cumulative distribution function together with the corresponding two-sided 95/95 tolerance limits have been calculated, while in case of time-dependent outputs the two-sided 95/95 tolerance limits have been determined for the whole simulation time. For the sensitivity analysis the Spearman's Rank correlation coefficient has been considered.

The time point of the vessel failure is one of the main results. The simulated results are shown in Figure 1. The lower and upper uncertainty limits are 3523s and 4684s, respectively. The left side of the Figure illustrates the cumulative distribution function as well. The right side of the figure shows the sensitivity analyses result: the heat conductivity of the ceramic melt, the relocation velocity of the metallic melt, the interfacial friction within the rod bundles, and the containment pressure proved to be the most influential input parameters.

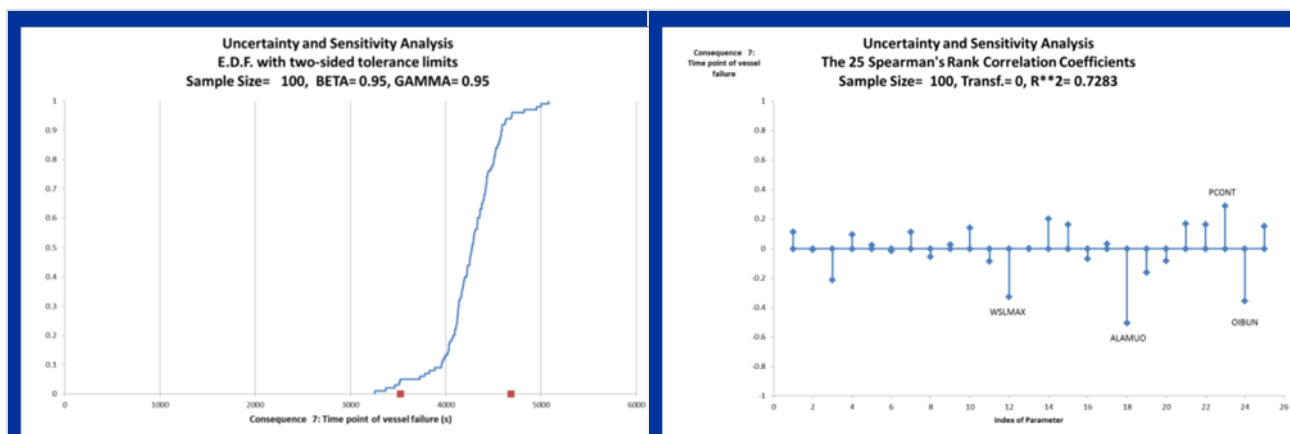


Figure 1: Time point of the vessel failure

Another important aspect of a severe accident is the hydrogen production. The simulated results concerning the cumulated hydrogen production are depicted in Figure 2. As it can be seen the uncertainty range is relatively large, especially after the melt relocation into the lower plenum has started. The most dominant input parameter is the containment pressure: the lower the backpressure, the larger the steam production and thus stronger the cladding oxidation.

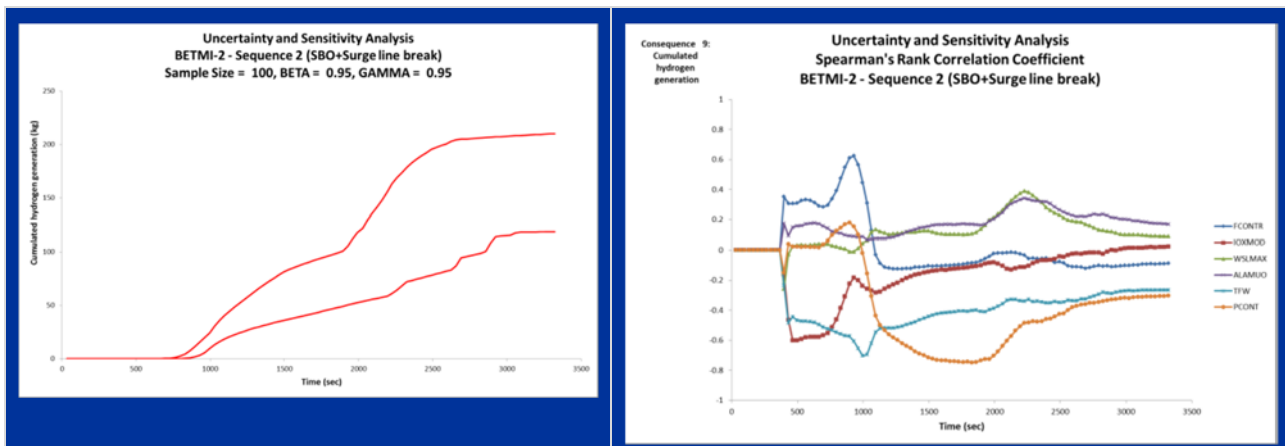


Figure 2: Cumulated hydrogen production

Another example of an UaSA performed by GRS is the Uncertainty and Sensitivity Analysis on the Iodine Model in the Containment Code COCOSYS.

Taken from [2] the uncertainty and sensitivity analysis of a COCOSYS-AIM calculation on the iodine behavior in the containment of PHEBUS test FPT1 delivered useful and detailed information on the accuracy of the iodine results in the sump, the gas phase and the potential source term.

The determination of the iodine source term to the environment under severe LWR accident conditions requires an accurate calculation of the iodine behavior in the containment. In order to investigate the iodine source term predictability by COCOSYS-AIM an uncertainty and sensitivity study on a post-test, multi-compartment calculation on PHEBUS test FPT1 was made. 93 uncertain input and model parameters including 56 iodine reaction rate constants were considered. The study was performed in two steps with 208 variation runs each.

The calculated statistical tolerance limits of the sum of all airborne iodine species masses in containment, which is a measure for the potential iodine source term, was found to be in average a quotient of 6.2 below and a factor of 5.3 above the best-estimate value. Only in the first hours of test FPT1, when the airborne iodine consisted mainly of CsI aerosol, the uncertainty range was significantly smaller.

The findings are qualitatively valid for reactor accident analyses as well, but larger uncertainties have to be assumed since the conditions in FPT1 were more controlled than in a severe reactor accident.

In the early phase of an accident when CsI aerosol is the dominant airborne iodine species in the containment the uncertainty of the calculated potential iodine source term is relatively small. Therefore, an improvement of the aerosol model in COCOSYS seems unnecessary at the moment.

In the late accident phase when CsI has settled and the iodine source term consists of the species I_2 , organic iodides and IOx the uncertainty of the source term is rather large. This confirms the experience made with numerous applications of COCOSYS-AIM and other codes.

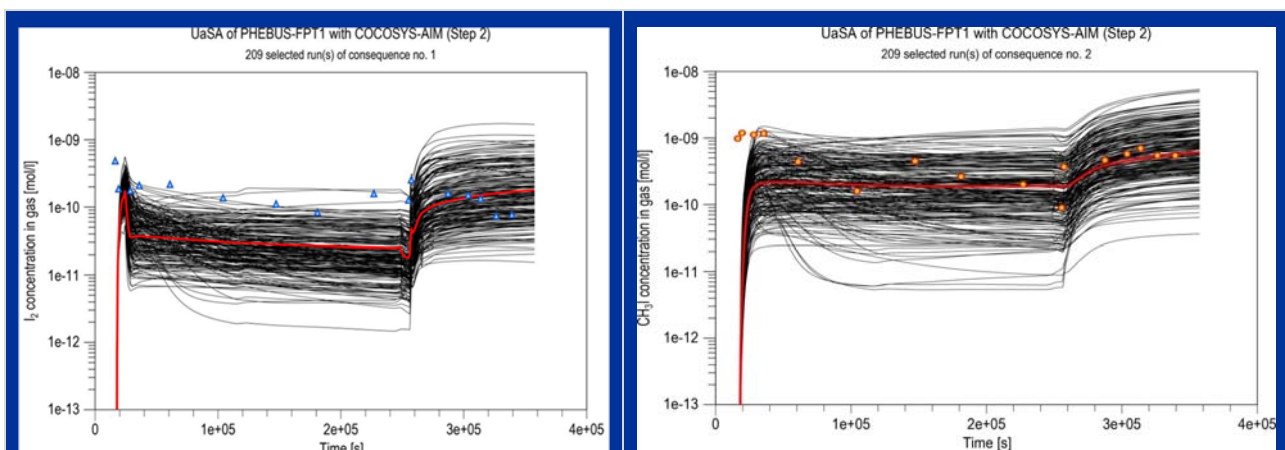


Figure 3: I_2 concentration in gas shown (209 selected runs; reference calculation of the I_2 concentration in gas (red) and experimental values (blue marks)); RI concentration in gas (209 selected runs; reference calculation of the RI concentration in gas (red) and experimental values (yellow marks))

It is further shown that only 5 of the 93 uncertain parameters investigated have an essential impact on the uncertainty of the potential iodine source term in the late phase. Four of them are used in different AIM sub-models: (1) radiolytic formation of I_2 from iodide in the sump, (2) iodine/silver reactions in the sump, (3) adsorption of I_2 onto paint in the gas phase and (4) radiolytic formation of CH_3I in the gas phase and the fifth parameter is an input parameter generally provided by a primary circuit code: the release rate of I_2 from the primary circuit into the containment. By a well-directed improvement of these AIM sub-models and a reduction of the uncertainty of the input parameter the accuracy of the iodine source term calculated with COCOSYS-AIM can be significantly improved.

In the international programs OECD-BIP, OECD-STEM and OECD-THAI aspects of the above mentioned reactions are also investigated experimentally. Within the national THAI program a test on the iodine/silver reaction in the sump is planned. The results of these projects form a valuable data base which can be used for the revision of the uncertain AIM sub-models.

1.2 Modelling of experiments using best estimate approach (LEI)

QUENCH experiment modelling and evaluation of the uncertainties. The full text of application of the best estimate approach for modelling of QUENCH-03 and QUENCH -06 experiments could be found in the article [3]. In this article the QUENCH-06 experiment analysis was provided using RELAP/SCDAPSIM code and SUSA computer tool. Uncertain input parameters used in the best estimate analysis consist of quenching water and injected gas flow rates, temperatures and pressures, thermal properties of ZrO_2 and contact resistance of sliding contacts.

For the uncertainty analysis two main test parameters were evaluated: a) cladding temperatures of the fuel rod imitator and b) amount of generated hydrogen (Figure 4).

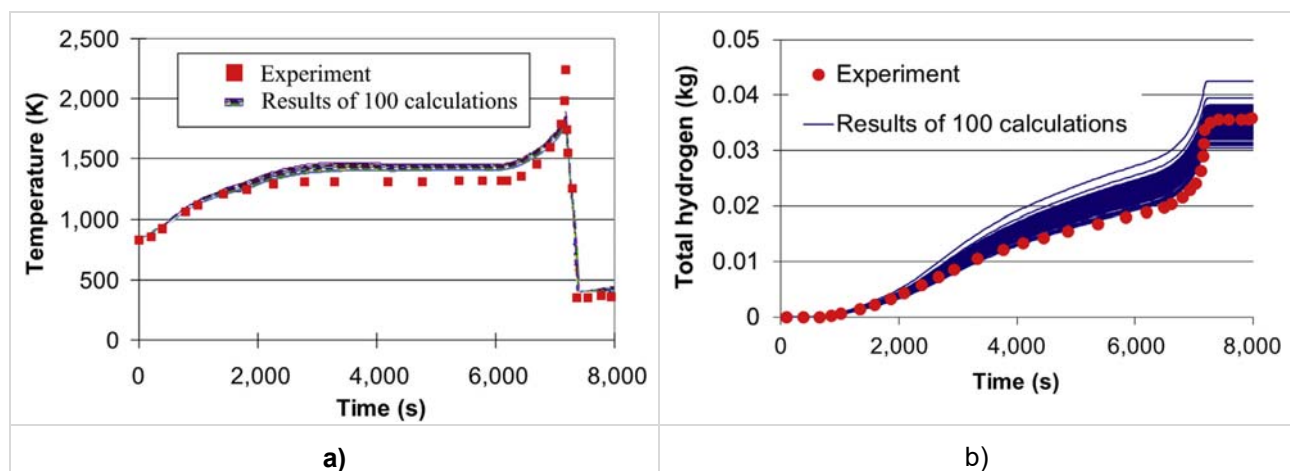


Figure 4: Results of RELAP/SCDAPSIM calculation of QUENCH-06 experiment: a) behaviour of cladding temperatures of the fuel rod imitator from the inner rod ring at 750 mm-height; b) amount of generated hydrogen

The analysis of sensitivity of uncertain parameters on the calculation results was performed using Spearman's rank correlation coefficient method. Influence of uncertain parameters to the calculation results presented in Figure 5. At the heat up phase and transient phase, the parameters mainly influencing the calculation results of fuel rod imitators' temperature are similar: additional resistance (parameter No. 9), steam flow rate and temperature (parameter No. 2 and 5), and thermal conductivity of ZrO_2 (parameter No. 7). The biggest influence on the hydrogen calculation results has the same parameters: additional resistance (parameter No. 9), steam flow rate and temperature (parameter No. 2 and 5), thermal conductivity of ZrO_2 (parameter No. 7).

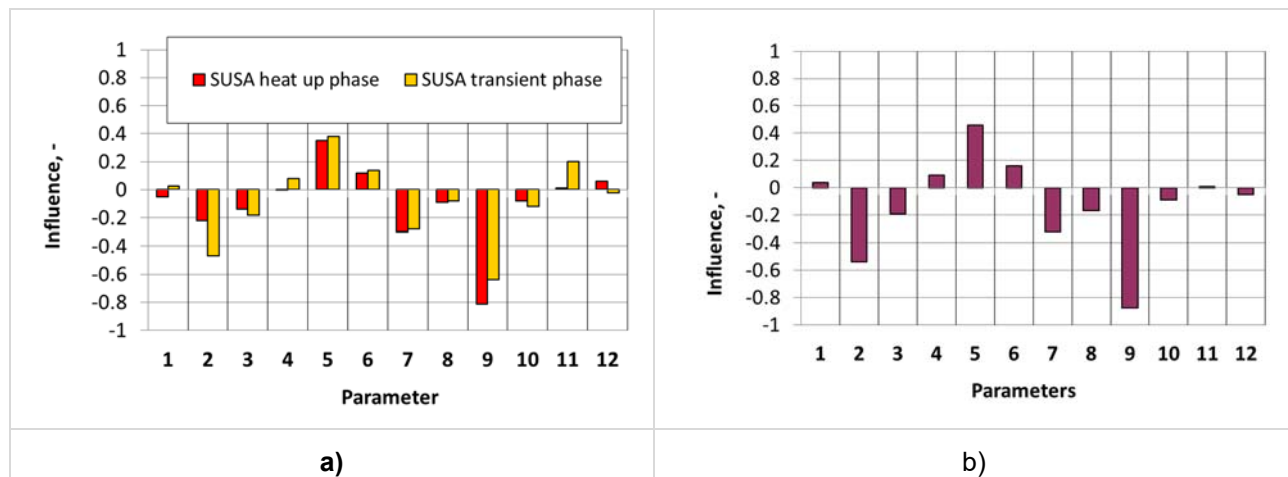


Figure 5: Influence of uncertain parameters to the calculation results: a) cladding temperature of the fuel rod imitators in the outer ring at 750 mm-height. Heat up phase and transient phase; b) hydrogen calculation results

PHEBUS FPT1 experiment modelling and evaluation of the uncertainties: The full text of application of the best estimate approach for modelling of PHEBUS FPT1 experiments could be found in the article [4]. In this article the best estimate analysis of the bundle degradation phase was provided using ASTEC V2.0 code ICARE module and SUSA 3.5 computer tool. In the uncertainty and sensitivity analysis 32 uncertain input parameters were chosen. These parameters could be divided into two groups - physical parameters and code parameters. Few calculation results are presented in Figure 6.

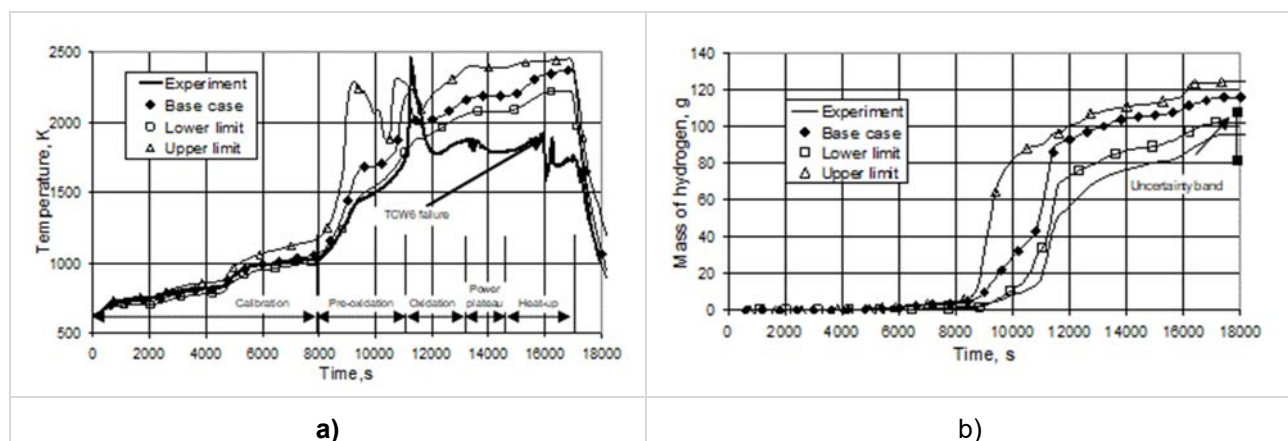


Figure 6: Results of ASTEC calculation of PHEBUS FPT1 experiment: a) fuel cladding temperature at 700 mm elevation; b) total hydrogen generation

Spearman's rank correlation coefficient method for the sensitivity analysis was chosen. The results of the sensitivity analysis showed that different parameters have the greatest influence during different subperiods of experiment. However, the performed sensitivity analysis for fuel and cladding temperatures indicated that the largest impact on the thermal behaviour modelling have good prediction of the fuel bundle power and variation of shroud thermal properties. For the calculation of the hydrogen generation the biggest influence has power of the bundle.

Uncertainty of aerosols deposition in containment in PHEBUS FPT-2: The results of analysis are presented in [5]. A detailed nodalisation of PHEBUS containment was developed for computer code COCOSYS. This nodalisation consists of 16 nodes and enables simulation of the convective flows of gases. Uncertainty and sensitivity analysis was performed using SUSA tool. 100 runs were performed using the COCOSYS code. A list of 24 parameters was developed and considered in the performed uncertainty and sensitivity analysis. In total 15 parameters are related to modelling of the particle transport in the AFP module of COCOSYS code, the rest 9 parameters are related to the thermal-hydraulic analysis.

In the performed sensitivity analysis, the calculated determination coefficient R^2 for all 24 parameters varied between 0.95 and 0.99; thus, the Spearman's rank correlation coefficient could be used for the sensitivity analysis.

Figure 7 shows the results of the uncertainty analysis for the aerosol mass suspended in the gas phase. The measured results are within the calculated uncertainty band. When the peak value is reached, the measured results are closer to the average calculated value, but then it decreases faster, and later it complies with the minimum calculated values.

Figure 12 shows 4 parameters giving the largest influence (Spearman's coefficient larger than ± 0.3 at least in one point) on the aerosol mass **suspended in the containment atmosphere**: the dynamic shape factor (parameter No. 2), the particle agglomeration factor (parameter No. 4), the Mass Median Diameter (parameter No. 6) and the geometric standard deviation (parameter No. 7).

The parameters that had the greatest influence on aerosol **deposition on the containment floor** are presented in Figure 9. These parameters were the same as those for aerosol mass suspended in the containment atmosphere. Compared to the results shown in Figure 8, one could see that the influence of parameters on the deposition on the floor is opposite, e. g., the increasing dynamic shape factor (increasing deviation from the spherical particle) leads to less deposition on the floor. Increasing the MMD and particle agglomeration factor leads to the increased deposition due to gravitational settling.

The parameters that had the greatest influence on aerosol **deposition on the condensers and in the sump** are presented in Figure 10. The dynamic shape factor (parameter No. 2), the MMD (parameter No. 6), the average thickness of water film (parameter No. 13) and the initial pressure (parameter No. 18) were the most important parameters for deposition on the condensers and in the sump.

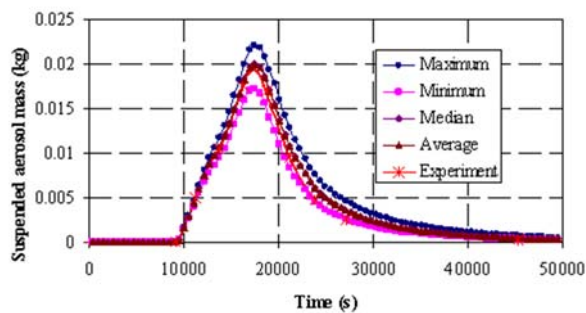


Figure 7: Mass of aerosols in gas phase of containment (maximum, minimum, median, average and experiment values)

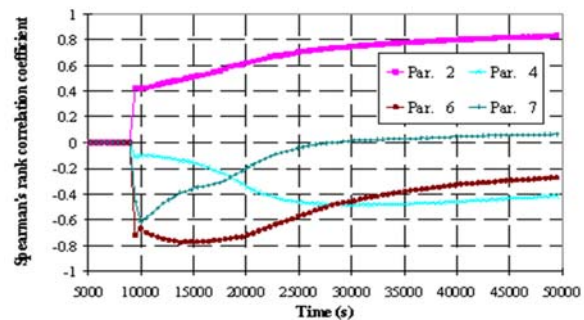


Figure 8: Spearman's rank correlation coefficients for suspended aerosol mass (only parameters with values >0.3 at least at one point are highlighted)

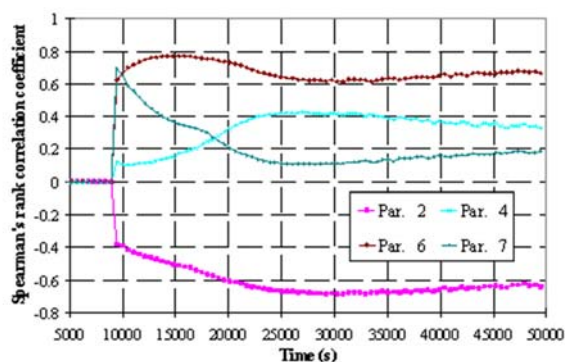


Figure 9: Spearman's rank correlation coefficients for aerosol deposition on containment floor

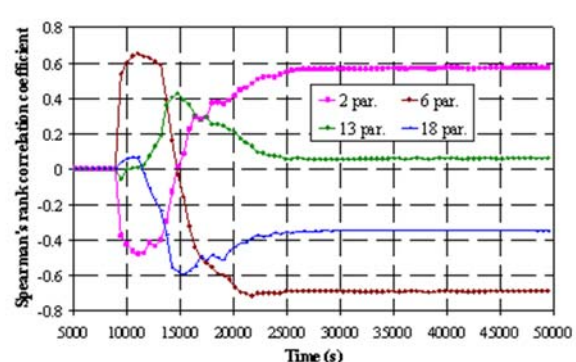


Figure 10: Spearman's rank correlation coefficients for aerosol deposition on the condensers and in a sump

The distribution of aerosol deposition on different surfaces in the containment is shown in Table 1. The largest deposition of aerosols was measured on the containment floor around the sump, where 74% of aerosols were

deposited. Besides, it was measured that 14% of aerosol mass was deposited on the condensers and in the sump, and 12% was deposited on the vertical containment walls and removed by sampling. The performed uncertainty analysis showed that the measured deposition on the elliptic floor and on the condensers is within the calculated range of the results; however, deposition on the containment vertical walls is far from the calculated results; the maximum value is only 0.9%.

Table 1: Distribution of aerosol deposition

	Floor of containment	Condenser surfaces and sump	Containment walls + samplings
Measured	74.0%	14.0%	12.0%
Min	71.44%	11.28%	0.42%
Max	86.88%	27.66%	0.9%

Generic containment SB-LOCA simulation and comparison of the parameter uncertainties and user-effect: The description of the study has been published in [6]. In this study an uncertainty and sensitivity analysis with the aim to investigate the effect of different input uncertainties related to the initial conditions, material properties and geometric definitions of the Generic Containment nodalisation in comparison to the user effect and computer code choice was performed. For the uncertainty and sensitivity analysis more than 30 uncertain input parameters were chosen and 200 calculation runs were performed using the ASTEC code CPA module. The impact of uncertainties on the containment pressure and temperature and hydrogen concentration in the characteristic locations was observed. Standard deviation bands of the sensitive parameters obtained from the analysis were compared to the corresponding bands obtained from the SARNET2 Generic Containment benchmark, which show the user-effect influence (Figure 11).

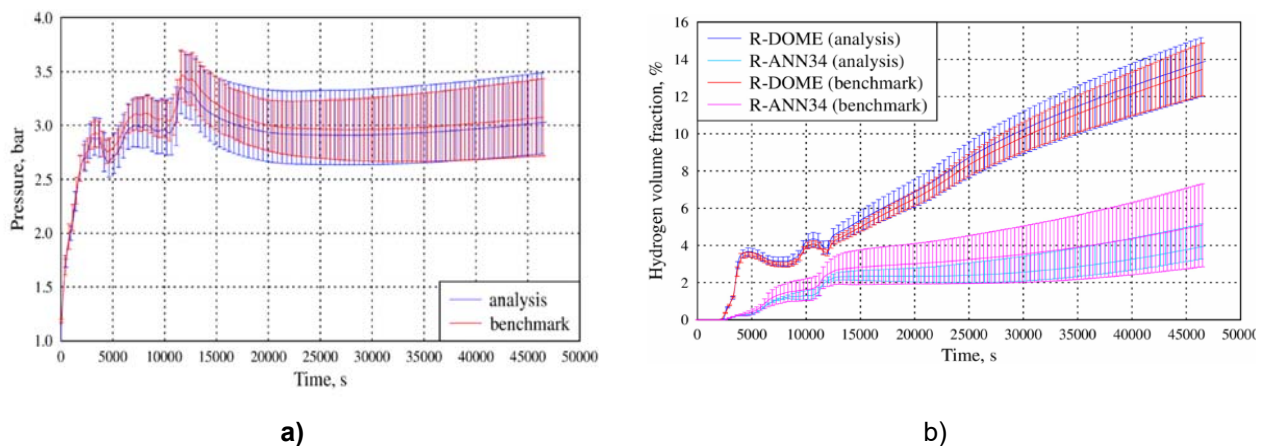


Figure 11: Comparison of the parameter uncertainty and the user effect standard deviation bands: a) pressure; b) hydrogen concentration

The study showed that while there are differences between bands of some parameters, general deviation bands caused by parameters' uncertainty vs. the computer code and the user effect are comparable and in the same order of magnitude, i.e. for a quantitative analysis, both must be considered.

Considering the selected sensitive parameters, there is a small number of significant uncertain input parameters and all of them are related to the modelling of containment structures – concrete and steel properties, areas of concrete structures', initial temperatures of the structures (Figure 12).

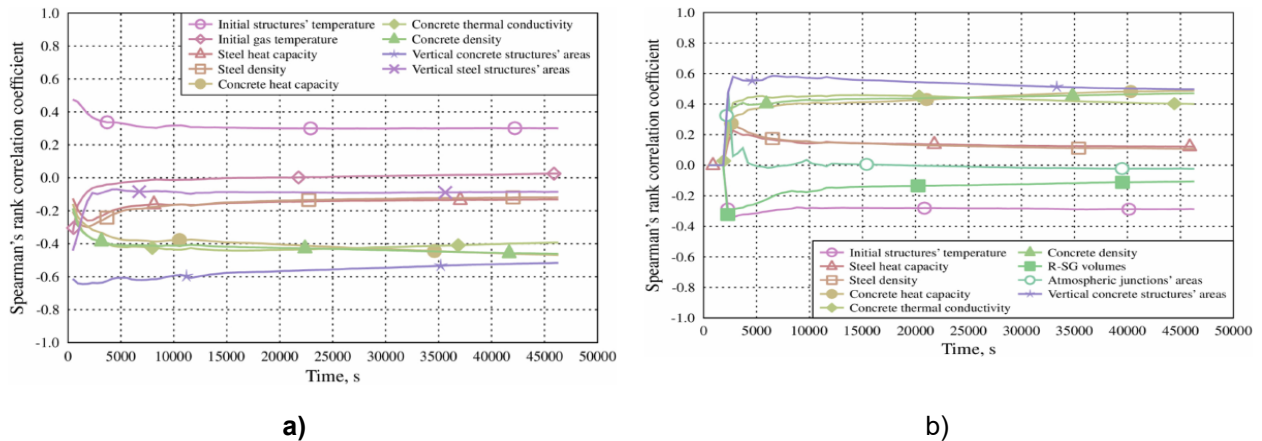


Figure 12: Obtained sensitivity measures (Spearman's coefficients): a) for pressure; b) for hydrogen concentration in the dome

Sensitivity and uncertainty analysis of atmosphere stratification modelling in MISTRA facility: The analysis has been published in [7]. The simulation of the steam injection driven gas mixing experiment M5 was performed using a lumped parameter code COCOSYS and a nodalisation scheme with jet/plume injection zones and plume path zones. The aim of the simulation was to obtain a stratified atmosphere conditions corresponding to the experimental ones.

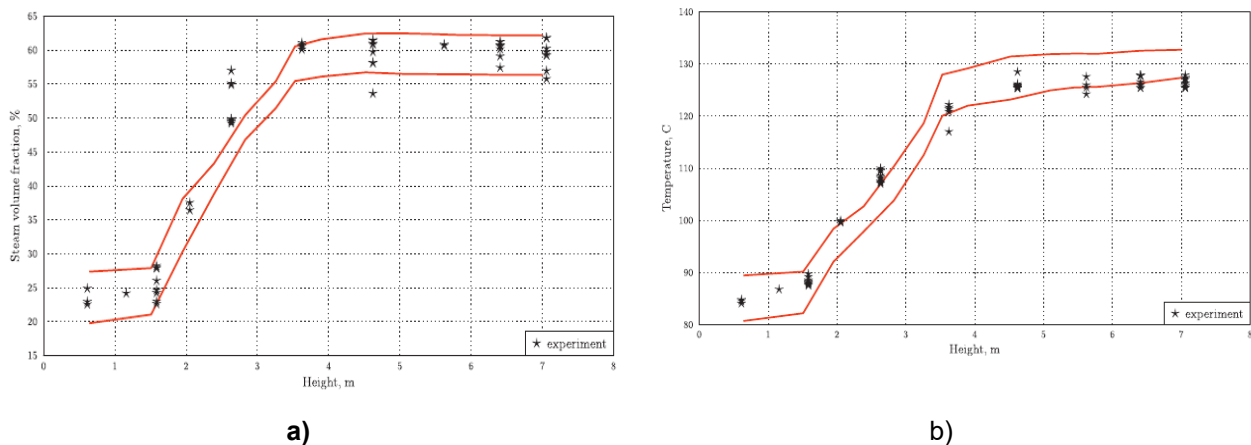


Figure 13: Obtained tolerance limits of vertical profiles at the end of the experiment: a) steam volume fraction; b) temperature

The analysis results showed that large uncertainties of some experimental facility data – effective heat losses and the pressure in the injection loop – have large influence on the sensitive results. Steam and temperature distribution in the facility was sensitive to the virtual junctions resistance. Obtained tolerance limits of pressure covered the experiment results, while the limits of final steam volume fraction and temperature included most, but not all of the measured values (Figure 13).

1.3 Modelling of accidents using Theory of Probabilistic Dynamics (LEI)

PWR accident modelling and evaluation of the uncertainties: The full-text description of the approach based on the Theory of Probabilistic Dynamics and the application for modelling of a severe accident in French 900 MWe PWR could be found in [8]. The considered case was supposed to be most relevant for level 2 PSA. In this article, SUSA computer tool application was also demonstrated. As a “basic transient” the following simplified object/situation was considered: A French 900 MWe PWR with 3 loops and Passive Autocatalytic Recombiners (PAR) operating at nominal power before the initiating event; LOCA after a 3” break size on cold leg of Reactor Coolant System (RCS); Failure of all water injection system and spray system.

In [8] the Theory of Probabilistic Dynamics (TPD) and its augmented version based on the concept of stimulus and delay are introduced for the dynamic reliability modelling and the simulation of accidents in hybrid

(continuous-discrete) systems considering uncertain events. An approach of non-Markovian simulation and uncertainty analysis is discussed in order to adapt the Stimulus-Driven TPD for practical applications.

Twelve uncertain input parameters were used in the analysis e.g. number of moles of steam, temperature inside the containment, pressure inside the containment, factor of spray efficiency to condensate hydrogen, factor of hydrogen mass flow rate in the range (1: [5875; 7000] or [9401; 14220]), factor of hydrogen mass flow rate in the range (2: [7001; 9400]), factor of water injection (SIS) availability, factor of spray injection (CHRS) availability, coefficient K1 of recombined hydrogen flow rate, coefficient K2 of recombined hydrogen flow rate, factor of peak pressure to cause a rupture, and activation of spray at 2.4 MPa pressure limit. For the uncertainty analysis the uncertain estimate of containment rupture probability (due to multiple hydrogen combustion) was considered (Figure 14).

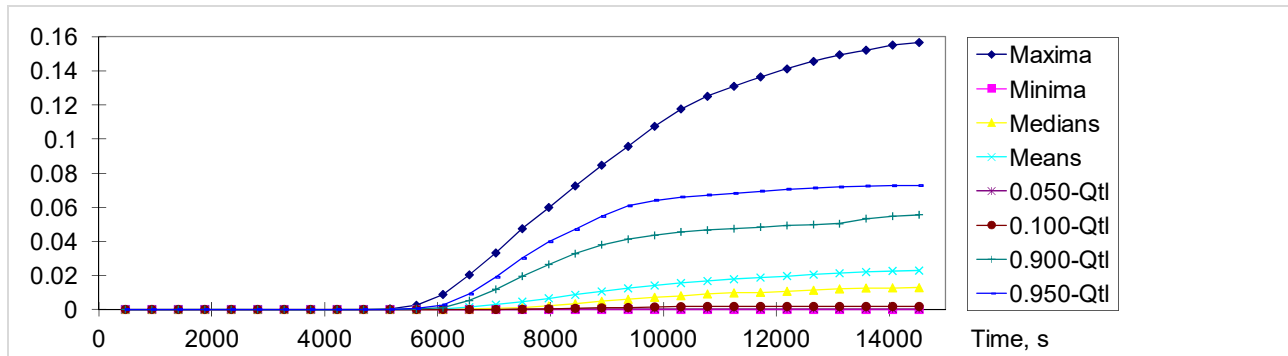


Figure 14: Example of time-dependent uncertainty analysis of rupture probability estimate

The analysis of the sensitivity of the calculation results due to uncertain parameters was performed using various sensitivity measures. An example of the time-dependent sensitivity of the calculation results due to uncertain parameters is presented providing Partial Correlation Coefficients (PCC) in Figure 15.

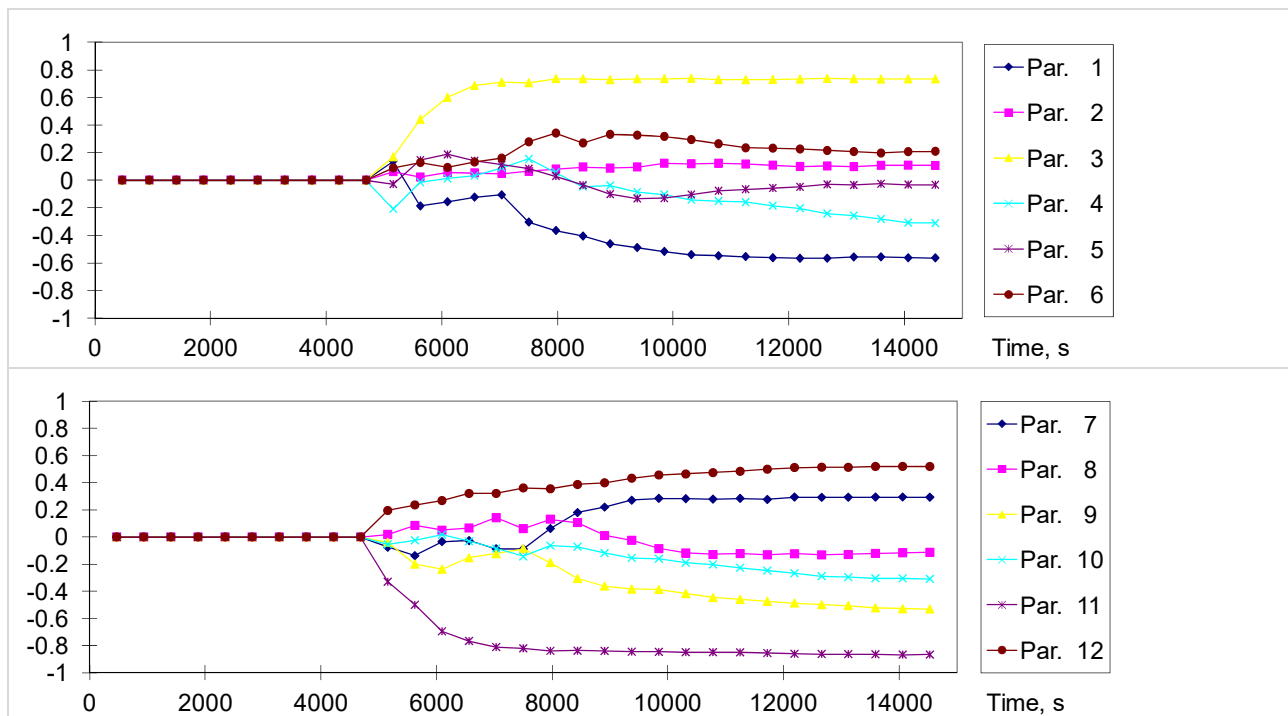


Figure 15: Example of time-dependent sensitivity analysis providing PCC

The set of considered parameters can also be extended and related to the timing, i.e. the set of input parameters can reflect uncertain delays and stochastically distributed time moments of events occurrence. For such an investigation, the extended analysis could be performed in the future. The additional uncertainty and

sensitivity analysis could be also useful in order to show how the uncertain timing is important for the modelling and analysis of a dynamic system trying to make it more robust and reliable.

The developed approach and related methods are used as a basis for a test case simulation in view of various methods applications for severe accident scenario simulation and uncertainty analysis. As shown in the test case, it is possible to reduce the computing time without meaningful change of the considered frequency mean and standard deviation, which is quite high due to uncertain parameters. For this and wider analysis of accident sequences, the initial test case specification is then extended and discussed.

Finally, it is concluded that enhancing the modelling of stimulated dynamics with uncertainty and sensitivity analysis allows the detailed simulation of complex system characteristics and representation of their uncertainty. The developed approach of accident modelling and analysis considering uncertain events can be efficiently used to estimate the reliability of hybrid systems and at the same time to analyze and possibly decrease the uncertainty of this estimate.

1.4 Experience from the application of SUSA (Bel V)

In general, results of code predictions are subjected to errors due to several sources of uncertainties like **model limits, approximations in the numerical solution, nodalization and homogenization approaches, or imperfect knowledge of boundary and initial conditions**. Therefore, it is necessary to investigate the uncertainty of the results as well as the sensitivity effects of the key parameters for a given phenomenon. This will allow identifying models that need improvement and areas where more validation data are needed.

In the following, SUSA uncertainty method was applied for the assessment of the coupled RELAP5/3.3-PARCS/2.6 code in predicting the experimental results issued from the Kozloduy VVER100 pump trip test [9]. Indeed, the code results show deviations with respect to the plant measurements (Figure 16). The origin of these discrepancies could not be identified at a first glance.

Therefore, the SUSA statistical code package was used to carry out sensitivity study that allows getting a qualitative and quantitative assessment of the code prediction capabilities. For this purpose, nine uncertain parameters with their distribution function are chosen according to a ranking process established by the author's expertise judgment or by using outcome from similar studies of the most influent parameters that govern the transient course.

Then a set of a random sample of input decks is generated by a random combination of the uncertain parameter over their probability distribution function. The number of samples is determined by the Wilk's formula according to the desired probability content and confidence level. This number is independent of the number of chosen uncertain parameters. In the current study dealing with uncertainty analysis of the code prediction, a random sample of 50 input decks is generated to get a 95% probability content and a confidence level of 90% of a two-sided statistical tolerance limits. Actually if the objective was to assess a parameter with respect to a safety criterion, the one-sided statistical tolerance limit would then have been chosen.

Figure 4 provides the SUSA calculation result related to the tolerance limits of the axial power distribution. The calculated upper and lower limits envelop completely the measured trend only at the upper part of the core zone. In the mid and lower part of the core, the measured trend is slightly out of the tolerance limit interval. Reasons for such effect could be explained due to **non-consideration of further uncertain input parameter** as mentioned above. However, more investigation should be performed to identify the source of the discrepancies, Table 2. The most significant parameter that governs the axial power distribution is the control rod worth (UP6), followed by UP5, UP1, UP4, and UP8. It is interesting to notice (see Figure 18) that the sign of these coefficient changes according to the position of the control rods in the core. For UP6, the effect on the power is negative in the upper part of the core where the control rods are inserted. Due to the axial coupling, this effect becomes positive in the lower part. The same trend effect is observed for UP1, which affect the axial distribution profile of the Doppler temperature. The effect is positive in the lower part of the core since higher value of ω leads to low Doppler temperature, and therefore lower Doppler feedback. The gap effect (UP5) it is negative in the lower part of the core since higher Xe fraction reduces the conductivity, and therefore the Doppler feedback becomes stronger.

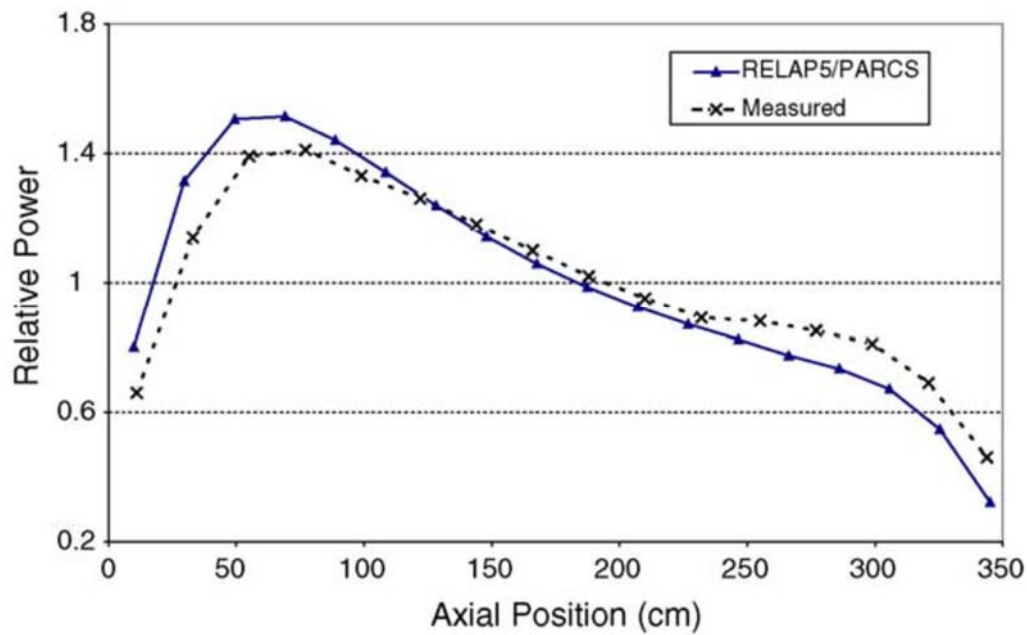


Figure 16: Mean axial power distribution during steady state¹.

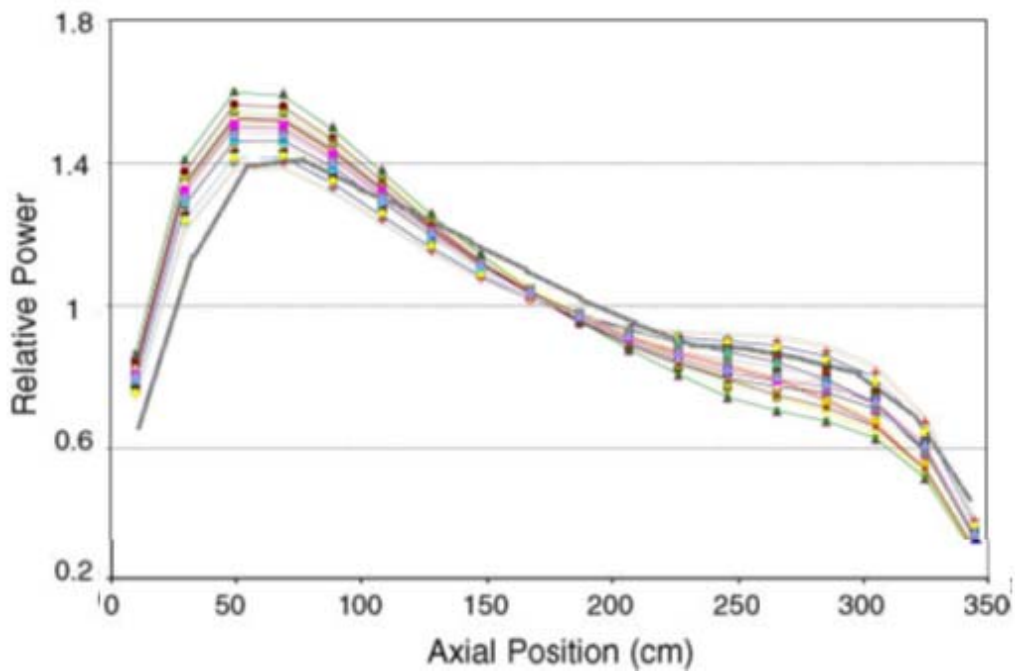


Figure 17: Uncertainty results for axial power profile during steady state.

¹ Steady state is selected here due to the availability of plant measurement.

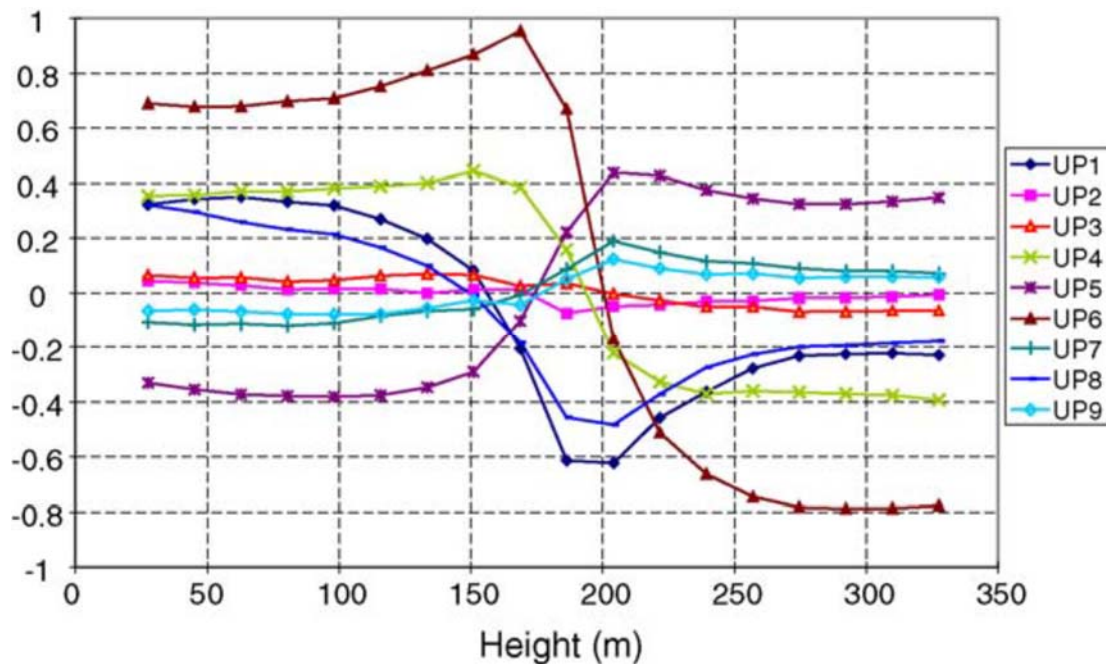


Figure 18: Spearman's Rank coefficients for the steady state axial power distribution.

Table 2: Rank of uncertain parameter according to their effect on the axial power distribution

Rank of uncertain parameters	Parameter
UP6	Control rod worth
UP1	Doppler temperature coefficient ω
UP5	Gap conductivity (xenon fraction)
UP4	Main steam header pressure
UP8	Global moderator coefficient

2 SUNSET (IRSN, INRNE, LEI, TUS)

2.1 Epistemic variables using probabilistic framework (IRSN)

The full text of an example of UQ study based on SUNSET-ASTEC tool can be found at the following reference [10]. It is summarized hereafter.

The study was based on version 2.0 of ASTEC. The aim of the study was to check the impact of several iodine related epistemic uncertainties on the source term at different times of a Loss of Feed Water of Steam Generator severe accident occurring on a French PWR1300, the containment spray system being unavailable. The six chosen epistemic variables were the following:

- Gaseous iodine mass fraction at primary circuit break
- Iodine oxides deposition rate in containment
- Ozone formation rates (forward and backward reactions)
- Organic iodine formation rate in containment atmosphere and sumps
- Release rate from paints of organic compounds that may react with molecular iodine in containment atmosphere and sumps to form organic iodides

The chosen framework was probabilistic, and the values chosen for the distribution were based on iodine experts' advice. The sample size was 100, which resulted in a good confidence level on the 5% and 95% percentile of the source term. Figure 19 illustrates the computed iodine source term. The order of magnitude

of the dispersion range is about a factor 20 between percentile 5 and percentile 95 by the end of the accident. It shall be noted that the farther from the initiator, the bigger the uncertainty range is.

Another comment from the study (not mentioned in the article, but mentioned internally at IRSN, see Figure 20) was that this order of uncertainty was comparable to the kind of difference between the source term from two different sequences (i.e. variability), which led to the conclusion that epistemic and stochastic uncertainties had to be considered altogether in the future.

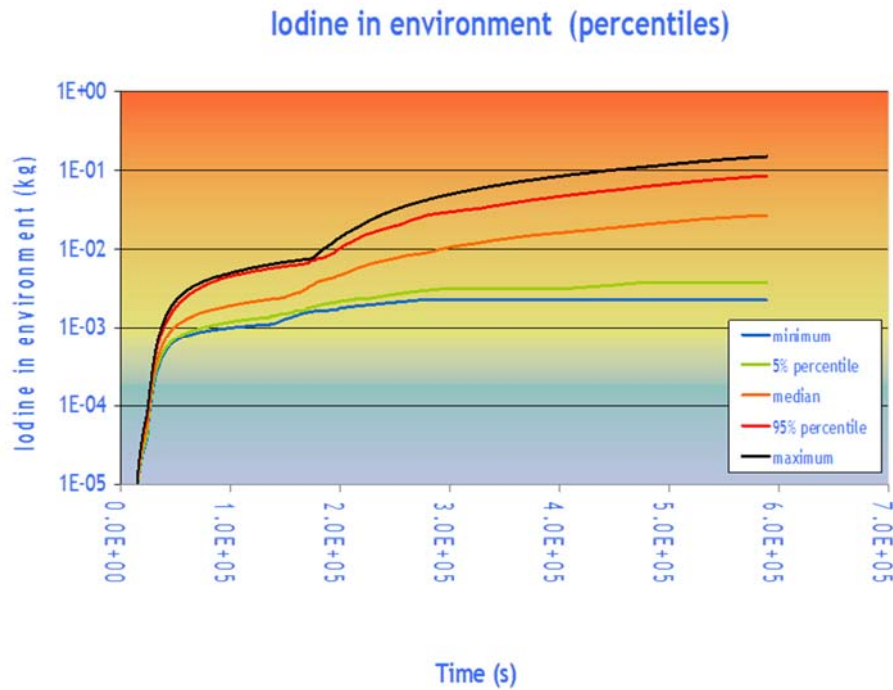


Figure 19: Experience from application of the UQ-methods, IRSN, epistemic variables using probabilistic framework: iodine related source term

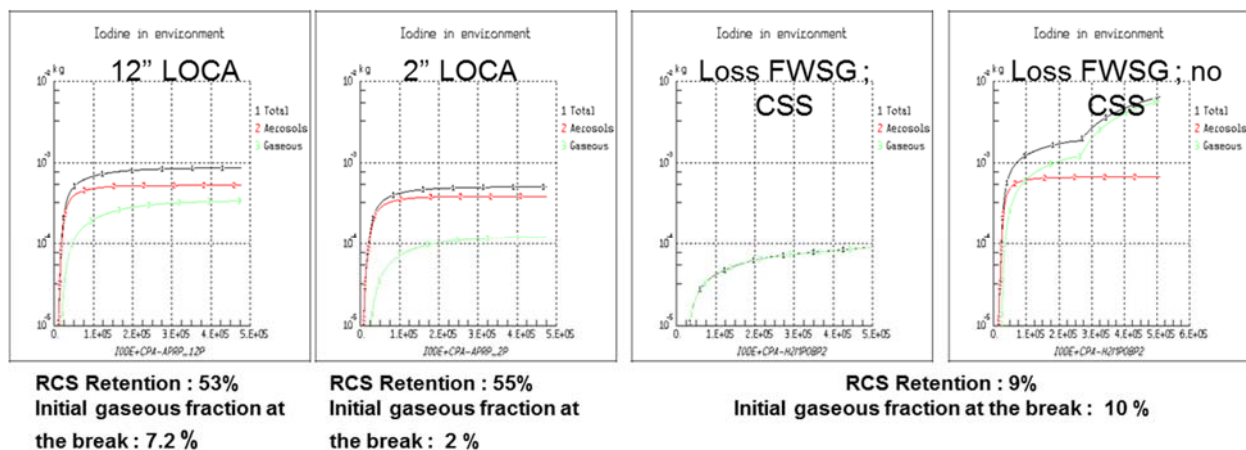


Figure 20 : Depending on the scenario the iodine release ranges from ~0.1g to ~5g

A sensitivity analysis performed at different instants of the accident showed that the influence of the parameters was variable through time, in order of magnitude and orientation as illustrated in Table 3.

Table 3: Variation of correlation coefficients through time

	1 day	6 days
Iodine gaseous mass fraction at primary circuit break	0.72	0.35
Iodine oxides deposition rate in containment	-0.75	-0.21
Organic iodine formation rate in containment atmosphere	0.26	0.14
Organic compound release rate in containment atmosphere	-0.05	0.13
Organic compound release rate from sumps	0.05	-0.09
Ozone formation rate (forward reaction)	0.52	-0.40
Ozone formation rate (backward reaction)	-0.30	0.14

2.2 Best estimate approach for modelling of QUENCH-03 experiment (LEI)

The full text of application of the best estimate approach for modelling of QUENCH-03 and QUENCH-06 experiments could be found in [3]. QUENCH-03 experiment analysis was performed using ASTEC V2.0 code ICARE module and SUNSET tool. The uncertainty analysis was performed using a two-side tolerance limit with 0.95 of probability and 0.95 confidence level. According to Wilks' formula, the number of calculations necessary for two-side tolerance intervals is 93. Using SUNSET computer tool, 100 different collections of 12 uncertain input parameters (quenching water and injected gas flow rates, temperatures and pressures; thermal properties of ZrO_2 and additional resistance outside the bundle) were generated. The deviation ranges of parameters were assumed based on experience and possible measurements errors.

Two parameters were evaluated: a) cladding temperatures of the fuel rod imitator and b) amount of generated hydrogen (Figure 21, Figure 4).

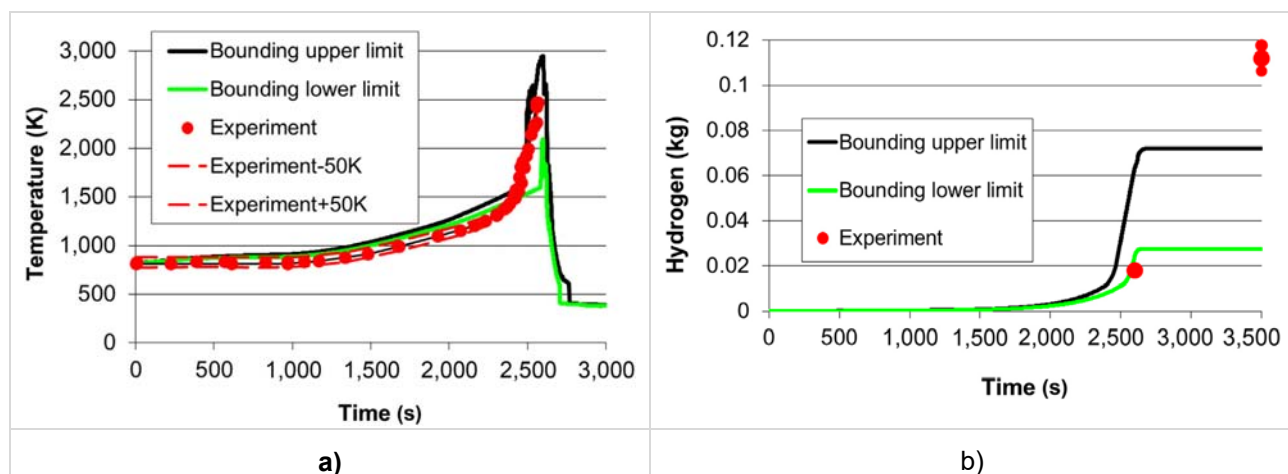


Figure 21: Results of ASTEC calculation of QUENCH-03 experiment: a) cladding temperatures of the fuel rod imitator from the outer ring at 750 mm height; b) amount of generated hydrogen

The analysis of sensitivity of uncertain parameters was performed employing Spearman's rank correlation coefficient method for two phases of experiment: for the bundle heat-up phase; and at the quenching phase (at time moment, when the maximal temperatures are reached). Influence of uncertain parameters to the calculation results presented in Figure 22. At the heat up phase, the parameters mainly influencing the calculation results of fuel rod imitators' temperature are: additional resistance (parameter number 9), thermal conductivity and specific heat of ZrO_2 (parameters No. 7 and 8), while at the quenching phase - additional resistance (parameter No. 9), steam flow rate (parameter No. 2) and thermal conductivity of ZrO_2 (parameter No. 7). The biggest influence on the hydrogen calculation results has: additional resistance (parameter No. 9), steam flow rate (parameter No. 2), thermal conductivity and specific heat of ZrO_2 (parameters No. 7 and 8).

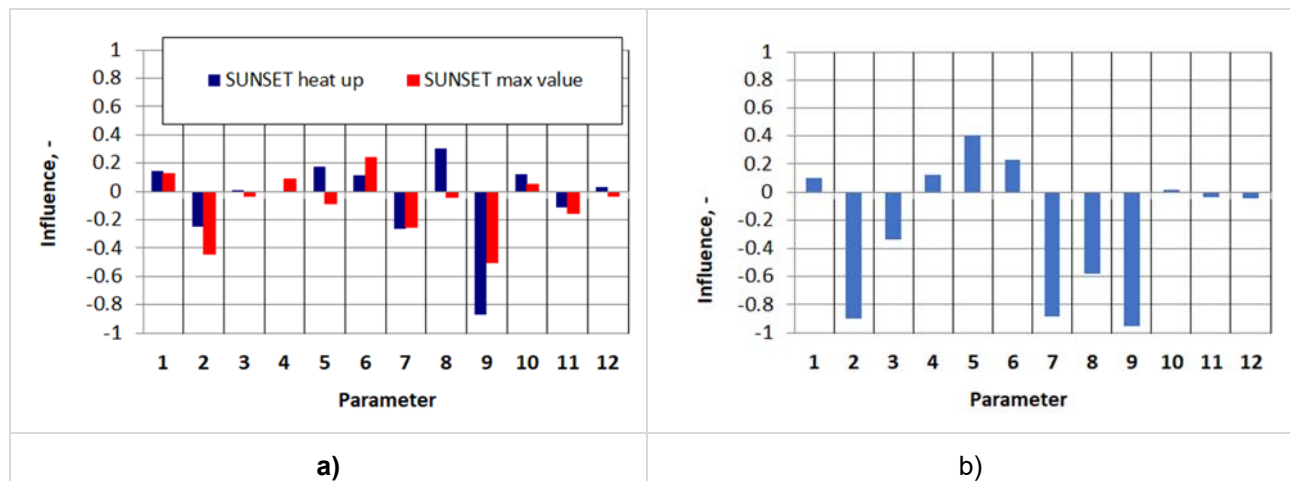


Figure 22: Influence of uncertain parameters to the calculation results: a) cladding temperature of the fuel rod imitators in the outer ring at 750 mm height; b) hydrogen calculation results

3 DAKOTA (ENEA, CIEMAT, TRACTEBEL)

3.1 MELCOR/DAKOTA/SNAP Applications (ENEA)

ENEA MELCOR/DAKOTA studies here reported, represents only first ENEA exercises aiming to show the complete application of the coupling procedure of MELCOR [11], [12] and DAKOTA in a SNAP environment/architecture. They do not want to represent a complete and representative analysis of the MELCOR code uncertainty; the main target of these applications is to show the feasibility and the great advantage to have everything integrated in a graphical user interface (SNAP) that permits to:

- Develop input-decks from scratch;
- Import existing input-deck developed in ASCII format;
- Develop the post processing of the simulations by using:
 - SNAP animation modelling capability;
 - APTPLOT plot capability.
- Perform uncertainty analyses:
 - Running automatically the different random sampling tasks;
 - Develop all the dispersion plots;
 - Develop the statistical analyses;
 - Characterize, through response correlations, the relationship between the selected uncertain input parameters and the FOMs
- Etc.

The ENEA applications of MELCOR/DAKOTA in a SNAP environment/architecture, here discussed, have been presented at the last European MELCOR User Group (EMUG) 2019 [13].

3.1.1 CASE 1: MELCOR/DAKOTA coupling against CSTF-AB1 test

This activity has been done by using the same MELCOR input-deck developed along the EU-JASMIN project (Joint Advanced Severe Accidents Modelling and Integration for Sodium-Cooled Fast Neutron Reactors) coordinated by IRSN and funded in the 7th Framework Programme of the European Commission [14]. In that project ENEA has been involved in the WP2.3 (ST) - Source term - coordinated by CIEMAT. A benchmark activity, coordinated by CIEMAT, has been performed with different codes as MELCOR, ASTEC-CPA, CONTAIN, FEUMIX, ASTEC-CPA (specific models for in-containment Na phenomena have been implemented). The tests selected for the benchmark were the CSTF-AB1, AB2, and FAUNA F2, F3 and EMIS10b (Pool Fire Tests) [14] [15]. ENEA used the MELCOR and ASTEC-CPA code for the simulation of the selected tests in order to support the benchmark of the CPA module of ASTEC-NA.

After JASMIN was finalized, ENEA did the first application (CASE1) of the MELCOR/DAKOTA coupling in a SNAP environment/architecture. The dispersion of the aerosol suspended mass (SUSP), aerosol mass median

diameter (MMD), geometric standard deviation of the aerosol distribution (SSD), and tot mass deposited (TOT_DEP) was analysed and compared against the CSTF-AB1 experimental data [16] having selected as a input uncertain parameters the aerosol constants. In relation to the input uncertainty parameters a first attempt, only to test the procedure, has been done to characterize them in term of PDF. The range value of the input uncertain parameter is reported in Table 4, and it is based on [17].

Figure 23 shows the DAKOTA Properties Tab for the ENEA Case 1 (FOMs selected, selection of Latin hypercube, and probability and confidence level of 98%). Based on the Wilks formula [18], 452 are the required tasks (as a results of the calculate samples bottom), to calculate the 0 order statistic for the specified FOMs with a 98.0% probability and a 98.0% confidence level. The data extracted to perform the uncertainty analyses is the value of the FOMs at the end of the pool fires. An initial DAKOTA run was performed using the specified input uncertain parameters, to generate a set of variates for each task. The individual tasks were then performed, and the FOMs were extracted from the completed calculations. A total of 452 tasks are required, 452 tasks were completed successfully. In Figure 24, the input uncertainty parameters, CHI, GAMMA, FSLIP, STICK has been plotted against the iteration index. In Figure 25, the FOM-SUSP and FOM-MMD have been reported against the CHI and GAMMA input uncertain parameters. Figure 26 shows the dispersion band, done with APTPLOT, for the suspended mass together with the cumulative distribution function and the probabilistic density function calculated by DAKOTA. Table 5 shows the statistical results reported in the automatically generated DAKOTA report for the SUSP FOM.

Table 4: Uncertainty input parameters range (ENEA CASE1) [12] [17] [11]

AEROSOL CONSTANT	Range Used	MELCOR NAME	Default Value MELCOR
Dynamic Shape factor	1.0-5.0	CHI	1
Agglomeration Shape factor	1.0-5.0	GAMMA	1
Slip Coefficient	1.14-1.257	FSLIP	1.257
Sticking Coefficient	0.5-1.0	STICK	1
Turbulence Dissipation (m2/s3)	0.001-0.02	TURBDS	1.00E-03
Thermal Accomodation Coefficient	2.18-2.25	FTHERM	2.25
Gas Thermal Conductivity/Particle Thermal Conductivity	0.06	TKGOP	0.05
Diffusion Boundary layer Thickness (m)	1.0e-5-1.0e-3	DELDIF	1.00E-05

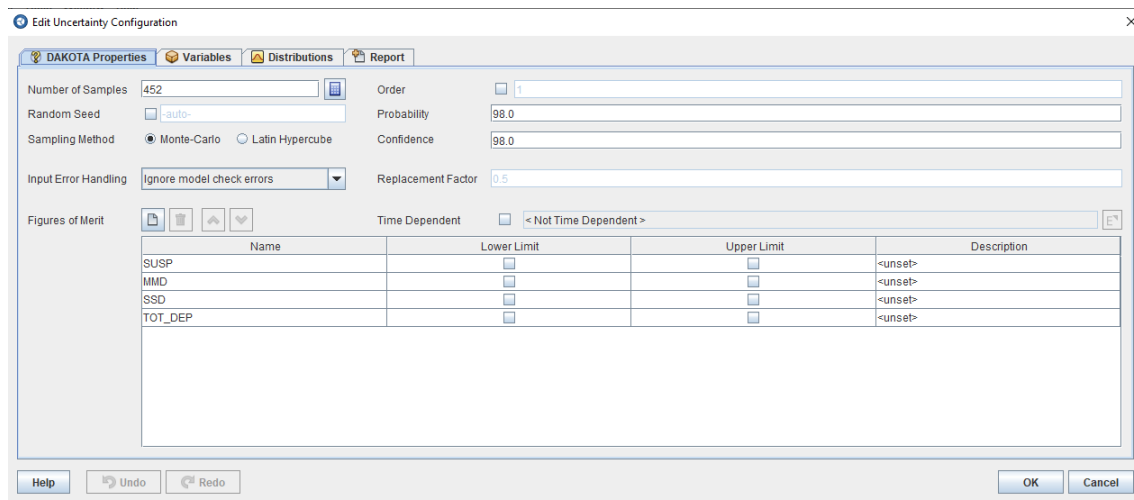


Figure 23 shows the DAKOTA Properties Tab for the ENEA Case 1. The window displays the following settings:

- Number of Samples:** 452
- Random Seed:** -auto-
- Sampling Method:** Monte-Carlo (selected), Latin Hypercube
- Order:** 1
- Probability:** 98.0
- Confidence:** 98.0
- Input Error Handling:** Ignore model check errors
- Replacement Factor:** 0.5
- Figures of Merit:**

Name	Lower Limit	Upper Limit	Description
SUSP	<input type="checkbox"/>	<input type="checkbox"/>	<unset>
MMD	<input type="checkbox"/>	<input type="checkbox"/>	<unset>
SSD	<input type="checkbox"/>	<input type="checkbox"/>	<unset>
TOT_DEP	<input type="checkbox"/>	<input type="checkbox"/>	<unset>

Figure 23: DAKOTA SNAP property Tab for the ENEA CASE 1.

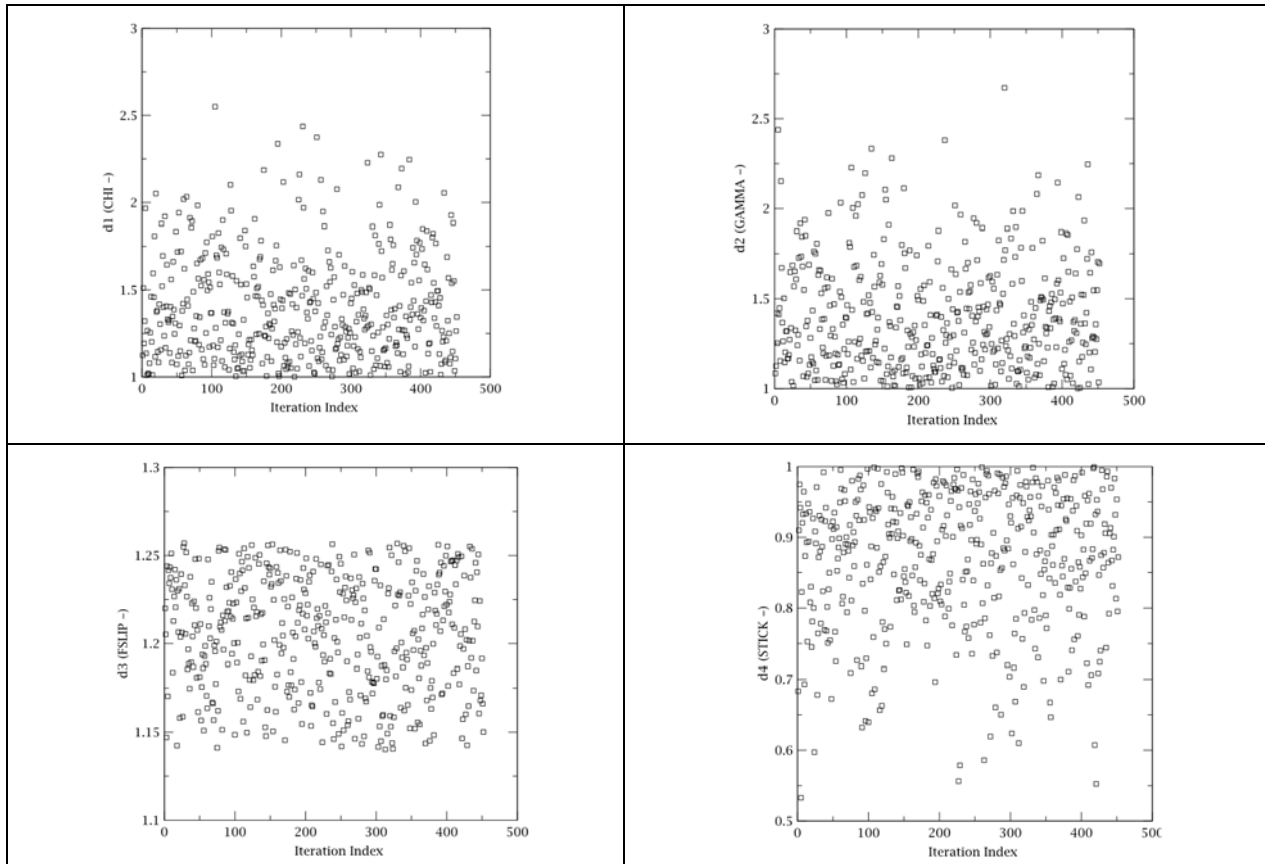


Figure 24: Variate and Response data: input uncertain parameter vs iteration index for the ENEA case1.

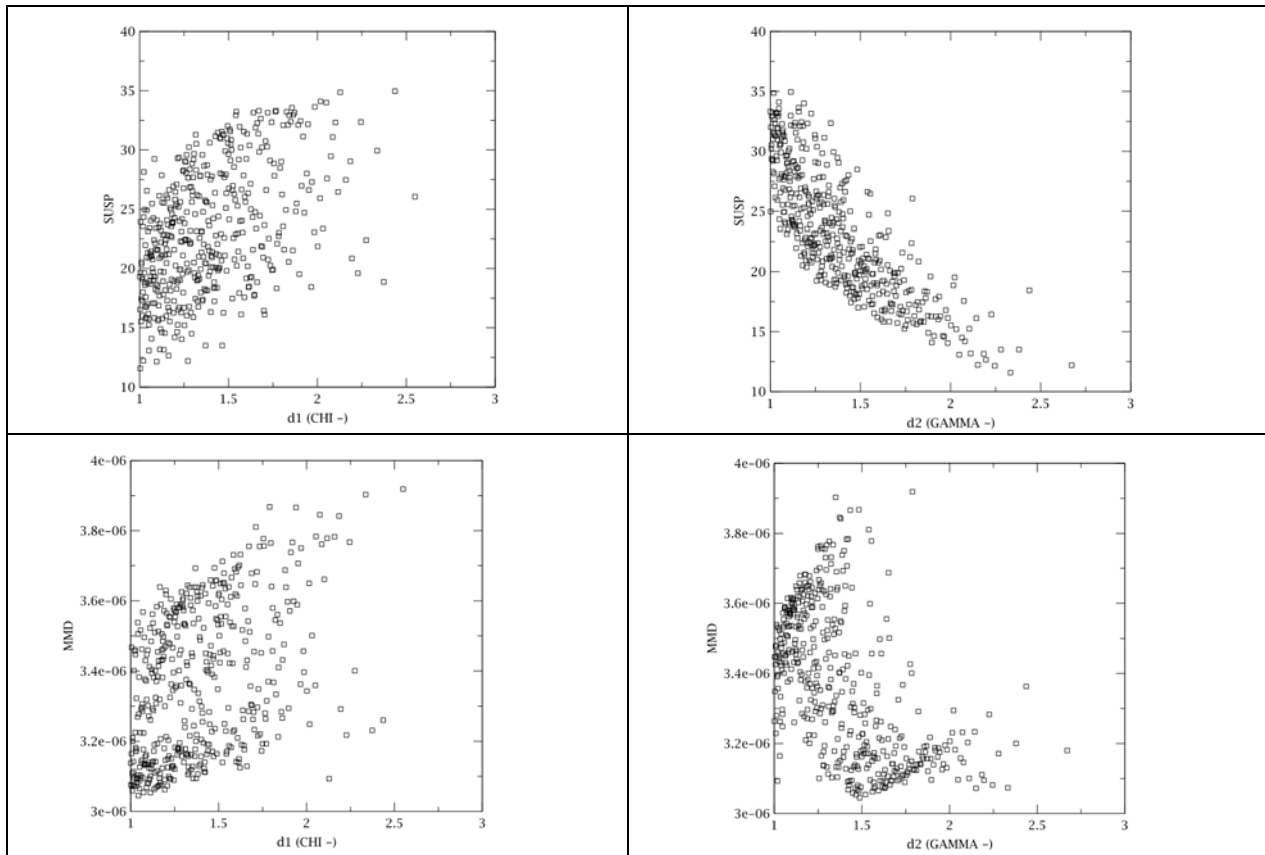


Figure 25: Variate and Response data: FOM VS input uncertain parameters: SUSP and MMD VS D1 (CHI) and d2 (GAMMA) for the ENEA Case 1.

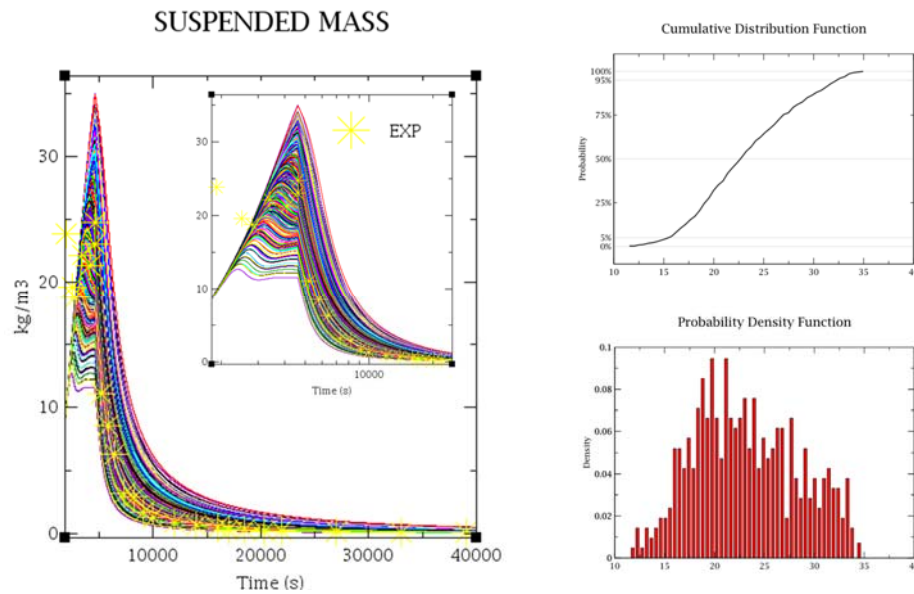


Figure 26: SUSP dispersion of the results against the experimental data, cumulative distribution function, and probability density function (ENEA CASE 1).

Table 5: Statistical results, reported in the automatically generated DAKOTA report, for SUSP-FOM (ENEA CASE 1).

Summary	Value	Task #
Min Value	11,5619	135
Max Value	34,94785	231
Mean	23,1486	-
Median	22,61615	average of 185 and 102
Standard Deviation	5,24126	-
Coefficient of Variance	0,20899	-

Table 6: Response correlation, reported in the automatically generated DAKOTA report, for SUSP FOM (ENEA CASE 1).

	Simple	Partial	Simple Rank	Partial Rank
d1	0.470256	0.87473	0.467447	0.91701
d2	-0.802127	-0.949568	-0.834265	-0.971159
d3	0.0224959	0.058378	0.0222934	0.0260806
d4	-0.168458	-0.604287	-0.180916	-0.639637
d5	-0.0273861	0.00756861	-0.0303348	-0.211284
d6	0.0183224	0.00143064	0.0099558	-0.0508664
d7	-0.00344123	0.0352195	0.00241676	-0.0439138
d8	0.0159181	-0.0395132	0.0320765	0.0407834
MMD	0.750518	-	0.820846	-
SSD	-0.683356	-	-0.604208	-

	Simple	Partial	Simple Rank	Partial Rank
TOT_DEP	-1.0	-	-1.0	-

Note: NaN values typically indicate an insufficient number of tasks were supplied to perform the analysis.

3.1.2 CASE 2: MELCOR/DAKOTA coupling for a PWR

In the CSARP framework, a MELCOR/DAKOTA sample input-deck has been developed by ENEA using the _PWR_v2-0.inp input available for MELCOR users. Since the file was available in ASCII format, the steps that have been done with SNAP are:

- Get the text file : _PWR_v2-0.inp;
- Imported through SNAP and create a .med file;
- Create the STREAM MELCOR and DAKOTA;
- Choose some input uncertain parameters and the related distribution type and related parameters;
- Run the analyses with SNAP.

As a FOM for this first analysis, only the total cumulative hydrogen production in the core from all the oxidation process (COR-DMH2-TOT) at the end the transient has been selected.

The uncertainty parameters that have been selected to apply the procedure, as examples, are:

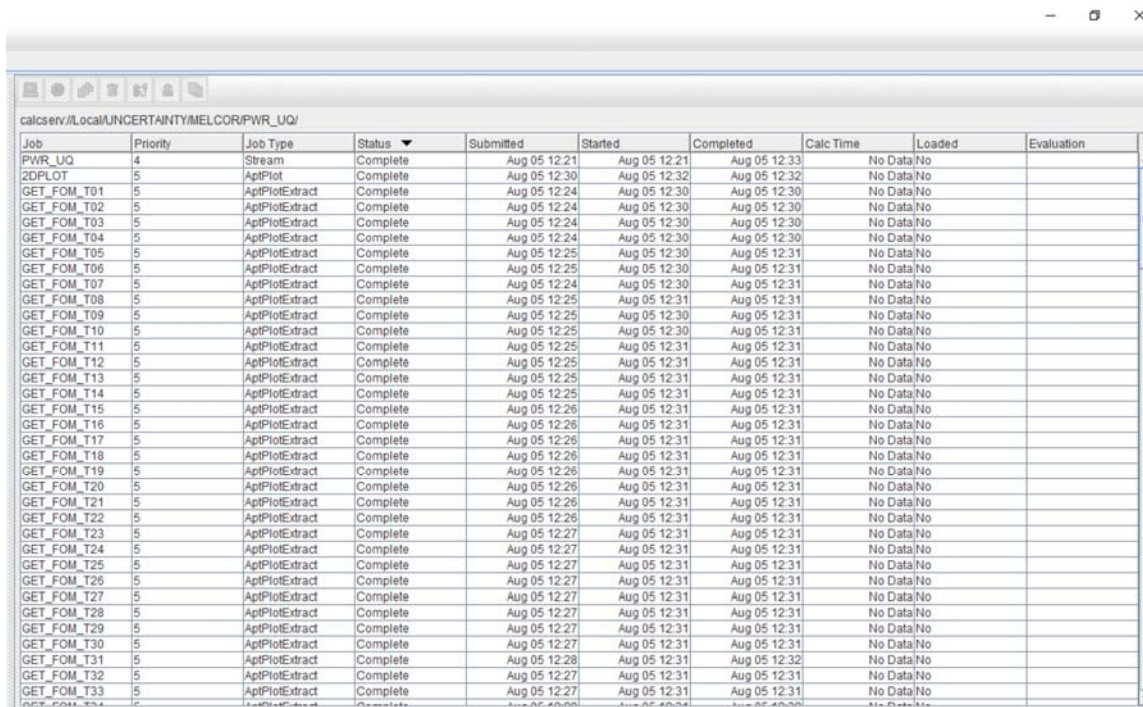
- Vfall : Velocity of falling debris;
- Hdblh: Heat transfer coefficient from debris to lower head;
- SC1132(1): Core Component Failure Parameters - Temperature to which oxidized fuel rods can stand in the absence of unoxidized Zr in the cladding;
- SC1131(2): Zircaloy melt breakout temperature;
- SC1141(2): Core Melt Breakthrough Candling Parameters - Maximum melt flow rate per unit width after breakthrough;
- SC1502(2): Minimum Component Masses - Minimum total mass of component subject to the maximum temperature change criterion for timestep control;
- SC1250(1): Conduction Enhancement for Molten Components - Temperature above which enhancement is employed.

In relation to the input uncertainty parameters a first attempt, only to test the procedure, has been done to characterize them in term of PDF. The type of PDF and the range value of the input uncertain parameters are based on [19] [20] . Table 7, shows the model variables and distribution as summarized in the DAKOTA automatically report.

Table 7: Uncertainty Quantification Input Options - Model Variables and Distributions (ENEA CASE2).

Distribution Name	Distribution Type	Application Rule	Distribution Parameters	Model Variables	Nominal
d1	Triangular	Scalar	a:2098.0, m:2400.0, b:2550.0	COR 1131-2	Replacement
d2	Triangular	Scalar	a:0.01, m:0.083, b:1.0	COR 1141-2	Replacement
d3	Triangular	Scalar	a:0.05, m:0.1, b:1.2	VFALL	Replacement
d4	Triangular	Scalar	a:50.0, m:1000.0, b:1100.0	HDBLH	Replacement
d5	Normal	Scalar	μ :2700.0, σ :120.0, $[-\infty, \infty]$	COR 1132-1	Replacement
d6	Normal	Scalar	μ :5.0, σ :1.0, $[-\infty, \infty]$	COR 1502-2	Replacement
d7	Normal	Scalar	μ :2800.0, σ :150.0, $[-\infty, \infty]$	COR 1250-1	Replacement

Figure 27 shows THE SNAP JOB-STATUS during the DAKOTA uncertainty application (in particular are visualized the different extraction steps). Figure 28 shows the tot hydrogen mass generated dispersion, cumulative distribution function, and probability density function (ENEA CASE 2). Table 8 shows the statistical results based on the 59 samples; Table 9 shows the response correlation reported in the automatically generated DAKOTA report based on the 59 samples (ENEA CASE 2). The input file used in a -pre_run DAKOTA invocation to generate the random variates, is reported in Figure 29.



Job	Priority	Job Type	Status	Submitted	Started	Completed	Calc Time	Loaded	Evaluation
PWR_UQ	4	Stream	Complete	Aug 05 12:21	Aug 05 12:21	Aug 05 12:33	No Data/No		
2DPLLOT	5	AptPlot	Complete	Aug 05 12:30	Aug 05 12:32	Aug 05 12:32	No Data/No		
GET_FOM_T01	5	AptPlotExtract	Complete	Aug 05 12:24	Aug 05 12:30	Aug 05 12:30	No Data/No		
GET_FOM_T02	5	AptPlotExtract	Complete	Aug 05 12:24	Aug 05 12:30	Aug 05 12:30	No Data/No		
GET_FOM_T03	5	AptPlotExtract	Complete	Aug 05 12:24	Aug 05 12:30	Aug 05 12:30	No Data/No		
GET_FOM_T04	5	AptPlotExtract	Complete	Aug 05 12:24	Aug 05 12:30	Aug 05 12:30	No Data/No		
GET_FOM_T05	5	AptPlotExtract	Complete	Aug 05 12:25	Aug 05 12:30	Aug 05 12:31	No Data/No		
GET_FOM_T06	5	AptPlotExtract	Complete	Aug 05 12:25	Aug 05 12:30	Aug 05 12:31	No Data/No		
GET_FOM_T07	5	AptPlotExtract	Complete	Aug 05 12:24	Aug 05 12:30	Aug 05 12:31	No Data/No		
GET_FOM_T08	5	AptPlotExtract	Complete	Aug 05 12:25	Aug 05 12:31	Aug 05 12:31	No Data/No		
GET_FOM_T09	5	AptPlotExtract	Complete	Aug 05 12:25	Aug 05 12:30	Aug 05 12:31	No Data/No		
GET_FOM_T10	5	AptPlotExtract	Complete	Aug 05 12:25	Aug 05 12:30	Aug 05 12:31	No Data/No		
GET_FOM_T11	5	AptPlotExtract	Complete	Aug 05 12:25	Aug 05 12:31	Aug 05 12:31	No Data/No		
GET_FOM_T12	5	AptPlotExtract	Complete	Aug 05 12:25	Aug 05 12:31	Aug 05 12:31	No Data/No		
GET_FOM_T13	5	AptPlotExtract	Complete	Aug 05 12:25	Aug 05 12:31	Aug 05 12:31	No Data/No		
GET_FOM_T14	5	AptPlotExtract	Complete	Aug 05 12:25	Aug 05 12:31	Aug 05 12:31	No Data/No		
GET_FOM_T15	5	AptPlotExtract	Complete	Aug 05 12:26	Aug 05 12:31	Aug 05 12:31	No Data/No		
GET_FOM_T16	5	AptPlotExtract	Complete	Aug 05 12:26	Aug 05 12:31	Aug 05 12:31	No Data/No		
GET_FOM_T17	5	AptPlotExtract	Complete	Aug 05 12:26	Aug 05 12:31	Aug 05 12:31	No Data/No		
GET_FOM_T18	5	AptPlotExtract	Complete	Aug 05 12:26	Aug 05 12:31	Aug 05 12:31	No Data/No		
GET_FOM_T19	5	AptPlotExtract	Complete	Aug 05 12:26	Aug 05 12:31	Aug 05 12:31	No Data/No		
GET_FOM_T20	5	AptPlotExtract	Complete	Aug 05 12:26	Aug 05 12:31	Aug 05 12:31	No Data/No		
GET_FOM_T21	5	AptPlotExtract	Complete	Aug 05 12:26	Aug 05 12:31	Aug 05 12:31	No Data/No		
GET_FOM_T22	5	AptPlotExtract	Complete	Aug 05 12:26	Aug 05 12:31	Aug 05 12:31	No Data/No		
GET_FOM_T23	5	AptPlotExtract	Complete	Aug 05 12:27	Aug 05 12:31	Aug 05 12:31	No Data/No		
GET_FOM_T24	5	AptPlotExtract	Complete	Aug 05 12:27	Aug 05 12:31	Aug 05 12:31	No Data/No		
GET_FOM_T25	5	AptPlotExtract	Complete	Aug 05 12:27	Aug 05 12:31	Aug 05 12:31	No Data/No		
GET_FOM_T26	5	AptPlotExtract	Complete	Aug 05 12:27	Aug 05 12:31	Aug 05 12:31	No Data/No		
GET_FOM_T27	5	AptPlotExtract	Complete	Aug 05 12:27	Aug 05 12:31	Aug 05 12:31	No Data/No		
GET_FOM_T28	5	AptPlotExtract	Complete	Aug 05 12:27	Aug 05 12:31	Aug 05 12:31	No Data/No		
GET_FOM_T29	5	AptPlotExtract	Complete	Aug 05 12:27	Aug 05 12:31	Aug 05 12:31	No Data/No		
GET_FOM_T30	5	AptPlotExtract	Complete	Aug 05 12:27	Aug 05 12:31	Aug 05 12:31	No Data/No		
GET_FOM_T31	5	AptPlotExtract	Complete	Aug 05 12:28	Aug 05 12:31	Aug 05 12:32	No Data/No		
GET_FOM_T32	5	AptPlotExtract	Complete	Aug 05 12:27	Aug 05 12:31	Aug 05 12:31	No Data/No		
GET_FOM_T33	5	AptPlotExtract	Complete	Aug 05 12:27	Aug 05 12:31	Aug 05 12:31	No Data/No		

Figure 27: SNAP JOB-STATUS during the DAKOTA uncertainty application (ENEA CASE2).

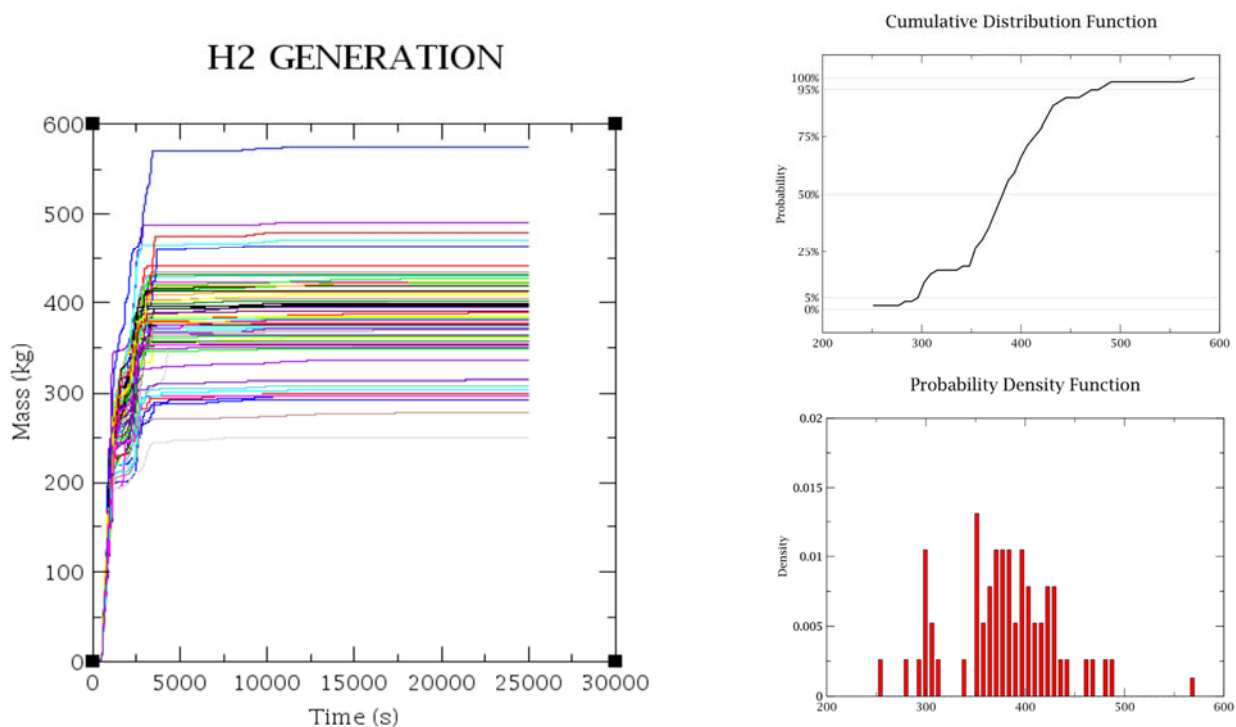


Figure 28: Total hydrogen mass generated dispersion, cumulative distribution function, and probability density function (ENEA CASE 2).

Table 8: Statistical results based on the 59 samples (ENEA CASE 2).

Summary	Value	Task #
Min Value	250.87505	54
Max Value	574.76666	51
Mean	381.43805	-
Median	382.44507	40
Standard Deviation	56.8461	-
Coefficient of Variance	0.38578	-

Table 9: Response correlation reported in the automatically generated DAKOTA report based on the 59 samples (ENEA CASE 2).

	Simple	Partial	Simple Rank	Partial Rank
d5	0.0979063	0.102384	0.135067	0.268539
d6	0.110172	0.146704	0.0338983	0.0599765
d7	0.098521	0.123725	0.126768	0.209831
d1	0.737284	0.791904	0.765926	0.855157
d2	-0.495872	-0.627241	-0.379486	-0.653184
d3	0.03035	0.00594472	0.0189947	0.0516358
d4	-0.0188159	0.0125986	-0.0151373	0.0108442

The input file used in a -pre_run DAKOTA invocation to generate the random variates.

```
method,
  nond_sampling,
    samples = 59
    # stub response levels
    response_levels = 0.0 1.0
    sample_type random
    distribution cumulative

variables,
  normal_uncertain = 3
  descriptors      = 'd5' 'd6' 'd7'
  means           = 2700.0 5.0 2800.0
  std_deviations  = 120.0 1.0 150.0
  lower_bounds    = -1.7976931348623157E308 -1.7976931348623157E308 -
1.7976931348623157E308
  upper_bounds    = 1.7976931348623157E308 1.7976931348623157E308
1.7976931348623157E308

  triangular_uncertain = 4
  descriptors          = 'd1' 'd2' 'd3' 'd4'
  lower_bounds         = 2098.0 0.01 0.05 50.0
  upper_bounds         = 2550.0 1.0 1.2 1100.0
  modes                = 2400.0 0.083 0.1 1000.0

interface,
  system
    analysis_driver = '<not used>'

responses,
  num_response_functions = 1
  no_gradients
  no_hessians
```

Figure 29: DAKOTA input reported in the automatically generated report.

3.2 Uncertainty quantification of in-pool fission product retention during BWR station Black-out sequences (CIEMAT)

This study investigates uncertainties on predictions of suppression pools decontamination. A stand-alone version of SPARC-90 (Suppression Pool Aerosol Removal Code) was used in combination with DAKOTA-6.4, to propagate the uncertainties in the input deck variables affecting the Decontamination Factor (DF). The input data for SPARC-90 was based on MELCOR 2.1 calculations of Fukushima Unit 1. The results indicate that DF uncertainties may spread around two orders of magnitude and the uncertainty margin stays roughly constant over time. In addition, a sensitivity analysis based on the Pearson and Spearman correlation coefficients was carried out and pointed that uncertainties associated to particle inertia (i.e., particle density and size) and in-pool phase change (i.e., non-condensable gas fraction in the carrier gas) dominate the uncertainties found in the DF for this specific scenario.

3.3 Uncertainty quantification for different codes (Tractebel)

An example of application at Tractebel is the following, published with the following reference [21]. The goal of this work was to test improvement of codes and methods for simulation of integral LOCA test experiments. It was focused on the simulation of Halden LOCA tests IFA-650.9 and IFA-650.10. The uncertainty quantification was used to determine if the uncertain bands on the simulation results could cover the experimental results. Without the uncertainty quantification, the simulation of the experiments involved 3 steps. First, the irradiation of the mother rod with the steady state FRAPCON code, then the re-fabrication into an experimental rodlet by adaptation of the restart file from the code, finally the simulation of the experiment with the transient code FRAPTRAN. For the uncertainty quantification, uncertainty parameters in fuel rod manufacturing data, operation and test boundary conditions, physical properties and key models were identified, with their ranges and distributions defined. The total number of contributors was 37. The DAKOTA tool has been used to sample these parameters 200 times and generate corresponding input models for the multi-step simulation. The relevant output parameters (cladding temperature, plenum gas pressure, cladding radius and elongation) were collected, then the lower and upper bounds were determined by using the order statistics. This permitted to confirm that some of the recent code and method improvements were adequate and that others shall be further reworked, Figure 30.

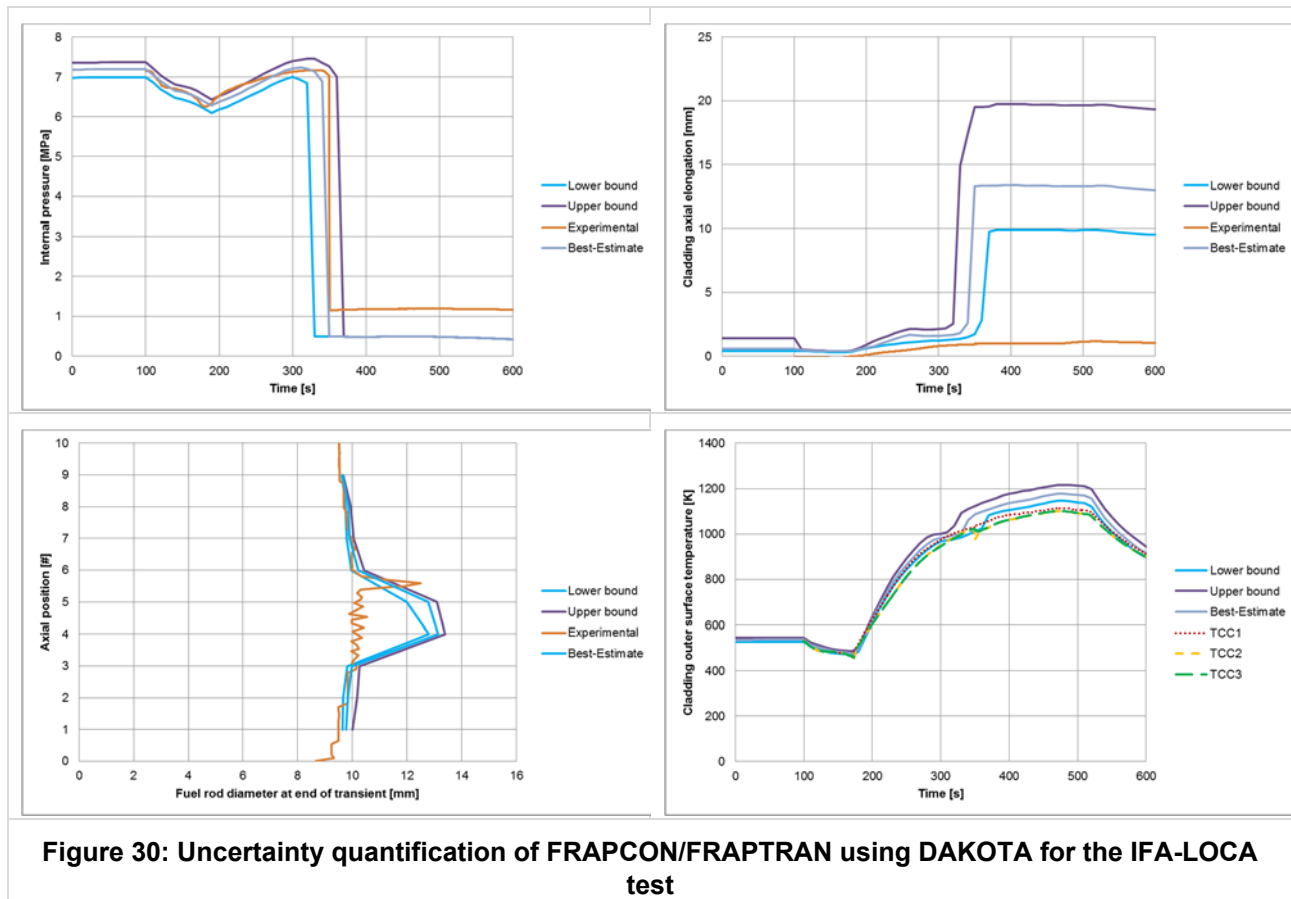
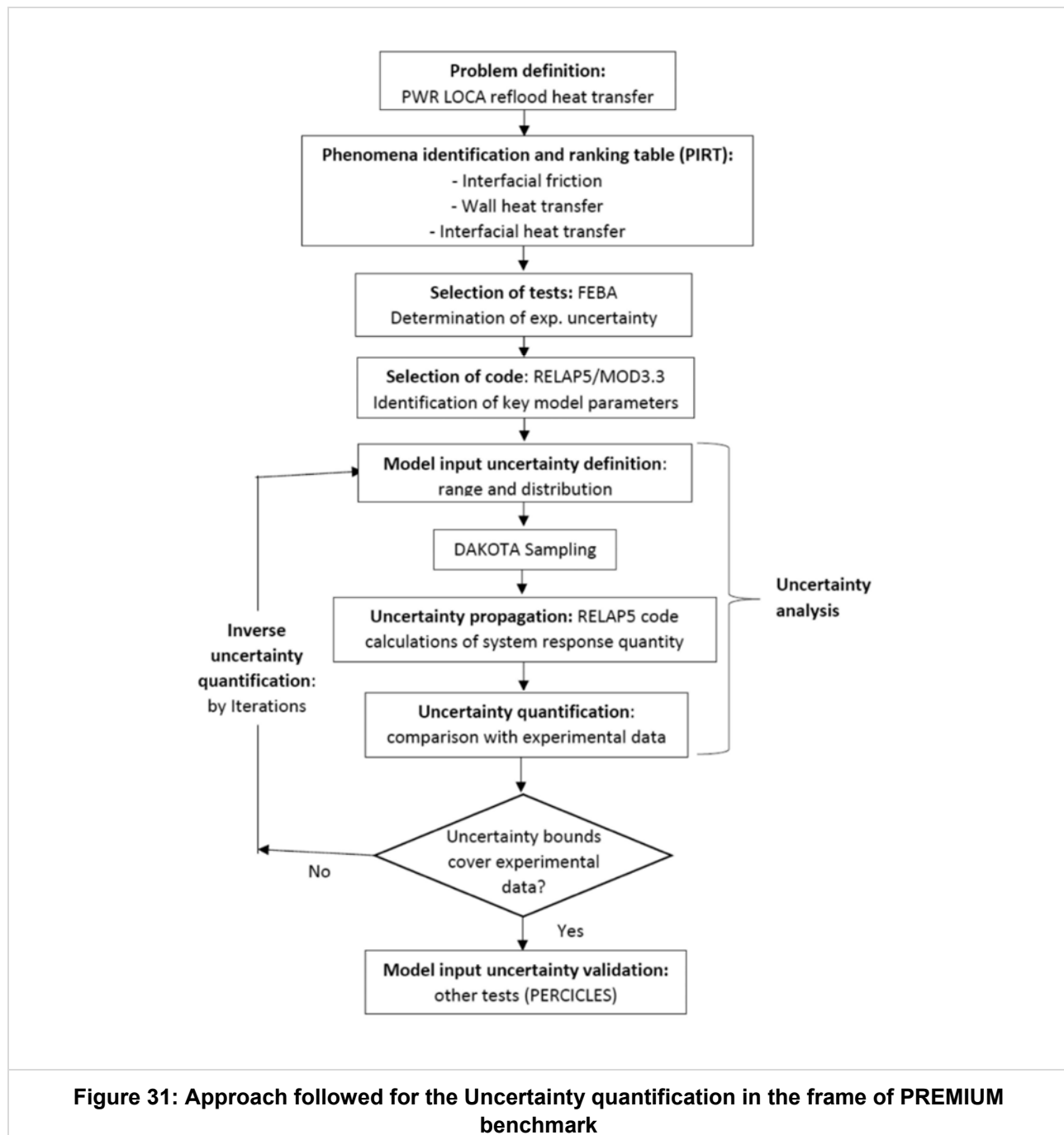


Figure 30: Uncertainty quantification of FRAPCON/FRAPTRAN using DAKOTA for the IFA-LOCA test

Note that the results are varying with time and along the fuel rod axial position. Finally, the important input uncertainty parameters were identified through the partial rank correlation coefficients obtained by the global sensitivity analysis. Other relatively similar applications were made in the previous years. In particular, there was uncertainty analyses in neutronics, fuel rod thermal-hydraulics and core thermal-hydraulics for the UAM benchmark organized by OECD [22]. Also, uncertainty analyses were included in the OECD/NEA REA benchmark [23]. Concerning severe accidents, the DAKOTA tool was interfaced with the EVNTRE code. This coupling has been made in order to develop the capability to perform uncertainty analysis as well as multiple sensitivity analysis on the most important basic events of the Probabilistic Safety Analysis (PSA) level 2. There is also an implementation of the DAKOTA tool with the MELCOR code. This coupling has been made in order to develop the capability to perform the quantification of some basic events of the Probabilistic assessment (PSA) level 2 through MELCOR calculations as well as multiple sensitivity analysis on important Severe Accident phenomena such as aerosols behavior, Molten-Core Concrete Interaction (MCCI), Direct Containment Heating (DCH), etc. There were however difficulties at the time linked to managing the necessary interactions between uncertain contributors and preventing combinations of sampled values that would cause code instability. Another interesting application was performed for the PREMIUM benchmark [14]. In that application of DAKOTA to system thermal-hydraulics code RELAP5/MOD3.3, the aim was to quantify the uncertainty ranges that had to be applied to the model input parameters. This was done by performing repeated uncertainty quantification studies on several relevant experiments. As shown in the following figures, the ranges of uncertain contributors of interest was modified in order to cover all the experimental values with the uncertain bounds on the simulation results by manual iterations.



The IUQ method can be also used to quantify the uncertainty of the major model input uncertainties of the Severe accidents codes.

4 URANIE (KIT, BELV)

4.1 The ASTEC/URANIE platform (KIT)

An interface based on C++ and Python scripts has been developed at KIT to integrate the ASTEC results in the URANIE framework [15][16]. The flowchart of the ASTEC/URANIE platform is shown in Figure 32. The interface performs three actions:

1. Pre-processing: the information related to the PDFs of the uncertainties of the input parameters are loaded in an URANIE DataServer object; after having defined the N numbers of ASTEC runs to be performed, the random Monte Carlo sampling is employed to assess the corresponding N ASTEC input decks; the N ASTEC input decks are run.

2. Export of the ASTEC results to the URANIE sampling: the ASTEC results for the output variables of interest are collected in *.plt files; such data are reorganized in a unique file suitable to be employed by URANIE.
3. Post-processing: the statistics is performed by URANIE; the results are sampled and provided as .txt or .csv files.

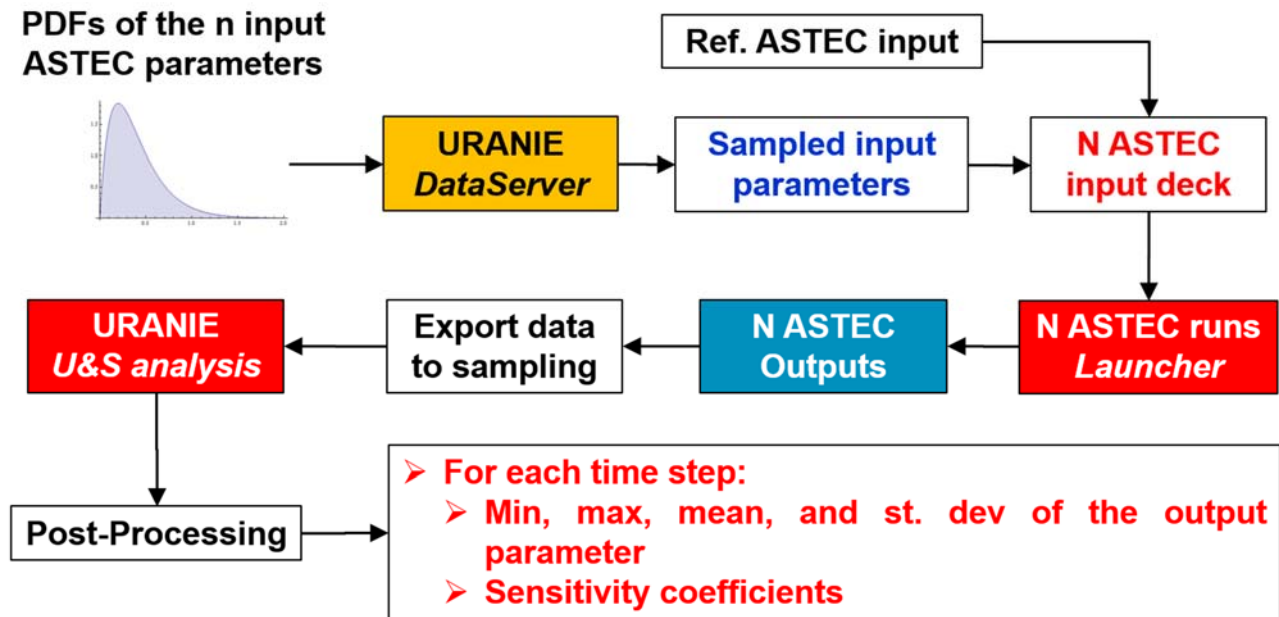


Figure 32: Flowchart of the ASTEC/URANIE Platform developed at KIT [24]

4.1.1 Application of the ASTEC/URANIE platform to QUENCH-08 Experiment

The ASTEC/URANIE platform has been employed to perform the U&S analysis of the ASTEC results for the QUENCH-08 experiment, performed at KIT [25].

The QUENCH-08 test aimed analyzing the effect of the injection of a low mass flow rate (steam) on H₂ production, namely representing the effect of the dispersed flow region located above the Transition Boiling Region on a pre-oxidized PWR sub-assembly. As shown in Figure 33, the bundle is loaded with 21 Zr-4 Fuel Rod Simulators (FRS) (20 heated+1 unheated) with identical radial dimensions as PWR fuel-element cladding (pin pitch=1.43 cm).

During the scenario, after a pre-heating phase and stabilization, the transient begins by increasing the power of the bundle Figure 34. The quenching phase is initiated by injecting saturated steam (15 g/s, 0.5 g/s/rod) when the temperature of the shroud at 950 mm elevation reaches 2073 K (@3776 s). The power continues to increase for ~40 s and then reduced from ~17.8 kW to ~4kW within 16 s and to zero.

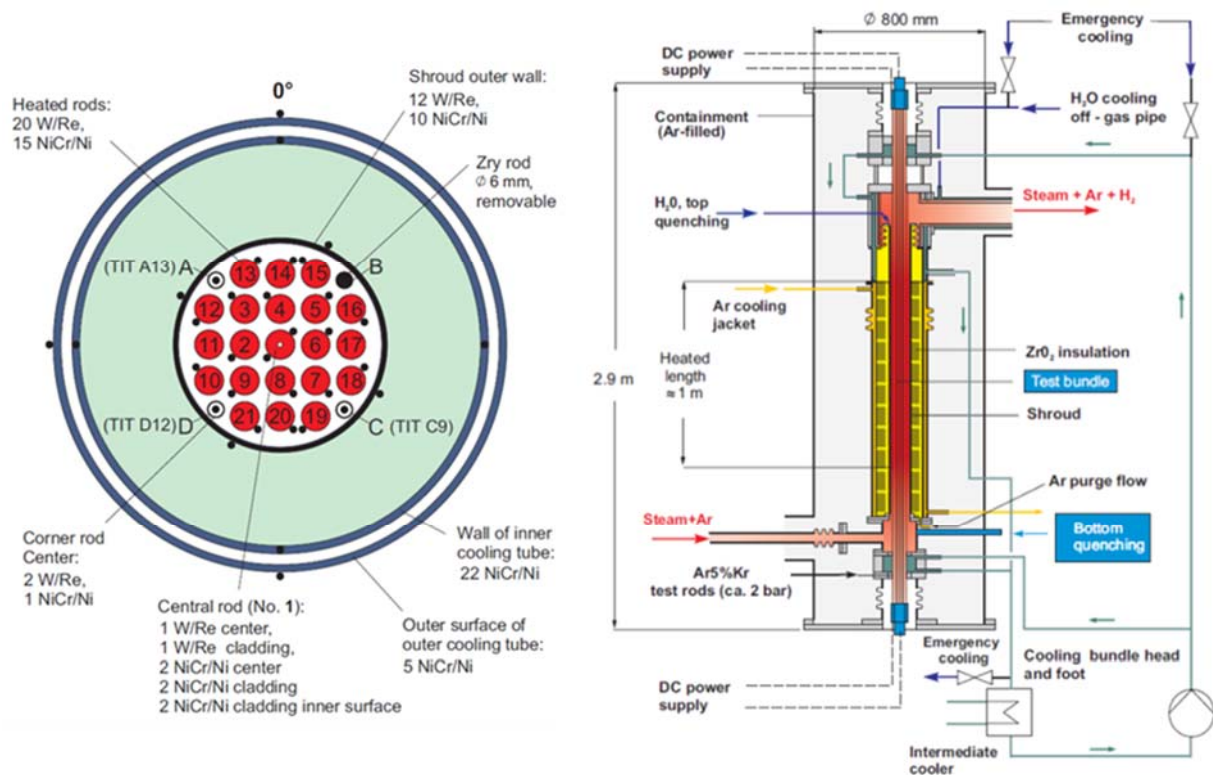


Figure 33: Sketch of the QUENCH facility [25]

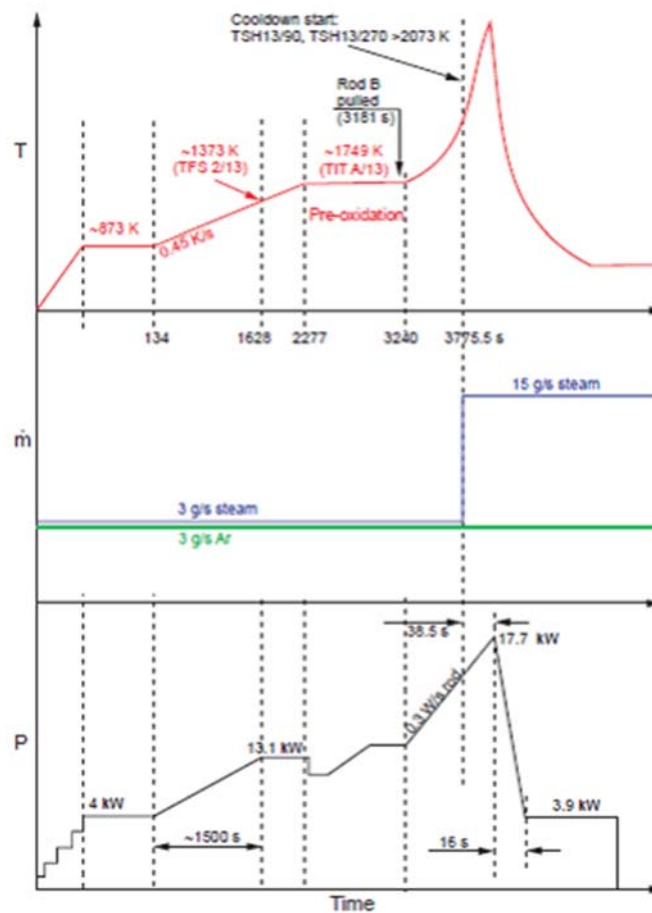


Figure 34: QUENCH-08 experiment

The FOMs of the QUENCH08 experiment are the total amount of H₂ produced, the oxide scales of selected rods, and the temperature behavior at different elevations in the bundle and in the shroud.

The U&S analysis of the ASTEC results has been carried out by employing the latest versions of the ASTEC code (v2) and of the URANIE tool (v4.1) with two main goals:

- Evaluating the performance of the calculation procedure when applied to 'real' ASTEC evaluations;
- Identifying the pros and contra of the application of URANIE to ASTEC in terms of volume of data to be managed and related CPU wall-clock time.

Having this in mind, a stress test has been performed to check the robustness of both the ASTEC/URANIE platforms and the URANIE tool when applied to severe accident codes. Therefore a quite large number of input and output parameters has been considered in the analysis, which has been performed for each time step of the ASTEC calculation.

The uncertainty of 24 input parameters has been propagated in the ASTEC/URANIE evaluation with respect to: the geometry model, the scenario, the clad integrity criteria, the radiative and convective heat exchange model, and the relocation and oxidation of the molten material. The list of input parameters and the information on the PDFs of the associated uncertainties are shown in Table 10. In order to assess the PDFs of the input parameters, the data in [17] have been considered.

Table 10: Input parameters of the ASTEC/URANIE analysis of the QUENCH-08 test [24]

Parameters	PDF	Mean	Std. Dev.	Min./Max.
Int. diameter Shroud	Uniform			0.99/1.01
Thickness Shroud	Uniform			0.99/1.30
Thickness Insulator	Uniform			0.99/1.01
Ar Mass Flow Rate	Normal	1.0	0.05	0.95/1.05
Steam Mass Flow Rate	Normal	1.0	0.05	0.95/1.05
Outlet Pressure	Normal	1.0	0.02	0.98/1.02
Fuel/Clad Internal Pressure	Uniform			0.99/1.01
Rod Anisotropic Factor	Uniform			0.00/1.00
Shroud Anisotropic Factor	Uniform			0.00/1.00
Threshold Thickness	Uniform			200/400
Failure T ZrO ₂	Uniform			2248/2500
HD (Average additional heat transfer coefficient due to droplet projection)	Normal	100.0	0.05	95/105
ZD (Height above the quench front concerned by droplet projection)	Normal	0.8	0.05	0.76/0.84
Alpha (Threshold void fraction to allow exchange with liquid droplets)	Uniform			0.99/0.999
CRES (Residual saturation)	Uniform			0.80/1.20
KEXP (Exponent for the saturation in the relative permeability)	Uniform			2.0/4.0
KSMX (Maximum value of Permeability/Viscosity)	Uniform			0.90/1.10
GRDR (Corrective factor for the gradient in the crust interfacing with the liquid)	Uniform			0.90/1.10
GREX (Corrective factor for the gradient in the crust interfacing with the steam)	Uniform			0.90/1.10

HSLX (Max value for the mass transfer coefficient HSL between solid and liquid)	Uniform			0.90/1.10
MULT (Factor applied on exchange area)	Uniform			0.90/1.10
RDZR (Relative diffusivity of ZR in the melt)	Uniform			0.90/1.10
KEXP (Exponent for the saturation in the relative permeability)	Uniform			2.0/4.0

The FoMs of the analysis are the H₂ production, the rods and shroud oxide scales, and the rods and shroud temperatures at different elevations for a total of 37 vectorial output parameters with a size of 2380 time steps. Therefore, the total number of variables is about 90000 (24+37*2380). Note that despite the employment of such large number of input and output parameters is most likely out of the scope of plant analyses, such big dimensions of the problem allow evaluating the performance of the ASTEC/URANIE platform.

4.1.2 The ASTEC/URANIE results for the QUENCH-08 Experiment

50 ASTEC runs have been performed. The results concerning mean, Std. Dev, minimum, and maximum of the H₂ mass produced and the H₂ production rate are shown in Figure 35. Attention is focused on the H₂ integral production. The results show that the mean value is about 60g, about 20 g below the best-estimate evaluation, with a Std. Dev of about 25 g.

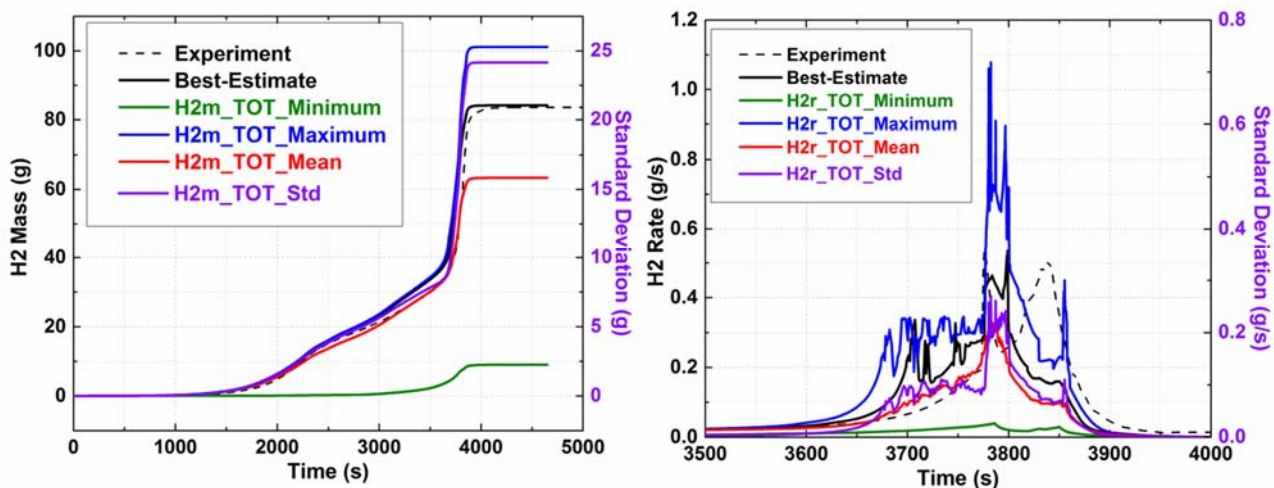


Figure 35: ASTEC/URANIE results: H₂ mass and production rate [24]

The Pearson's sensitivity coefficients related to the input parameters for the geometry model and the scenario are shown in Figure 36. The results show a significant impact of the uncertainty on the internal diameter of the shroud on the H₂ production in the quench phase. The internal diameter and the thickness of the shroud, as well as the Ar and steam mass flow rate influence the pre-quenching phase.

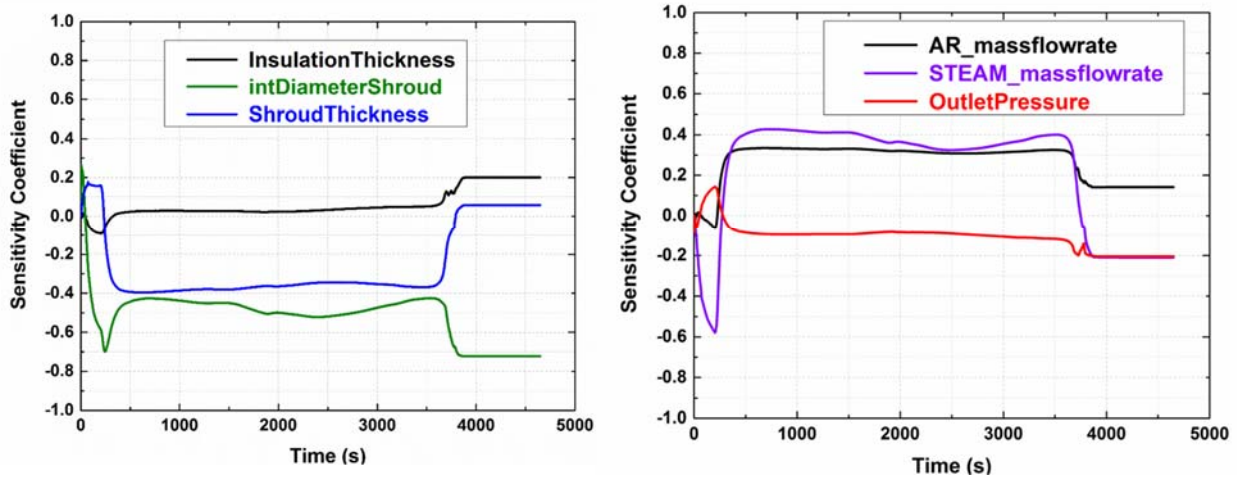


Figure 36: Sensitivity of the H₂ production on the input parameters for the geometry and the scenario [24]

The Pearson's sensitivity coefficients related to the input parameters for the radiative and convection heat exchange are shown in Figure 37. As expected, the uncertainty on the convection model have no meaningful influence on this scenario. On the contrary, the anisotropic factor of the rods and of the shroud have a not negligible impact of the H₂ production in the pre-heating and during the stabilization phases, respectively.

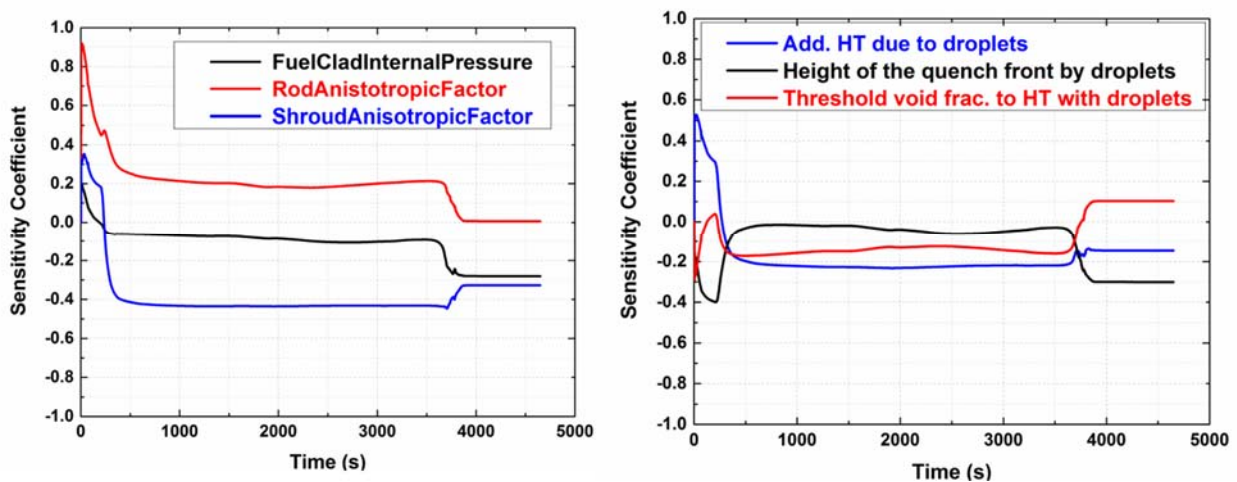


Figure 37: Sensitivity of the H₂ production on the input parameters for radiative and convection heat exchange [24]

The Pearson's sensitivity coefficients related to the input parameters for the relocation and oxidation of the molten material are shown in Figure 38. The results show that the most significant impact on the H₂ production after quenching comes from the uncertainty on the diffusivity of Zr in the melt (about 60%) and on the heat exchange area of the melt (about 40%). This is in line with the ASTEC results, which predict the melt formation between 950 mm and 1100 mm elevation as also observed in the experiment.

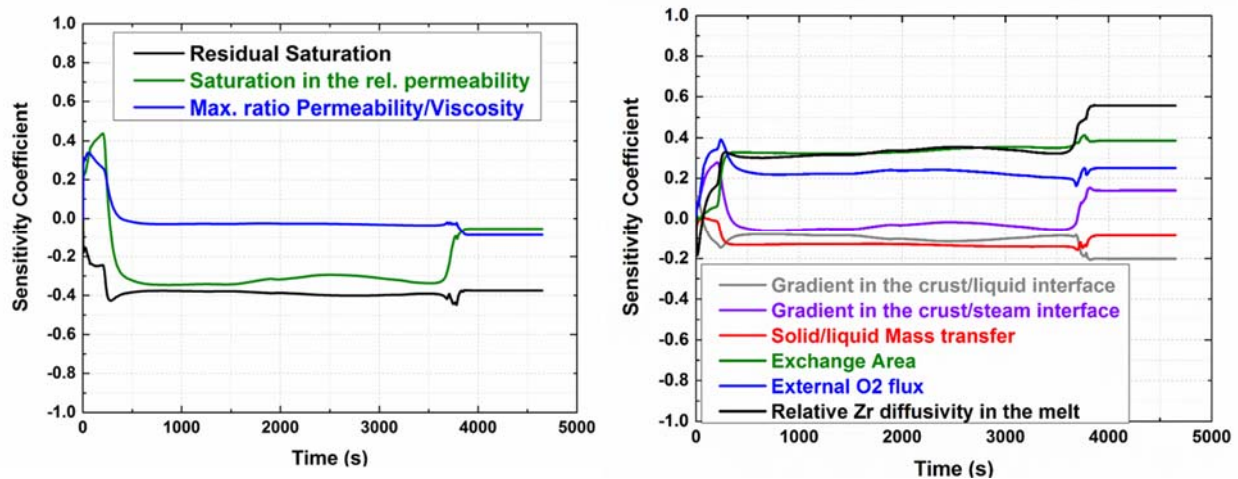


Figure 38: Sensitivity of the H₂ production on the input parameters for relocation and oxidation of the molten material [24]

4.1.3 Performance of the ASTEC/URANIE application to the QUENCH-08 Experiment

The ASTEC/URANIE are rather consistent, namely the trends of the results were expected. From this point of view, the URANIE tool shows to be able to be applied to severe accident codes. Further, the ASTEC/URANIE platform demonstrates to be a powerful tool for U&S analyses of severe accident scenarios.

The stress test allowed further improving the performance of the URANIE. The original version of the ASTEC/URANIE interface employed a read/write mode by columns, namely for each line the data on each columns were read/written. The CPU wall-clock time employed is huge (about 32.6 hours) despite the parallel option activated, as shown in Table 11. URANIE developers suggested employing the 'vector mode', namely each column is read/written as a vector of elements. By extending the URANIE input deck with the 'read/write by vectors mode', the URANIE tool takes about 6 minutes (Table 11), which is rather reasonable.

Table 11: CPU wall-clock time of URANIE: original vs. update

Action	Original	Update
Read/write mode	by columns	by vectors
Reading input file	10 minutes	21 s
Computing statistics	4.2 hours	58 s
Writing Output Files	28.4 hours	4 minutes
Total	~ 32.6 hours	~ 6 minutes

An important aspect refers to the CPU wall-clock time for the ASTEC simulations. The ASTEC part of the analysis of the QUENCH-08 experiment took about 850 minutes (50 runs, 2 CPUs on a VirtualBox). In view of performing similar analysis at plant level, running on clusters look mandatory, or at least recommended. Efforts at KIT are going on in this direction.

4.2 Bel V Experience from the application of URANIE

URANIE [26] has been used by Bel V for the OCDE/NEA PREMIUM benchmark [27] [28], coupled with the thermal-hydraulic system code CATHARE2, and the probability density functions of the uncertain input parameters determined by the CIRCE methodology [29]. The study addressed the uncertainties in the physical models involved in predicting the reflooding of fuel rods in the core, such as heat transfer downstream of the quench front, enhance of thermal transfer near the quench front, the phases relative velocity to the downstream of the quench front.

Hereafter, the different phases of the study performed by Bel V are listed.

- I. Identification of the physical models of the CATHARE2 code associated with physical phenomena considered to be predominant [30] [31] [32].
- II. Determination of the most Influential Uncertain Input parameters (IUIP) associated with these physical models by performing sensitivity analyses on the basis of a CATHARE2 reference calculation of one test of FEBA reflooding experimental program.
- III. Quantification of the uncertainties of the IUIP based on the results of several FEBA tests, by using CATHARE2 and the CIRCE methodology.
- IV. Propagation of uncertainty for the FEBA and PERICLES reflooding experiments by using CATHARE2 coupled with URANIE, to verify the quality of the method prediction, and confirm the uncertainties found in the previous phase.

The most influential uncertain input parameters, selected thanks to CATHARE2 analysis, were: the interfacial friction, the global wall to fluid heat transfer, and the very local quench front progression reflood parameter.

A total of 74 responses derived from the CIRCE approach and associated to 6 FEBA tests have been used as input for the propagation of the uncertainties in URANIE: cladding temperatures downstream the quench front for various times and elevations (46) and quenching time at various elevations (28).

For the multipliers of the coefficients used in physical models of CATHARE2, a log-normal law formulation of the probability density function has been chosen in CIRCE, **a normal formulation has been discarded because leading to negative multipliers.**

For both series of experiments (6 tests for each series), the characteristics of the uncertainty propagation in URANIE were the following:

- Simple Random Sampling
- No truncation performed
- Sample size set to 200; that is 2400 calculations

Uncertainty analysis of the 1D Reflooding FEBA tests shows that the results of the reference calculations and the experimental data are generally inside uncertainty bands.

Uncertainty analysis of the 2D Reflooding PERICLES (blind) tests shows that the results of the reference calculations and experimental data are generally outside uncertainty bands, moreover, reference calculations is very different from the experimental data (see for example the cladding temperature in Figure 39).

One of the main reason of unsatisfactory results is connected with the use of CIRCE (hypothesis of linearity not always fulfilled). Note that CIRCE has also a limitation: the application to the quantification of input uncertain parameters larger than 1-3 not recommended.

Nevertheless, **URANIE has proven to be an adequate tool to manage the propagation of uncertainties on two series of experiments of six tests each, on which 200 runs per test were performed.** Its application to severe accident codes is possible since URANIE is able to handle a code in a non-intrusive manner, considering it as a black box.

Another issue is the **selection of experiments and their adequacy for the purpose of the study**, e.g. for the current case, the lack of representativeness of the FEBA experiment (used for input uncertainty quantification) for PERICLES (used for input uncertainty validation, blindly).

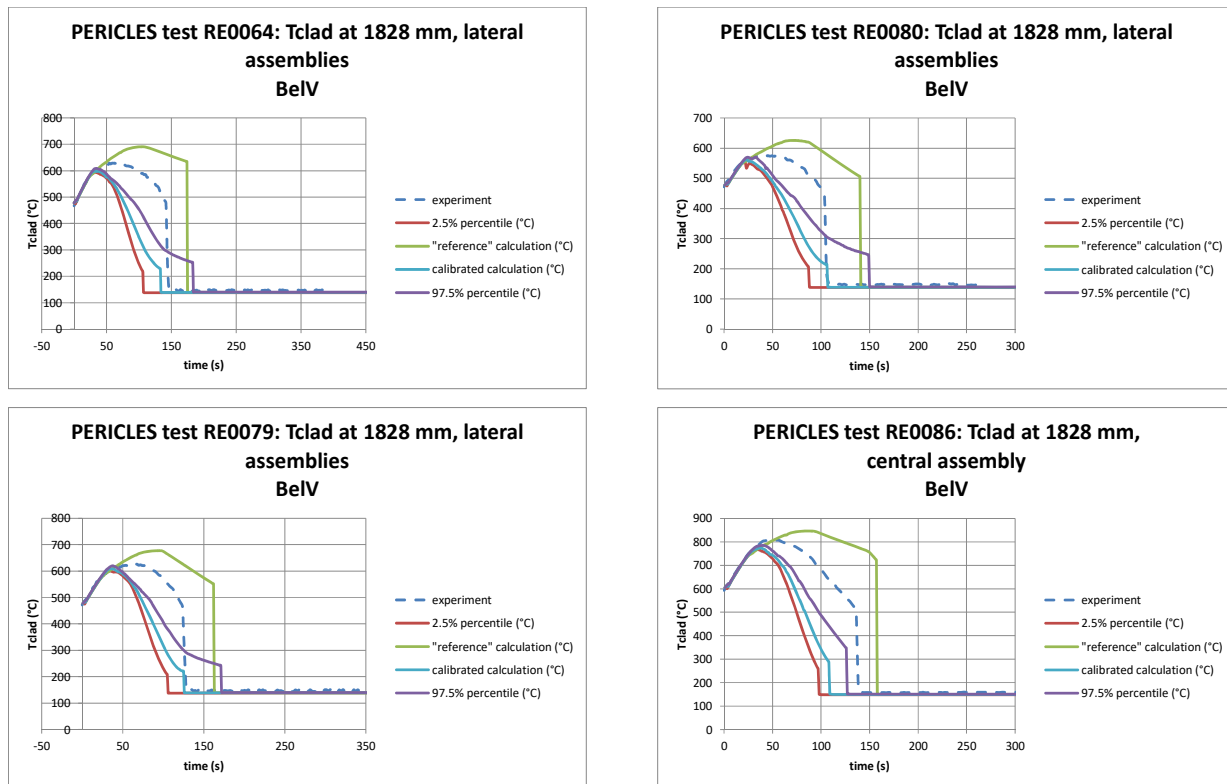


Figure 39: Uncertainty Propagation for PERICLES tests – Cladding Temperatures

5 RAVEN (UNIRM1, JAEA)

5.1 Source term uncertainty quantification and global sensitivity analysis

As the previous UQSA experience, JAEA developed a specific methodology, consisting of a sampling-based UQ and surrogate-based GSA. The UQ part consists of

1. parameter screening (one-at-a-time method and Morris method),
2. LHS sampling considering parameter correlations,
3. MELCOR1.8.5 running,
4. probability density functions of representative source terms of Cs and I.

The GSA part consists of

1. training of a statistical surrogate model using Bayesian nonparametric method,
2. global sensitivity analysis using Sobol' sensitivity index. For the MUSA project, MELCOR 2.2 is currently usable at JAEA, and will be used to coupling with RAVEN [33] [34].

5.2 Other applications

JAEA has used RAVEN for simulation-based probabilistic risk assessment (also known as dynamic PRA), by coupling with a simplified thermal-hydraulic code.

6 References

- [1] O. NEA, "NEA/CSNI/R(2015)3 : Ability of current advanced codes to predict In-vessel core melt progression and degraded core coolability, Benchmark exercise on the Three Mile Island-2 Plant", 2015.
- [2] G. e. a. Weber, "Uncertainty and sensitivity analysis on the Iodine model in the containment Code COCOSYS," in *NUTHOS10*, Japan, 2014.
- [3] T. Kaliatka, A. Kaliatka and a. V. Vileiniskis, "Application of Best Estimate Approach for Modelling of QUENCH-03 and QUENCH-06 Experiments," *Nucl. Eng. Technol.*, p. 419–433, Nr.2 Vol.48 2016.
- [4] V. Vileiniskis and A. Kaliatka, "Best estimate analysis of PHEBUS FPT1 experiment bundle phase using ASTEC code ICARE module," *Kerntechnik*, Nr.4 Vol.76 2011.
- [5] A. Kontautas and E. Urbonavičius, "Uncertainty and sensitivity evaluation of aerosol deposition in PHEBUS containment during FPT-2 experiment," *Energetika*, pp. 12-24, Nr. 1 Vol. 6 2015.
- [6] M. Povilaitis, S. Kelm and E. Urbonavičius, "The Generic Containment SB-LOCA accident simulation: Comparison of the parameter uncertainties and user-effect," *Ann. Nucl. Energy*, p. 1–10, 2017.
- [7] M. Povilaitis, E. Urbonavičius, S. Rimkevičius and E. Babilas, "Sensitivity and uncertainty analysis of atmosphere stratification modelling in MISTRA using lumped-parameter code COCOSYS," *Nucl. Eng. Design*, p. 108–119, 2013.
- [8] R. Alzbutas, "Probabilistic Dynamics for Integrated Analysis of Accident Sequences considering Uncertain Events," *Sci. Technol. Nucl. Install*, 2015.
- [9] A. B. Salah, S. Kliem, U. Rohde, F. D'Auria and A. Petrucci, "Uncertainty and sensitivity analyses of the Kozloduy pump trip test using coupled thermal-hydraulic 3D kinetics code," *Nucl. Eng. Design*, p. 1240–1255, No.12 Vol.236 206.
- [10] K. Chevalier-Jabet, F. Cousin, L. Cantrel and C. Séropian, "Source term assessment with ASTEC and associated uncertainty analysis using SUNSET tool," *Nucl. Eng. Design*, p. 207–218, Vol.272 2014.
- [11] L. L. Humphries, R. K. Cole, D. L. Louie, V. G. Figueroa and a. M. F. Young, "MELCOR Computer Code Manuals, Vol. 1: Primer and Users' Guide. SAND2015-6691 R," SANDIA Nat. Lab, USA, 2015.
- [12] L. L. Humphries and e. al., "MELCOR Computer Code Manuals: Vol. 3: MELCOR Assessment Problems SAND2015-6693," Sandia Nat. Lab., USA, 2015.
- [13] F. Mascari, "ENEA ACTIVITIES IN THE FIELD OF SEVERE," ENEA, Italy, 2019.
- [14] L. E. Herranz, M. Garcia, L. Lebel, F. Mascari and C. Spengler, "In-containment source term predictability of ASTEC-Na: Major insights from data-predictions benchmarking," *Nucl. Eng. Des*, p. 269–281, Vol. 320 2017.
- [15] L. E. Herranz, L. Lebel, F. Mascari and C. Spengler, "Progress in modeling in-containment source term with ASTEC-Na," *Ann. Nucl. Energy*, p. 84–93, Vol.112 2018.
- [16] R. K. Hilliard, J. D. McCormack and A. K. Postma, "Aerosol behavior during sodium pool fires in a large vessel - CSTF tests AB1 and AB2.HEDL-TME 79-28," Hanford Engineering Development Laboratory, UK, 1979.

- [17] L. E. Herranz, M. Garcia and S. Morandi, "Benchmarking LWR codes capability to model radionuclide deposition within SFR containments: An analysis of the Na ABCOVE tests," *Nucl. Eng. Des.*, p. 772–784, vol. 265 2013.
- [18] S. S. Wilks, "Determination of Sample Sizes for Setting Tolerance Limits," *Ann. Math. Stat.*, p. 91–96, 1941.
- [19] P. Mattie and et.al., "State-of-the-Art Reactor Consequence Analyses Project , Uncertainty Analysis of the Unmitigated Long-Term Station Blackout of the Peach Bottom Atomic Power Station, NUREG/CR-7155," USA, 2016.
- [20] M. D'onorio, F. Giannetti, F. Mascari and G. Caruso, "Uncertainty Analyses Using The Raven Software Tool Coupled With Melcor Severe Accident Code," UNI Rome, Italy , 2018.
- [21] J. Zhang, A. Dethioux, T. Drieu, B. Quivy and C. Schneidesch, "Statistical Uncertainty and Sensitivity Analysis on the FRAPTRAN-TE-1.5 Modelling of the Halden LOCA Tests IFA-650.9 and IFA650.10," TRACTEBEL, Belgium, 2017.
- [22] J. Zhang, A. Dethioux, T. Drieu and C. Schneidesch, "Development and Application of Statistical Uncertainty Analysis Method to Multi-Physics Modelling to Support Reactor Core Design and Operation," Tractebel, Belgium, 2018.
- [23] O. Marchand, J. Zhang and M. Cherubini, "Uncertainty and sensitivity analysis in reactivity-initiated accident fuel modeling: synthesis of organisation for economic co-operation and development (OECD)/nuclear energy agency (NEA) benchmark on reactivity-i," *Nuclear Engineering and Technology*, pp. 140-152, Nr. 2 Vol. 50 2018.
- [24] F. Gabrielli and V. Sanchez-Espinoza, "Uncertainty and Sensitivity Analysis by means of ASTEC/URANIE Platform of the QUENCH-08 Experiment," KIT, Karlsruhe, 2019.
- [25] J. Stuckert and et.al., "Experimental and computational results of the QUENCH-08 experiment. (Reference to QUENCH-07), report FZKA-6970," Karlsruhe, 2005.
- [26] J.-B. Blanchard, G. Damblin, J.-M. Martinez, G. Arnaud and a. F. Gaudier, "The Uranie platform: an open-source software for optimisation, meta-modelling and uncertainty analysis," *EPJ Nucl. Sci. Technology*, p. 4, Vol5 2019.
- [27] OECD PREMIUM, "Post-BEMUSE Reflood Model Input Uncertainty Methods (PREMIUM) Benchmark Final Report, NEA/CSNI/R(2016)18," NEA, Paris, 2016.
- [28] T. Skorek and e. al., "Quantification of the uncertainty of the physical models in the system thermal-hydraulic codes – PREMIUM benchmark," *Nucl. Eng. Design*, p. 110199, Vol- 354 2019.
- [29] A. d. Crécy, "CIRCÉ: A methodology to quantify the uncertainty of the physical models of a code, STMF/LGLS," IRSN, France, 2012.
- [30] F. Barre and M. Bernard, "The CATHARE code strategy and assessment," *Nucl. Eng. Design*, p. 257–284, Nr.3 Vol.124 1990.
- [31] D. Bestion, "The physical closure laws in the CATHARE code," *Nucl. Eng. Design*, p. 229–245, Nr.3 Vol124 1990.
- [32] J. Bartak, D. Bestion and T. Haapalehto, "The top-down reflooding model in the CATHARE code," *Nucl. Eng. Design*, p. 141–152, Nr.1 Vol 149 1994.
- [33] X. Zheng, H. Itoh, K. Kawaguchi, H. Tamaki and Y. Maruyama, "Application of Bayesian nonparametric models to the uncertainty and sensitivity analysis of source term in a BWR severe accident," *Reliab. Eng. Syst. Safety*, p. 253–262, Vol.138 2015 .

- [34] X. Zheng, H. Itoh, H. Tamaki and Y. Maruyama, "An integrated approach to source term uncertainty and sensitivity analyses for nuclear reactor severe accidents," *J. Nucl. Sci. Technology*, p. 333–344, Vol. 53 2016.
- [35] Fukushima Daiichi Unit 1 Accident Progression Uncertainty Analysis and Implications for Decommissioning of Fukushima Reactors – Volume I", , January 2016., "Fukushima Daiichi Unit 1 Accident Progression Uncertainty Analysis and Implications for Decommissioning of Fukushima Reactors," Sandia, USA, 2016.
- [36] M. R. Denman and D. M. Brooks, "Fukushima Daiichi Unit 1 Uncertainty Analysis – Exploration of Core Melt Progression Uncertain Parameters," Sandia, 2015.
- [37] M. M. D., R. J. Beckman and C. and W. J., "A comparison of three methods for selecting values of input variables in the analysis of output from a computer code," *Technometrics*, p. pp. 55–61, 42 No.1 2000.
- [38] A. Hoefer, O. Buss, M. Hennebach, M. Schmid and a. D. Porsch, " "MOCABA: A general Monte Carlo-Bayes procedure for improved predictions of integral functions of nuclear data," *Annals of Nuclear Energy*, p. 514–521, 2015.
- [39] G. Cecchini, U. Farinelli, A. Gandini and a. M. Salvatores, "Analysis of Integral Data for Few-Group Parameter Evaluation of Fast Reactors," 1964.
- [40] M. Humi, J. J. Wagschal and a. Y. Yeivin, "Multi-Group Constants from Integral Data," 1964.
- [41] A. Hoefer, O. Buss and a. M. Schmid, "Applications of Multivariate Normal Bayesian Models in Nuclear Engineering," *Nuclear Technology*, p. 1578–1587, Vol 205 12 2019.
- [42] A. H. a. O. Buss, "Assessing and Improving Model Fitness in MOCABA Data Assimilation," 2020.
- [43] E. Peters, F. Sommer and a. M. Stuke, "Modeling of critical experiments and its impact on integral covariance matrices and correlation coefficients," , *Ann. Nucl. Energy*, p. 355–362, 2016.
- [44] A. H. a. O. Buss, "Impact of Covariances between Criticality Benchmark Experiments on Licensing," 2019.
- [45] E. Castro, C. Ahnert, O. Buss, N. García-Herranz, A. Hoefer and a. D. Porsch, "Improving PWR core simulations by Monte Carlo uncertainty analysis and Bayesian inference," , *Ann. Nucl. Energy*, p. 148–156, 2016.
- [46] D. Siefman, M. Hursin, D. Rochman, S. Pelloni and a. A. Pautz, "Stochastic vs. sensitivity-based integral parameter and nuclear data adjustments," , *Eur. Phys. J. Plus*, p. 429, Vol 133 No 10 2018.
- [47] Steinbuch Centre for Computing, 2014. [Online].
- [48] E. Chonacki and a. J. Baccou, "SUNSET V2.1: Theory Manual and User Guide," IRSN, Cadarache, 2013.
- [49] U. NRC, "AN APPROACH FOR DETERMINING THE TECHNICAL ADEQUACY OF PROBABILISTIC RISK ASSESSMENT RESULTS FOR RISK-INFORMED ACTIVITIES, Regulatory Guide 1.203," December 2005. [Online]. Available: Available: <https://www.nrc.gov/docs/ML0535/ML053500170.pdf>.
- [50] R. Orive, I. C. G. P. J., J. Arias, J. R. Alonso and a. J. Á. Martinez, "Uncertainties Study into the LWR Containment Analyses," in *ICAPP-5023*, Seoul, Korea, 2015.
- [51] R. Bocanegra, G. Jimenez and a. M. Fernandez-Cosials, "Development of a PWR-W GOTHIC 3D model for containment accident analysis," *Ann. Nucl. Energy*, p. 547–560, 2016.
- [52] K. W. Ross, J. Phillips, R. O. Gauntt and a. K. C. Wagner, "MELCOR Best Practices as Applied in the State-of-the-Art Reactor Consequence Analyses (SOARCA) Project, Nureg/Cr-7008, p. 133," ANL , USA, 2014.

- [53] Sandia National Lab, "Severe Accident Analysis Department, State-of-the-Art Reactor Consequence Analyses (SOARCA) Project. Sequoyah Integrated Deterministic and Uncertainty Analyses, NUREG/CR-7245," US NRC, USA, 2019.
- [54] R. E. Walpole, R. H. Myers, S. L. Myers and a. K. E. Ye, Probability & Statistics for Engineers & Scientists, MyLab Statistics Update. Pearson..
- [55] J. C. Helton, J. D. Johnson, W. L. Oberkampf and and C. J. Sallaberry, "Representation of Analysis Results Involving Aleatory and Epistemic Uncertainty, SAND2008-4379," Sandia Nat. Lab, USA, 2008.
- [56] S. Destercke, *Epistemic uncertainty propagation in risk/reliability analyses: an introduction to imprecise probabilities.*, 2017., France: CRNS, 2017.
- [57] P.-S. D. Laplace, "Essai Philosophique sur les probabilités," France, 1814.
- [58] S. S. Wilks, "Statistical Prediction with Special Reference to the Problem of Tolerance Limits," *Ann. Math. Stat.*, p. 400–409, Nr.4 Vol.13 1942.
- [59] F. Galton, "Co-relations and their measurement, chiefly from anthropometric data," *Proc. R. Soc. London*, p. 135–145, Vol 45 1889.
- [60] Student, "The Probable Error of a Mean," *Biometrika*, pp. 1-25, Nr.1 Vol.6 1908.
- [61] "Dakota homepage," Sandia Nat. Lab., 2020. [Online]. Available: <https://dakota.sandia.gov/>.
- [62] B. M. Adams et al., "Dakota, A Multilevel Parallel Object-Oriented Framework for Design Optimization, Parameter Estimation, Uncertainty Quantification, and Sensitivity Analysis: Version 6.6 User's Manual,SAND2014-4633," Sandia, USA, 2014.
- [63] F. Mascari, G. Vella, B. G. Woods, K. Welter and a. F. D'Auria, "Analysis of Primary/Containment Coupling Phenomena Characterizing the MASLWR Design During a SBLOCA Scenario," IntechOpen, 2012, p. Ch. 8., Vienna, Austria.
- [64] F. Mascari, J. C. D. L. R. Blul, M. Sangiorgi and a. G. Bandini, " Analyses of an Unmitigated Station Blackout Transient in a Generic PWR-900 with ASTEC , MAAP and MELCOR Codes, NUREG/IA-0515," 2019., US NRC, USA, 2019.
- [65] H. Glaeser, " "GRS method for uncertainty and sensitivity evaluation of code results and applications," *Sci. Technol. Nucl. Install.*, 2008.
- [66] S. M. Bajorek and a. C. Gingrich, "Uncertainty Methods Framewor. Development for the TRACE Thermal-Hydraulics Code by the U.S.NRC," in *Proc. OECD/CSNI Work. Best Estim. Methods Uncertain. Eval. NEA/CSNI/R(2013)8/PART2*, pp. 148–157, 2013.
- [67] K. A. Gamble and a. L. P. Swiler, "Uncertainty quantification and sensitivity analysis applications to fuel performance modeling," in *Top Fuel 2016: LWR Fuels with Enhanced Safety and Performance*, SAND2016-4597C, 2016, pp. 1289–1298.
- [68] M. E. Stephens, B. W. Goodwin and a. T. H. Andres, "Deriving parameter probability density functions," *Reliab. Eng. Syst. Safety*, p. 271–291, Vol.42 1993.
- [69] F. Gaudier, "URANIE : The CEA/DEN Uncertainty and Sensitivity platform," *Procedia Social and Behavioral Sciences*, p. 7660–7666, 2 2010.
- [70] R. Brun and F. Rademakers, "ROOT- An object oriented data analysis framework," *Nuclear Instruments and Methods in Physics Research, Section A*, pp. 81-86, 1997.
- [71] I. Antcheva, .: M. Ballintijn, B. Bellenot, M. Biskup, R. Bruna, N. Buncica, P. Canal, D. Casadei, O. Couet, V. Fine, 1. G. G. L. Franco, A. Gheata, D. G. Maline, M. Goto, J. Iwaszkiewicz, A. Kreshuk, D. M. Segura, R. Maunder, L. Moneta and A. Naumann, "ROOT-A C++ framework for petabyte data storage, statistical analysis and visualization," *Computer Physics Communications*, pp. 2499-2512, 180 2009.

- [72] URANIE, “Uranie,” 2020. [Online]. Available: <https://sourceforge.net/projects/uranie>.
- [73] E. d. Rocquigny, “Quantifying uncertainty in an industrial approach: an emerging consensus in an old epistemological debate,” *Surveys and Perspectives Integrating Environment and Society*, Vol.2 2.1 2009.
- [74] Raven, “RAVEN homepage on github,” Idaho National Laboratory, 2020. [Online]. Available: <https://github.com/idaholab/raven>.
- [75] A. Alfonsi, “Raven as a tool for dynamic probabilistic risk assessment: Software overview,” INL, USA, 2013.
- [76] A. Alfonsi et al., “RAVEN User Guide. INL/EXT-18-44465,” INL, USA, 2017.
- [77] V. Narcisi, P. Lorusso, F. Giannetti, A. Alfonsi and a. G. Caruso, “Uncertainty quantification method for RELAP5-3D© using RAVEN and application on NACIE experiments,” *Ann. Nucl. Energy*, p. 419–432, Vol.127 2019.
- [78] J. Baccou and et.al., “SAPIUM: Development of a Systematic Approach for Input Uncertainty quantification of the physical Models in thermal-hydraulic codes, Good Practices Guidance Report,” NEA/CSNI/R(2019)xx, Paris, France, 2019.
- [79] B. M. Adams and et.al., “Dakota, A Multilevel Parallel Object-Oriented Framework for Design Optimization, Parameter Estimation, Uncertainty Quantification, and Sensitivity Analysis: Version 6.6 Reference Manual. SAND2014-5015,” Sandia Nat. Lab, USA, 2014.
- [80] F. Mascari and et.al., “Analysis of the OSU-MASLWR 001 and 002 Tests by using TRACE code, NUREG/IA-0466,” US NRC, USA, 2016.
- [81] A. Bersano and F.Mascari, “Evaluation of a Double-Ended Guillotine Break Transient in a Three-Loop PWR-900 Like with TRACE Code Coupled with DAKOTA Uncertainty Analysis,” *Int. J. Nucl. Power, November/December, Oct. 2019*, no. 64 Issue 11/12 vol. 1 2019.
- [82] B. M. Adams and e. al., “Dakota, A Multilevel Parallel Object-Oriented Framework for Design Optimization, Parameter Estimation, Uncertainty Quantification, and Sensitivity Analysis: Version 6.6 Theory Manual. SAND2014-4253,” Sandia Nat. Lab., USA, 2014.
- [83] A. Guba, M. Makai and L. Pál, “Statistical aspects of best estimate method-I,” *Reliab. Eng. Syst. Safety*, p. 217–232, Nr.3 Vol.80 2003.
- [84] USNRC, “TRACE TRACE V5.840 Theory manual, Field equations, solution mtrhods, and physical models,” U. S. Nuclear Regulatory Commission, Washington, DC, U.S., 2013.
- [85] A. Alfonsi and et.al., “RAVEN Theory Manual,RAVEN Theory Manual,INL/EXT-16-38178 Revision 3,” INL, Idaho Falls, 2016.
- [86] C. J. Roy and W. L. Oberkampf, “A comprehensive framework for verification, validation, and uncertainty quantification in scientific computing,” *Comput. Methods Appl. Mech. Eng.*, p. 2131–2144, Nr. 25-28 Vol.200 2011.
- [87] M. Kloos, “ Main features of the tool SUSA 4.0 for uncertainty and sensitivity anal-yses. Proceedings of,” in *ESREL Conference*, Zürich, Schweiz, 2015.
- [88] M. Kloos, “SUSA - Software for uncertainty and sensitivity analyses, Version 4.2, User’s Guide and Tutorial. GRS-P-5, Vol. 1, Rev. 5,” GRS, Garching, 2019.
- [89] H. JC and D. FJ, “Latin hypercube sampling and the propagation of uncertain-ty in analyses of complex systems.,” *Reliab Eng Syst Safety*, p. 23–69., 81 2003.
- [90] H. JC, D. FJ and J. JD, “A comparison of uncertainty and sensitivity analysis results obtained with random and Latin hypercube sampling,” *Reliab Eng Syst Safety*, p. 305–330, 89 2005.

- [91] K. S. and J. N. L., Encyclopedia of statistical sciences, Volume 4, Wiley & Sons, 1983.
- [92] M. Kloos, "Sensitivity analyses supplemented to epistemic uncertainty analyses for PSA results," in *Proceedings of PSAM 11*, Helsinki, Finland., 2012.
- [93] E. Hofer, "Sensitivity analysis in the context of uncertainty analysis for computationally intensive models," *Computer Physics Communications*, , pp. 21-34, 1999.
- [94] K. M. G. and S. A., The advanced theory of statistics, Vol. 2: Inference and relationship. 3rd ed, New York: MacMillan Publishing Co., 1973. .
- [95] M. D. McKay, "Variance-based methods for assessing uncertainty importance, NUREG-1150 analyses. LA-UR-96-2695; 1–27.," USA , 1996.
- [96] I. Sobol, "Sensitivity estimates for nonlinear mathematical models.," *Math Model & Computational Experiments*, p. 407–414, 1 1993.
- [97] S. A., K. Chan and E. Scott, Sensitivity analysis, Wiley Series in Probability and Statistics, Wiley, 2000.
- [98] G. L. A. and K. W. H., "Measures of Association for Cross Classification," *Journal American Statistical Association*, pp. 310-364, 1963.
- [99] I. R.L. and H. S. C., "A robust measure of uncertainty importance for use in fault tree system analysis," *Risk Analysis*, p. 401–406, 1990 .
- [100] M. Kloos and e. al., "MCDET: A Tool for Integrated Deterministic Probabilistic Safety Analyses," in *Advanced Concepts in Nuclear Energy Risk Assessment and Management*, World Scientific Publishing Company., 2018.
- [101] Applied Programming Technology Inc., "Symbolic Nuclear Analysis Package (SNAP). User ' s Manual.," APT, USA, 2012.
- [102] G. Weber, B. Krzykacz-Hausmann and a. F. Funke, "Specific Validation of COCOSYS and ASTEC and Uncertainty and Sensitivity study on Iodine. GRS-A-3676," GRS , Garching, 2012.
- [103] I. Pasichnyk, K. Velkov, O. Schumacher and a. R. Donderer, "Quantitative Bestimmung der Unsicherheitsbandbreiten in aktuell verwendeten Berechnungsverfahren für Reaktivitätsstörfälle," GRS, Garching, 2012.
- [104] K.-H. Walter, C. Hsiao-Wei, K. Dominic and R. Nils O., "Analyse kernzerstörungs- und quelltermrelevanter Prozesse mit ASTEC und ATHLET-CD/COCOSYS. GRS - 351 ISBN 978-3-944161-31-0," GRS, Cologne, 2014.
- [105] S. P. and etal., "Tools for Validation and Uncertainty Quantification with ANSWERS Software," 2019.
- [106] G. e. a. Weber, "Uncertainty and sensitivity analysis on the iodine model in the containment COCOSYS," in *NUTHOS 10*, Japan, 2014.

Appendix 3: Potential of UQ for HPC applications (Task 4)

K. Chevalier (IRSN), V. Sanchez (KIT)

Version 06 – 08/04/2021

Content

Content 3

1 SUSAN (GRS, SSTC,CNSC)..... 4

2 SUNSET (IRSN, INRNE, TUS)..... 4

3 DAKOTA (ENEA, CIEMAT, TRACTEBEL)..... 4

4 URANIE (KIT, BELV) 4

5 RAVEN (UNIROM1, JAEA) 5

6 References 5

1 SUSAN (GRS, SSTC,CNSC)

To start a large number of simulation runs within a standard high-performance computing (HPC) cluster environment, the software Cluster Computing Processor (CCP) may be used (Berner 2017). The simulation runs must be based on corresponding input files each considering a different set of values sampled for the uncertain input parameters. These input files may be automatically generated by SUSAN. Since the simulation runs do not depend from each other, the collectively launched computation processes can be easily executed in parallel by distributing the individual runs over the nodes of a cluster computing environment. The advantage of performing the simulation runs in parallel (and not sequential) is the considerable decrease of the total computation time. CCP offers basic assistance to launch a set of parallel simulation processes within a standard high-performance computing (HPC) cluster environment. The implementation of the current CCP version supports the input name scheme and output data format necessary to perform uncertainty and sensitivity analyses with SUSAN.

The commands of the CCP provide the basic functionalities in order to perform a set of simulation runs in parallel on an HPC cluster in an automated and convenient manner. The CCP is implemented in the interpreter language python. The software in its current version supports running the ATHLET simulation code based on a set of SUSAN-generated input files on an HPC cluster. Nevertheless, in principle the CCP can be adapted to any simulation code and input file name scheme. Since so far SUSAN depends on a Windows operating system (OS) and the domain of application of the CCP depicts an HPC (Unix OS) cluster, the software is per design an independent and auxiliary add-on tool to SUSAN.

2 SUNSET (IRSN, INRNE, TUS)

SUNSET is designed for personal computers or computer cluster. The calculations may be parallel or sequential.

3 DAKOTA (ENEA, CIEMAT, TRACTEBEL)

If the MPI package (specialised in parallel computing) is installed on Linux and with cautious management of the intermediate files to avoid conflicts (for example having each run in its dedicated subdirectory), the user can specify in the DAKOTA input that the sampled cases are to be distributed on a given number of CPU. Each case will run on one CPU and will be replaced by another when finished.

4 URANIE (KIT, BELV)

URANIE can run in Windows and Linux environments in parallel or sequential (MPI) mode. URANIE can also be launched on clusters with SLURM (curie at CCRT), LSF (tantale, platine at CCRT) or SGE (mars) with BSUB directives. It is also possible to use batch clusters in order to run several instances of a parallel code, mixing two levels of parallelism: one for the code, one for the design-of-experiments.

In order to distribute computation the TLauncher run method can be also employed. It allows creating directories, copying files, executing jobs, and creating the output DataServer. All these operations are performed simultaneously, so that it is possible to delete execution directories as the computation are performed.

Concerning the severe accident analyses, the ASTEC code can be run on clusters. KIT is exploring the possibility of performing ASTEC multi-runs on the ForLHR II cluster at the KIT Steinbuch Center of Computing (SCC) [1]. The architecture of the cluster allows working on up to 1155 nodes with 20 cores each with a theoretical peak performance of 832 GFLOPS at 2.6 GHz and 64 GB of main memory per node.

5 RAVEN (UNIROM1, JAEA)

RAVEN is designed for personal computers and supercomputers, and computation can be in parallel or sequential. In collaboration with ENEA, MELCOR2.2-RAVEN will be used for large number of simulations at supercomputers of ENEA CRESCO HPC. This implementation is similar to the one of INL HPC which was replicated into the Sapienza Nuclear area HPC.

6 References

[1] Steinbuch Centre for Computing, 2014. [Online].

Appendix-4: Data Assimilation

K. Chevalier (IRSN), V. Sanchez (KIT)

Version 06 – 08/04/2021

Content

Appendix-4: Data Assimilation.....	1
Content	3
List of figures	4
List of Tables	5
1 Data assimilation methods (Task 1)	6
1.1 MOCABA (FRAMATOME).....	6
1.1.1 Description of the method.....	6
1.1.2 Description of main features	7
1.1.3 Pros and Cons	8
1.2 NEMM (NINE).....	8
1.2.1 Description of the method.....	8
1.2.2 Description of main features	10
1.2.3 Initial conditions	11
1.2.4 Boundary conditions	11
1.2.5 Model parameters.....	11
1.2.6 Propagation of uncertainties	12
1.2.7 Pros and Cons	12
1.3 Experience from the application of data assimilation methods (Task 2)	12
1.3.1 MOCABA (FRAMATOME).....	12
1.3.2 NEMM (NINE).....	12
1.4 Potentials for HPC-applications (task4).....	13
1.4.1 MOCABA (FRAMATOME).....	13
1.4.2 NEMM (NINE).....	13
2 References	14

List of figures

Figure 1: General scheme of the complex relationship between NEMM modules 9

List of Tables

Table 1: Short description of NEMM modules relative to TH application. 10

1 Data assimilation methods (Task 1)

1.1 MOCABA (FRAMATOME)

1.1.1 Description of the method

MOCABA [1] is a Bayesian data assimilation methodology for improving predictions of integral observables by combining uncertainty information on basic input parameters with information from integral measurements. In contrast to the widely used Generalized Linear Least Squares (GLLS) methodology [2], [3] MOCABA uses Monte Carlo sampling instead of first-order perturbation theory for uncertainty propagation. This allows one to apply Bayesian updating directly to the integral observables of interest without taking the detour via updating the input parameter distributions. As a result, MOCABA does not require the computation of any sensitivities of the integral response variables with respect to input parameter variations.

The objective of the MOCABA framework is to make predictions about an (in general multidimensional) observable, represented by a vector function $\mathbf{y}_A(\boldsymbol{\alpha}_A)$ of a parameter vector $\boldsymbol{\alpha}_A$, taking into account observations \mathbf{v}_B of a vector function $\mathbf{y}_B(\boldsymbol{\alpha}_B)$ of a parameter vector $\boldsymbol{\alpha}_B$. For example, $\mathbf{y}_A(\boldsymbol{\alpha}_A)$ may represent the time-dependent source term during a severe accident, $\mathbf{y}_B(\boldsymbol{\alpha}_B)$ may represent a set of observables measured during accident progression (e.g. dose rate measurements), and $\boldsymbol{\alpha}_A$ and $\boldsymbol{\alpha}_B$ may represent sets of input parameters determining the values of \mathbf{y}_A and \mathbf{y}_B , e.g. physical parameters determining the fission product release rates from the core melt.¹

It is assumed that the uncertainties of $\mathbf{y}_A(\boldsymbol{\alpha}_A)$ and $\mathbf{y}_B(\boldsymbol{\alpha}_B)$ are completely determined by the uncertainties of the corresponding parameter vectors $\boldsymbol{\alpha}_A$ and $\boldsymbol{\alpha}_B$. Hence, collecting the components of $\boldsymbol{\alpha}_A$ and $\boldsymbol{\alpha}_B$ in a combined parameter vector $\boldsymbol{\alpha}$, the uncertainties of \mathbf{y}_A and \mathbf{y}_B are defined by the uncertainty of $\boldsymbol{\alpha}$. To quantify this uncertainty, $\boldsymbol{\alpha}$ is identified with a random vector defined by a probability density function (pdf) $p(\boldsymbol{\alpha})$. Collecting \mathbf{y}_A and \mathbf{y}_B in a combined vector,

$$\mathbf{y}(\boldsymbol{\alpha}) = (\mathbf{y}_A^T(\boldsymbol{\alpha}_A), \mathbf{y}_B^T(\boldsymbol{\alpha}_B))^T, \quad (1)$$

allows us to express the uncertainties of \mathbf{y}_A and \mathbf{y}_B in terms of the pdf $p(\mathbf{y})$ of the response vector \mathbf{y} , which is completely defined by $p(\boldsymbol{\alpha})$.

Bayes' theorem allows us to combine information from measurements \mathbf{v}_B of \mathbf{y}_B , expressed in terms of a likelihood function $p(\mathbf{v}_B|\mathbf{y}_B)$, with the prior information represented by $p(\mathbf{y})$. This yields the posterior pdf $p(\mathbf{y}|\mathbf{v}_B)$ of \mathbf{y} :

$$p(\mathbf{y}|\mathbf{v}_B) \propto p(\mathbf{v}_B|\mathbf{y}_B) p(\mathbf{y}). \quad (2)$$

If the Bayesian updating shall be applied to the input parameter vector $\boldsymbol{\alpha}$, $\mathbf{y}_A(\boldsymbol{\alpha}_A)$ is simply identified with $\boldsymbol{\alpha}$ in Eq. (2), which yields the posterior pdf of $\boldsymbol{\alpha}$:

$$p(\boldsymbol{\alpha}|\mathbf{v}_B) \propto p(\mathbf{v}_B|\mathbf{y}_B(\boldsymbol{\alpha})) p(\boldsymbol{\alpha}). \quad (3)$$

Within the basic MOCABA framework, a multivariate normal distribution model is assumed for the prior pdf $p(\mathbf{y})$ of the integral observable \mathbf{y} :²

$$p(\mathbf{y}) = N(\mathbf{y}_0, \boldsymbol{\Sigma}_0) \propto \exp\left(-\frac{Q_0}{2}\right), \quad Q_0 = (\mathbf{y} - \mathbf{y}_0)^T \boldsymbol{\Sigma}_0^{-1} (\mathbf{y} - \mathbf{y}_0), \quad (4)$$

with

$$\mathbf{y}_0 = (\mathbf{y}_{0A}^T, \mathbf{y}_{0B}^T)^T, \quad \boldsymbol{\Sigma}_0 = \begin{pmatrix} \boldsymbol{\Sigma}_{0A} & \boldsymbol{\Sigma}_{0AB} \\ \boldsymbol{\Sigma}_{0AB}^T & \boldsymbol{\Sigma}_{0B} \end{pmatrix}. \quad (5)$$

¹ It should be noted that we are generally interested in observables \mathbf{y}_B for which the uncertainties of \mathbf{y}_A and \mathbf{y}_B are dominated by parameters common to both $\boldsymbol{\alpha}_A$ and $\boldsymbol{\alpha}_B$. If this is the case, observations \mathbf{v}_B of \mathbf{y}_B have the potential to significantly improve our knowledge about \mathbf{y}_A [21].

² As mentioned in [22], it is straightforward to extend the model space to more general classes of multivariate distribution models by making use of invertible variable transformations. However, such model expansions hardly change the inferences for most application of interest (see [5]).

\mathbf{y}_0 is the vector of prior application case and benchmark observables, and Σ_0 is the corresponding prior covariance matrix due to input parameter uncertainties.

To calculate the prior model parameters, \mathbf{y}_0 and Σ_0 , random samples of the parameter vector α are drawn from the pdf $p(\alpha)$. For each random draw α_j^{MC} , the corresponding value $\mathbf{y}_j^{MC} = \mathbf{y}(\alpha_j^{MC})$ is calculated. The prior mean vector and prior covariance matrix are then estimated by applying the corresponding unbiased estimators to the Monte Carlo data:

$$\mathbf{y}_0 = \frac{1}{m} \sum_{j=1}^m \mathbf{y}_j^{MC}, \quad \Sigma_0 = \frac{1}{m-1} \sum_{j=1}^m (\mathbf{y}_j^{MC} - \mathbf{y}_0)(\mathbf{y}_j^{MC} - \mathbf{y}_0)^T. \quad (6)$$

In the above equations, m is the number of Monte Carlo draws. The measurements of \mathbf{y}_B are expressed in terms of the measurement vector \mathbf{v}_B , whose uncertainty is expressed in terms of the likelihood function $p(\mathbf{v}_B|\mathbf{y}_B)$. For the basic MOCABA framework, the likelihood function is also expressed in terms of a normal distribution model:

$$p(\mathbf{v}_B|\mathbf{y}_B) \propto \exp\left(-\frac{Q_V}{2}\right), \quad Q_V = (\mathbf{y}_B - \mathbf{v}_B)^T \Sigma_{VB}^{-1} (\mathbf{y}_B - \mathbf{v}_B). \quad (7)$$

Here, Σ_{VB} is the covariance matrix of \mathbf{y}_B due to experimental or measurements uncertainties. Inserting Eqs. (4) and (7) into Eq. (2), yields a normal posterior pdf of \mathbf{y} :

$$p(\mathbf{y}|\mathbf{v}_B) = N(\mathbf{y}^*, \Sigma^*) \propto \exp\left(-\frac{Q^*}{2}\right), \quad Q^* = (\mathbf{y} - \mathbf{y}^*)^T \Sigma^{*-1} (\mathbf{y} - \mathbf{y}^*), \quad (8)$$

with the posterior model parameters:

$$\mathbf{y}^* = (\mathbf{y}_A^*, \mathbf{y}_B^*)^T, \quad \Sigma^* = \begin{pmatrix} \Sigma_A^* & \Sigma_{AB}^* \\ \Sigma_{AB}^{*T} & \Sigma_B^* \end{pmatrix}, \quad (9)$$

$$\mathbf{y}_A^* = \mathbf{y}_{0A} + \Sigma_{0AB}(\Sigma_{0B} + \Sigma_{VB})^{-1}(\mathbf{v}_B - \mathbf{y}_{0B}), \quad (10)$$

$$\mathbf{y}_B^* = \mathbf{y}_{0B} + \Sigma_{0B}(\Sigma_{0B} + \Sigma_{VB})^{-1}(\mathbf{v}_B - \mathbf{y}_{0B}), \quad (11)$$

$$\Sigma_A^* = \Sigma_{0A} - \Sigma_{0AB}(\Sigma_{0B} + \Sigma_{VB})^{-1}\Sigma_{0AB}^T, \quad (12)$$

$$\Sigma_B^* = \Sigma_{0B} - \Sigma_{0B}(\Sigma_{0B} + \Sigma_{VB})^{-1}\Sigma_{0B}, \quad (13)$$

$$\Sigma_{AB}^* = \Sigma_{0AB} - \Sigma_{0AB}(\Sigma_{0B} + \Sigma_{VB})^{-1}\Sigma_{0B}. \quad (14)$$

Instead of parameterizing the experimental uncertainties in terms of the likelihood covariance matrix Σ_{VB} , they may also be included in the prior covariance matrix Σ_{0B} . If all experimental uncertainties are included in Σ_{0B} , the likelihood covariance matrix Σ_{VB} becomes zero in the above updating formulas.

Generalizations of the basic MOCABA framework, taking into account measurements and constraints of linear combinations of variables and more general classes of distribution models, are discussed in [4] and [5].

1.1.2 Description of main features

MOCABA is a general mathematical framework, which is not restricted to any specific computer implementation. Software implementations have been realized by different institutions for different applications, including criticality safety analysis ([1], [6], [4], [7], [8]), reactor cycle predictions [9], and nuclear data adjustment ([10]).

Within the MUSA project, the MOCABA framework will be used for the prediction of severe accident quantities, such as the source term, taking into account the information from measured plant data.

Typical software implementations of MOCABA calculate as “by-products” other useful statistical quantities such as correlations between different responses and between input parameters and responses, as well as sensitivities of responses w.r.t. input parameter variations.

1.1.3 Pros and Cons

Because of its generality, the MOCABA framework is applicable to a wide class of different application cases. Applying MOCABA to a Monte Carlo uncertainty propagation analysis, Monte Carlo sampling of input parameters has to be performed with a dedicated Monte Carlo code.

It has been demonstrated by different institutions that the MOCABA method is very efficient and has the potential to significantly improve the predictions of integral observables.

Statistical software packages commonly used in nuclear engineering (URANIE, DAKOTA, SUNSET etc.) generally do not include MOCABA implementations. Hence, analysts may have to write their own software implementations in order to use the MOCABA method within their Monte Carlo uncertainty propagation analyses. Writing such software implementations is straightforward but requires some knowledge in computer programming and numerical linear algebra algorithms.

1.2 NEMM (NINE)

1.2.1 Description of the method

NINE Evaluation Model Methodology (NEMM) is a comprehensive methodology capable to address the essential requirements of the safety analysis process:

- Validation and improvement of the computational tools;
- Development of adequate plant models;
- Qualification of the simulation results;
- Quantification of the uncertainties associated with the predicted results.

NEMM was developed as a flexible and modular tool primarily for licensing applications either using Best Estimate Plus Uncertainty (BEPU) methodology or a conservative approach. Currently, NEMM can be applied for the development of Thermal-Hydraulics (TH) Evaluation Models, as well as coupled TH and Reactor Physics codes. However, the concepts and the elements of NEMM are applicable to the SA domain. Thus, NEMM can be extended from DBA or DEC to SA analysis, although with some simplifications and adaptations, as illustrated in the next Subsection.

The key characteristics of NEMM can be summarized as:

- The extensive use of experimental data;
- The possibility to validate and as well to improve a system code;
- The application of a systematic procedure to qualify simulation results;
- The comprehensive treatment of the uncertainty sources;

In order to deal with all the features listed above, specific procedures have been developed. As depicted in **Figure 1** and summarized in Table 1, NEMM is organized in semi-independent modules. Depending on the objectives of the analysis and on the adopted approaches, only selected modules may be applied focusing on the considered target applications. For example, code validation process can be addressed by the “*Computation Tools Development and Validation*” module.

Within MUSA framework, the “*SM & SMT Uncertainty Quantification*” module will be the focus of NEMM application to SA domain. NEMM provides two steps for the computation of Uncertainty:

- Code with Internal Assessment of Uncertainty (CIAU), which will be detailed in the next subsection;
- Predictive Model Methods, which employ a Data Assimilation strategy to optimize some parameters of the code models in order to improve the code response.

In MUSA only the CIAU method will be applied, since the Predictive Model Methods are not yet mature enough for the transition from TH to SA. It must be pointed out that the application of CIAU envisages the execution of at least the first two NEMM modules, namely the “*NPP Selection*” and the “*Computation Tools Development & Validation*”, in order to guarantee the correctness of uncertainty evaluation.

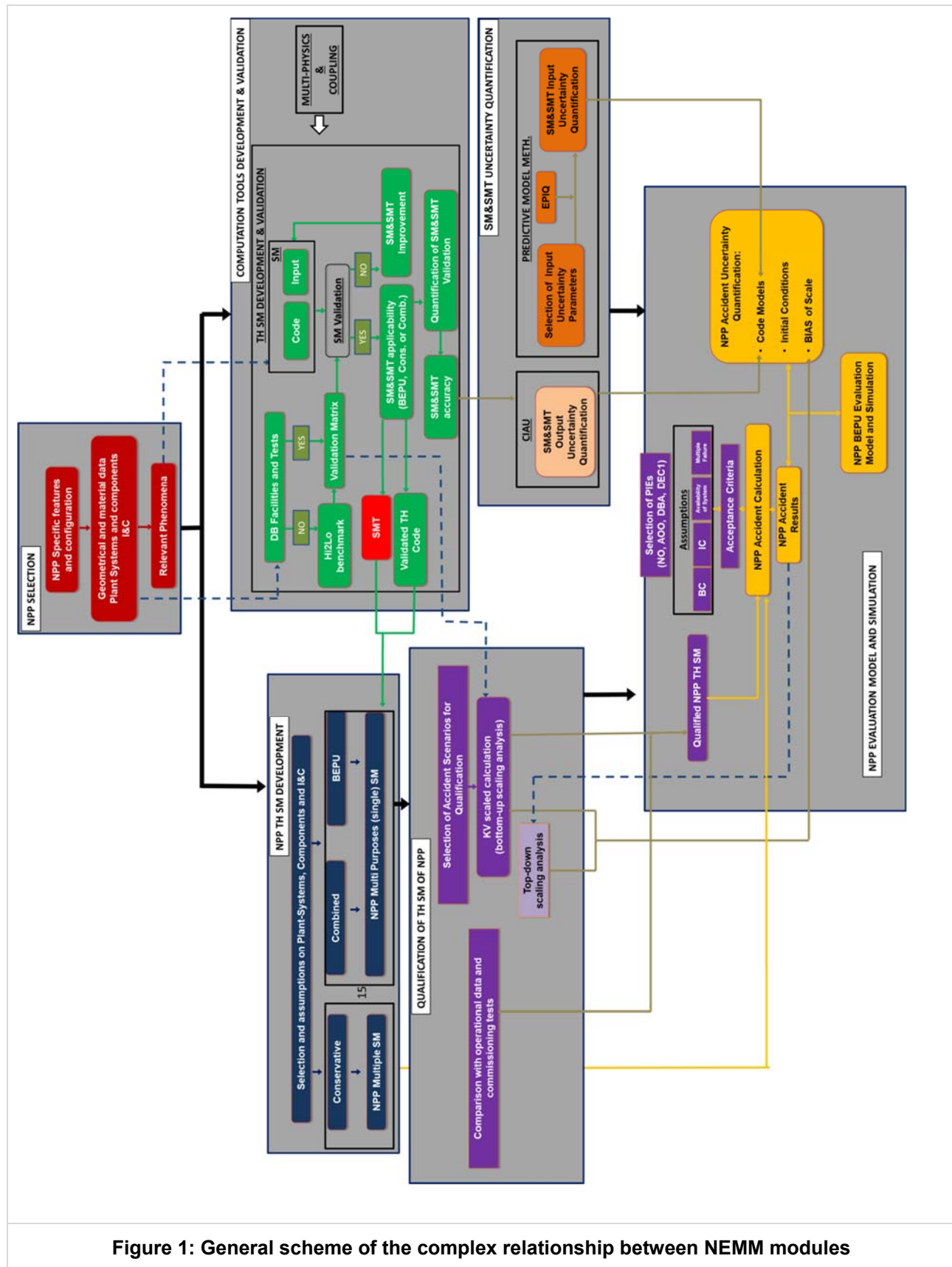


Figure 1: General scheme of the complex relationship between NEMM modules

Table 1: Short description of NEMM modules relative to TH application.

#	MODULE	DESCRIPTION	OUTPUT
1	NPP Selection	The NPP, object of the analysis, is identified. All the necessary information and data to simulate the NPP are collected including the relevant phenomena.	<ul style="list-style-type: none"> • The data necessary to build a SM of the plant • The phenomena to be considered in the SM
2	Computational Tools Development and Validation	Selection of the computational tools to perform the analysis and execution of the validation process of Computational tools to demonstrate the capability to simulate needed phenomena.	<ul style="list-style-type: none"> • The validated SM techniques and the validated code to be applied for the target application • SM accuracy data to be used for uncertainty evaluation
3	NPP Simulation Model Development	Use of the collected information (SM Techniques) and data to develop a NPP SM	<ul style="list-style-type: none"> • The NPP SM
4	Qualification of NPP Simulation Model	Demonstration that the SM of the NPP is capable to properly simulate the selected transients/accidents. Adoption of the “Kv Scaled calculation”	<ul style="list-style-type: none"> • The qualified NPP SM
5	Simulation Model (SM) and Simulation Model Techniques (SMT) Uncertainty Quantification	Evaluation of uncertainty due to code models, input code model parameters, initial conditions of the NPP. Consideration of the scaling issue for uncertainty evaluation.	<ul style="list-style-type: none"> • Uncertainty Quantification
6	NPP Evaluation Model and Simulation	Selection of the PIE and Assumptions for the carrying out the NPP safety analysis. Top-down scaling analysis to support the NPP Evaluation Model and Simulation results.	<ul style="list-style-type: none"> • NPP evaluation model and the calculation results adopting BE/BEP, Conservative or Combined approach

1.2.2 Description of main features

NEMM breaks down the Uncertainty Quantification into three main components, each of which is treated separately:

1. Code phenomenological models;
2. Initial conditions;
3. Scaling.

For the quantification of the uncertainty related to code phenomenological models, NEMM envisages the use of CIAU (Code with the capability of Internal Assessment of Uncertainty). The main feature of CIAU is the estimation of uncertainty through the comparison with experimental results. However, a thorough selection of the experimental data available must be obtained before the CIAU application to the selected Simulation Model. The experimental facilities that can indeed be considered as part of the analysis must be characterized by the reproduction of the phenomena of the NPP under examination. Thus, Integral Test Facilities (ITF) or Separate Effect Test Facilities (SETF) reproducing downscaled conditions of selected NPP systems are used, in addition to available data from accidents/transients occurring in the full scale plants

The CIAU method can be summarized in the following steps:

1. First of all, the phenomena involved in the analysis of the selected NPP and accident scenario must be identified, along with the associated code models;

2. Once the object of analysis is selected, the main variables driving the selected NPP accident scenario are identified, constituting the so-called Driving Quantities;
3. Available experiments reproducing the selected NPP accident phenomena are identified;
4. Special procedures are employed in order to develop the Simulation Models reproducing the selected experiments. In particular, Simulation Model Techniques (SMT) for the creation of the SM and criteria for the SM validation are established;
5. A multidimensional database is built, with each driving quantity corresponding a different dimension. The database is divided into hypercubic cells, each representing a NPP state identified by the coordinates of the hypercube in the dimensions of the data base.

The final output consists of the NPP uncertainty related to the code phenomenological models inside each hypercube obtained treating the accuracy in the hypercubes collected comparing experimental data and the related calculations by code application. Once the multidimensional database is filled with uncertainty NPP level can be finally computed. The list of output quantities, on which the uncertainty is calculated, is associated and limited to the experimental measurements available for analysis, both at the test facility and NPP level.

For this reason, the extension to SA is associated with the crucial issue of the availability of experiments. While in TH domain numerous ITFs reproducing NPPs phenomena with high degree of fidelity are available, in SA field it is more difficult to find facilities reproducing NPP systems, either due to a smaller number of ITFs available and due to the minor attention to reproduce downscaled NPP systems in SETFs, often devoted to a specific group of phenomena. As a consequence the application of CIAU method to SA must be adapted and simplified.

The idea is to build up one multidimensional database for each key phase/phenomenon occurring in most of SA sequences, such as Core degradation, FP release and deposition, etc.. Focusing on few phenomena reduces the requirements for the full scale experimental facilities and will enable to widen the spectrum of ITFs and SETFs selectable for the application of the CIAU method. This modification has the consequence to create several multidimensional databases, where the hypercubic cells do not represent anymore a state of the NPP, but a state of a selected system referred to a particular phenomenon. The uncertainty calculated for each phase/phenomenon will be finally aggregated to find a unique value of uncertainty related to the code phenomenological models.

Regarding the uncertainty related to the initial conditions, the UQ is performed through the statistical methods. The initial condition quantities are sampled from probability density functions and multiple calculations are performed in order to compute a statistical distribution of results.

The scaling uncertainty component is related to the different scale and distortion between the test facilities and the full-scale NPP. Scaling uncertainty can be estimated through a combination of top-down and bottom-up scaling analyses (e.g. Fractional Scaling Analysis). However the evaluation of this components is quite complicated and preliminary a bias can be considered base on engineering judgment.

Finally, the component of uncertainty are aggregated together in order to provide for the final uncertainty value for the NPP analysis.

1.2.3 Initial conditions

The uncertainty on initial conditions is treated completely with the statistical method by NEMM.

1.2.4 Boundary conditions

The uncertainty on boundary conditions is treated completely with the statistical method by NEMM.

1.2.5 Model parameters

The uncertainty on code phenomenological models is calculated through the application of the CIAU model by the comparison of the Simulation Model results with the experimental data from Integral Test Facilities (ITF) and Separate Effect Test Facilities (SETF).

1.2.6 Propagation of uncertainties

The three components of uncertainty are connected with Simulation Model by (code and nodalization), initial and boundary conditions and scaling. They are aggregated with special mathematical functions. While the uncertainty related to initial and boundary conditions is propagated through the code applications, the simulation model uncertainty is not propagated by the code application, but is obtained by accuracy treatment and applied at the code output. Currently, the scaling uncertainty is a bias directly applied to the code output.

1.2.7 Pros and Cons

The CIAU method is able to provide a quantification of the validation of the Simulation Model and of the Simulation Model techniques. Namely, the UQ takes into account not only the accuracy related to the application of the code model correlations to the spectrum of the selected phenomena, but considers as well the influence of the nodalization applied to the NPP.

Moreover, the application of the CIAU method points at a broader definition of uncertainty with respect to a simple statistical method. The experimental results are taken into account in the UQ by estimating the accuracy affected by the deviation between the predictions of the code model and the experimental measurements.

The application of CIAU requires a preliminary deep analysis of the phenomena occurring in Severe Accident domain. A large number of simulations of experiments are necessary in order to build CIAU multidimensional database, requiring an important effort in terms of time, computational resources and availability of qualified users. Moreover, the limited number of experiments poses a limitation of the extent of CIAU application to SA domain. The scope of NINE for MUSA is to focus NEMM application to the Core Degradation phase. On the opposite the application by the final user does not request multiple calculations and HPC application

Finally, CIAU application is strongly code-dependent: CIAU multidimensional database must be entirely built from scratch when passing from one code to another.

1.3 Experience from the application of data assimilation methods (Task 2)

1.3.1 MOCABA (FRAMATOME)

Framatome GmbH is the developer of the MOCABA methodology. Since its introduction in 2014, Framatome and other institutions (including GRS, UPM, PSI, EPFL, and ANSWERS) have been using MOCABA for different applications, including criticality safety analysis, reactor cycle predictions, and nuclear data adjustment [1], [9], [6], [10], [4], [7], [8]. Since 2019, there is an R&D cooperation between KIT and Framatome involving the development of data assimilation methods and tools based on the MOCABA methodology for severe accident analysis.

1.3.2 NEMM (NINE)

NEMM has been extensively applied to the TH domain and is nowadays accepted by regulatory bodies in the frame of Best Estimate Plus Uncertainty (BEPU), conservative and combined approaches. It was fully applied to the licensing activities of the Atucha II NPP with a BEPU approach for the preparation of the Chapter 15 of the Final Safety Analysis Report (FSAR), which envisaged the analysis of 83 accident scenarios. The Atucha II NPP was successfully licensed in 2015. In addition, NEMM was also applied in the frame of core design activities for a SMR-PWR in Brazil. Some NEMM modules were applied for the Multiphysics analysis of the core response due to a postulated Control Rod Ejection, using the BEPU approach.

The Uncertainty Quantification module of NEMM has not been yet applied to any Severe Accident analysis. However, the concepts and the elements of NEMM are theoretically directly applicable to the SA-domain. Thus, NEMM can be extended from DBA or DEC to SA analysis, although with some simplifications and adaptations.

1.4 Potentials for HPC-applications (task4)

1.4.1 MOCABA (FRAMATOME)

MOCABA is a general data assimilation framework, which is not linked to any specific software implementation. Implementations for HPC are possible if necessary.

1.4.2 NEMM (NINE)

The use of HPC is not envisaged since the final user application of NEMM for the UQ does not request either multiple calculations or the use of large computational power. The most demanding phase of the CIAU method is represented by the setup of the multidimensional database, which requires the use of tens of experimental tests in order to provide an appropriate uncertainty quantification. This in turn requires an important effort in terms of time, computational resources and availability of qualified user.

2 References

- [1] A. Hoefer, O. Buss, M. Hennebach, M. Schmid and a. D. Porsch, “ “MOCABA: A general Monte Carlo-Bayes procedure for improved predictions of integral functions of nuclear data,” *Annals of Nuclear Energy*, p. 514–521, 2015.
- [2] G. Cecchini, U. Farinelli, A. Gandini and a. M. Salvatores, “Analysis of Integral Data for Few-Group Parameter Evaluation of Fast Reactors,” 1964.
- [3] M. Humi, J. J. Wagschal and a. Y. Yeivin, “Multi-Group Constants from Integral Data,” 1964.
- [4] A. Hoefer, O. Buss and a. M. Schmid, “Applications of Multivariate Normal Bayesian Models in Nuclear Engineering,” *Nuclear Technology*, p. 1578–1587, Vol 205 12 2019.
- [5] A. H. a. O. Buss, “Assessing and Improving Model Fitness in MOCABA Data Assimilation,” 2020.
- [6] E. Peters, F. Sommer and a. M. Stuke, “Modeling of critical experiments and its impact on integral covariance matrices and correlation coefficients,”,” *Ann. Nucl. Energy*, p. 355–362, 2016.
- [7] A. H. a. O. Buss, “Impact of Covariances between Criticality Benchmark Experiments on Licensing,” 2019.
- [8] S. P. and etal., “Tools for Validation and Uncertainty Quantification with ANSWERS Software,” 2019.
- [9] E. Castro, C. Ahnert, O. Buss, N. García-Herranz, A. Hoefer and a. D. Porsch, “Improving PWR core simulations by Monte Carlo uncertainty analysis and Bayesian inference,”,” *Ann. Nucl. Energy*, p. 148–156, 2016.
- [10] D. Siefman, M. Hursin, D. Rochman, S. Pelloni and a. A. Pautz, “Stochastic vs. sensitivity-based integral parameter and nuclear data adjustments,”,” *Eur. Phys. J. Plus*, p. 429, Vol 133 No 10 2018.

Appendix-5: Noise Analysis

K. Chevalier (IRSN), V. Sanchez (KIT)

Version 06 – 08/04/2021

Content

Content 3

List of figures 5

List of Tables 6

1 Numerical Noise 7

 1.1 Introduction to Numerical Noise 7

 1.2 Investigations into Numerical Noise 8

 1.3 Time Step Optimisation Study 19

 1.4 Guidelines and Recommendations..... 21

2 References 23

List of figures

Figure 1: The variation in time to lower head failure for a set of different small-perturbation input uncertainties for the small-scale PWR deck.	10
Figure 2: The variation in time to lower head failure for a set of different small-perturbation input uncertainties for the full-plant BWR deck.	11
Figure 3: The variation in fission product vapour mass released to the environment FOM for a set of different small-perturbation input uncertainties for the small-scale PWR deck.	12
Figure 4: The partial correlation matrix between all inputs and outputs for the small-scale PWR deck.	13
Figure 5: The variation in the fission product vapour mass released to the environment FOM for a set of different small-perturbation input uncertainties to the full-plant BWR deck (equivalent to Figure 3).	14
Figure 6: The outputs of a series of MELCOR calculations with the ordering of the flow paths randomly shuffled in the small-scale PWR deck.	16
Figure 7: The spread in time to lower head failure for different input perturbations to reactor operating power for the small-scale PWR deck.	17
Figure 8: The spread in mass of radioactive vapour released to the environment for different input perturbations to reactor operating power for the small-scale PWR deck.	17
Figure 9: The correlation matrices for reactor operating power for an input uncertainty of 10-1W (left) 106W (middle) and 108W (right).	18
Figure 10: The correlation between reactor operating power and the seven output metrics for a range of different input uncertainties.	18
Figure 11: The distributions of time to lower head failure for the PWR deck for the four different time step regimes.	20
Figure 12: A direct comparison of the distributions in the time for the onset of oxidation for the small and large sets of time steps.	20

List of Tables

Table 20 - The inputs to the parameter perturbation studies. 8

Table 21: The mean, standard deviation and percentage variation (defined as the std. dev. divided by the mean) of the output quantities for both input decks with all input parameters varied. 14

Table 22: The mean and standard deviation of all selected output quantities for the four time step regimes.21

1 Numerical Noise

1.1 Introduction to Numerical Noise

Complex, iterative calculations such as those performed by integral severe accident codes can be subject to numerical noise. This is the effect of small perturbations to the inputs of the calculation causing chaotic (i.e. unpredictable) and non-trivial changes to the output quantities that are not necessarily commensurate with the scale of that perturbation. Numerical noise is distinct from an aleatory and epistemic uncertainties, where the output values should be well behaved (or change) with respect to some correlation function of the input quantities. Output variability due to numerical noise has been noted by users of integral severe accident codes and studies have been reported by Sandia National Laboratories as part of its Fukushima Daiichi Unit 1 uncertainty analyses [1], [2]. In these MELCOR studies, numerical noise was exhibited as a result of both small perturbations to input parameters and extrinsic effects, such as the ordering of input deck units such as flow paths. Flow path reordering can occur automatically when an input deck is processed through the analysis platform SNAP and results in a reordering of the elements of the matrices that are loaded into MELCOR's implicit solvers. This produces slight calculational variations due to the non-commutative nature of mathematical operations on floating point binary numbers.

A simple quantitative example demonstrating the effect of numerical noise in a MELCOR calculation was set up, in which the radius of the lower head of a test deck was varied from its nominal value by less than the width of a hydrogen atom ($\sim 10^{-10}\text{m}$). The resulting time to lower head failure was observed to change by roughly 5%. Clearly, such observations are not physical and prompted further investigation. Two potential problems were identified: there is an inherent numerical uncertainty in some integral severe accidents codes that needs to be understood for a rigorous uncertainty calculation, and it is possible that any genuine, physical uncertainty could be conflated with the effects of numerical noise causing an incorrect assessment of the results.

Mathematical simulations of classical physics will perfectly reproduce the experiment on the condition that the equations that describe the physics are comprehensive, such that all physical phenomena that describe the behaviour of the Figure of Merit (FOM) are captured mathematically. Unfortunately, this ideal case is typically limited to physics that can be fully described by explicit equations and often relates to simple hypothetical case studies. In practice, the simulation of physics phenomena in a nuclear plant will involve the solutions to implicit and semi-implicit equations and the integration of equations that do not have an analytical solution. In these situations, numerical methods are required to determine the solutions to these problems. However, the solution often involves the iterative convergence of equations where the accuracy of the solution will depend on a subjective convergence tolerance, which is chosen to balance accuracy with pragmatic code run times.

The growth of these initially very small differences between similar calculations may be attributed to the large number of steps the calculation must make, the finite precision of how computers store data, and the feedback of a single initial perturbation ultimately causing perturbations to many different values. For example, consider the following sequence of events:

1. A calculation is started in which the pressure in a single control volume has been modified from the original value by a tiny amount;
2. MELCOR will attempt to equalise the pressure between adjacent control volumes and thus the perturbation will quickly spread to all linked control volumes;
3. This will affect the heat transfer rate to and from the control volumes, as well as the flow rate between control volumes (which will further change the heat transfer rate);
4. The temperature of the core and any surrounding heat structures will change because of the different heat transfer rates into the control volumes;
5. The change in temperature of the surrounding materials will cause a pressure difference in the system, including the control volume with the single initial difference.

With this particular example, it is quite clear that an initial perturbation to an input of the calculation can affect large areas of the calculation in relatively small number of time steps. Although in a single iteration of the given example, the perturbations to the calculation will not grow in any meaningful way, continued iterations as the transient progresses can cause significant divergences between different calculations.

For MELCOR, which models a large number of different phenomena, it is postulated that different parts of the calculation will be more susceptible to numerical noise than others as the underlying physics and equations that describe that physics will be very different. The growth of noise is expected to be especially prominent in non-linear parts of the calculation. For example, calculations involving exponents, particularly to large powers, will increase the divergences between two initially similar values. For this reason, the oxidation of core materials is expected to cause the largest divergence between different calculations.

The discussions of numerical noise in this subsection are primarily with respect to observations in MELCOR, with which the analyses presented were performed. However, it should be noted that numerical noise will likely be present and affect all similar calculations, including those performed by other integral severe accident codes.

1.2 Investigations into Numerical Noise

To characterise numerical noise, four key questions need to be answered:

1. Which input parameters, if any, are most responsible for noise?
2. Do the effects of noise grow if multiple input parameters are varied?
3. How can a physical uncertainty be distinguished from numerical noise?
4. How does the geometric size and complexity of the input model affect numerical noise?

Two test cases were prepared for the purpose of answering these questions. The first was a small-scale, simple PWR deck that was designed to run quickly and was loosely based on a single module of a NuScale SMR which undergoes a loss of coolant accident. A short run time was useful due to the large number of calculations that were performed to produce the results presented in this section. The second deck was a full-plant model of a typical BWR which undergoes a complete station blackout. This deck was developed to be distinct from the small PWR deck, in that it is large-scale, complex, and takes longer to run. Any differences in the results between the two decks could be used to interpret how scale and complexity affect numerical noise.

A series of studies was performed to address the questions listed above, in which the following input parameters were trialled:

- The inner radius curvature of the lower head;
- The initial temperature of the water in the lower head;
- The mass fraction of carbon in the definition of stainless steel (with a corresponding change in the mass fraction of iron);
- The free fall velocity of debris into the lower head;
- The operating power of the reactor prior to SCRAM;
- Multiplicative coefficient of the Arrhenius equation governing the rate of Zircaloy oxidation;
- The emissivity of the cladding inner surface;
- The equivalent hydraulic diameter of the cladding's outer surface.

The parameters were chosen not for their suspected inherent uncertainty within the input deck model but because they can each be a source of noise that would affect very different parts of the calculation. It can then be identified if any can be precluded from contributing to a variation in the output distributions or if any are particularly responsible for numerical noise. They also have different relative importance to the calculation to assist in understanding the sensitivity of the calculation to the different parameters. The nominal values of these parameters are given in Table 1 along with the standard deviations governing a set of tiny perturbations that would be small enough to be immeasurable with respect engineering tolerances. The sampling method assumes that each parameter is perturbed with respect to a normal probability density function.

Table 1 - The inputs to the parameter perturbation studies.

Parameter	PWR Mean	PWR Std. Dev	BWR Mean	BWR Std. Dev
Lower head radius of curvature	2.6715m	10^{-6} m	5.325m	10^{-6} m
Lower head initial temperature	531.0K	10^{-6} m	551.15K	10^{-6} m
Carbon (iron) mass fraction in steel	0.0003, (0.74)	10^{-10}	0.0003, (0.74)	10^{-10}
Debris fall velocity	4.4m/s	10^{-8} m/s	1.0m/s	10^{-8} m/s
Reactor operating power	300MW	1W	3.926GW	1W
Zirconium oxidisation coefficient	$29.6\text{kg}^2/\text{m}^4\text{s}$	$10^{-6}\text{kg}^2/\text{m}^4\text{s}$	$29.6\text{kg}^2/\text{m}^4\text{s}$	$10^{-6}\text{kg}^2/\text{m}^4\text{s}$
Cladding emissivity	0.325	10^{-8}	0.325	10^{-8}
Cladding equivalent hydraulic diameter	9.5×10^{-3} m	10^{-10} m	0.01026m	10^{-10} m

A series of output quantities were used to assess the effects of noise on key quantities of interest throughout the progression of a severe accident, ranging from timings of events occurring early in the transient, through to source term FOMs. These are:

- The time to the onset of oxidation (denoted T_OXID);
- The time to the onset of core melting (denoted T_MELT);
- The time to lower head failure (denoted LH_FAIL);
- The total mass of hydrogen produced in-vessel (denoted MH2);
- The total radioactive mass released from the core (denoted RN1_REL);
- The total mass of radioactive aerosol released to the environment (denoted ARM);
- The total mass of radioactive vapour released to the environment (denoted VRM).

Each of the input parameters was varied within separate uncertainty analyses, using a method in which DAKOTA was coupled to MELCOR using Python code, in order to determine how the output quantities varied with the input values individually. The amount of variation in the input parameters was chosen to be sufficiently small so as to expect no significant change in the output due to any real physical process, refer to Table 1. An additional analysis was performed where all eight input parameters were perturbed simultaneously. The results of these tests can be seen in Figure 1, which illustrates the spread in the calculated time to lower head failure. The ranges of the plots in Figure 1 were chosen to include all the data and to match between subplots to allow an easy visual comparison of the results.

Three key points of interest in Figure 1 are, firstly, that the spread in the results is much larger than would be naïvely expected. This shows that perturbations to the inputs to a calculation can lead to output variations far larger than the relative size of the perturbation, without necessarily corresponding to any physical response. In this case, the standard deviations of the distributions in Figure 1 are approximately 3%, which, compared to the perturbations from the nominal input values defined in Table 1 is several orders of magnitude higher. Secondly, the individual inputs tend to produce similar outputs, suggesting that numerical noise is not dominated by a particular input parameter or set of parameters (though this pilot study was necessarily limited to a subset of all possible parameters). Lastly, the spread in results when all eight parameters were varied is very similar to the other individual plots. This indicates that numerical noise does not accumulate with the number of parameters varied. This is important, since it qualifies numerical noise as an underlying and relatively fixed uncertainty to a calculation, rather than a quantity that could overwhelm a calculation if a large

number of input uncertainties were considered. However, it is clear that the effect of numerical noise could be conflated with a genuine physical uncertainty and therefore must be well understood as part of a rigorous uncertainty analysis.

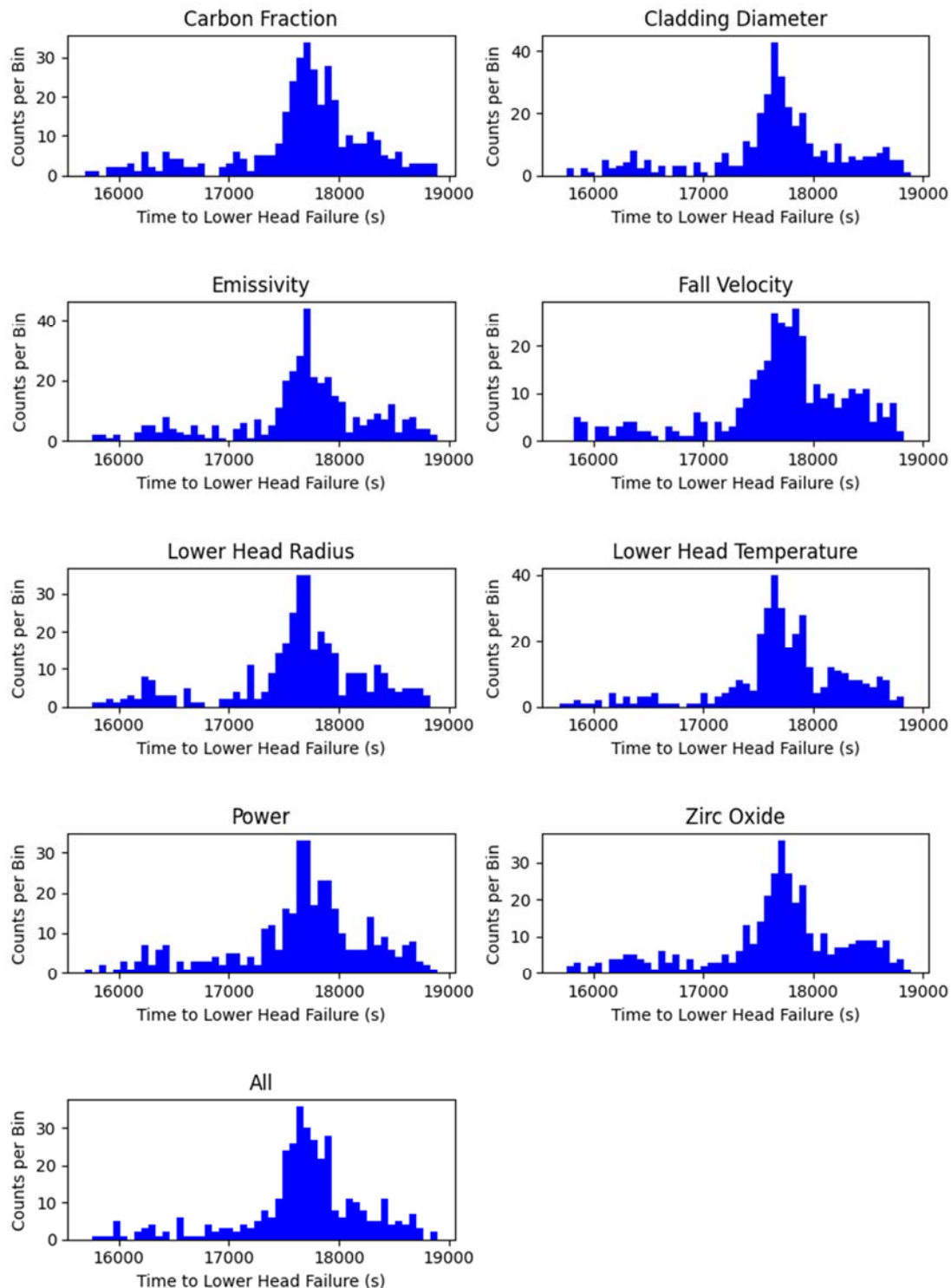


Figure 1: The variation in time to lower head failure for a set of different small-perturbation input uncertainties for the small-scale PWR deck.

Figure 2 shows the equivalent plot to Figure 1 but for the full-plant BWR deck instead of the small-scale PWR deck. The differences between the plots demonstrates that the effects of numerical noise can differ between input decks. In particular, Figure 2 includes outliers that exist further from the central tendency of lower head failure time than in Figure 1, illustrating the need to understand numerical noise as part of a rigorous uncertainty quantification, as an analyst would have no indication whether a single deterministic result was an outlier in such a distribution when viewed in isolation.

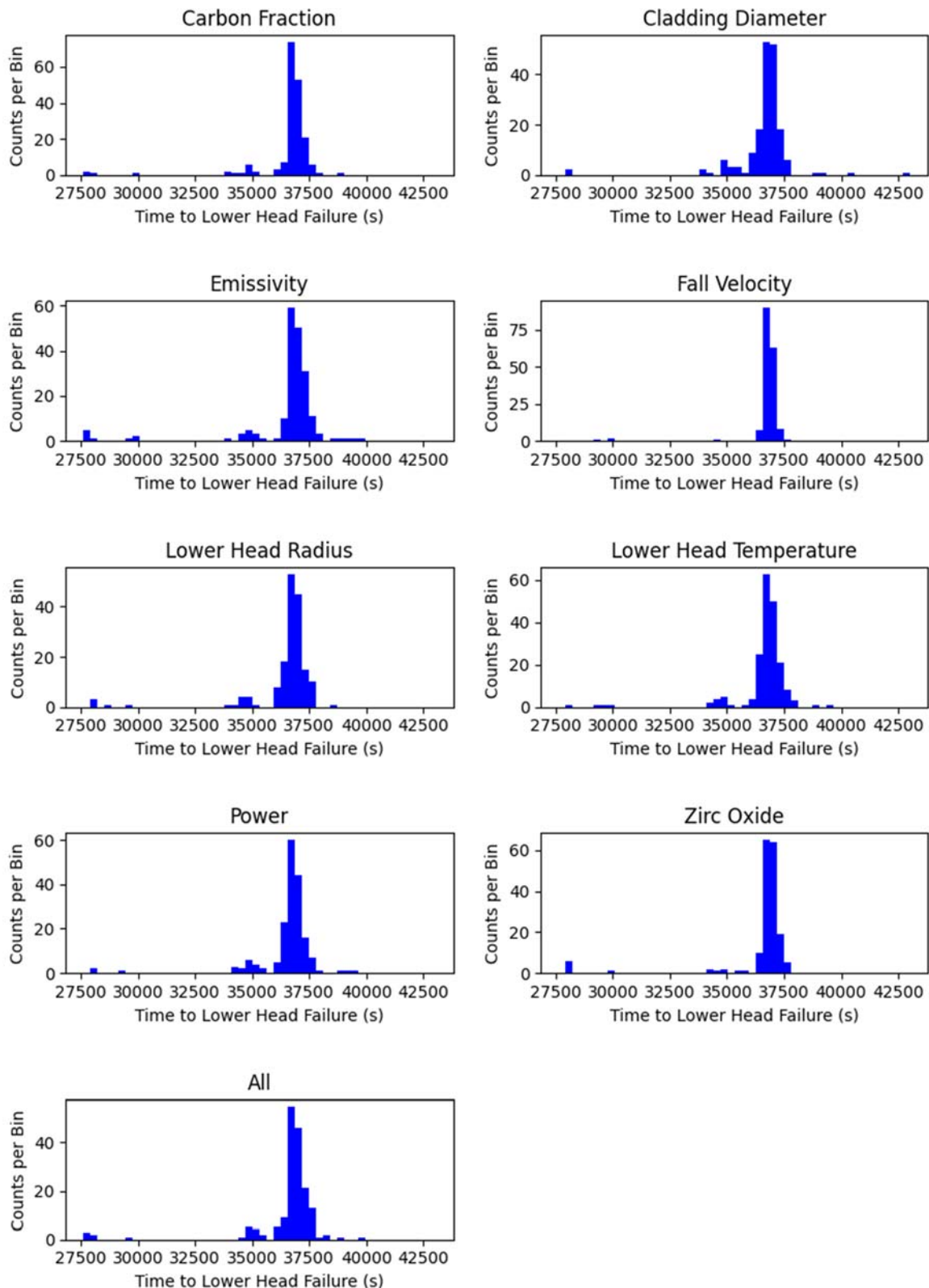


Figure 2: The variation in time to lower head failure for a set of different small-perturbation input uncertainties for the full-plant BWR deck.

The distributions in Figure 1 and Figure 2 are not perfectly normal. In some cases, the MELCOR calculation may diverge to a degree where a different physical model is applied or some process does or does not happen; such divergences become more likely as the accident sequence progresses. This can lead to more complicated distributions of results, as seen in Figure 3. This is the analogous plot to Figure 1 but shows the total mass of radioactive vapour released to the environment at the end of the calculation, instead of the time

to lower head failure. Since this value is obtained from the calculation after lower head failure has occurred, there will have been a greater number of calculation cycles and therefore increased opportunity for different runs to diverge. These more complicated distributions demonstrate an important result that cliff-edge effects can manifest even in cases that are almost identical physically, with the divergence entirely due to numerical noise.

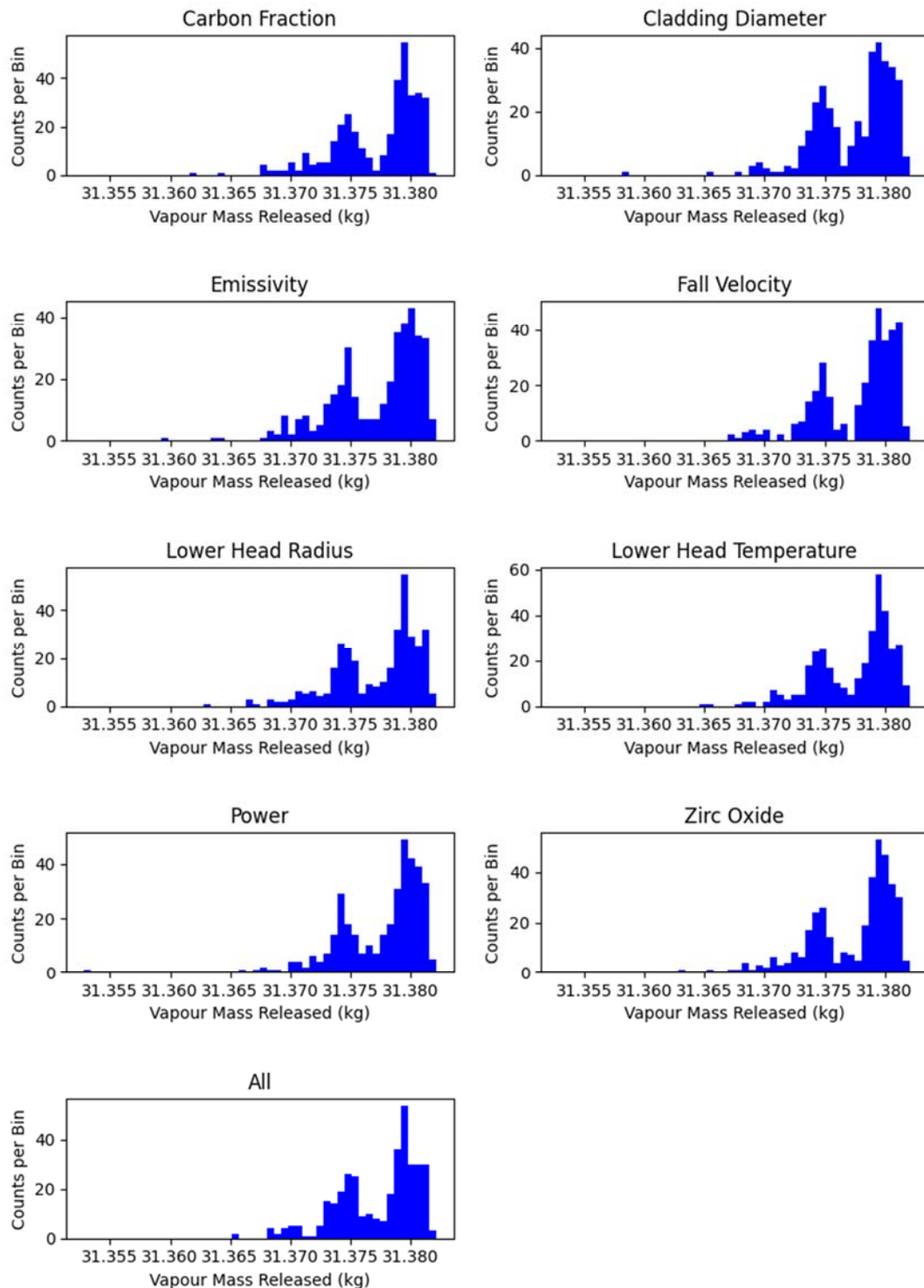


Figure 3: The variation in fission product vapour mass released to the environment FOM for a set of different small-perturbation input uncertainties for the small-scale PWR deck.

The chaotic nature of numerical noise was confirmed by examining the correlation (based on Pearson's product-moment method) between the inputs and the outputs. Figure 4 shows that there is no statistically significant correlation between any of the inputs and outputs when the input perturbations are minuscule, as in this study.

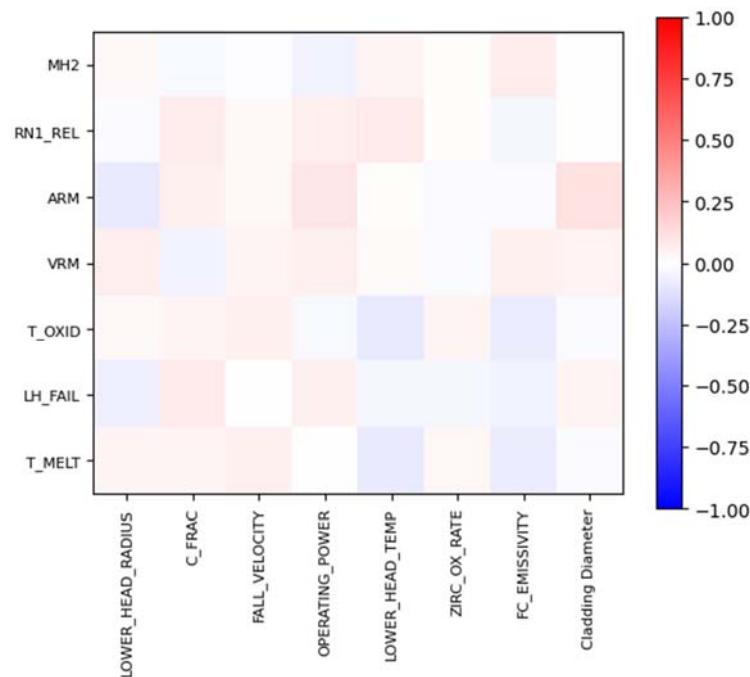


Figure 4: The partial correlation matrix between all inputs and outputs for the small-scale PWR deck.

Similar results are observed for the large-scale BWR deck. Figure 5 shows the equivalent plot to Figure 3, but for the BWR deck instead of the PWR deck. The plots in Figure 5 are significant because they demonstrate that numerical noise can cause divergences such that in some cases, no radioactive vapours are released to the environment during the calculation period, while in other cases, significant masses are released. This indicates that numerical noise has the potential to affect whether or not important cliff-edge events, such as containment failure, are invoked. For example, a Fuel-Coolant Interaction (FCI) event may trigger a pressure spike that is sufficient to breach a defined containment failure threshold in some runs, while not quite reaching that threshold in others. Alternatively, a quantity such as pressure may be slowly approaching a defined threshold, meaning that small differences between runs can result in large variations in the time at which that threshold is reached or whether it is reached at all before the calculation end-point is reached. It is also important to note that limits such as withstand pressures, and criteria for the failure of structures such as fuel rods and components such as Safety Relief Valves (SRVs), are themselves subject to significant uncertainty.

Additionally, the differences in shapes between Figure 3 and Figure 5 indicate that effect of numerical noise is plant model and accident scenario dependent, and therefore should be analysed on a case-by-case basis.

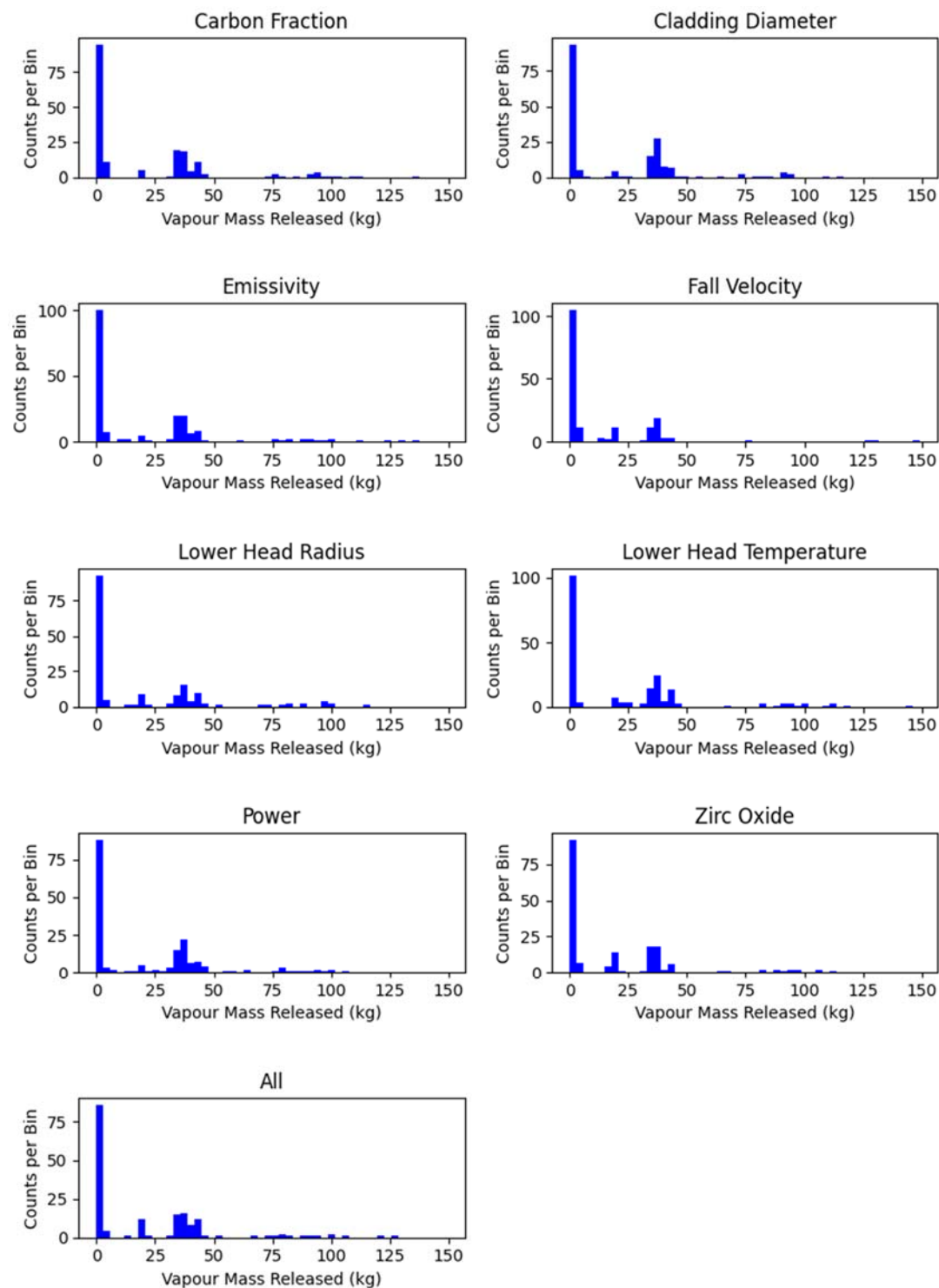


Figure 5: The variation in the fission product vapour mass released to the environment FOM for a set of different small-perturbation input uncertainties to the full-plant BWR deck (equivalent to Figure 3).

A direct comparison of the results of the small-scale PWR deck and the full-plant BWR deck runs with all parameters varied is provided in Table 2. Note that although the standard deviation is used to compare the spread in results for the two test decks, an actual assessment of the uncertainties on these quantities would likely be more complicated, depending on the distribution of results. This limitation is clear for distributions such as those in Figure 5, which, due to a significant fraction of the outputs returning zero, lead to very large percentage uncertainties. It also means that, for cases where the distributions are not the same shape, such as the vapour mass released for the PWR and BWR decks, that a direct comparison is not valid. These are, however, included in Table 2 as a clear demonstration of how different the results can be between input decks.

Table 2: The mean, standard deviation and percentage variation (defined as the std. dev. divided by the mean) of the output quantities for both input decks with all input parameters varied.

	PWR			BWR		
Output	Mean	Std. Dev.	%	Mean	Std. Dev.	%
MH2 (kg)	38.63	1.12	2.9	2342	50	2.1
RN1_REL (kg)	130.7	1.2	0.92	975.3	65.4	6.7
ARM (kg)	78.36	0.75	0.10	2.15	2.51	117
VRM (kg)	31.377	0.003	0.010	21.4	27.6	129
T_OXID (s)	1752	2	0.11	4620	49	1.1
T_MELT (s)	1936	2	0.10	7058	55	0.78
LH_FAIL (s)	17669	569	3.2	36544	1731	4.7

It is clear from Table 2 that the magnitude of numerical noise is significantly different between the two test decks. The percentage uncertainties are larger for the full-plant BWR deck than the small-scale PWR deck for most of the output quantities. This could be due to either the increased complexity of the BWR deck or that the transient occurs over a significantly longer time period with a greater number of time steps, or some combination of the two. Rigorously determining the effects of deck complexity and transient duration is not possible without significant further analysis. However, this limited study indicates that more complex decks with long transient times may be more susceptible to numerical noise. These results further demonstrate that numerical noise should be addressed on a case-by-case basis.

As mentioned in Section 1.1, shuffling of input deck units such as control volumes, flow paths and heat structures, reorders the elements of the matrices that are loaded into MELCOR's implicit solvers. Small calculational variations are then introduced due to the inherent nature of floating point binary numbers, which are often an imprecise representation of the real decimal number from which they are converted. This limitation in precision means that the outputs of mathematical operations cannot be guaranteed to behave as commutative when executed with machine code and can therefore be dependent on the order in which they are performed. Once a small perturbation is introduced, it will propagate in a similar way to a minuscule change to an input parameter, producing a similar numerical noise distribution when a large set of unique input decks is run.

A further study was performed to assess numerical noise driven by changes to the ordering of input deck units, with the example of flow paths considered. For this study, a series of calculations was set up for the PWR deck that differed only by the ordering of the flow paths, which were randomly shuffled for each case. Figure 6 shows the spread in results from this study. The distributions of the results appear similar to those where the parameters have been subjected to minor perturbations, indicating that the underlying cause of the differences in results with the flow paths shuffled is also numerical noise and that the re-ordering is equivalent to a minuscule perturbation in input values.

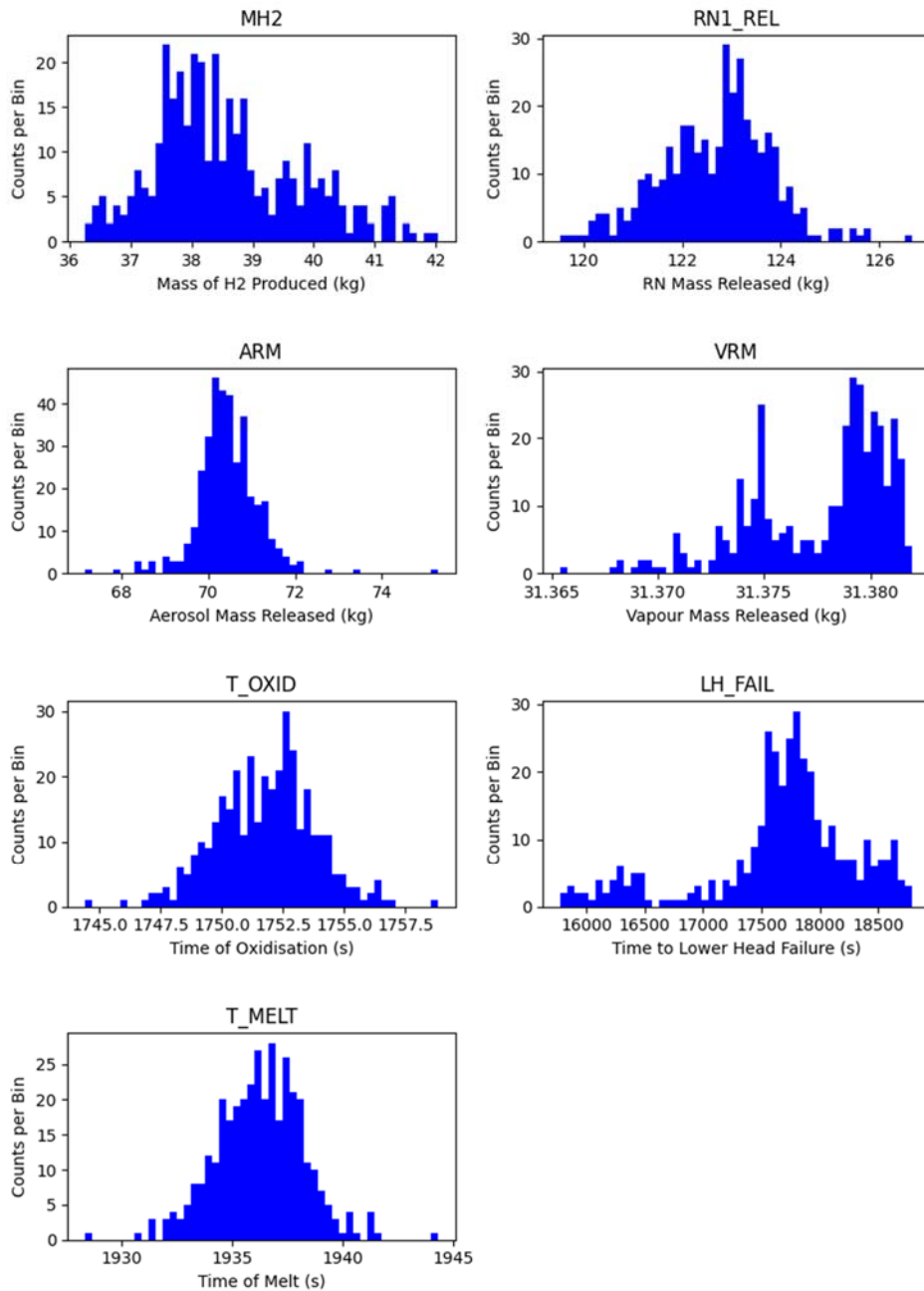


Figure 6: The outputs of a series of MELCOR calculations with the ordering of the flow paths randomly shuffled in the small-scale PWR deck.

To understand the distinction between numerical noise and a genuine uncertainty, the analysis where the parameters were varied was repeated for the variation in reactor operating power, but for a series of different input perturbation sizes. Input perturbations were chosen according to a normal distribution, in sets, with standard deviations covering several orders of magnitude. Figure 7 and Figure 8 show how the spread in output results changes with the size of the input perturbation for the output quantities of time to lower head failure and mass of radioactive vapour released, respectively. For lower values of the perturbation, there is no statistically significant change in the spread in the output quantities, indicating that there is no “physics signal” and that numerical noise dominates in this region with no correlative physical effects observable. At an uncertainty value of around $10^6\text{W} - 10^7\text{W}$ (corresponding to roughly a 0.3% - 3% uncertainty in reactor power), the spread in results starts to grow, suggesting that the threshold between noise and uncertainty is around this value. Above this threshold, the spread in results is much larger, indicating that the physical uncertainty on the input parameter is dominating over numerical noise.

The transition between numerical noise and physical uncertainty appears to be different between Figure 7 and Figure 8. This indicates, as would be expected, that different output quantities are affected differently for a

particular input quantity, i.e. each chosen parameter will have a distinct signal to noise threshold for a given uncertainty analysis.

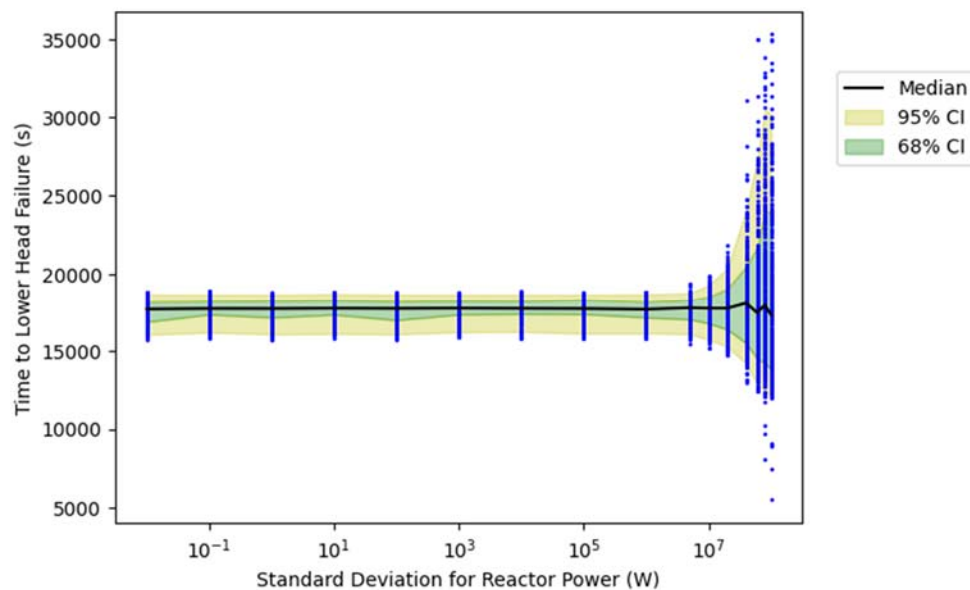


Figure 7: The spread in time to lower head failure for different input perturbations to reactor operating power for the small-scale PWR deck.

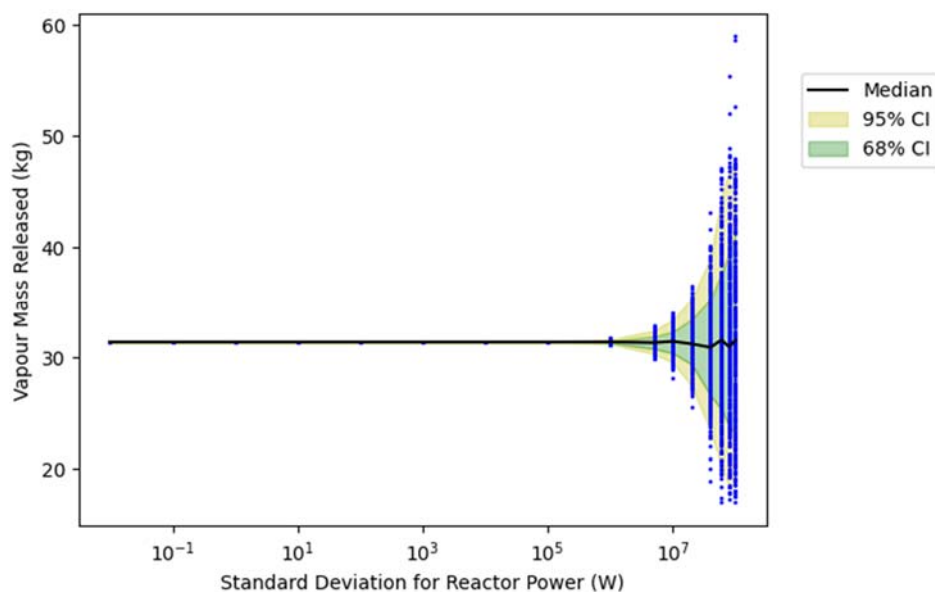


Figure 8: The spread in mass of radioactive vapour released to the environment for different input perturbations to reactor operating power for the small-scale PWR deck.

Figure 7 and Figure 8 demonstrate that as the input uncertainty increases, the output uncertainty will at some point dominate over numerical noise, while Figure 1 and Figure 3 demonstrate that the effects of noise do not combine. It may therefore be tempting to an analyst to discard an input parameter as having a negligible effect on results if the corresponding output cannot be distinguished from numerical noise. However, it is possible that there is a point where the input perturbation is not large enough to dominate over noise when studied in isolation, but is still having an effect on the results, particularly if there are several such parameters. In this case, the effects of multiple input parameters may combine, and thus it may not be appropriate to neglect the input parameter, depending on the magnitude of the uncertainty from other parameters.

To check for this, and to test whether the increase in the spread of results seen in Figure 7 and Figure 8 is not due to noise that is simply of a larger magnitude, the partial correlation matrices between input and outputs are shown in Figure 9 for the 10^{-1} , 10^6 and 10^8 perturbations. The correlations for all tested input perturbation sizes are shown in Figure 10. The correlation between reactor operating power and the seven output metrics

is much stronger with the larger perturbations, with no statistically significant correlation for the $10^{-1}W$ perturbation, demonstrating that noise is chaotic in nature. It is clear when comparing these to Figure 7 and Figure 8 that the correlation starts to increase before the output distribution becomes dominated by the physical uncertainty. This also shows that the threshold between noise and a physical uncertainty can be characterised by the correlation between inputs and outputs. However, it is clear from the 10^6W case, that the threshold where physical uncertainty dominates is different for different output quantities, with the mass of the radioactive vapour (VRM) released being the most sensitive.

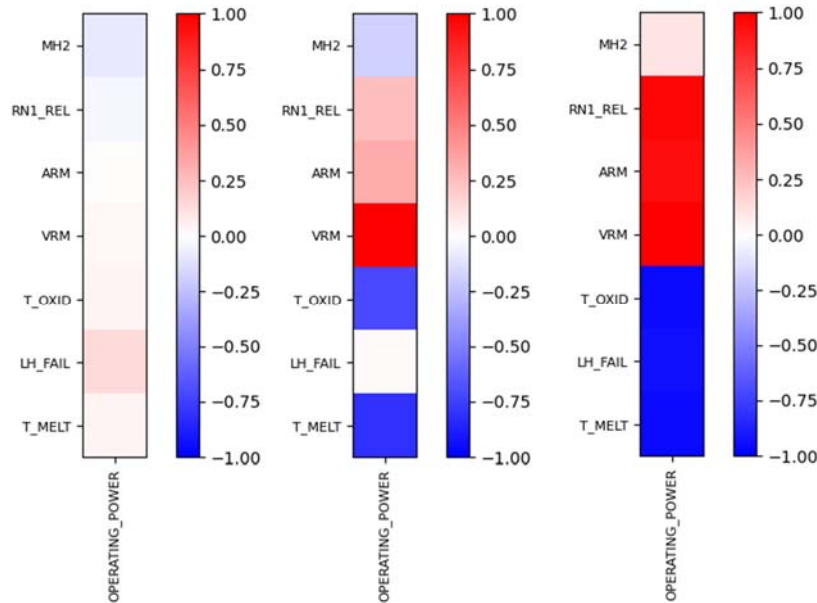


Figure 9: The correlation matrices for reactor operating power for an input uncertainty of $10^{-1}W$ (left) 10^6W (middle) and 10^8W (right).

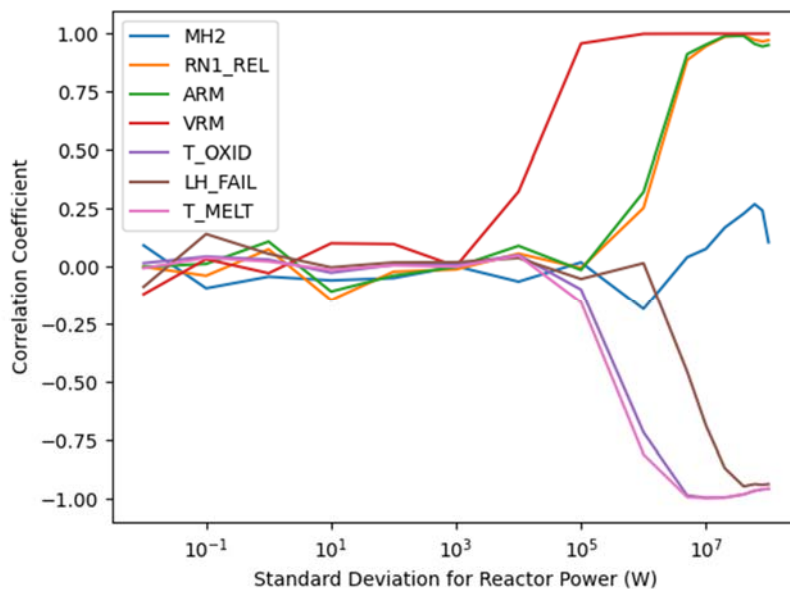


Figure 10: The correlation between reactor operating power and the seven output metrics for a range of different input uncertainties.

Figure 9 and Figure 10 demonstrate that the distinction between numerical noise and a physical uncertainty should be made using both the size of the output distributions and the strength of the correlation between inputs and outputs.

1.3 Time Step Optimisation Study

The choice of time step in a calculation is made to balance pragmatic run times with the convergence of the solution. This trade-off may be further complicated by numerical noise, which is expected to grow with each time step. It may be that with smaller time steps, any biases intrinsic to the method of using time steps are reduced, but the distribution grows as a result of the larger number of calculation cycles required to reach a given problem time.

Many different sources of physical uncertainty feed into an uncertainty analysis of a severe accident calculation. Some of these uncertainties are known to be very large, and for input parameters to which a given output FOM is particularly sensitive, only a small uncertainty can have a large effect on that FOM (as observed in Figure 8). It is therefore expected that, for a full-plant calculation which considers the most important input parameters, the uncertainty in the outputs will be dominated by physical uncertainties rather than numerical noise. Nevertheless, a study into the potential for time step optimisation against numerical noise is considered valuable, given that numerical noise has been observed to be significant in some calculations for some output quantities, and because numerical noise could broaden the distributions of results or reduce correlations even if it is sub-dominant to the physical uncertainties.

In order to establish a well-defined set of guidelines for mitigating numerical noise, the effects of time steps need to be well understood. To this end, a study was conducted in which the same eight input parameters were varied through small perturbations, as with the previous study (see Section 1.2), but using a series of four different time step regimes. The actual MELCOR parameter that was modified for each case was the maximum time step size (DTMAX). The minimum time step size (DTMIN) was set at 1×10^{-8} s for all cases for all times to allow MELCOR to adjust the time step to small enough values to satisfy internal convergence criteria without the calculation aborting. The four cases trialled were:

1. Small time steps with DTMAX set to 1×10^{-2} s for the entire calculation;
2. Large time steps with DTMAX set to 10s for the entire calculation (encouraging MELCOR to progress at a pace determined by its time-step management algorithm);
3. Nominal time steps with DTMAX set to 1×10^{-1} s except for during the oxidation of core components, when the time step was set to 1×10^{-3} s;
4. Nominal time steps with DTMAX set to 1×10^{-1} s except for during the core uncover phase, when the time step was set to 1×10^{-3} s.

As with a normal MELCOR run, the choice of the smaller values of DTMAX was made to allow the analysis to complete in a reasonable run time. It should be noted that, in practice the actual time step used for these runs will not always be DTMAX, as the code will force a smaller time step during certain parts of the calculation. This is particularly true for the second case, which uses a DTMAX value that is significantly higher than would be applied in a detailed severe accident analysis; reduction of time steps to satisfy convergence criteria occurred frequently in this case.

The four cases were chosen to enable direct comparison of the use of smaller and larger time steps to examine their effect on the output distributions, and to target specific areas of the calculation that may be responsible for numerical noise. The last two cases were chosen due to oxidation of core components being a highly non-linear process and the core liquid level during boil-off having been observed to often be unstable for larger time steps. These cases are intended to give an indication of how time steps may be optimised for different phases of the accident. The analyses were only performed for the simple, small-scale PWR deck.

The distributions for the time to lower head failure can be seen in Figure 11 for the four time step regimes. It can be seen that, in addition to the anticipated variation in results due to numerical noise, some bias is also evident. This is particularly manifest when comparing the case in which time steps of 10^{-3} s are applied during the oxidation phase with the others; in this case, the main cluster of results for lower head failure occurs around 10% later in terms of overall calculation time, compared with the other cases. The consequence of this with regard to the effect on the other output quantities considered is discussed later.

A direct comparison of the results for onset of oxidation between the small and large time step cases is shown in Figure 12. This provides a clear example of how the solution can be biased depending on the choice of time step duration, with difference of around 0.4% observed in the median time to the onset of oxidation. However, it is noted that this distinction is not visible in all the output quantities. The distribution of the results for the larger time steps in Figure 12 is slightly narrower than the smaller time step case. This is believed to be due to the smaller number of calculation cycles required to reach this point.

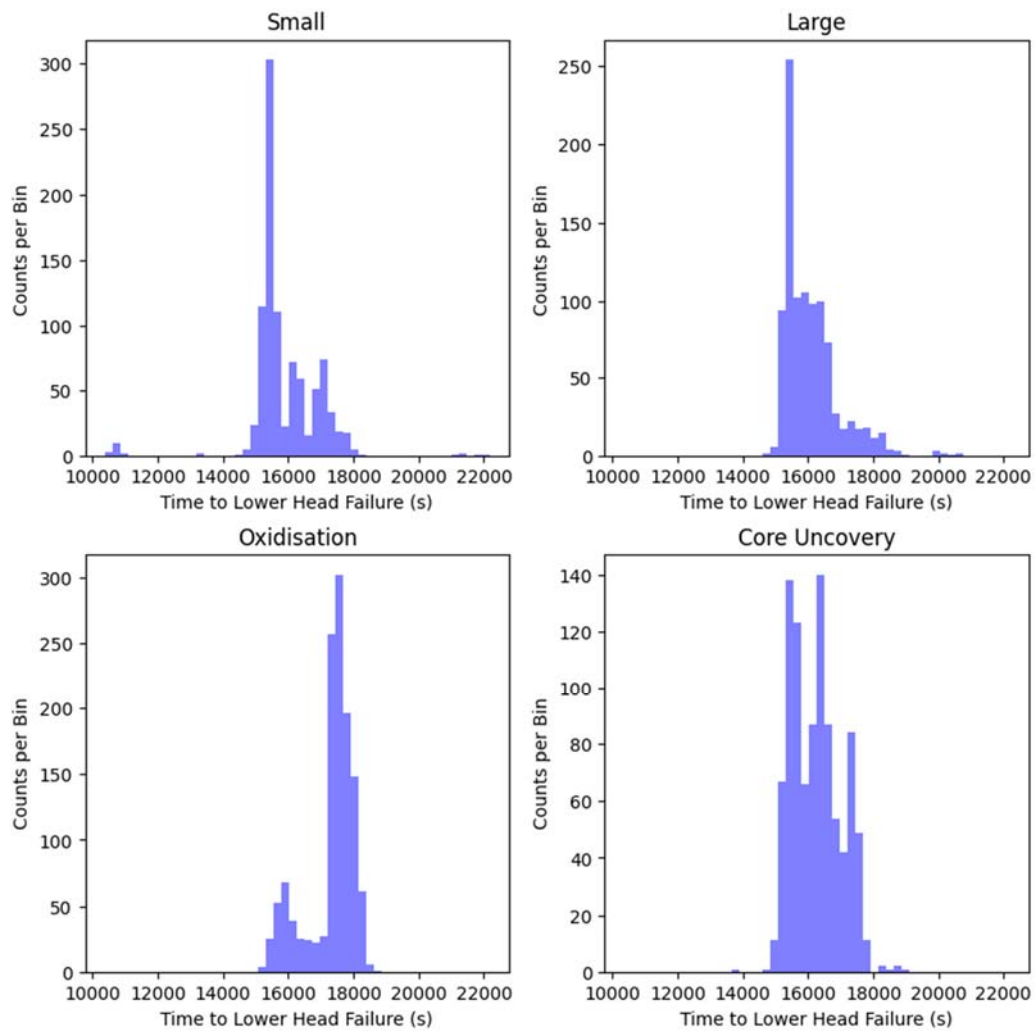


Figure 11: The distributions of time to lower head failure for the PWR deck for the four different time step regimes.

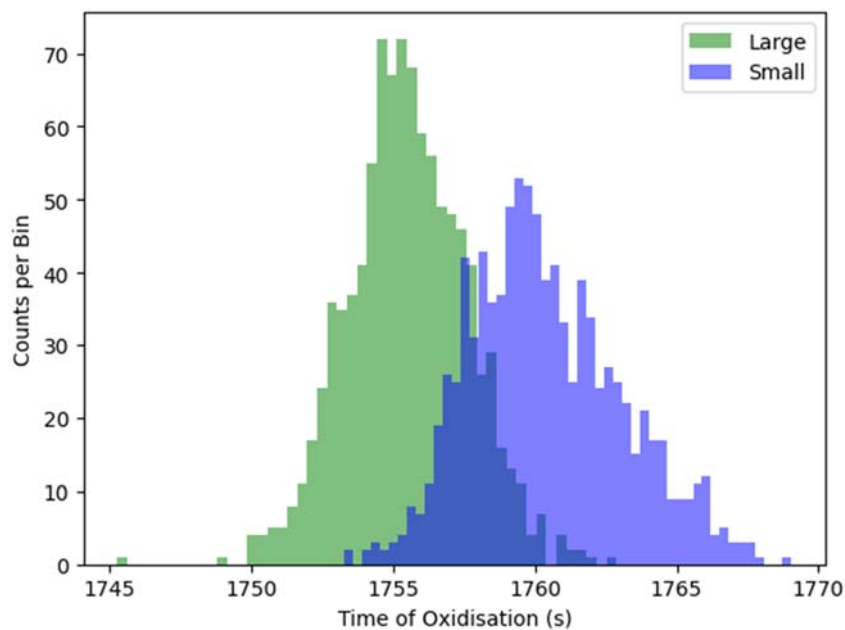


Figure 12: A direct comparison of the distributions in the time for the onset of oxidation for the small and large sets of time steps.

The results of the tests for the four time step regimes are provided in Table 3. The smallest and largest standard deviations of the distributions are highlighted in green and red respectively. It should be noted that the standard deviation is used to measure the spread in the results, but the interpretation of this with respect to a confidence level should not be assumed to be consistent with Gaussian statistics. It does however allow a crude comparison of the widths of the distributions for the four cases and is more valid for results such as the time to the onset of core melting and the mass of aerosol released to the environment, which more closely resemble normal distributions.

Table 3: The mean and standard deviation of all selected output quantities for the four time step regimes.

Result	Small		Large		Oxidation		Core uncover	
	Mean	Std. Dev	Mean	Std. Dev	Mean	Std. Dev	Mean	Std. Dev
MH2	41.52	1.98	40.02	1.86	41.40	1.41	39.34	1.61
RN1_REL	82.30	1.24	83.27	0.86	81.93	1.11	81.22	1.02
ARM	33.48	0.75	32.35	0.88	32.79	1.12	32.46	0.98
VRM	31.361	0.018	31.368	0.011	31.362	0.015	31.357	0.010
T_OXID	1760.4	2.7	1755.5	2.1	1749.2	2.5	1755.0	2.7
LH_FAIL	15889	1092	16076	848	17323	728	16261	745
T_MELT	1946.9	2.9	1940.4	2.1	1934.7	2.5	1941.0	2.9

The results given in Table 3 do not provide an obvious strategy for guaranteeing minimal numerical noise in a calculation, due to inconsistencies across the output quantities. However, the general trend reveals that smaller time steps will result in slightly wider distributions of results than the larger time steps. Since this trend is fairly loose and the narrowing of the distributions is small with larger time steps, it is expected that for most analyses the reduction in bias expected when smaller time steps are used would be preferable to a narrower distribution. This trade-off between bias reduction and the desire to minimize numerical noise will be at the discretion of the analyst on a case-by-case basis since the results shown in Table 3 are a specific case that does not replicate all possible input decks. It is further noted that the tendency towards a later time of lower head failure for the case with small time steps during the oxidation phase did not noticeably affect the other output quantities, for which all cases are relatively consistent.

Clearly further work is needed to rigorously understand the effects of time step on the output distributions. This would be required before more thorough recommendations can be made regarding mitigation of numerical noise, such as whether time steps can be optimised for different phases of the accident.

It was noted previously that the underlying cause of numerical noise was likely the fact that so many quantities in a calculation depend on each other, and the feedback of small initial differences repeated across many time steps. Since a typical severe accident calculation will evolve and change significantly near the start of the calculation, i.e. during boil-down, oxidation and melting, whereas in later parts of the calculation, such as the ex-vessel phase, changes occur relatively slowly, it would be expected that numerical noise grows faster in the earlier phases. This is important because it means an analyst need not be overly concerned about the duration of the calculation having a large effect on the extent to which the results are affected by numerical noise. Though it should be noted that calculations that run to a later problem time would be expected to have a slightly larger width of the output distributions resulting from numerical noise.

1.4 Guidelines and Recommendations

The following guidelines and recommendations with regard to numerical noise have been proposed based on the presented results and observations:

- Numerical noise should be considered to form an inherent uncertainty to a calculation in severe accident codes. The results of a calculation should be treated as a distribution, rather than a single value, since there is no guarantee that any deterministic result is not an outlier within the noise spectrum. As demonstrated in Figure 1 and Figure 3, the results are not likely to be normally distributed and so use of a simple mean and standard deviation may not be sufficient to describe the distribution;

- For any comprehensive uncertainty quantification analysis, an appreciation of the extent to which the inherent numerical noise is affecting the relevant outputs to the calculation should be obtained. This can be achieved by running a large set of calculations in which input variables are perturbed by negligible amounts (i.e. well below the level at which any physical effect would be expected) to understand the magnitude of numerical noise. Similarly, a set of input decks that are physically identical and differ only in the ordering of input deck units such as control volumes, flow paths or heat structures, will also demonstrate a numerical noise distribution;
- It is likely that input decks with greater complexity are more susceptible to numerical noise than simple decks. An analyst should consider this when preparing the input deck so as to avoid adding unnecessary complexity to the calculation. There may also be a trade-off between reducing biases and reducing numerical noise when considering extrinsic factors like model nodalisation, although this has yet to be studied;
- An analyst should be aware that changes in results to calculations with varied inputs may not necessarily be physical. Any change to the inputs of a calculation will result in both a genuine, physical difference to the outputs of the calculation, and a resampling of the noise distribution. Failing to distinguish between these effects could lead to the incorrect interpretation of the relationship between the input and the results. A sufficient number of runs should be performed to enable a clear distinction between numerical noise and a physical uncertainty;
- The uncertainty on the results of a calculation due to the uncertainty on an input parameter should be compared to the effects of numerical noise. This is to ensure that an input uncertainty is not incorrectly overstated in terms of its significance to the calculation. If the distribution of results for a set of input perturbations is not distinguishable from numerical noise, and the correlation between the inputs and all of the outputs is statistically indistinguishable from zero, then numerical noise is likely dominating over any genuine effects of the input parameters. If these criteria are met, and at the analysts discretion, these input uncertainties may be neglected from a full uncertainty analysis;
- Numerical noise will still be present even in an uncertainty analysis strongly dominated by physical uncertainties. In this case, it will be a largely irreducible uncertainty. However, the analyst should still be mindful of this, and that numerical noise will tend to act to reduce the calculated correlation between inputs and outputs;
- It has been observed that numerical noise can invoke cliff-edge effects in the calculation, where key events may or may not happen within a set of very similar or nominally identical input decks. This can lead to multiple peaks in the output distributions which are not related to the physical uncertainty of the input parameters being tested. Ideally, effort should be made to understand the cause of such divergences to determine whether the scenario being analysed is particularly vulnerable to these effects, though this may not always be possible due to the limited information available to the analyst;
- The effect of time steps on numerical noise is complex, and is dependent on the output quantity. However, a general observation is that larger time steps will result in a narrower distribution of results, given that a smaller number of cycles will be required to progress the calculation by a given amount of time. This means that there will likely be a trade-off between time step sizes to balance accuracy with the desire to minimise the size of the noise distribution. The reduction in width of the output distributions was only small with larger time steps and was not observed for all output quantities. It is therefore anticipated that smaller time steps would be preferred for most applications, which is to be balanced with the requirement for calculations to run to completion within practical timescales. Further work would be needed to determine optimal time step sizes or ranges for the different phases of the accident;
- Given the size of typical uncertainties in severe accidents, it is expected that time step optimisation will not be necessary for most cases. This was demonstrated using the small-scale PWR deck. However, a repeat of this analysis would be required for more complex decks in order to conclude if this holds true in general. It is recommended therefore, that an analyst gains an appreciation of the numerical noise distributions in the context of the overall uncertainty distributions, and understands how the time steps may affect these distributions, as part of a rigorous uncertainty quantification.

2 References

- [1] Fukushima Daiichi Unit 1 Accident Progression Uncertainty Analysis and Implications for Decommissioning of Fukushima Reactors – Volume I”, , January 2016., “Fukushima Daiichi Unit 1 Accident Progression Uncertainty Analysis and Implications for Decommissioning of Fukushima Reactors,” Sandia, USA, 2016.
- [2] M. R. Denman and D. M. Brooks, “Fukushima Daiichi Unit 1 Uncertainty Analysis – Exploration of Core Melt Progression Uncertain Parameters,” Sandia, 2015.